

CR-151966

**SIMULATOR EVALUATION OF OPTIMAL THRUST  
MANAGEMENT/FUEL CONSERVATION STRATEGIES  
FOR AIRBUS AIRCRAFT ON SHORT HAUL ROUTES  
FINAL REPORT**

**(March 1976 through November 1976)**

**By John H. Bochem, David C. Mossman,  
and Philip D. Lanier**

January 1977

(NASA-CR-151966) SIMULATOR EVALUATION OF  
OPTIMAL THRUST MANAGEMENT/FUEL CONSERVATION  
STRATEGIES FOR AIRBUS AIRCRAFT ON SHORT HAUL  
ROUTES Final Report, Mar. - Nov. 1976  
(Sperry Flight Systems, Phoenix, Ariz.)

N77-18137  
HC A08  
MF A01

Unclas

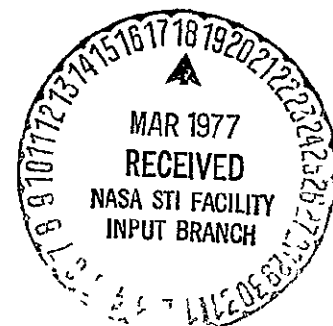
G3/05 20871

Distribution of this report is provided in the interest  
of information exchange. Responsibility for the contents  
resides in the author or organization that prepared it

Prepared under Contract No NAS 2-9174 by  
Sperry Flight Systems  
Phoenix, Arizona

For

NATIONAL AERONAUTICS AND SPACE ADMINISTRATION  
AMES RESEARCH CENTER  
MOFFETT FIELD, CALIFORNIA



Sperry Flight Systems is a Division of the Sperry Rand Corporation

**SIMULATOR EVALUATION OF OPTIMAL THRUST  
MANAGEMENT/FUEL CONSERVATION STRATEGIES  
FOR AIRBUS AIRCRAFT ON SHORT HAUL ROUTES  
FINAL REPORT  
(March 1976 through November 1976)**

**By John H. Bochem, David C. Mossman,  
and Philip D. Lanier**

January 1977

Distribution of this report is provided in the interest  
of information exchange. Responsibility for the contents  
resides in the author or organization that prepared it.

Prepared under Contract No. NAS 2-9174 by  
Sperry Flight Systems  
Phoenix, Arizona

For

NATIONAL AERONAUTICS AND SPACE ADMINISTRATION  
AMES RESEARCH CENTER  
MOFFETT FIELD, CALIFORNIA

Sperry Flight Systems is a Division of the Sperry Rand Corporation

## TABLE OF CONTENTS

Section		Page No.
I	INTRODUCTION AND SUMMARY	1-0
	A. Objectives	1-0
	B. Background	1-0
	C. Summary of Results	1-1
	D. Recommendations	1-4
II	SIMULATOR FACILITY AND AIRBORNE EQUIPMENT	2-0
	A. Simulator/Validation Facility	2-0
	B. Aircraft Simulation and Airborne Guidance and Control System	2-3
	C. Engine Model	2-3
	D. Instruments and Displays	2-7
	E. CRT Conversational Utility	2-7
III	BASELINE FLIGHT PLAN	3-0
IV	DISCUSSION OF RESULTS	4-0
	A. Aircraft Fuel Consumption Characteristics	4-0
	B. Baseline Runs: Las Vegas to Los Angeles	4-7
	C. Delayed Flap Approach Development	4-21
	D. Baseline Flight with Delayed Flap Approach: Las Vegas to Los Angeles	4-39
	E. Baseline Flight at Optimal Cruise Mach: Las Vegas to Los Angeles	4-45
	F. FORTRAN Fuel Optimization Program	4-50
	G. Constrained Altitude Optimal Flight: Las Vegas to Los Angeles	4-61
	H. Unconstrained Altitude Optimal Flight: Las Vegas to Los Angeles	4-74

TABLE OF CONTENTS (cont)

Section		Page No.
	I. Unconstrained Altitude Optimal Flight with Delayed Flap Approach: Las Vegas to Los Angeles	4-78
	J. Baseline Flight: Chicago to Las Vegas	4-92
	K. Constant Altitude Cruise Optimal Flight with Delayed Flap Approach: Chicago to Las Vegas	4-97
	L. Climbing Cruise Optimal Flight with Delayed Flap Approach: Chicago to Las Vegas	4-110
	M. Great Circle Route Analysis	4-118
V	CONCLUSIONS AND RECOMMENDATIONS	5-0
	REFERENCES	R-1
	<b>NOTE: APPENDICES ARE NOT INCLUDED IN THIS REPORT. SEE LAST PAGE FOR AVAILABILITY.</b>	<b>R-2</b>
Appendix		
A-1	OPTIMUM CRUISE TABLE (STANFORD DATA)	A. 1-1
A-2	ASCENT TABLE (STANFORD DATA)	A. 2-1
A-3	DESCENT TABLE (STANFORD DATA)	A. 3-1
A-4	OPTIMUM CRUISE TABLE (SIMULATION DATA)	A. 4-1
A-5	ASCENT TABLE (SIMULATION DATA)	A. 5-1
A-6	DESCENT TABLE (SIMULATION DATA)	A. 6-1
A-7	ASCENT TABLE (SIMULATION DATA WITH FINAL PROGRAM VERSION)	A. 7-1
A-8	DESCENT TABLE (SIMULATION DATA WITH FINAL PROGRAM VERSION)	A. 8-1
B	PROGRAM LISTINGS	B-1
C-1	ASCENT TABLE: CONSTRAINED ALTITUDE: LAS VEGAS TO LOS ANGELES	C. 1-1



TABLE OF CONTENTS (cont)

Appendix		Page No.
C-2	DESCENT TABLE: CONSTRAINED ALTITUDE: LAS VEGAS TO LOS ANGELES	C.2-1
D-1	ASCENT TABLE: UNCONSTRAINED ALTITUDE: LAS VEGAS TO LOS ANGELES	D.1-1
D-2	DESCENT TABLE: UNCONSTRAINED ALTITUDE: LAS VEGAS TO LOS ANGELES	D.2-1
E-1	ASCENT TABLE: UNCONSTRAINED ALTITUDE/DELAYED FLAP: LAS VEGAS TO LOS ANGELES	E.1-1
E-2	DESCENT TABLE: UNCONSTRAINED ALTITUDE/DELAYED FLAP: LAS VEGAS TO LOS ANGELES	E.2-1
F-1	CRUISE TABLE: CHICAGO TO LAS VEGAS	F.1-1
F-2	ASCENT TABLE: OPTIMAL FLIGHT/DELAYED FLAP: CHICAGO TO LAS VEGAS	F.2-1
F-3	DESCENT TABLE: OPTIMAL FLIGHT/DELAYED FLAP: CHICAGO TO LAS VEGAS	F.3-1
G	OPTIMAL CRUISE MACH TABLES	G-1
H-1	DEFINITION OF $K_{1flap}$ AS USED IN THE DRAG EQUATION	H.1-1
H-2	DEFINITION OF $K_{2flap}$ AS USED IN THE DRAG EQUATION	H.2-1
I	CF6-6 ENGINE SIMULATION CALCULATION PROCEDURE AND EQUATIONS	I-1

## LIST OF TABLES

Table No.		Page No.
1-1	Summary of Simulator Flight Results, Las Vegas to Los Angeles	1-2
1-2	Summary of Simulator Flight Results, Chicago to Las Vegas	1-3
3-1	VOR Stations: Las Vegas to Los Angeles	3-2
3-2	VOR Stations: Chicago to Las Vegas	3-6
4-1	Baseline Flight Data	4-21
4-2	$\Delta V/\Delta x$ for Various Flap Settings	4-35
4-3	Desired Flap Deployment Schedule	4-38
4-4	Flight Data: Baseline Flight with Delayed Flap Approach	4-42
4-5	Flight Data: Baseline Flight at Optimal Cruise Mach	4-50
4-6	Mach-Altitude Profiles: Constrained Altitude Flight: Las Vegas to Los Angeles	4-64
4-7	Flight Data: Constrained Altitude Optimal Flight: Las Vegas to Los Angeles	4-74
4-8	Mach-Altitude Profiles: Unconstrained Altitude Optimal Flight: Las Vegas to Los Angeles	4-77
4-9	Flight Data: Unconstrained Altitude Optimal Flight: Las Vegas to Los Angeles	4-78
4-10	Mach-Altitude Profiles: Unconstrained Altitude Optimal Flight with Delayed Flap Approach: Las Vegas to Los Angeles	4-83
4-11	Flight Data: Unconstrained Altitude Optimal Flight with Delayed Flap Approach: Las Vegas to Los Angeles	4-92
4-12	Mach-Altitude Profiles: Optimal Flight with Delayed Flap Approach: Chicago to Las Vegas	4-101
5-1	Summary of Simulator Flight Results: Las Vegas to Los Angeles	5-0
5-2	Summary of Simulator Flight Results: Chicago to Las Vegas	5-1

## LIST OF ILLUSTRATIONS

Figure No.		Page No.
2-1	Sperry DC-10 Simulator	2-1
2-2	Detailed View of Airborne Hardware Simulator and Multiport Peripheral Controller	2-2
2-3	Overall View of DC-10 Simulation Facility	2-2
2-4a	Six-Degree-of-Freedom Equations of Motion Programmed on Sperry Simulator	2-5
2-4b	Supplemental Definitions for Six-Degree-of-Freedom Equations of Motion	2-5
2-5	Block Diagram of Simulation and Integrated Thrust Management System	2-9
2-6	Detailed View of Simulator Cab Instrument Panel	2-10
2-7	Simulation CRT Display Showing Conversational Control of Simulation Features a) Selecting and Scaling Plotter Outputs b) Selecting Flight Plan	2-11
3-1	Lateral Approach Profile: Las Vegas to Los Angeles (Not to Scale)	3-1
3-2	Baseline Climb-Out Profile: Las Vegas to Los Angeles (Not to Scale)	3-4
3-3	Baseline Descent Profile: Las Vegas to Los Angeles (Not to Scale)	3-5
3-4	Baseline Vertical Profile: Chicago to Las Vegas (Not to Scale)	3-7
4-1	$F_D$ vs Mach at Constant Altitude, $W = 300,000$ , $H = 5K$ to $20K$	4-1
4-2	$F_D$ vs Mach at Constant Altitude, $W = 300,000$ , $H = 25K$ to $40K$	4-2
4-3	$F_D$ vs Mach at Constant Altitude, $W = 350,000$ , $H = 5K$ to $20K$	4-3
4-4	$F_D$ vs Mach at Constant Altitude, $W = 350,000$ , $H = 25K$ to $40K$	4-4

LIST OF ILLUSTRATIONS

Figure No.		Page No.
4-5	$F_D$ vs Mach at Constant Altitude, $W = 400,000$ , $H = 5K$ to $20K$	4-5
4-6	$F_D$ vs Mach at Constant Altitude, $W = 400,000$ , $H = 25K$ to $35K$	4-6
4-7	Baseline Lateral Profile, Las Vegas to Los Angeles	4-8
4-8	Barometric Altitude vs Range, Baseline Flight, Las Vegas to Los Angeles, $R = 0$ to $120$	4-9
4-9	Barometric Altitude vs Range, Baseline Flight, Las Vegas to Los Angeles, $R = 104$ to $224$	4-10
4-10	Calibrated Airspeed vs Range, Baseline Climb-Out, Las Vegas to Los Angeles, $R = 0$ to $120$	4-11
4-11	Calibrated Airspeed vs Range, Baseline Descent, Las Vegas to Los Angeles, $R = 104$ to $224$	4-12
4-12	Mach vs Altitude, Baseline Climb-Out, Las Vegas to Los Angeles	4-14
4-13	Mach vs Altitude, Baseline Descent, Las Vegas to Los Angeles	4-15
4-14	Flight Path Angle vs Range, Baseline Flight, Las Vegas to Los Angeles, $R = 0$ to $120$	4-16
4-15	Flight Path Angle vs Range, Baseline Flight, Las Vegas to Los Angeles, $R = 104$ to $224$	4-17
4-16	$F_D$ vs Range, Baseline Flight, Las Vegas to Los Angeles, $R = 0$ to $120$	4-18
4-17	$F_D$ vs Range, Baseline Flight, Las Vegas to Los Angeles, $R = 104$ to $224$	4-20
4-18	Fuel Consumed vs Range, Baseline Flight, Las Vegas to Los Angeles, $R = 0$ to $120$	4-22
4-19	Fuel Consumed vs Range, Baseline Flight, Las Vegas to Los Angeles, $R = 104$ to $224$	4-23
4-20	$F_D$ vs Mach at Constant Altitude, Flaps = $0$ , $\gamma = 0$	4-24
4-21	$F_D$ vs Mach at Constant Altitude, Flaps = $10$ , $\gamma = 0$	4-25

LIST OF ILLUSTRATIONS (cont)

Figure No.		Page No.
4-22	$F_D$ vs Mach at Constant Altitude, Flaps = 22, $\gamma = 0$	4-26
4-23	$F_D$ vs Mach at Constant Altitude, Flaps = 35, $\gamma = 0$	4-27
4-24	$F_D$ vs Mach at Constant Altitude, Flaps = 50, $\gamma = 0$	4-28
4-25	$F_D$ vs Mach at Constant Altitude, Flaps = 0, $\gamma = 3$	4-30
4-26	$F_D$ vs Mach at Constant Altitude, Flaps = 10, $\gamma = 3$	4-31
4-27	$F_D$ vs Mach at Constant Altitude, Flaps = 35, $\gamma = -2.75$	4-32
4-28	$F_D$ vs Mach at Constant Altitude, Flaps = 50, $\gamma = -2.75$	4-33
4-29	Flight Path Angle vs Calibrated Airspeed, Various Flaps	4-34
4-30	Calibrated Airspeed vs Distance on a 2.7 Degree Glide Slope with Retarded Throttles, Flaps = 0 to 40	4-36
4-31	Barometric Altitude vs Range, Baseline Flight with Delayed Flap Approach, Las Vegas to Los Angeles, R = 104 to 224	4-40
4-32	$F_D$ vs Range, Baseline Flight with Delayed Flap Approach, Las Vegas to Los Angeles, R = 104 to 224	4-41
4-33	Flap Position vs Range, Baseline Descent with Delayed Flap Approach, Las Vegas to Los Angeles	4-43
4-34	Calibrated Airspeed vs Range, Baseline Descent with Delayed Flap Approach, Las Vegas to Los Angeles, R = 104 to 224	4-44
4-35	Barometric Altitude vs Range, Baseline Flight at Optimal Cruise Mach, Las Vegas to Los Angeles, R = 0 to 120	4-46
4-36	Barometric Altitude vs Range, Baseline Flight at Optimal Cruise Mach, Las Vegas to Los Angeles, R = 104 to 224	4-47
4-37	$F_D$ vs Range, Baseline Flight at Optimal Cruise Mach, Las Vegas to Los Angeles, R = 0 to 120	4-48
4-38	$F_D$ vs Range, Baseline Flight at Optimal Cruise Mach, Las Vegas to Los Angeles, R = 104 to 224	4-49

LIST OF ILLUSTRATIONS (cont)

Figure No.		Page No.
4-39	Optimal Climb-Out Trajectories (Assuming No Change in Kinetic Energy)	4-54
4-40	Optimal Climb-Out Trajectories (Comparing Constant Kinetic Energy Case to Changing Kinetic Energy Case)	4-60
4-41	Barometric Altitude vs Range, Constrained Altitude Optimal Flight, Las Vegas to Los Angeles, R = 0 to 120	4-62
4-42	Barometric Altitude vs Range, Constrained Altitude Optimal Flight, Las Vegas to Los Angeles, R = 104 to 224	4-63
4-43	Mach vs Barometric Altitude, Constrained Altitude Optimal Flight, Las Vegas to Los Angeles, Climb-Out	4-65
4-44	Mach vs Barometric Altitude, Constrained Altitude Optimal Flight, Las Vegas to Los Angeles, Descent	4-66
4-45	Calibrated Airspeed vs Range, Constrained Altitude Optimal Flight, Las Vegas to Los Angeles, R = 0 to 120	4-68
4-46	Calibrated Airspeed vs Range, Constrained Altitude Optimal Flight, Las Vegas to Los Angeles, R = 104 to 224	4-69
4-47	Flight Path Angle vs Range, Constrained Altitude Optimal Flight, Las Vegas to Los Angeles, R = 0 to 120	4-70
4-48	Flight Path Angle vs Range, Constrained Altitude Optimal Flight, Las Vegas to Los Angeles, R = 104 to 224	4-71
4-49	$F_D$ vs Range, Constrained Altitude Optimal Flight, Las Vegas to Los Angeles, R = 0 to 120	4-72
4-50	$F_D$ vs Range, Constrained Altitude Optimal Flight, Las Vegas to Los Angeles, R = 104 to 224	4-73
4-51	Fuel Consumed vs Range, Constrained Altitude Optimal Flight, Las Vegas to Los Angeles, R = 0 to 120	4-75
4-52	Fuel Consumed vs Range, Constrained Altitude Optimal Flight, Las Vegas to Los Angeles, R = 104 to 224	4-76
4-53	Barometric Altitude vs Range, Unconstrained Altitude, Las Vegas to Los Angeles, R = 0 to 120	4-79

LIST OF ILLUSTRATIONS (cont)

Figure No.		Page No.
4-54	Barometric Altitude vs Range, Unconstrained Altitude, Las Vegas to Los Angeles, R = 104 to 224	4-80
4-55	$F_D$ vs Range, Unconstrained Altitude, Las Vegas to Los Angeles, R = 0 to 120	4-81
4-56	$F_D$ vs Range, Unconstrained Altitude, Las Vegas to Los Angeles, R = 104 to 224	4-82
4-57	Barometric Altitude vs Range, Unconstrained Optimal with Delayed Flap Approach, Las Vegas to Los Angeles, R = 0 to 120	4-85
4-58	Barometric Altitude vs Range, Unconstrained Optimal with Delayed Flap Approach, Las Vegas to Los Angeles, R = 104 to 224	4-86
4-59	$F_D$ vs Range, Unconstrained Optimal with Delayed Flap Approach, Las Vegas to Los Angeles, R = 0 to 120	4-87
4-60	$F_D$ vs Range, Unconstrained Optimal with Delayed Flap Approach, Las Vegas to Los Angeles, R = 104 to 224	4-88
4-61	Flap Position vs Range, Unconstrained Optimal with Delayed Flap Approach, Las Vegas to Los Angeles	4-89
4-62	Calibrated Airspeed vs Range, Unconstrained Optimal with Delayed Flap Approach, Las Vegas to Los Angeles, R = 0 to 120	4-90
4-63	Calibrated Airspeed vs Range, Unconstrained Optimal with Delayed Flap Approach, Las Vegas to Los Angeles, R = 104 to 224	4-91
4-64	Baseline Lateral Profile, Chicago to Las Vegas	4-93
4-65	Barometric Altitude vs Range, Baseline Flight, Chicago to Las Vegas, R = 0 to 300	4-94
4-66	Barometric Altitude vs Range, Baseline Flight, Chicago to Las Vegas, R = 540 to 840	4-95
4-67	Barometric Altitude vs Range, Baseline Flight, Chicago to Las Vegas, R = 1,100 to 1,400	4-96
4-68	$F_D$ vs Range, Baseline Flight, Chicago to Las Vegas, R = 0 to 300	4-98

LIST OF ILLUSTRATIONS (cont)

Figure No.		Page No.
4-69	$F_D$ vs Range, Baseline Flight, Chicago to Las Vegas, R = 540 to 840	4-99
4-70	$F_D$ vs Range, Baseline Flight, Chicago to Las Vegas, R = 1,100 to 1,400	4-100
4-71	Barometric Altitude vs Range, Constant Altitude Cruise Optimal Flight with Delayed Flap Approach, Chicago to Las Vegas, R = 0 to 300	4-103
4-72	Barometric Altitude vs Range, Constant Altitude Cruise Optimal Flight with Delayed Flap Approach, Chicago to Las Vegas, R = 1,100 to 1,400	4-104
4-73	$F_D$ vs Range, Constant Altitude Cruise Optimal Flight with Delayed Flap Approach, Chicago to Las Vegas, R = 0 to 300	4-105
4-74	$F_D$ vs Range, Constant Altitude Cruise Optimal Flight with Delayed Flap Approach, Chicago to Las Vegas, R = 1,100 to 1,400	4-106
4-75	Flap Position vs Range, Constant Altitude Cruise Optimal Flight with Delayed Flap Approach, Chicago to Las Vegas	4-107
4-76	Calibrated Airspeed vs Range, Constant Altitude Cruise Optimal Flight with Delayed Flap Approach, Chicago to Las Vegas, R = 0 to 300	4-108
4-77	Calibrated Airspeed vs Range, Constant Altitude Cruise Optimal Flight with Delayed Flap Approach, Chicago to Las Vegas, R = 1,100 to 1,400	4-109
4-78	Barometric Altitude vs Range, Climbing Cruise Optimal Flight with Delayed Flap Approach, Chicago to Las Vegas, R = 0 to 300	4-111
4-79	Barometric Altitude vs Range, Climbing Cruise Optimal Flight with Delayed Flap Approach, Chicago to Las Vegas, R = 1,100 to 1,400	4-112
4-80	$F_D$ vs Range, Climbing Cruise Optimal Flight with Delayed Flap Approach, Chicago to Las Vegas, R = 0 to 300	4-113



LIST OF ILLUSTRATIONS (cont)

Figure No.		Page No.
4-81	$F_D$ vs Range, Climbing Cruise Optimal Flight with Delayed Flap Approach, Chicago to Las Vegas, R = 1,100 to 1,400	4-114
4-82	Flap Position vs Range, Climbing Cruise Optimal Flight with Delayed Flap Approach, Chicago to Las Vegas	4-115
4-83	Calibrated Airspeed vs Range, Climbing Cruise Optimal Flight with Delayed Flap Approach, Chicago to Las Vegas, R = 0 to 300	4-116
4-84	Calibrated Airspeed vs Range, Climbing Cruise Optimal Flight with Delayed Flap Approach, Chicago to Las Vegas, R = 1,100 to 1,400	4-117

SECTION I

INTRODUCTION AND SUMMARY

## SECTION I

### INTRODUCTION AND SUMMARY

#### A. OBJECTIVES

The objective of this study was to demonstrate and evaluate various fuel conservation techniques for airbus aircraft on short haul routes. The study was to determine the feasibility of incorporating optimal concepts into a practical system, to confirm various earlier theoretical analyses, and to gain some insight into the sensitivity of fuel conservation strategies to nonlinear and second order aerodynamic and engine characteristics not represented in the earlier theoretical studies. In addition to the investigation of optimal trajectories the study was to ascertain combined fuel savings by utilizing various procedure-oriented improvements such as delayed flap/decelerating approaches and great circle navigation.

#### B. BACKGROUND

The study was performed in Sperry's Advanced Avionics Systems Laboratory using one of the digital simulator facilities contained in that laboratory. The specific simulator/validation facility used for this study had been developed previously to provide a software/hardware validation capability for an advanced digital flight guidance and control system for the DC-10 aircraft. The airborne equipment that was flight tested in a DC-10 in 1974 (Reference 1) was used to mechanize the guidance and control laws that defined the optimal flight guidance and thrust management strategies. The integrated digital flight guidance system consisted of an autopilot, flight director, autothrottle and thrust rating system representative of state-of-the-art airborne computer technology. The airborne system was interfaced with an accurate and realistic array of airborne sensing subsystems. A complete complement of DC-10 flight guidance displays permitted realistic monitoring of the demonstration flights. A more detailed description of the validation facility is given in Section II.

Optimal flight path and thrust strategies were computed from procedures developed at Stanford University (References 2 and 3) and NASA Ames Research Center (Reference 4). A FORTRAN program that computed fuel optimal flight

paths was obtained from Stanford University, Department of Aeronautics and Astronautics and was run on the Sperry Flight Systems UNIVAC® 1108 computer. Several modifications were made to the Stanford program in order to more accurately predict the actual performance of the DC-10 aircraft. The program was then used to generate the optimal climb-out and descent profiles for the various flights under study.

### C. SUMMARY OF RESULTS

Trajectories based on optimal control theory were implemented and tested on the Sperry Flight Systems 1819B airborne computer interfaced with a real time simulation of the DC-10 aircraft. The computer was programmed for a fully automated flight, with the autopilot/autothrottle system providing automatic take-off, climb, cruise, descent, approach, landing, and roll-out control. This control was accomplished by sequencing the existing repertoire of autopilot/autothrottle flight path guidance modes. The sequence was controlled by a simulated navigation subsystem which stored the aircraft's flight plan and computed the aircraft's horizontal position with respect to the reference flight plan. All vertical navigation and state estimation was performed by the autopilot/autothrottle computer.

Assurance that the optimal concepts studied are attainable and practical has been provided through utilization of state-of-the-art airborne computer equipment, a very complete simulation of the aircraft and engines, and realistic hardware interfaces representing airborne sensing devices. The results obtained have been encouraging and in general have confirmed earlier theoretical results. The results for a short flight (Las Vegas to Los Angeles) are summarized in Table 1-1. Results for an intermediate range flight (Chicago to Las Vegas) are summarized in Table 1-2.

Conclusions obtained from the study are:

- Fuel consumption sensitivity to nonoptimal airspeed is least during climb-out.
- Fuel consumption sensitivity to changes in airspeed is low in the vicinity of the optimum airspeed at all conditions.

TABLE 1-1  
SUMMARY OF SIMULATOR FLIGHT RESULTS  
LAS VEGAS TO LOS ANGELES

Flight	Average Fuel Consumed (lb)	Average F <sub>D</sub> (lb/nmi)	Average Flight Time (min,sec)	Fuel Saved		Time Change	
				(lb)	%	(min,sec)	%
Baseline	10,072	45.25	39,0	-	-	-	-
Baseline with Delayed Flap Approach (A)	9,791	44.02	37,8	281	2.79	-(1,52)	-4.79
Baseline at Optimal Cruise Mach	9,638	43.31	42,20	434	4.31	3,20	8.55
Optimal with Constrained Altitude	9,480	42.58	43,6	592	5.9	4,6	9.4
Optimal with Unconstrained Altitude	9,316	41.85	42,28	756	7.51	3,28	8.89
Optimal with Unconstrained Altitude and Delayed Flap Approach	8,993	40.42	41,16	1079	10.7	2,16	5.8
Optimal with Unconstrained Altitude and Delayed Flap Approach on Great Circle Route	8,524	41.18	38,52	1548	15.4	-(0,8)	-.34

TABLE 1-2  
SUMMARY OF SIMULATOR FLIGHT RESULTS  
CHICAGO TO LAS VEGAS

Flight	Average Fuel Consumed (lb)	Average $F_D$ (lb/nmi)	Average Flight Time (hr,min,sec)	Fuel Saved		Time Change	
				(lb)	%	(hr,min,sec)	%
Baseline	41,566	30.79	3,3,15	-	-	-	-
Constant Altitude Cruise Optimal with Delayed Flap Approach	39,914	29.56	3,15,9	1652	3.97	0,11,54	6.5
Climbing Cruise Optimal with Delayed Flap Approach	39,860	29.52	3,14,55	1706	4.1	0,11,40	6.37
Climbing Cruise Optimal with Delayed Flap Approach on Great Circle Route	39,050	29.58	3,10,50	2516	6.05	-(0,4,5)	-2.1

- It is advantageous to climb to the optimal altitude that the route length and FAA regulations permit.
- The current airline practice of flying a low altitude cruise segment at a high calibrated airspeed is least efficient on short routes (e.g., Las Vegas to Los Angeles).
- Delayed flap/decelerating approaches can provide a substantial fuel savings if the procedures can be made compatible with air traffic control management of aircraft metering into the final approach paths.
- Great circle routes could significantly reduce both fuel consumption and flight time.

#### D. RECOMMENDATIONS

Results obtained thus far have provided assurance that the optimal concepts under study are realizable and practical. However, additional work should be done to evaluate the desirability of making the strategies adaptive in order to account for drag variations in individual aircraft and loss of engine efficiency with age. The optimal trajectory formulation should be expanded to include the time factor. Procedure-oriented techniques should be explored to maintain the aircraft in the lowest possible drag trim state. In short, while the demonstrated gains are impressive, there appear to be significant effects that bear further investigation.

We also recommend that these concepts be incorporated into a system with sufficient pilot interfaces to allow evaluation of augmented manual (flight director) as well as fully automatic systems. Further, we recommend the ultimate flight testing of a complete system with enough flexibility to evaluate manual, automatic, and semi-automatic fuel conservation techniques.

SECTION II

SIMULATOR FACILITY AND AIRBORNE EQUIPMENT DESCRIPTION



## SECTION II

### SIMULATOR FACILITY AND AIRBORNE EQUIPMENT DESCRIPTION

#### A. SIMULATOR/VALIDATION FACILITY

Figure 2-1 shows a general block diagram of the DC-10 aircraft simulator/validation facility which identifies those elements providing guidance and control system study and/or evaluation capability. The availability of an airborne guidance and control computer complex interfaced with an array of airborne sensing subsystems is an important consideration when conducting this type of work. This capability is provided by the Airborne Hardware Simulator (AHS) unit shown on the left in Figure 2-2. This unit duplicates the electrical and mechanical characteristics of the airborne equipment. The airborne guidance and control system consisting of the data adapter unit, the 1819B digital computer, the electronic control unit (servo drive and excitation interface) and associated panels and controls is interfaced with sensing and control hardware items that are precise electrical replicas of the equipment existing in a DC-10 aircraft. The Multiport Peripheral Controller (Percon) unit, shown on the right in Figure 2-2, contains the simulation computer (a ground-based version of the Sperry 1819B), a 32K auxiliary memory, dual magnetic cartridge units (for program assemblies, program loading, etc), and the electronics that interface the simulation computer with magnetic tape, magnetic cartridge, CRT and printers.

Figure 2-3 shows a view of the simulation facility equipment from the rear of the two-seat cab. The system integration bench, designed to provide the necessary redundancy for fail operative digital Automatic Flight Control System (AFCS) testing, is shown on the right. The front connectors that are in view are test interface points for troubleshooting system components or system wiring. The airborne equipment is mounted behind the trays which are visible. The CRT in the right corner is always on line with the airborne computer.

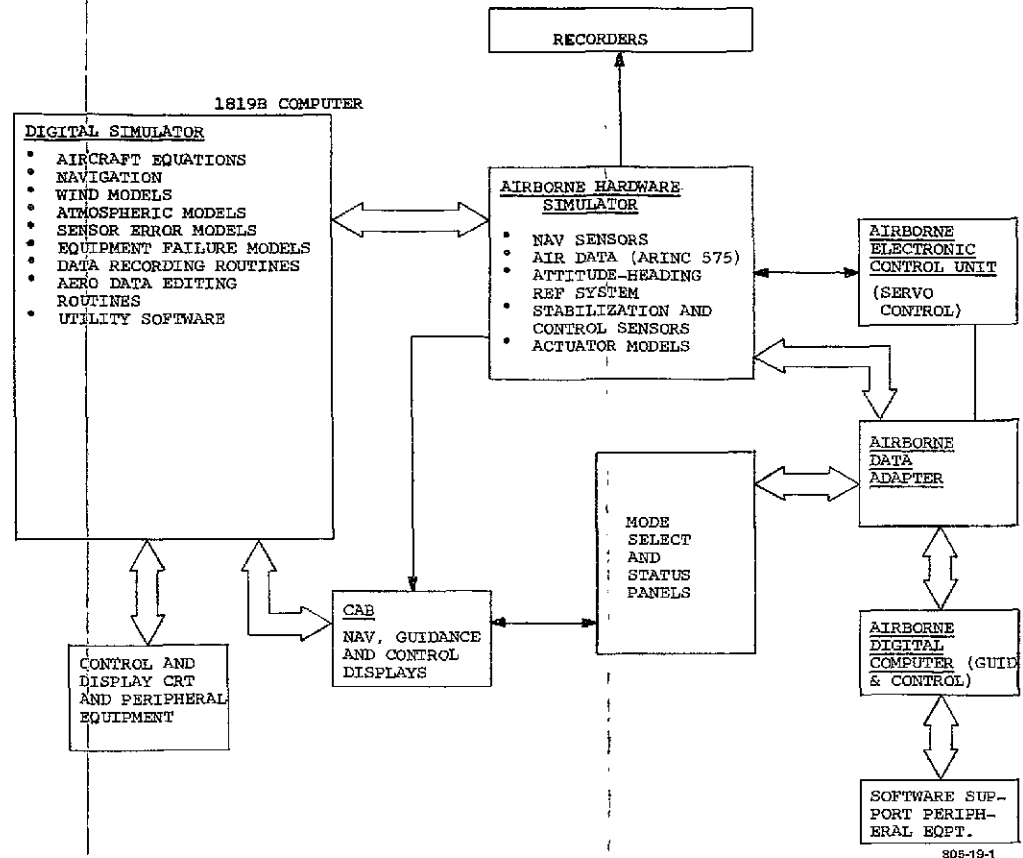
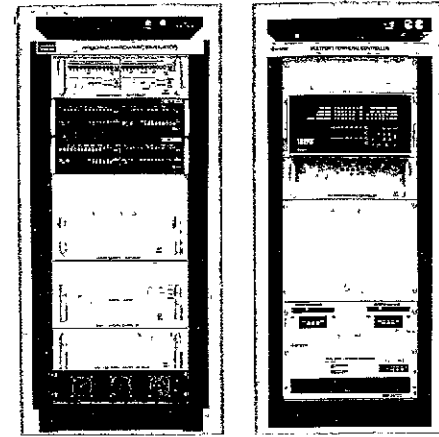
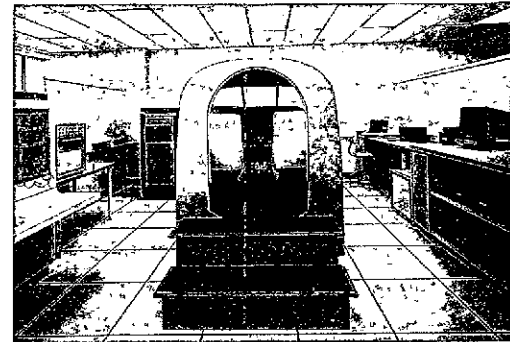


Figure 2-1  
Sperry DC-10 Simulator



815-37-22

Figure 2-2  
Detailed View of Airborne Hardware Simulator  
and Multipoint Peripheral Controller



815-37-20

Figure 2-3  
Overall View of DC-10 Simulation Facility

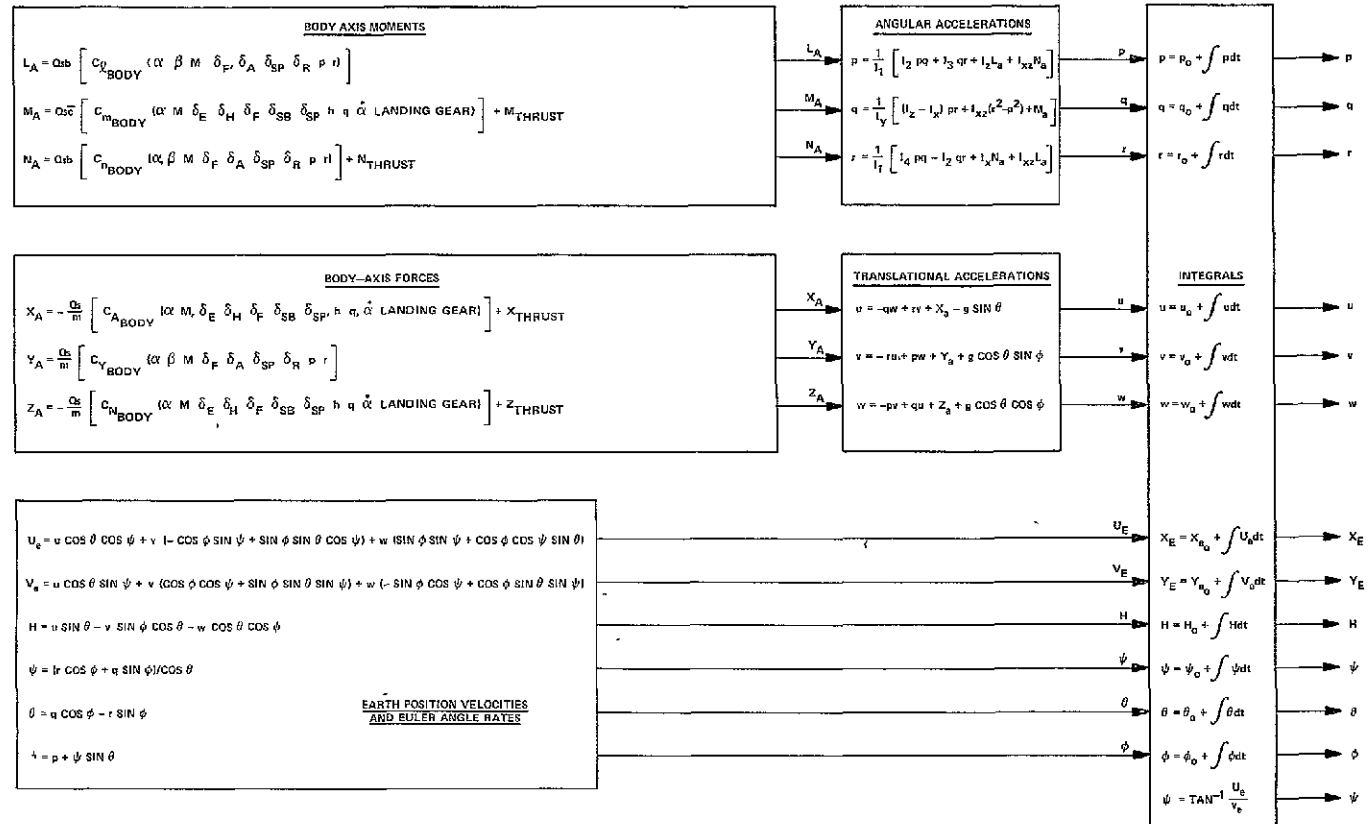
## B. AIRCRAFT SIMULATION AND AIRBORNE GUIDANCE AND CONTROL SYSTEM

The aircraft simulation includes complete six-degree-of-freedom, quasi-rigid body equations of the DC-10 covering its entire flight regime plus ground roll/landing gear equations. These equations are shown in Figures 2-4a and 2-4b. The simulation was developed from Douglas Aircraft Company data given in Reference 5. Detailed aero data is stored in tables which are utilized in the computation of the equations of motion. Moreover, the Airborne Hardware Simulator includes a nonlinear electronic model of the hydromechanical actuation system including hysteresis effects due to compliance, friction, and backlash. The simulation can be flown manually or automatically from take-off to a full stop after landing.

The automatic flight path guidance modes resident in the airborne hardware include autopilot cruise and landing guidance, autopilot control wheel steering with flight director guidance, autothrottle/speed command and thrust rating. The autothrottle/speed command system provides continuous, inflight computation of aircraft weight and angle of attack using inertial and air data measurements. A general block diagram of the aircraft simulation and integrated pitch guidance/thrust management system is shown in Figure 2-5. To facilitate completely automatic flights, flap deployment and course selection are preprogrammed into the simulation and airborne software. Lateral and vertical flight path data for several flight legs, as obtained from United Airlines, are included in the simulation.

## C. ENGINE MODEL

An extensive model of the General Electric CF6-6 jet engine is included in the simulation. Necessary equations and tables are found in Reference 6. The engine power lever is used exclusively for control of the thrust by controlling the high pressure core rotor speed,  $N_2$ . Net engine thrust, fuel flow, and percent low pressure fan rotor speed,  $N_1$ , are then calculated as functions of  $N_2$ , flight condition, and the air bleeds. Typical customer air bleeds as obtained from McDonnell Douglas are adjusted according to the flight mode (climb, cruise, or descent), the altitude, and the aircraft weight. Throttle levers are provided to allow individual manual control of the two wing engines, while the tail engine assumes the average of the other



711 19 143 B1

PRECEDING PAGE BLANK NOT FILMED

Figure 2-4a  
Six-Degree-of-Freedom Equations of  
Motion Programmed on Sperry Simulator

FOLDOUT FRAME /

2-5  
FOLDOUT FRAME

$$I_1 = I_X I_Z - (I_{XZ})^2 \quad M - \text{MASS}$$

$$I_2 = I_{XZ} (I_X - I_Y + I_Z) \quad S - \text{SURFACE AREA}$$

$$I_3 = I_Z (I_Y - I_Z) - (I_{XZ})^2$$

$$I_4 = I_X (I_X - I_Y) + (I_{XZ})^2$$

$b = \text{WING SPAN (FT)}$

$\bar{c} = \text{MEAN AERO CHORD (FT)}$

CONSTANTS  
FOR EQUATIONS OF MOTION

$$\begin{bmatrix} C_{l_{\text{BODY}}} \\ C_{m_{\text{BODY}}} \\ C_{n_{\text{BODY}}} \end{bmatrix} = \begin{bmatrix} \cos \alpha_F & 0 & -\sin \alpha_F \\ 0 & 1 & 0 \\ \sin \alpha_F & 0 & \cos \alpha_F \end{bmatrix} \begin{bmatrix} C_{l_{SA}} \\ C_{m_{SA}} \\ C_{n_{SA}} \end{bmatrix}$$

$$\begin{bmatrix} C_{A_{\text{BODY}}} \\ C_{Y_{\text{BODY}}} \\ C_{N_{\text{BODY}}} \end{bmatrix} = \begin{bmatrix} \cos \alpha_F & 0 & -\sin \alpha_F \\ 0 & 1 & 0 \\ \sin \alpha_F & 0 & \cos \alpha_F \end{bmatrix} \begin{bmatrix} C_{D_{SA}} \\ C_{Y_{SA}} \\ C_{L_{SA}} \end{bmatrix}$$

STABILITY TO BODY AXIS  
TRANSFORMATION

$$u' = u + u_w$$

$$v = v + v_w$$

$$w = w + w_w$$

$u_w, v_w, w_w$  ARE WIND COMPONENTS EQUAL TO

$$u_w = u_{\text{mean}} + u_{\text{gust}}$$

$$v_w = v_{\text{mean}} + v_{\text{gust}}$$

$$w_w = w_{\text{mean}} + w_{\text{gust}}$$

WIND COMPONENT ADDITIONS\*

\*WIND COMPONENTS ENTER BODY MOMENT AND FORCE EQUATIONS THROUGH  $\alpha, \beta, Q$  AND MACH

$$V_T = (u'^2 + v'^2 + w'^2)^{1/2}$$

$$M = V_T / V_A \quad (V_A = \text{SPEED OF SOUND AS A FUNCTION OF ALTITUDE})$$

$$Q = 1/2 \rho V_T^2 \quad (\rho = \text{AIR DENSITY})$$

$$\alpha = \tan^{-1} \frac{w'}{u'}$$

$$\beta = \sin^{-1} \frac{v'}{V_T}$$

$$\gamma = \tan^{-1} \frac{h}{(u_e^2 + v_e^2)^{1/2}}$$

$$V_E = (2Q/\rho_0)^{1/2}$$

AIR DATA COMPUTATIONS

Figure 2-4b  
Supplemental Definitions for  
Six-Degree-of-Freedom Equations of Motion

two. The engine model receives a throttle rate command from the autopilot/autothrottle system (when engaged) which is used to adjust the position of the power lever. The complete engine model is then incorporated into the simulation as shown in Figure 2-5.

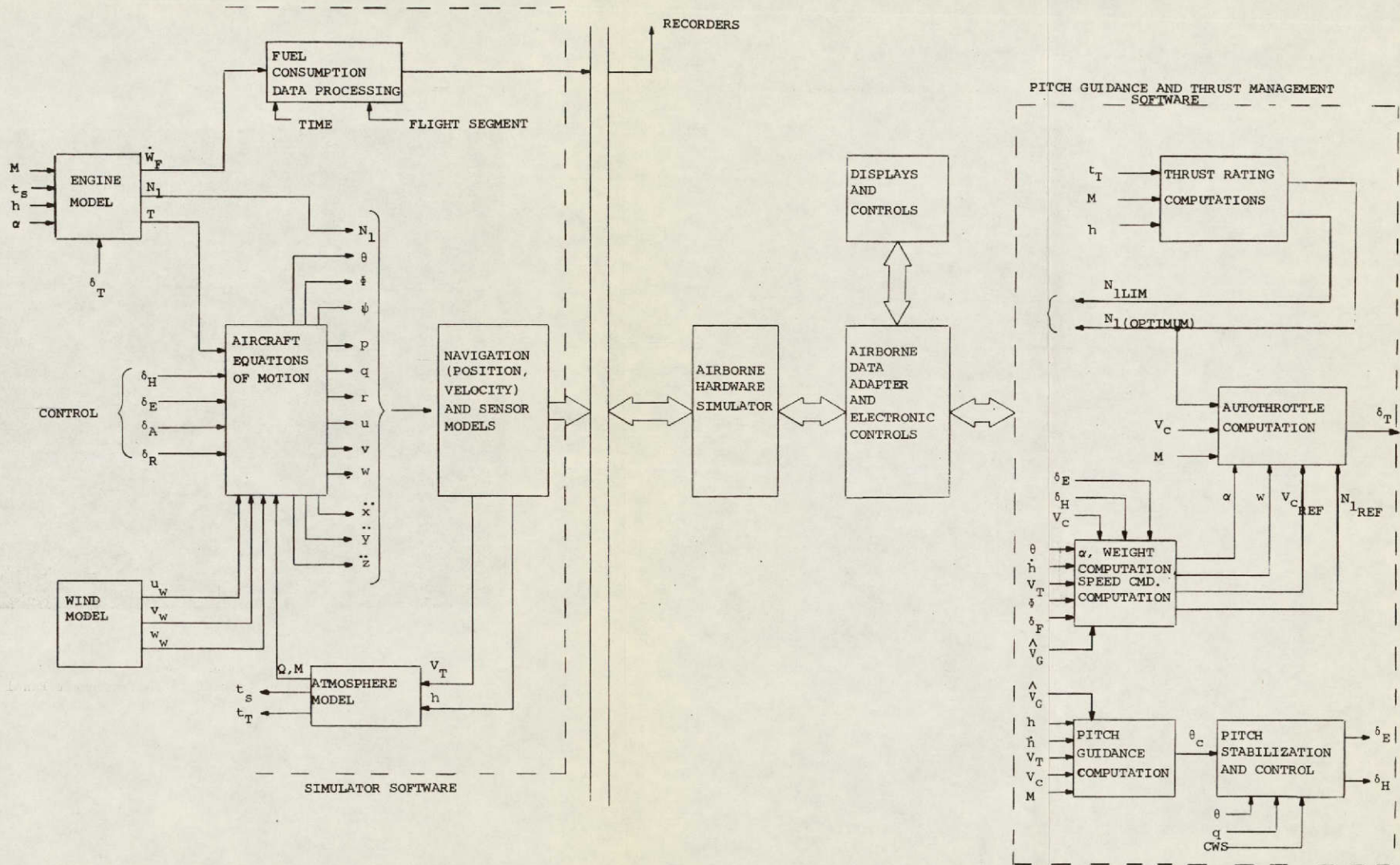
#### D. INSTRUMENTS AND DISPLAYS

The aircraft simulation facility is equipped with a two-seat cab that contains a complete complement of flight displays and controls representative of a transport aircraft. Figure 2-6 shows the instrument panel inside the cab. Instruments interfaced with the simulation include a Mach airspeed indicator, an altimeter, a vertical speed indicator (VSI), an attitude director indicator (ADI), a horizontal situation indicator (HSI), and the total air temperature (TAT) scale of the thrust rating indicator. The airborne computer is interfaced with flight director bars on the ADI, the thrust rating ( $N_1$  limit) indicator, and an alphanumeric mode status display. The Flight Mode Annunciator (FMA) indicates (left to right, top to bottom) the engaged throttle mode, any armed modes, the engaged roll mode, the autopilot status, and the engaged pitch mode. The autopilot status is defined as off, control wheel steering (CWS), or autopilot command.

#### E. CRT CONVERSATIONAL UTILITY

Editing the simulation equations and incorporating additional features are achieved by a simulation utility resident in the simulation computer. Some of the features of this utility are illustrated in Figure 2-7 which shows the simulator's control CRT display calling conversational routines. Figure 2-7a allows selection of any output variable for plotting (including scaling) on an 8-channel strip chart recorder, and Figure 2-7b allows selection of preprogrammed flight plans. Other features include selection of ILS facility beam bends, wind profiles and shears, and setup of X-Y plotters. These same English language conversational routines allow setting of aircraft trim conditions at any point in the aircraft's operating envelope. Turbulence models can be selected or changed, redundant sensor model failure mechanisms can be selected or added, and aero data can be edited.



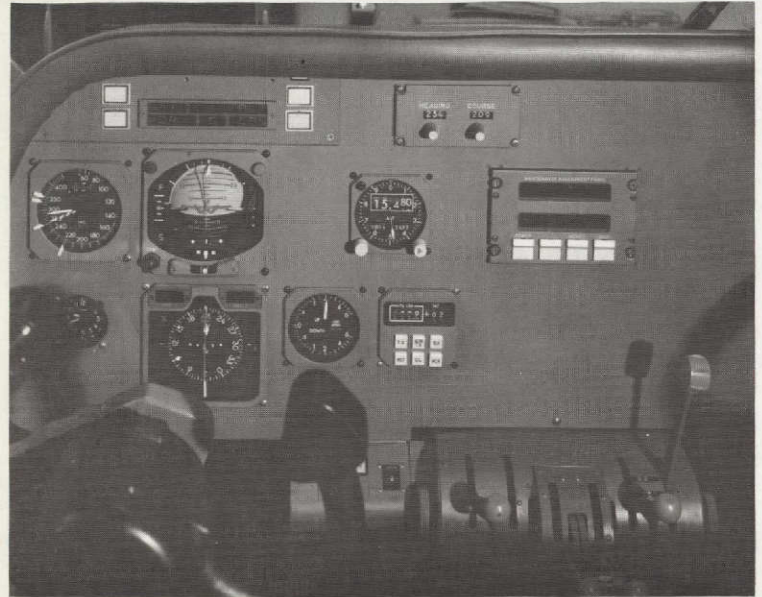


805-19-2

Figure 2-5  
Block Diagram of Simulation and  
Integrated Thrust Management System

ORIGINAL PAGE IS  
OF POOR QUALITY  
FOLDOUT FRAME /

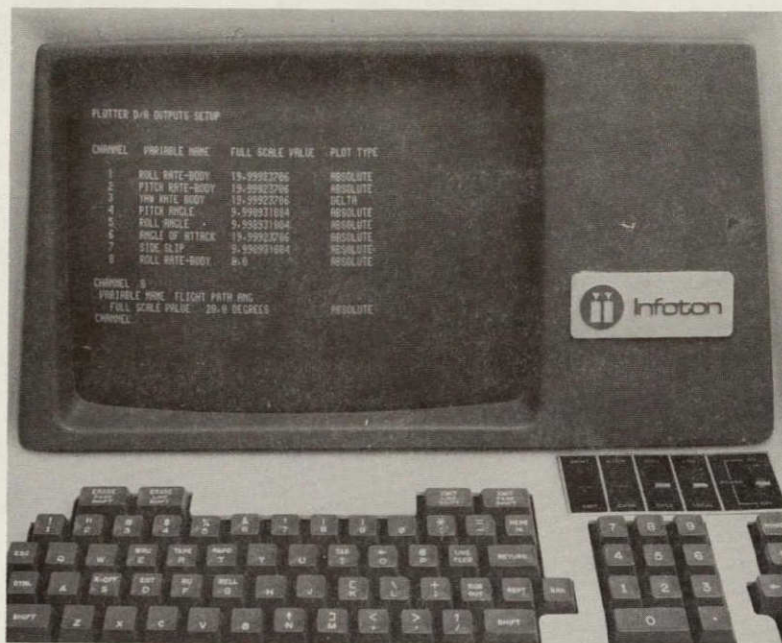




716-72-1

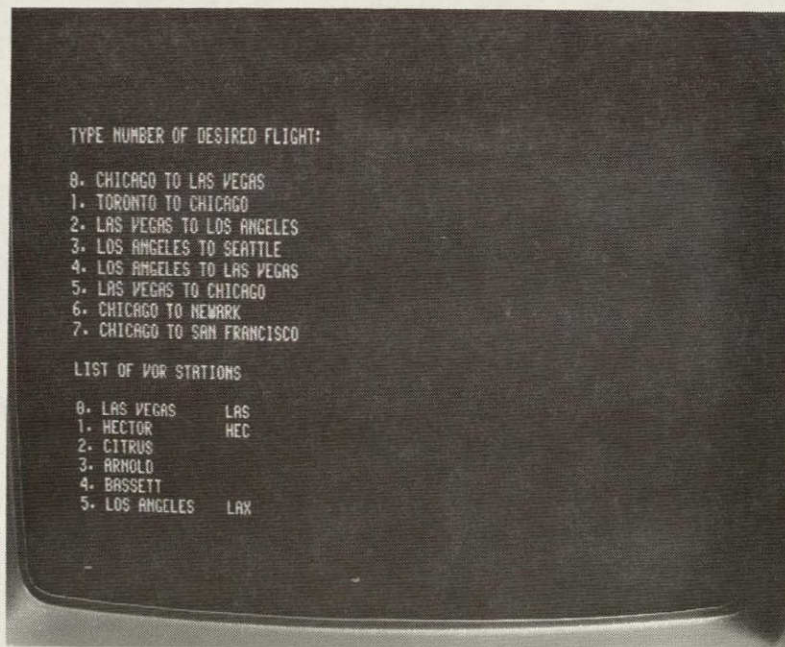
Figure 2-6  
Detailed View of Simulator Cab Instrument Panel

ORIGINAL PAGE IS  
OF POOR QUALITY



15-37-17 ①

a) Selecting and Scaling Plotter Outputs



716-72-2

b) Selecting Flight Plan

Figure 2-7

Simulation CRT Display Showing Conversational Control of Simulation Features

ORIGINAL PAGE IS OF POOR QUALITY

SECTION III  
BASELINE FLIGHT PLAN

### SECTION III

#### BASELINE FLIGHT PLAN

Two flight routes were obtained from United Airlines for use in the fuel conservation study. These routes are:

- United Airlines Flight 345 (as on November 21, 1975)

- Toronto (YYZ) to Chicago (ORD)
- Chicago (ORD) to Las Vegas (LAS)
- Las Vegas (LAS) to Los Angeles (LAX)
- Los Angeles (LAX) to Seattle (SEA)

- United Airlines Flight 358 (as on November 21, 1975)

- Los Angeles (LAX) to Las Vegas (LAS)
- Las Vegas (LAS) to Chicago (ORD)
- Chicago (ORD) to Newark (EWR)

There are seven individual legs with three being short range (LAS to LAX and LAX to LAS, about 220 nautical miles and YYZ to ORD, 398 nautical miles).

The leg from Las Vegas to Los Angeles was chosen as the short range baseline flight, while the leg from Chicago to Las Vegas was chosen as the intermediate range flight. Table 3-1 lists the longitudes and latitudes of the VOR stations that defined the lateral profile for the short haul route. Note that some of the stations listed are not really VOR stations but simply checkpoints. These checkpoints were treated as VOR stations in order to simplify the simulation of pilot action during the automatic flights. Figure 3-1 shows the lateral approach profile used in the baseline short haul route for a landing at Los Angeles.

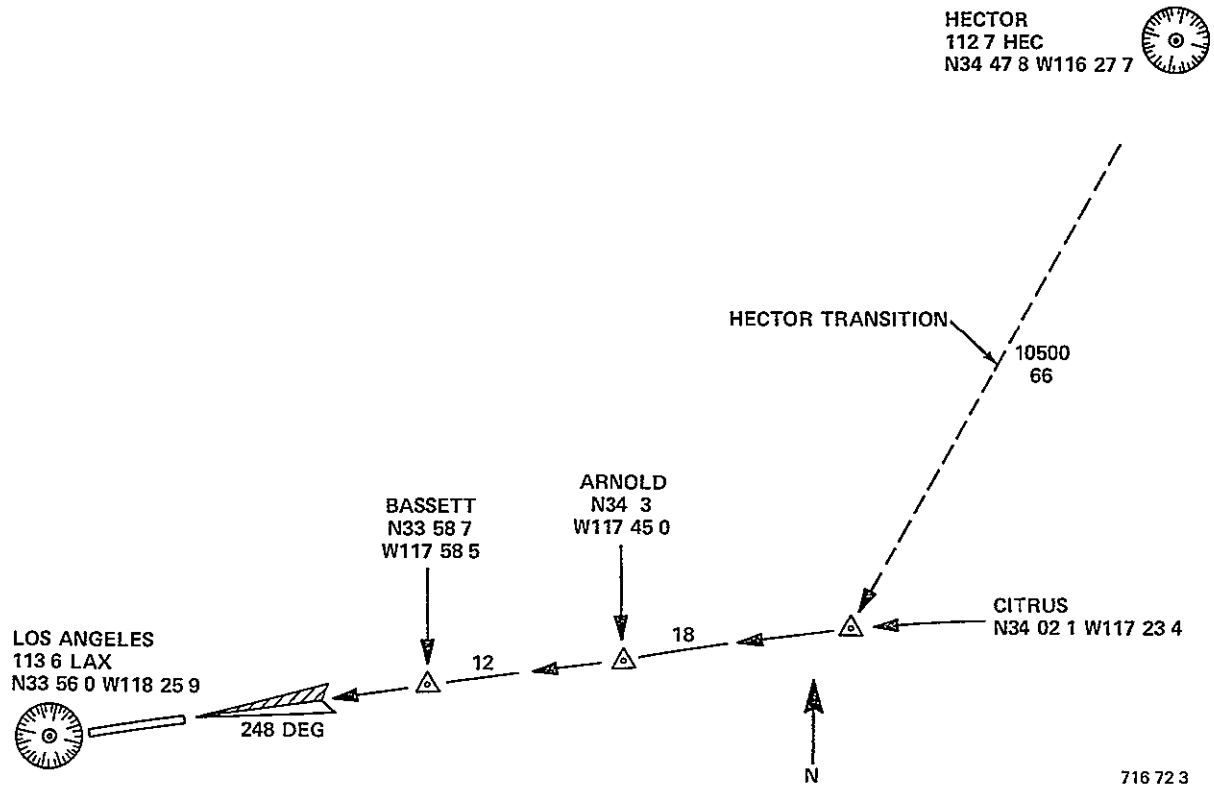


Figure 3-1  
Lateral Approach Profile.  
Las Vegas to Los Angeles (Not to Scale)

TABLE 3-1  
VOR STATIONS  
LAS VEGAS (LAS) TO LOS ANGELES (LAX)

VOR Station	Latitude (deg)	Longitude (deg)	Course (deg)
Las Vegas	36.08	-115.158	219.088
Hector	34.797	-116.462	224.643
Citrus	34.035	-117.39	263.037
Arnold	34.005	-117.75	260.04
Bassett	33.978	-117.975	262.219
Los Angeles	33.933	-118.432	--
Total Initial Weight: 324,900 pounds			
Weight Without Fuel: 279,500 pounds			

Current climb-out procedure, per United Airlines, is to take off with the flaps set to 10 degrees and the throttles set at the take-off  $N_1$  limit. When the speed reaches  $V_R = V_2 + 13$  knots, the aircraft is rotated to 15 degrees nose-up at 3 degrees per second. The speed is then maintained at  $V = V_2 + 10$  knots while the aircraft lifts off and climbs. At 1,500 feet above ground level (AGL), the speed is maintained at  $V_2 + (\text{flap setting})$  in knots, flaps are retracted and the throttles are set at the maximum climb  $N_1$  limit. At 3,000 feet AGL, the vertical speed is reduced to about 600 feet per minute to allow the aircraft to gain airspeed. When 250 knots IAS is attained, this speed is held on pitch, and the throttles are set to the maximum cruise  $N_1$  limit. At 10,000 feet mean sea level (MSL), the vertical speed is again reduced to about 600 feet per minute. At 290 knots IAS, this speed is held on pitch. When .82 Mach is reached, it is held on pitch. As the climb rate drops below 1,000 feet per minute, the throttles are set back to the maximum climb  $N_1$  limit for the remainder of the climb-out.

Current descent procedure, per United Airlines, is to retard the throttles and maintain 340 knots IAS on pitch. When 12,000 feet MSL is reached, the descent rate is reduced to about 800 feet per minute in order to slow the aircraft. At 250 knots IAS, this speed is held on pitch until the approach altitude of 3,000 feet AGL is reached. This altitude is then captured and held on pitch with the throttles still retarded, allowing the

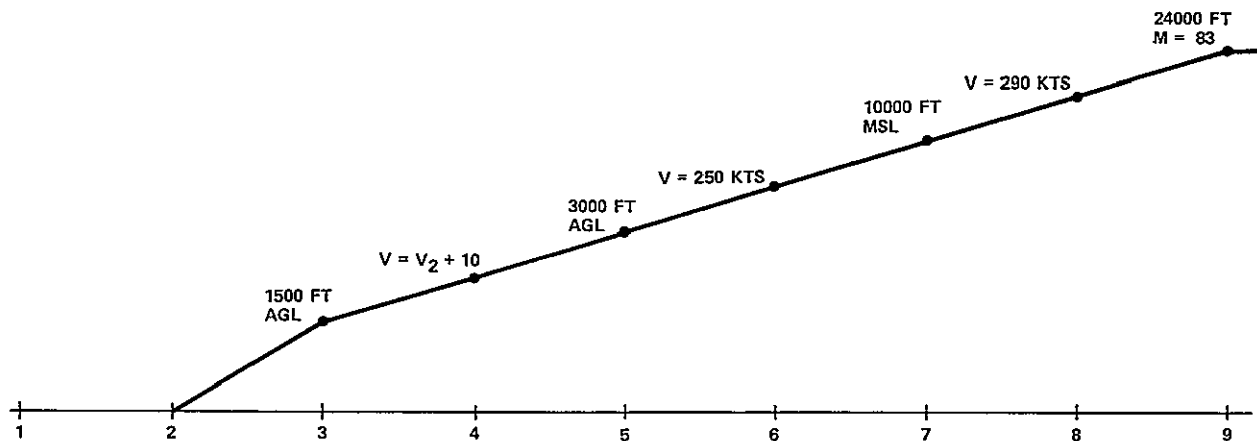
aircraft to slow down. At 190 knots, the flaps are deployed to 15 degrees. When the airspeed reaches the approach speed with respect to the weight and flaps, this speed is held with the throttles. Concurrent with glideslope capture, the flaps are deployed to 22 degrees. Full landing flaps are deployed at 1,500 feet AGL and the aircraft completes the final approach to touchdown. Figures 3-2 and 3-3 show the climb-out and descent profiles, respectively, for the baseline flight from Las Vegas to Los Angeles.

The total initial weight of the aircraft for the short range route was taken as 324,900 pounds, while the weight without fuel was 279,500 pounds. Cruise altitude was 24,000 feet MSL and the cruise Mach was .83. Take-off was due west from Las Vegas. At 1,500 feet AGL, a heading of 165 degrees (magnetic) was selected in order to intercept the 32 degree radial from Hector. The ILS approach into Los Angeles was a Citrus Three arrival made on runway 25L, at a magnetic heading of 248 degrees.

Table 3-2 lists the longitudes and latitudes of the VOR stations that were used for the intermediate range flight from Chicago to Las Vegas. As in the previous case some of the points listed were not really VOR stations but simply checkpoints.

The climb-out and descent procedures for the Chicago to Las Vegas flight were the same as those between Las Vegas and Los Angeles. Initial cruise altitude was 35,000 feet MSL; the cruise Mach was .824. About 140 nautical miles before Denver, an enroute climb to 39,000 feet was effected. Throttles were set to the maximum climb  $N_1$  limit and Mach was held on pitch. Figure 3-4 shows the vertical profile of the flight from Chicago to Las Vegas.

Total initial weight for the intermediate range flight was 348,300 pounds, while the weight without fuel was 288,200 pounds. Take-off was due west from Chicago. At 1,500 feet AGL, a magnetic heading of 165 degrees was selected in order to intercept a 34 degree radial from Joliet. The ILS approach into Las Vegas was a Crowe One arrival (Bryce Canyon transition) made on runway 25 at a magnetic heading of 255 degrees.



CLIMB OUT FROM LAS VEGAS

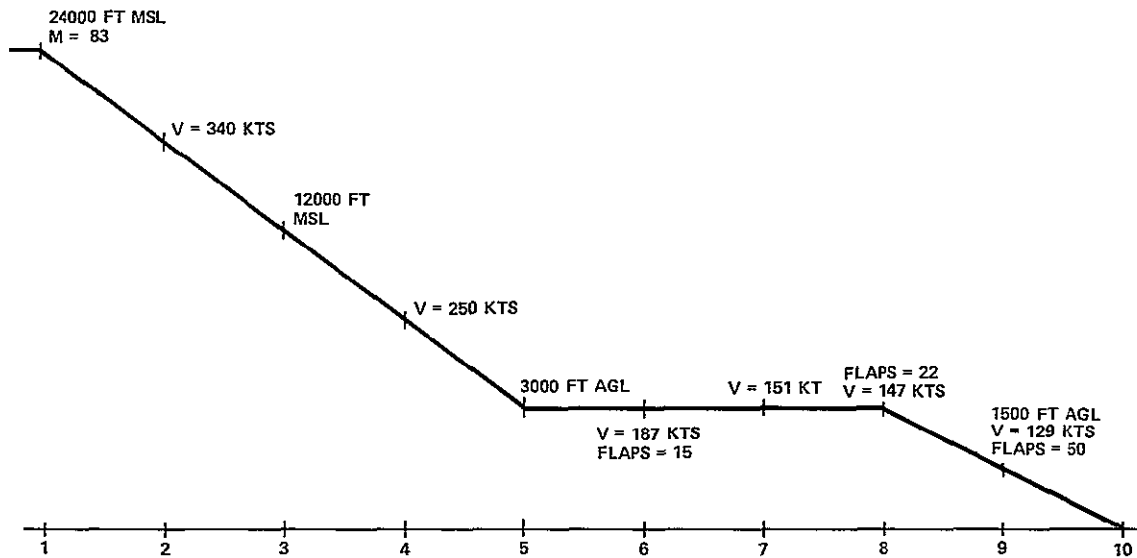
- |   |  |
|---|--|
| <ol style="list-style-type: none"> <li>1 With the flaps set to 10 degrees set the throttles for the <math>N_1</math> limit in the take off mode</li> <li>2 When the speed reaches <math>V_R = V_2 + 13</math> rotate to 15 degrees nose up at 3 degrees per second. Maintain <math>V = V_2 + 10</math> and take off thrust. Heading is due west.</li> <li>3 At 1500 feet above ground level select <math>V = V_2 + \text{Flap (10)}</math> and begin to retract flaps. Set the throttles for the <math>N_1</math> limit in the climb mode. Turn to a heading of 165 degrees in order to intercept the 32 degree radial from the VOR at Hector.</li> <li>4 Maintain <math>V = V_2 + 10</math> knots</li> </ol> | <ol style="list-style-type: none"> <li>5 At 3000 feet above ground level, set the flight path angle mode to maintain ~ 600 feet per minute climb rate</li> <li>6 When the speed reaches 250 knots hold this speed on pitch</li> <li>7 At 10 000 feet (mean sea level) again set the flight path angle mode to maintain ~ 600 feet per minute climb rate</li> <li>8 When the speed reaches 290 knots hold this speed on pitch</li> <li>9 At 24 000 feet (MSL) hold altitude on pitch and hold 83 Mach on autothrottle with the <math>N_1</math> limit in the cruise mode</li> </ol> |
|---|--|

716 72-4

Figure 3-2  
 Baseline Climb-out Profile:  
 Las Vegas to Los Angeles  
 (Not to Scale)

ORIGINAL PAGE IS  
 OF POOR QUALITY





DESCENT AND APPROACH INTO LOS ANGELES

- |  |  |
|--|--|
| <ol style="list-style-type: none"> <li>1 At point of descent (35 miles past Hector), retard the throttles and maintain altitude</li> <li>2 When the speed reaches 340 knots hold this speed on pitch</li> <li>3 At 12,000 feet (MSL) set the flight path angle mode for a descent rate of 800 feet per minute</li> <li>4 When the speed reaches 250 knots hold this speed on pitch</li> <li>5 At 3 000 feet above ground level hold altitude on pitch</li> </ol> | <ol style="list-style-type: none"> <li>6 When the speed reaches 187 knots deploy flaps to 15 degrees</li> <li>7 When the approach speed is reached hold this speed on autothrottle</li> <li>8 When the glide slope is intercepted deploy the flaps to 22 degrees and hold 147 knots on autothrottle</li> <li>9 At 1 500 feet above ground level deploy full landing flaps (50 degrees) and hold 135 knots on autothrottle</li> <li>10 Land at Los Angeles</li> </ol> |
|--|--|

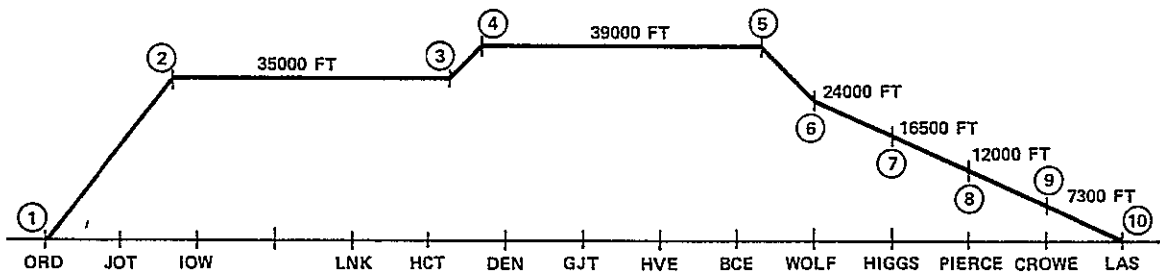
716 72 5

Figure 3-3  
 Baseline Descent Profile:  
 Las Vegas to Los Angeles  
 (Not to Scale)

ORIGINAL PAGE IS  
 OF POOR QUALITY

TABLE 3-2  
 VOR STATIONS  
 CHICAGO (ORD) TO LAS VEGAS (LAS)

VOR Station	Latitude (deg)	Longitude (deg)	Course (deg)
Chicago	41.988	-87.905	214.077
Joliet	41.547	-88.318	268.035
Iowa City	41.518	-91.613	250.240
111 Miles Past IOW	40.927	-93.922	268.879
Lincoln	40.923	-96.742	260.112
Hayes Center	40.453	-100.923	257.131
Denver	39.86	-104.752	254.251
Grand Junction	39.06	-108.792	245.687
Hanksville	38.417	-110.698	239.439
Bryce Canyon	37.69	-112.303	222.133
Wolf	36.693	-113.455	222.034
Higgs	36.415	-113.772	220.810
Pierce	36.075	-114.147	267.074
Crowe	36.073	-114.357	269.621
Las Vegas	36.08	-115.163	--
Total Initial Weight: 348,300 pounds			
Weight Without Fuel: 288,200 pounds			



- 1 LEAVE CHICAGO, ELEVATION 595 FEET
- 2 REACH CRUISE ALTITUDE OF 35000 FEET AT 126 MILES PAST JOLIET MACH = 82
- 3 BEGIN ENROUTE CLIMB IN ALTITUDE AT 38 MILES PAST HAYES CENTER, MACH = 82.
- 4 REACH NEW CRUISE ALTITUDE OF 39000 FEET AT 90 MILES PAST HAYES CENTER  
MACH = 827
- 5 POINT OF DESCENT AT 52 MILES PAST BRYCE CANYON, MACH = 825
- 6 PASS OVER WOLF
- 7 PASS OVER HIGGS
- 8 PASS OVER PIERCE
- 9 PASS OVER CROWE
- 10 ARRIVE AT LAS VEGAS, ELEVATION 2030 FEET

716-726

Figure 3-4  
 Baseline Vertical Profile:  
 Chicago to Las Vegas  
 (Not to Scale)

ORIGINAL PAGE IS  
 OF POOR QUALITY

SECTION IV  
DISCUSSION OF RESULTS

## SECTION IV

### DISCUSSION OF RESULTS

#### A. AIRCRAFT FUEL CONSUMPTION CHARACTERISTICS

Figures 4-1 through 4-6 show the simulated DC-10 aircraft's fuel consumption per unit distance versus Mach number at constant altitude for weights of 300,000, 350,000, and 400,000 pounds. The altitudes ranged from 5,000 to 40,000 feet in 5,000 foot increments. It was determined that the center of gravity location has little, if any, effect on the altitude or Mach number for optimal fuel consumption per unit distance.

All the curves tend to be very shallow and have a wide range of Mach numbers over which the fuel consumption per unit distance,  $F_D$ , does not change appreciably. As an example, for a weight of 300,000 pounds and an altitude of 15,000 feet, the minimum  $F_D$  of 36.25 pounds per nautical mile occurs at .52 Mach. If the Mach number is increased 10.6 percent to .575 Mach, the value of  $F_D$  increases to 37.0 pounds per nautical mile, or only about 2.1 percent.

The Mach number where the optimal  $F_D$  occurs increases with altitude for a given weight. For example, with a weight of 300,000 pounds, the optimal Mach number is about .42 for an altitude of 5,000 feet. The optimal Mach then increases with each succeeding altitude until at 40,000 feet the Mach number is .79.

The altitude at which the optimal  $F_D$  occurs is a function of the weight. The optimal altitude decreases with increasing weight. Figure 4-2 shows that the optimal altitude for a weight of 300,000 pounds is approximately 40,000 feet. Figure 4-6 shows that the optimal altitude is about 35,000 feet for a weight of 400,000 pounds.

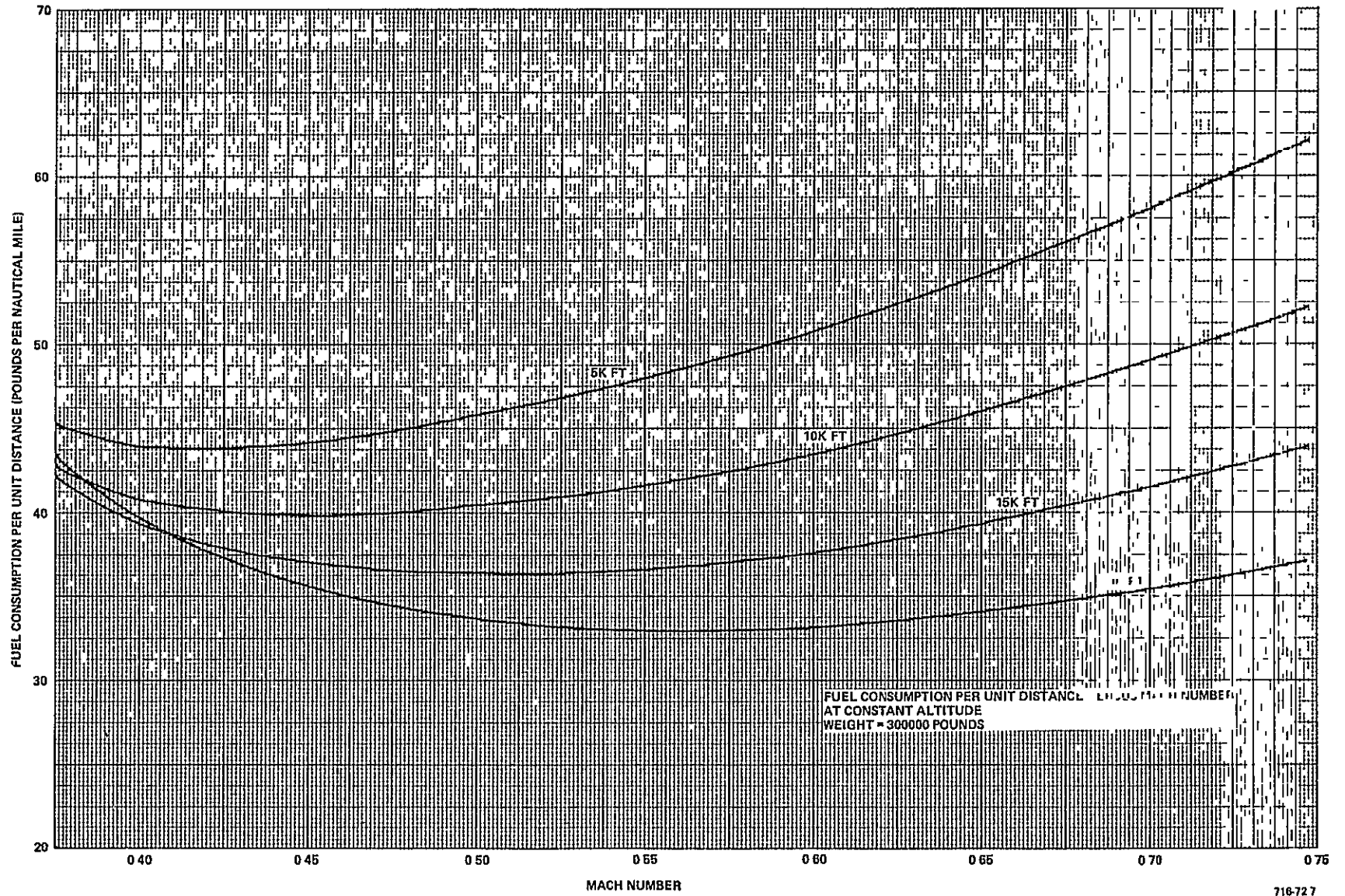


Figure 4-1

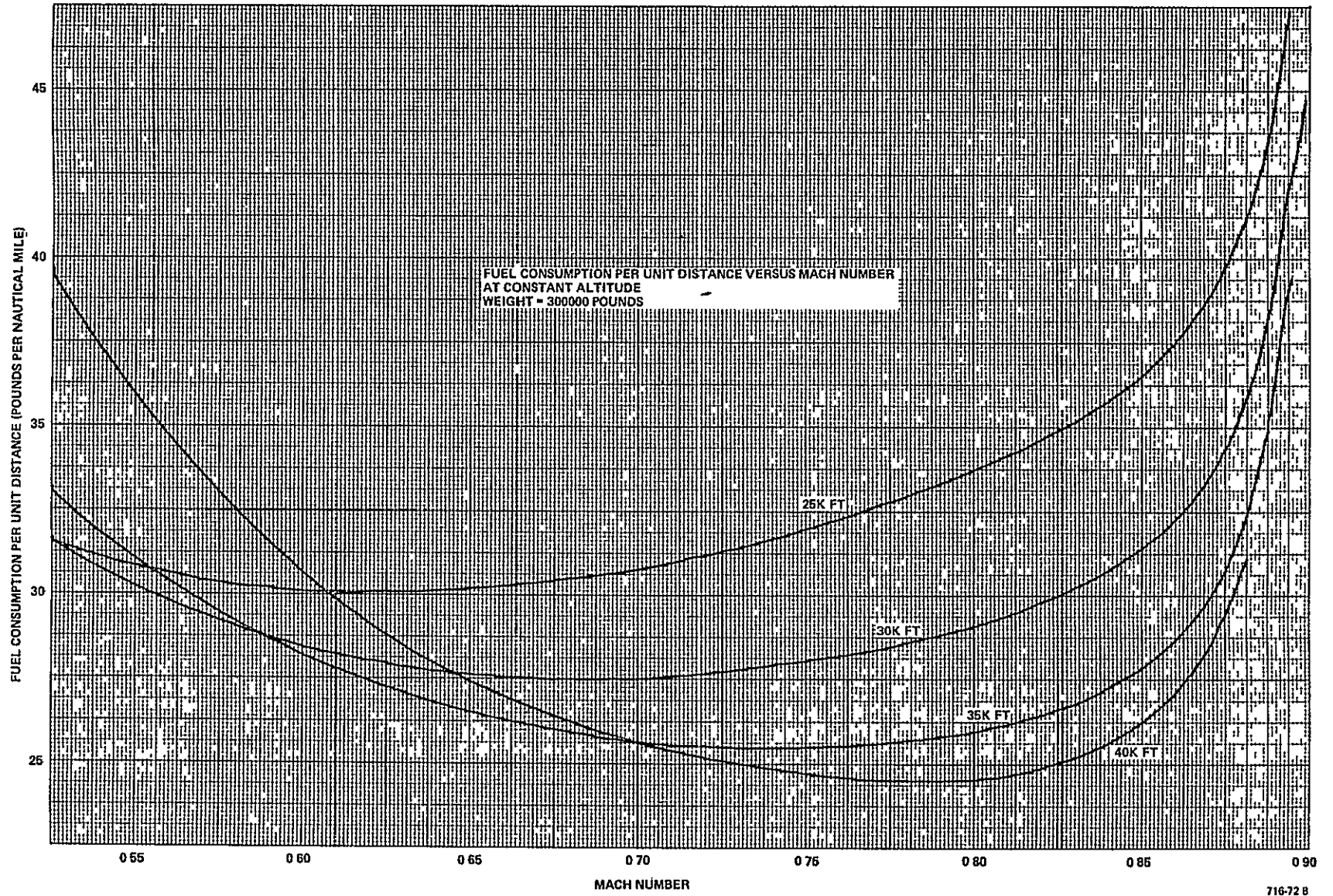


Figure 4-2

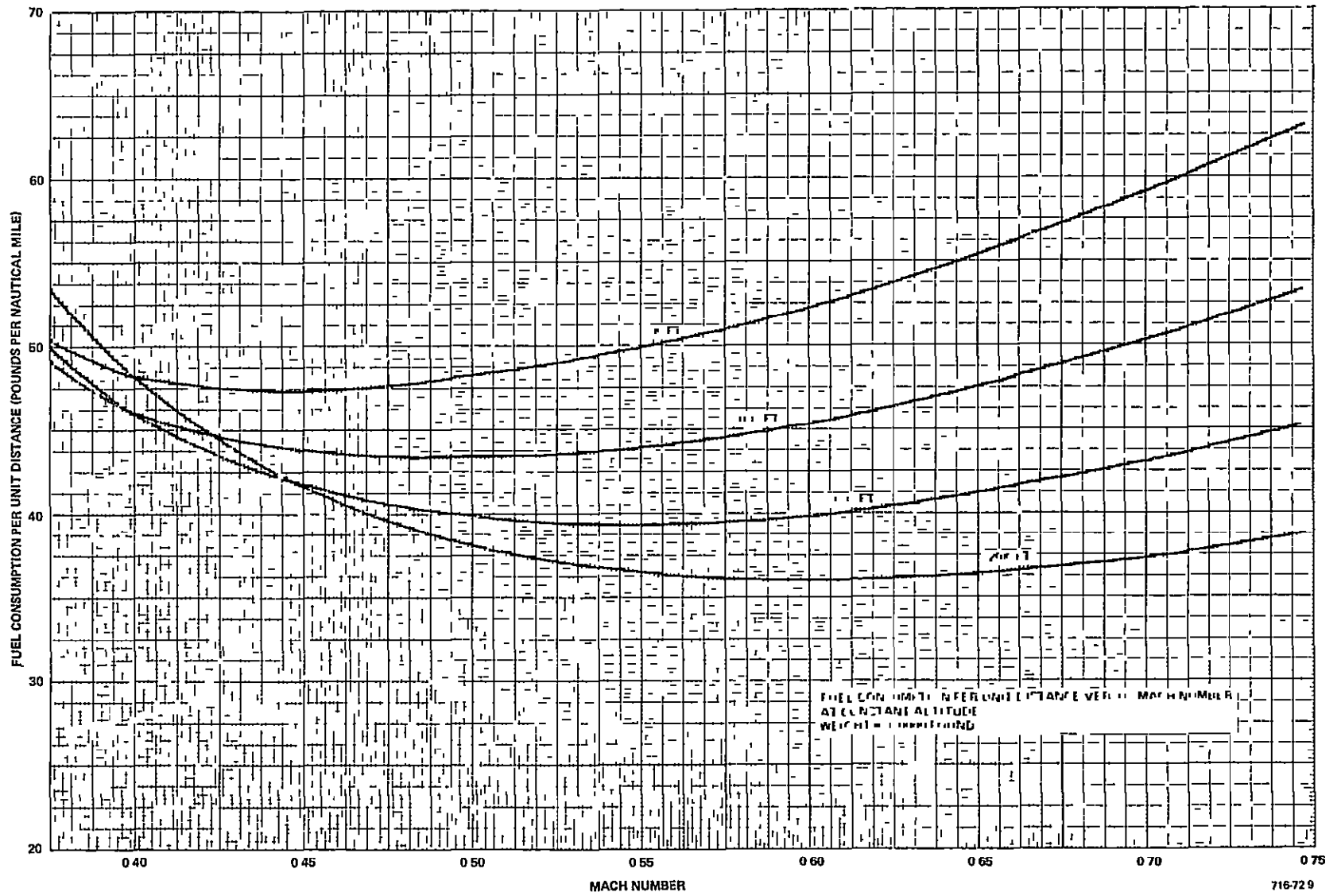


Figure 4-3



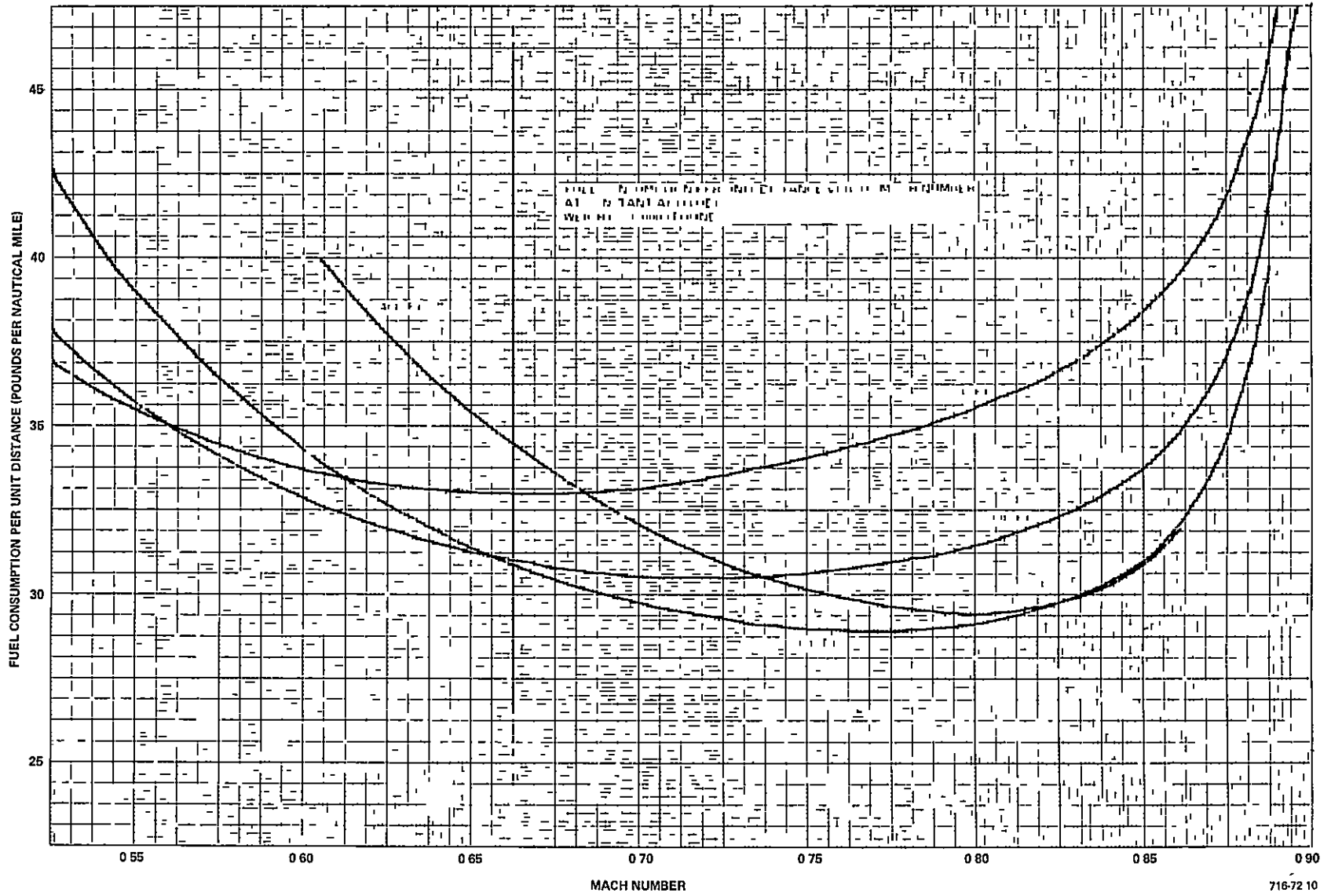


Figure 4-4

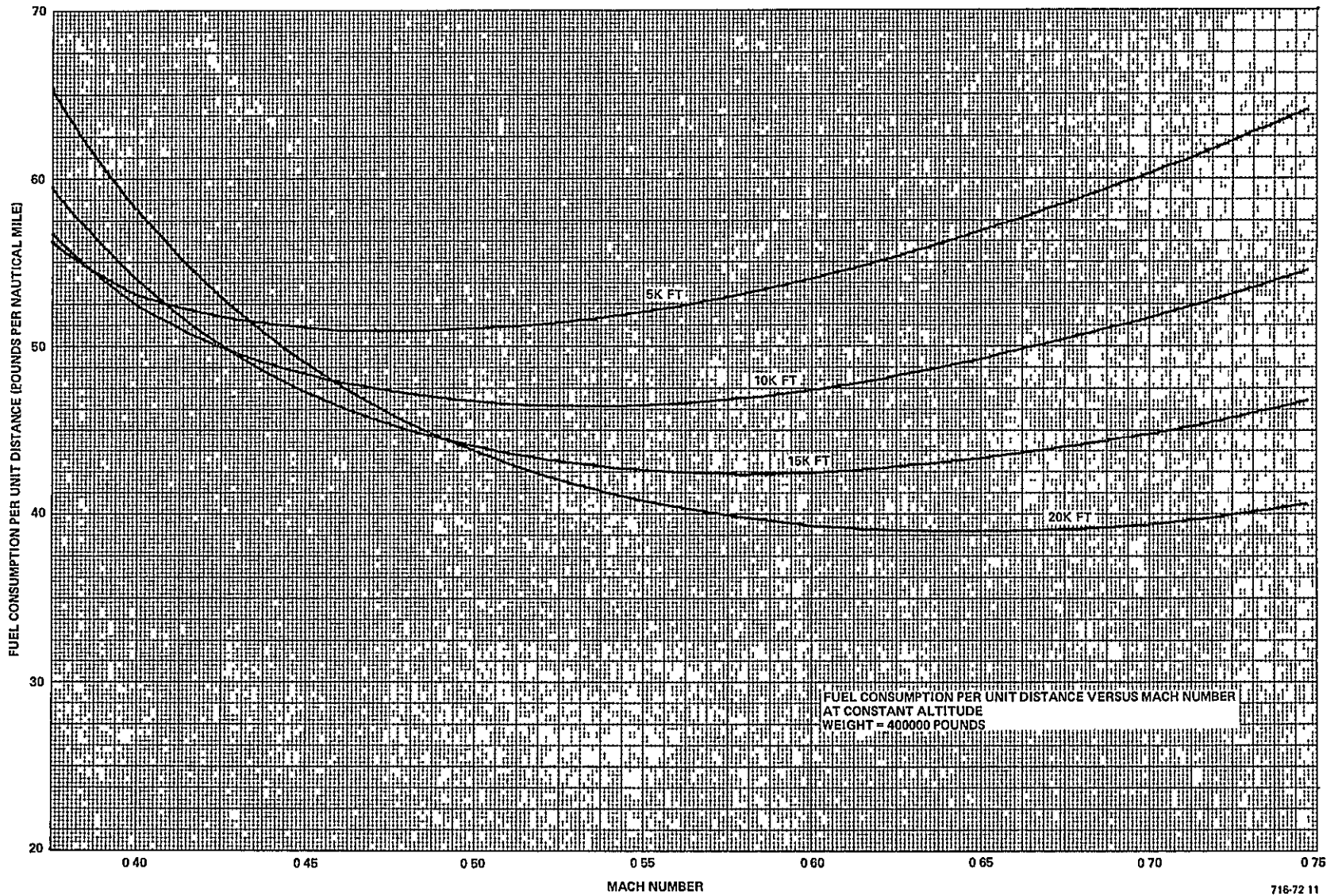


Figure 4-5

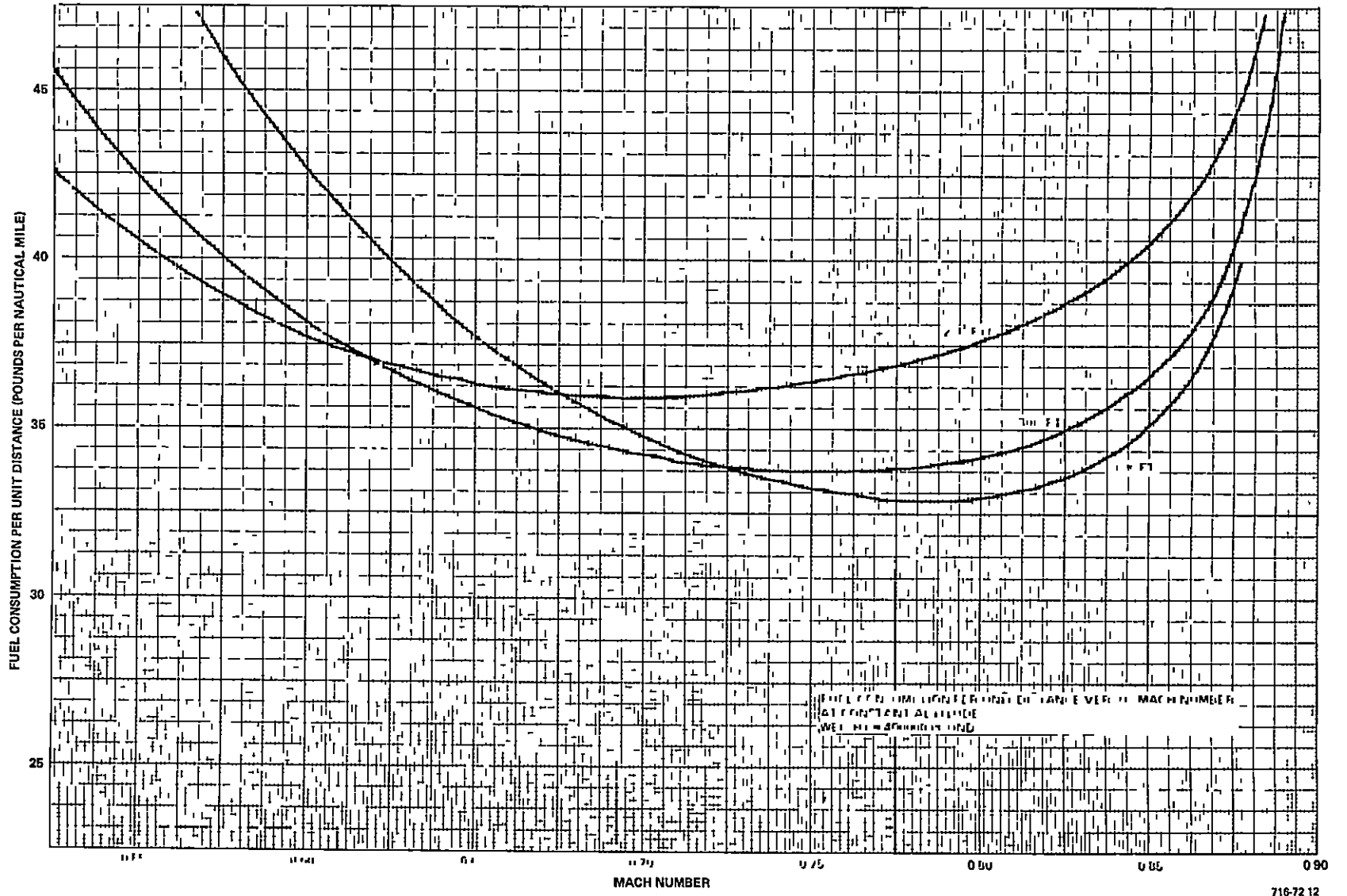


Figure 4-6

## B. BASELINE FLIGHT: LAS VEGAS TO LOS ANGELES

Figure 4-7 shows the baseline lateral profile in terms of the longitude and latitude. The flight follows the lateral profile for a Citrus Three arrival at Los Angeles. Points of particular interest during the flight are indicated on the figure. The initial heading is due west (true). At 1,500 feet above ground level, a heading of 165 degrees (180 degrees true) is flown in order to intercept the 32 degree (47 degrees true) radial from Hector. The rest of the flight follows the lateral flight plan given in Section III.

Figure 4-8 shows the barometric altitude versus the range for the baseline climb-out from Las Vegas. Climb-out procedure is given in Section III. The flattening of the profile at about 5,000 and 10,000 feet is due to holding the vertical speed at about 600 feet per minute while the calibrated airspeed increases. The value of  $V_2$  shown in the figure is dependent on the weight and flap position. For this flight, the initial weight is 324,900 pounds, the initial flap setting is 10 degrees, and the value of  $V_2$  is about 150 knots. A cruise altitude of 24,000 feet MSL is reached approximately 62 nautical miles into the flight.

Figure 4-9 shows the barometric altitude versus the range for the baseline descent into Los Angeles. The point of descent is reached about 138 miles into the flight. Since the cruise airspeed is 360 knots, the aircraft must maintain altitude with retarded throttles in order to slow down to 340 knots specified by the descent procedure given in Section III. The flattening of the curve at 12,000 feet is due to holding a descent rate of 800 feet per minute while the aircraft slows to 250 knots. Approach altitude is reached at 207 nautical miles and glide slope is captured about 4 miles later. The aircraft lands at Los Angeles with a total range of 222 nautical miles.

Figures 4-10 and 4-11 show the calibrated airspeed versus the range for climb-out and descent, respectively. The two flat regions during climb-out are when 250 and 290 knots are being held on pitch. At 62 miles, cruise altitude is reached and the aircraft increases airspeed to about 360 knots, corresponding to a Mach of .83. Similar flat regions during the descent are

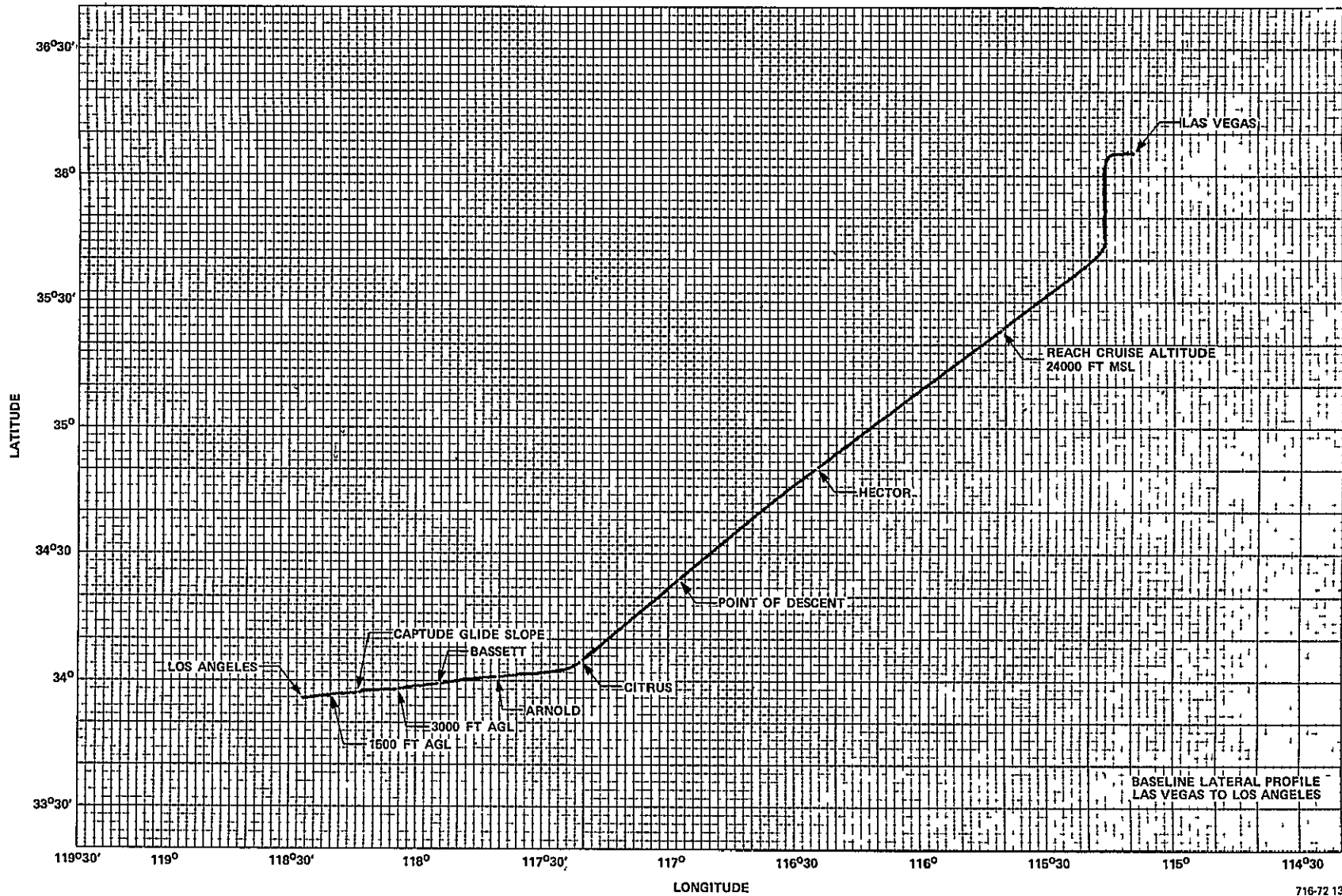


Figure 4-7

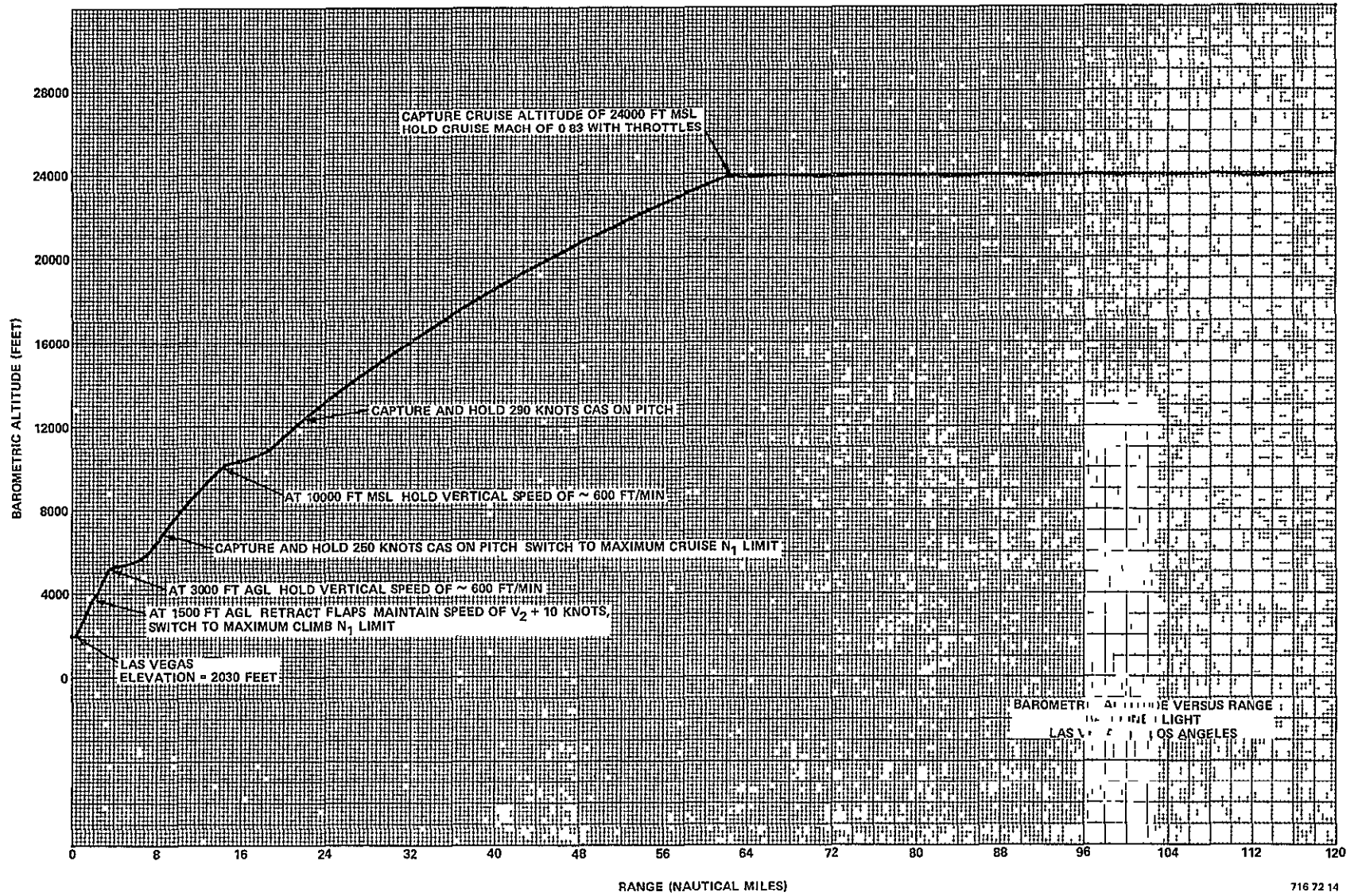


Figure 4-8



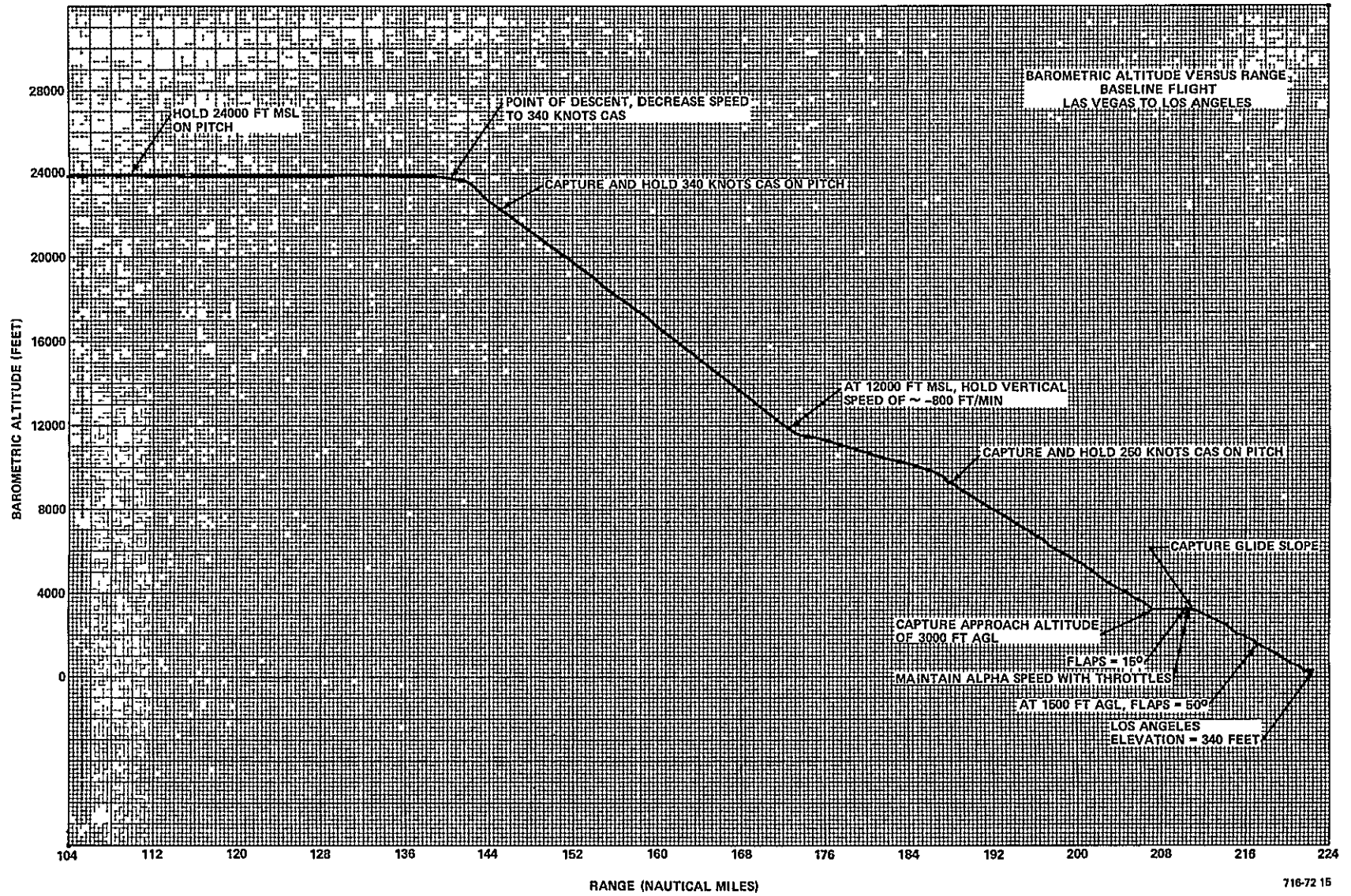


Figure 4-9

ORIGINAL PAGE IS  
OF POOR QUALITY

11-7

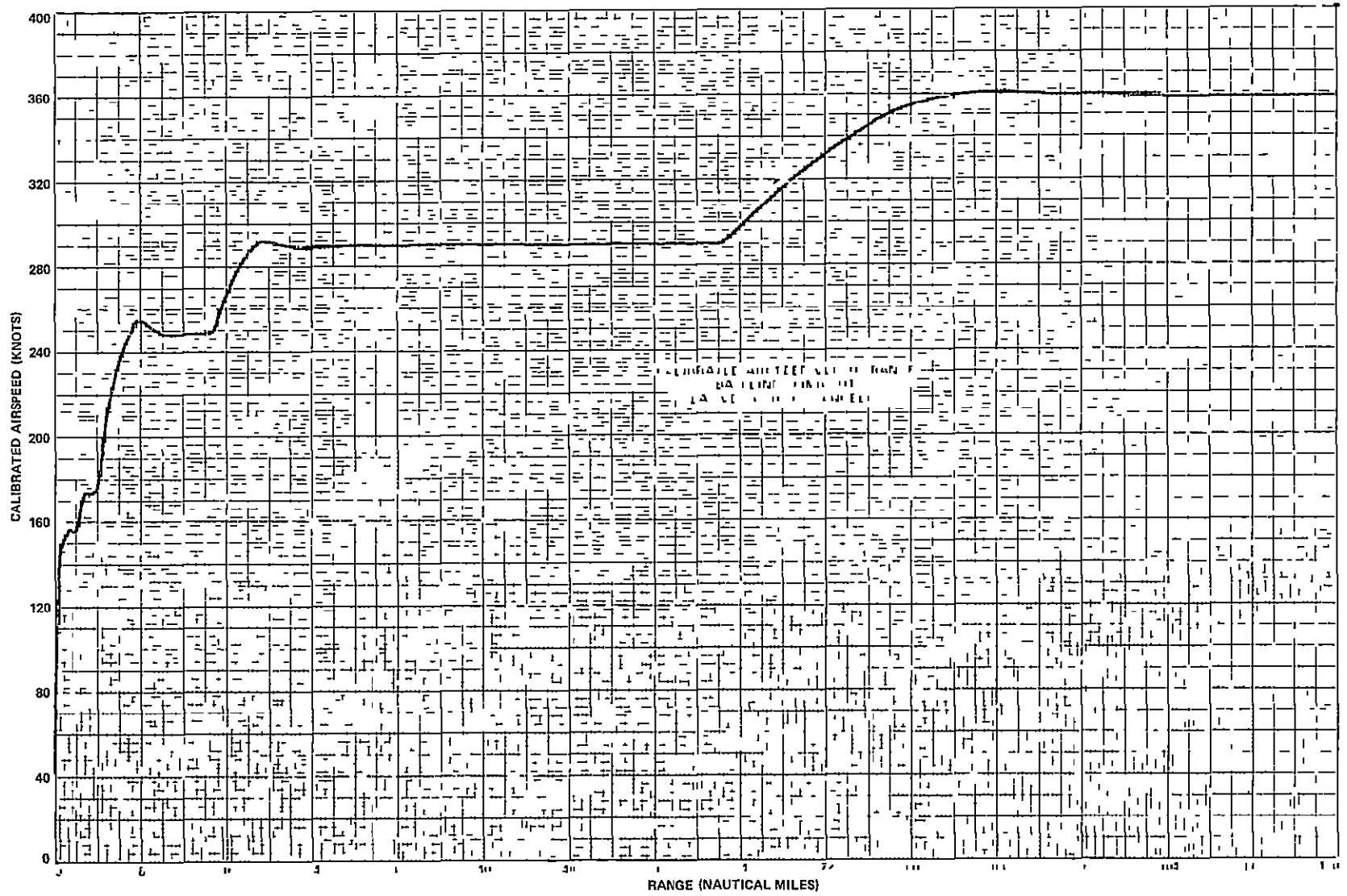


Figure 4-10



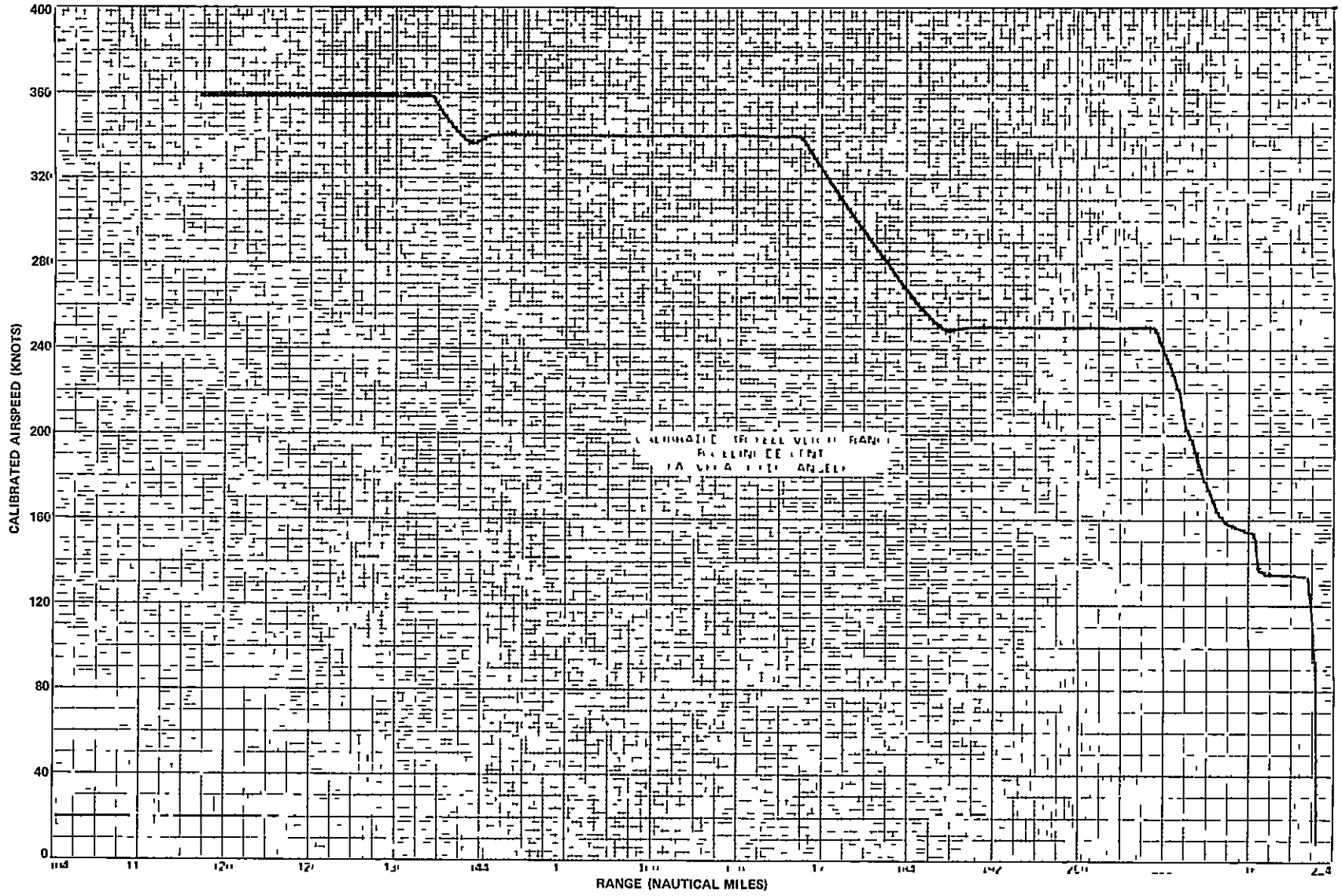


Figure 4-11

due to holding 340 and 250 knots on pitch. The aircraft slows to the approach speed while holding altitude before capturing the glide slope.

Figures 4-12 and 4-13 show the Mach number versus the range for both the climb-out and descent. For a constant airspeed, the Mach number increases with altitude. This is the reason for the near-linear sloping regions during climb-out and descent corresponding to the regions where the calibrated airspeed is being held on pitch.

The flight path angle versus the range during climb-out is shown in Figure 4-14. It should be noted that the scale is somewhat exaggerated, the full width of the plot being only 10 degrees. The depressions centered around 5 miles and 16 miles are due to the autopilot holding a vertical speed of about 600 feet per minute in order to increase the airspeed to 250 and 290 knots, respectively. Sloping regions following the depressions occur when the calibrated airspeed is being held on pitch. About 62 miles into the flight, the cruise altitude is captured and the flight path angle goes to zero.

Figure 4-15 shows the flight path angle versus the range for the descent into Los Angeles. After the point of descent, the autopilot holds 340 knots CAS on pitch. The flight path angle decreases to -3.5 degrees and is relatively constant between 145 and 172 miles. One hundred seventy-four miles into the flight, the autopilot begins to slow the aircraft to 250 knots by increasing the flight path angle. The autopilot captures CAS at 188 miles and the flight path angle again decreases. Approach altitude is reached at 207 miles and the flight path angle goes to zero. Spikes at 210, 211, and 216.5 miles are due to the flaps being deployed to 15, 22, and 50 degrees, respectively. At 211 miles, the glide slope is captured and the flight path angle drops to the nominal value of -2.7 degrees.

Fuel consumption per unit distance,  $F_D$ , for the climb-out versus the range is shown in Figure 4-16. During the take-off ground roll and the initial climb-out,  $F_D$  is high because the throttles are against the  $N_1$  limit and the airspeed is relatively low. The value of  $F_D$  decreases as the speed picks up on climb-out. At 1,500 feet AGL, the flaps are retracted and less

ORIGINAL PAGE IS  
OF POOR QUALITY

4-14

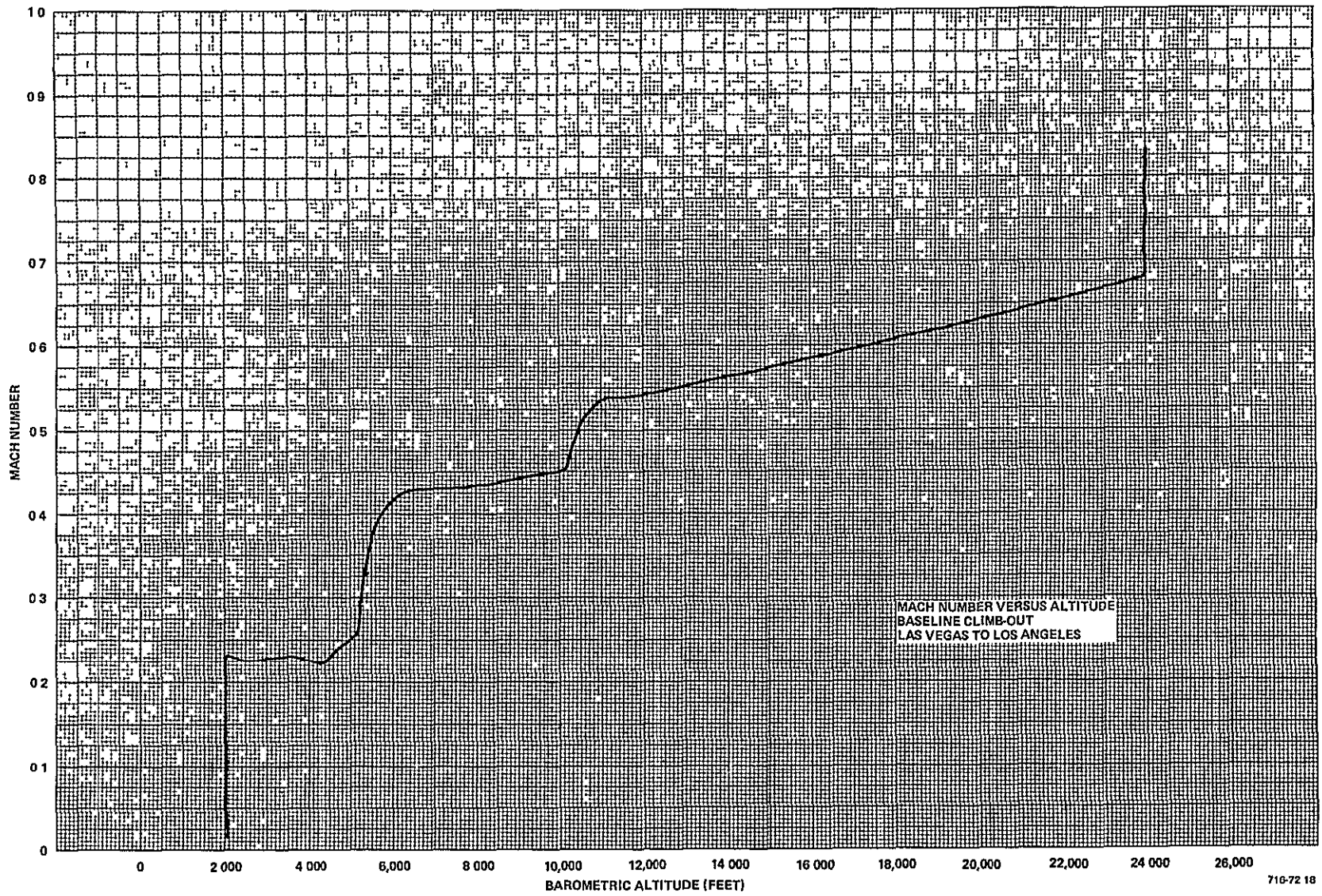


Figure 4-12

ORIGINAL PAGE IS  
OF POOR QUALITY

4-15

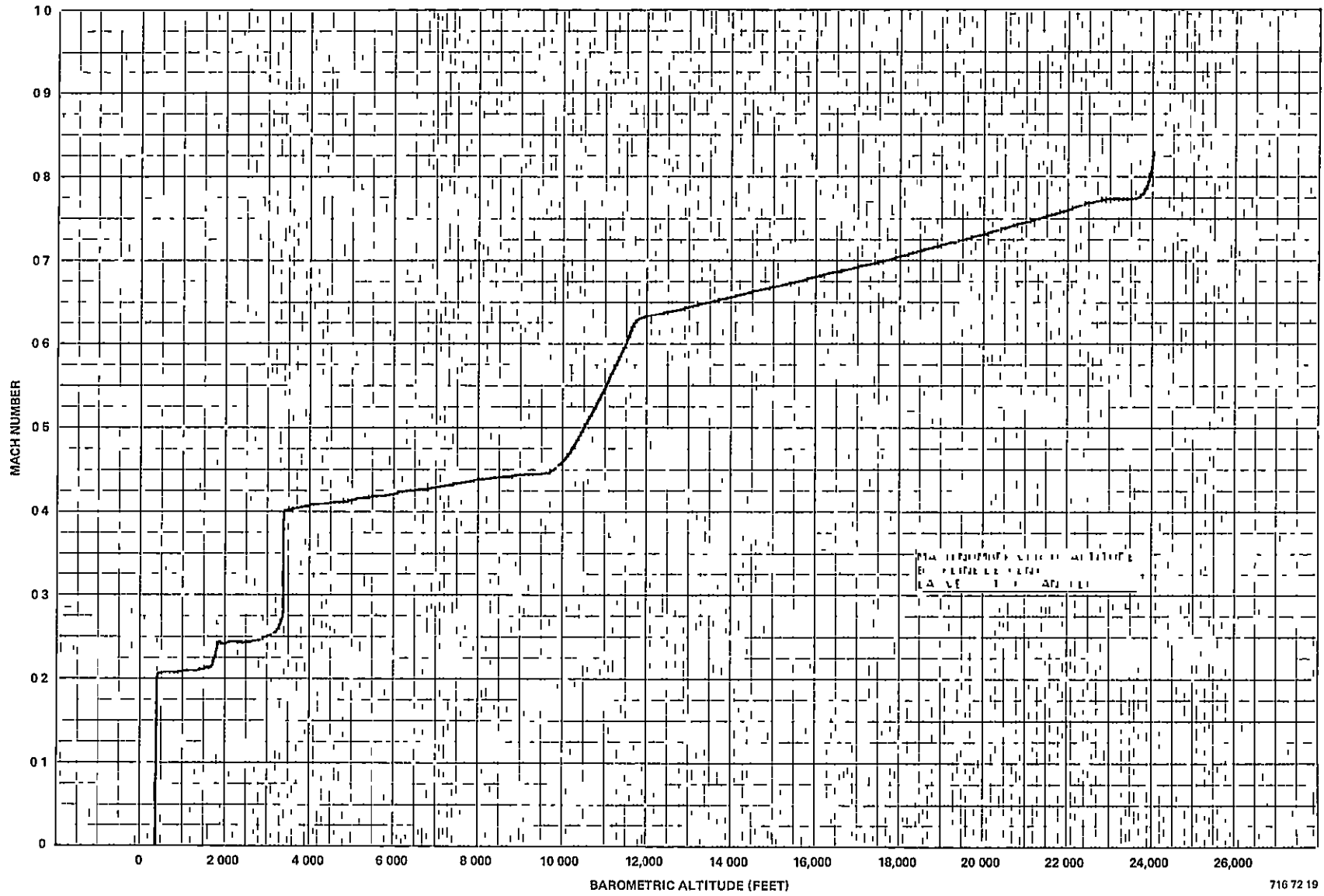


Figure 4-13

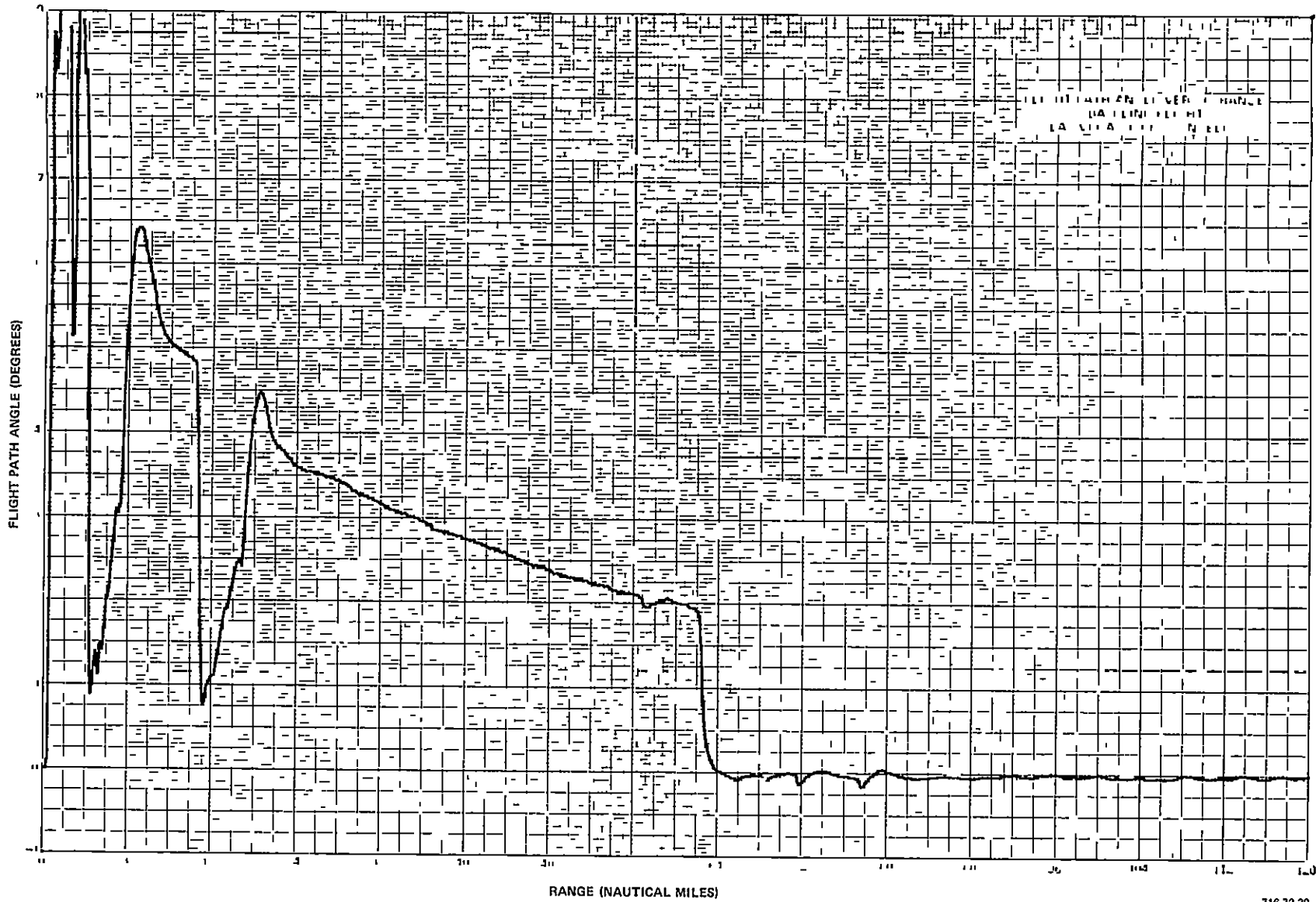


Figure 4-14

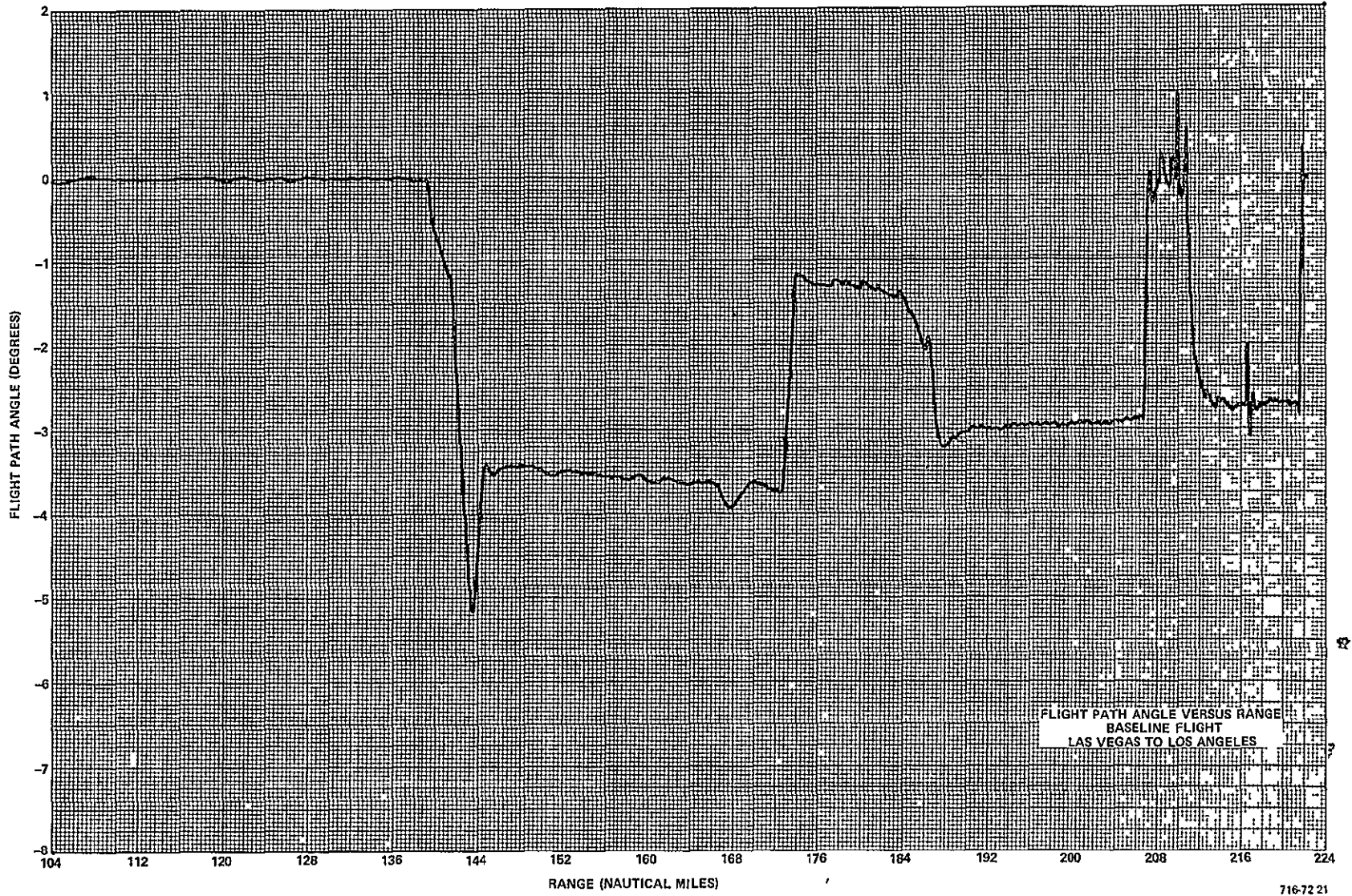


Figure 4-15



ORIGINAL PAGE IS  
OF POOR QUALITY

4-18

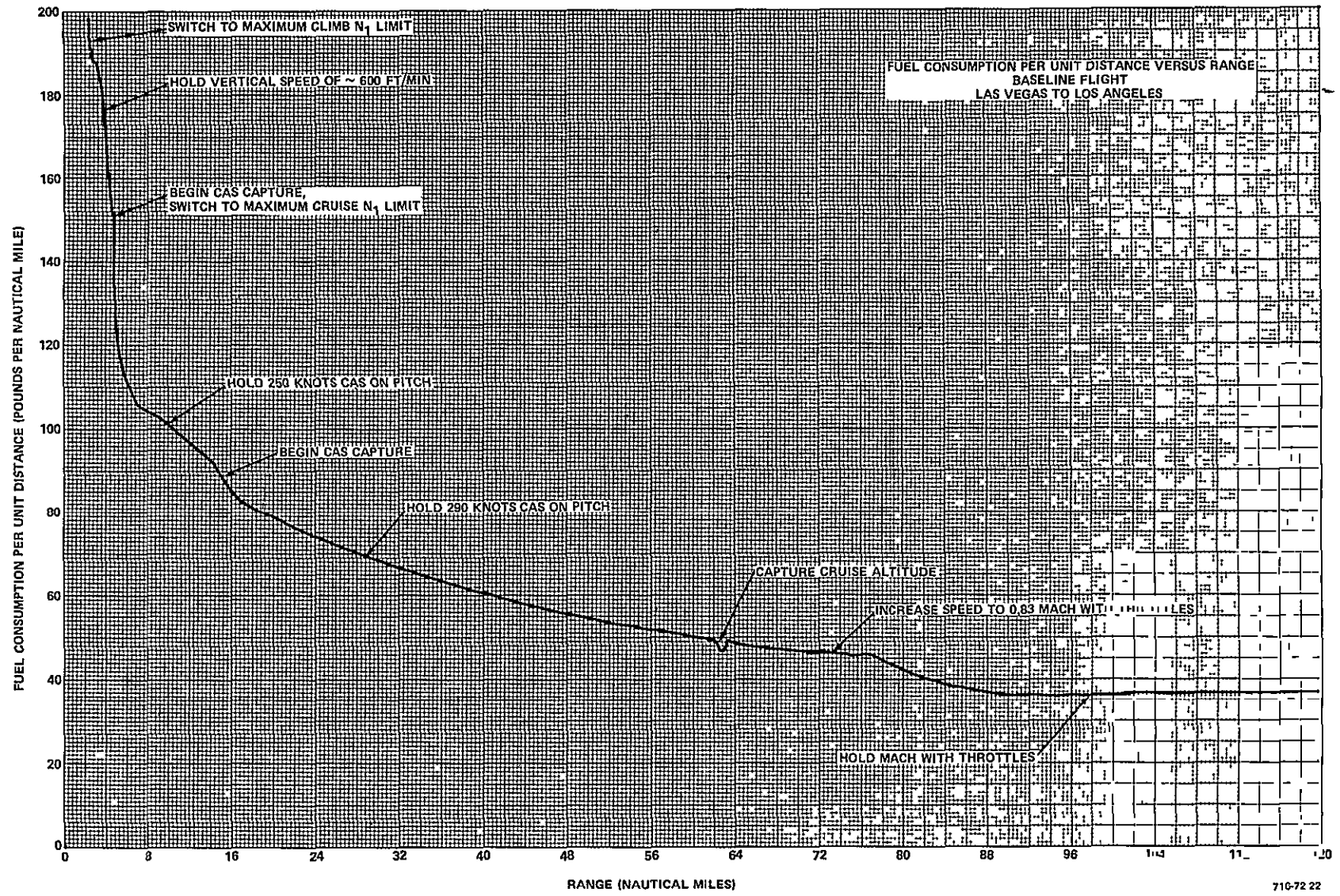


Figure 4-16

fuel is required to maintain an airspeed of  $V_2 + 10$  knots. The throttles are also set for the maximum climb  $N_1$  limit and are pulled back slightly. At 3,000 feet AGL, a vertical speed of about 600 feet per minute is held while the aircraft speed increases to 250 knots; the throttles are set to the maximum cruise  $N_1$  limit. The airspeed overshoots so the aircraft must pitch up slightly to slow back to speed. This causes  $F_D$  to level off at a range of about 8 miles. The 250 knot airspeed is held while the altitude increases, which causes the groundspeed to increase and  $F_D$  to decrease. At 10,000 feet MSL, the aircraft goes through the second vertical speed hold maneuver to increase the airspeed to 290 knots. Once the aircraft captures airspeed,  $F_D$  steadily decreases with increasing groundspeed. At a range of 62 miles, the cruise altitude is captured and the throttles are used to hold the cruise Mach of .83. This requires the throttles to stay against the  $N_1$  limit until 77 miles into the flight.

Figure 4-17 shows  $F_D$  versus the range for the descent. At the point of descent, the throttles are retarded and  $F_D$  drops to 5 pounds per nautical mile. An airspeed of 340 knots is then held while the altitude decreases. The groundspeed therefore decreases and  $F_D$  begins to rise. At 12,000 feet MSL the aircraft goes through the slow down maneuver until the airspeed reaches 250 knots. This airspeed is then held on pitch and  $F_D$  continues to rise. The approach altitude is captured at 207 miles and the airspeed begins to drop rapidly. At approximately 190 knots, the flaps are deployed to 15 degrees and the aircraft slows even more rapidly. The autothrottle is set to hold the initial approach speed and tries to reduce the deceleration rate by pushing the throttles forward. This causes  $F_D$  to rise slightly at 210.5 miles. As the rate of deceleration decreases, the throttles are pulled back again and  $F_D$  correspondingly drops. Glide slope is captured at 211 miles and the flaps are deployed to 22 degrees. Again, the throttles are increased to compensate for the sudden deceleration, then decreased shortly thereafter. At 213 miles, the throttles increase to maintain the approach speed. The flaps are deployed to 50 degrees at 1,500 feet AGL and the throttles must increase tremendously to compensate for the extra drag;  $F_D$  increases accordingly. Just prior to touchdown, the throttles are retarded and  $F_D$  drops sharply. The value of  $F_D$  then increases again as the groundspeed decreases during ground roll.



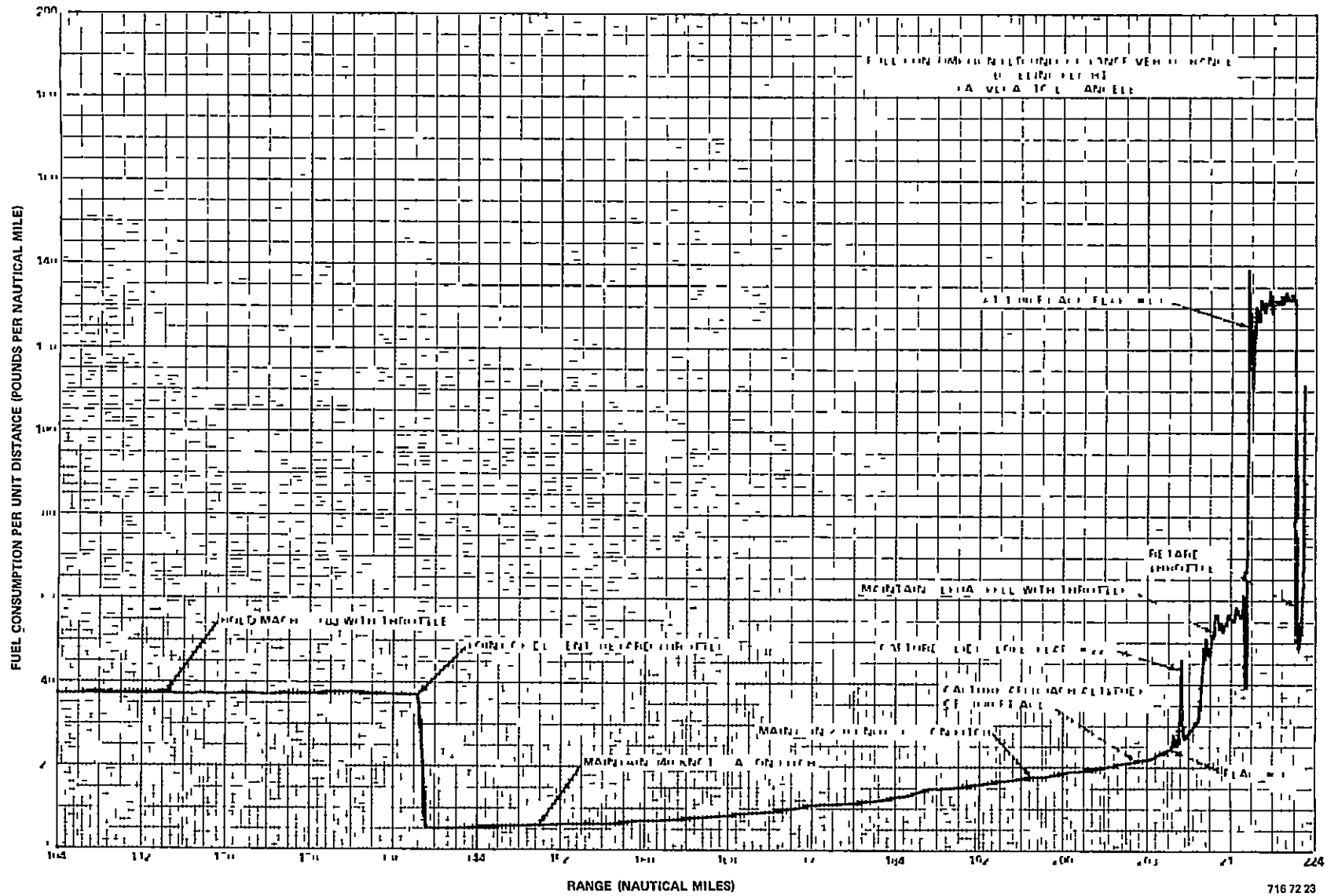


Figure 4-17

Figures 4-18 and 4-19 show the amount of fuel consumed versus the range for the climb-out and descent. These figures represent the integrals of Figures 4-16 and 4-17. The fuel consumption is obviously highest during take-off; thus, the slope of Figure 4-18 is greatest during this segment of the flight. At the midpoint of the flight, or 111 miles, 7,320 pounds of the total 10,075 pounds of fuel have already been consumed. In Figure 4-19, the slope drops drastically at the point of descent when the throttles are retarded. The visible slope increase at 217 miles is due to the 50 degree flap deployment and the resultant sharp increase in  $F_D$ .

A summary of the results of several baseline flights from Las Vegas to Los Angeles is given in Table 4-1. Fuel consumption ranged from a minimum of 10,067 pounds to a maximum of 10,075 pounds, displaying an average value of 10,072 pounds with a standard deviation of 3.4 pounds. The average  $F_D$  was 45.25 pounds per nautical mile with a standard deviation of .01; average flight time was 39 minutes. Since an airborne hardware simulator and a data adapter are being used, and since the simulation and airborne computers are asynchronous, a slight deviation in the data is expected.

TABLE 4-1  
BASELINE FLIGHT DATA

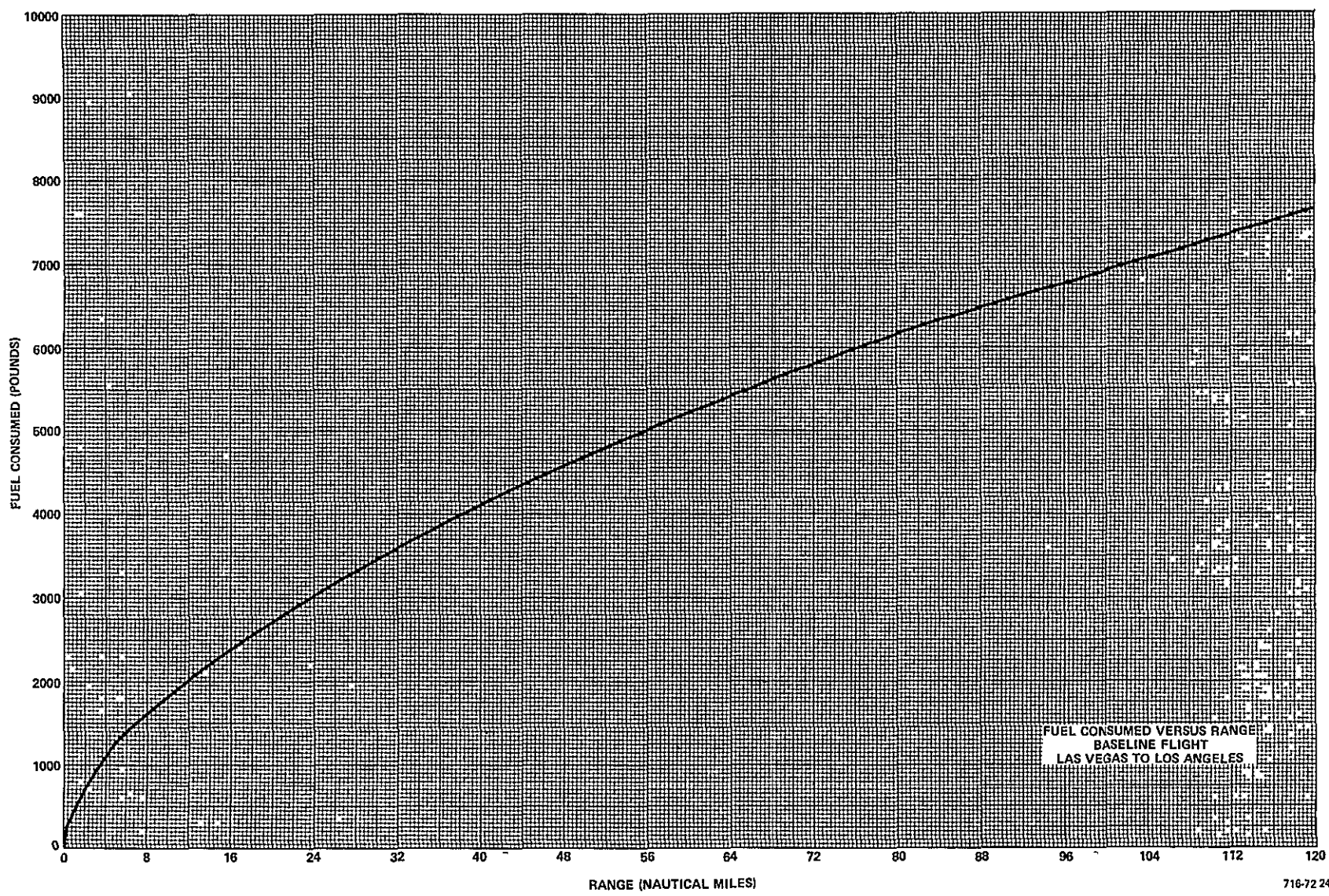
Flight No.	Fuel Consumed (pounds)	$F_D$ (lb/nmi)	Time (min, sec)
1	10,067	45.23	38, 59
2	10,073	45.25	39, 2
3	10,075	45.26	38, 59
4	10,072	45.25	38, 59
Averages	10,072	45.25	39, 0

#### C. DELAYED FLAP APPROACH DEVELOPMENT

Figures 4-20 through 4-24 show the fuel flow per unit distance,  $F_D$ , versus the Mach number for various altitudes at five different flap settings. The flap settings are those typically used during a flight; they are 0, 10, 22, 35 and 50 degrees. The weight of the aircraft is 300,000 pounds and the flight path angle, gamma, is zero.

ORIGINAL PAGE IS  
OF POOR QUALITY

4-22



716-72 24

Figure 4-18

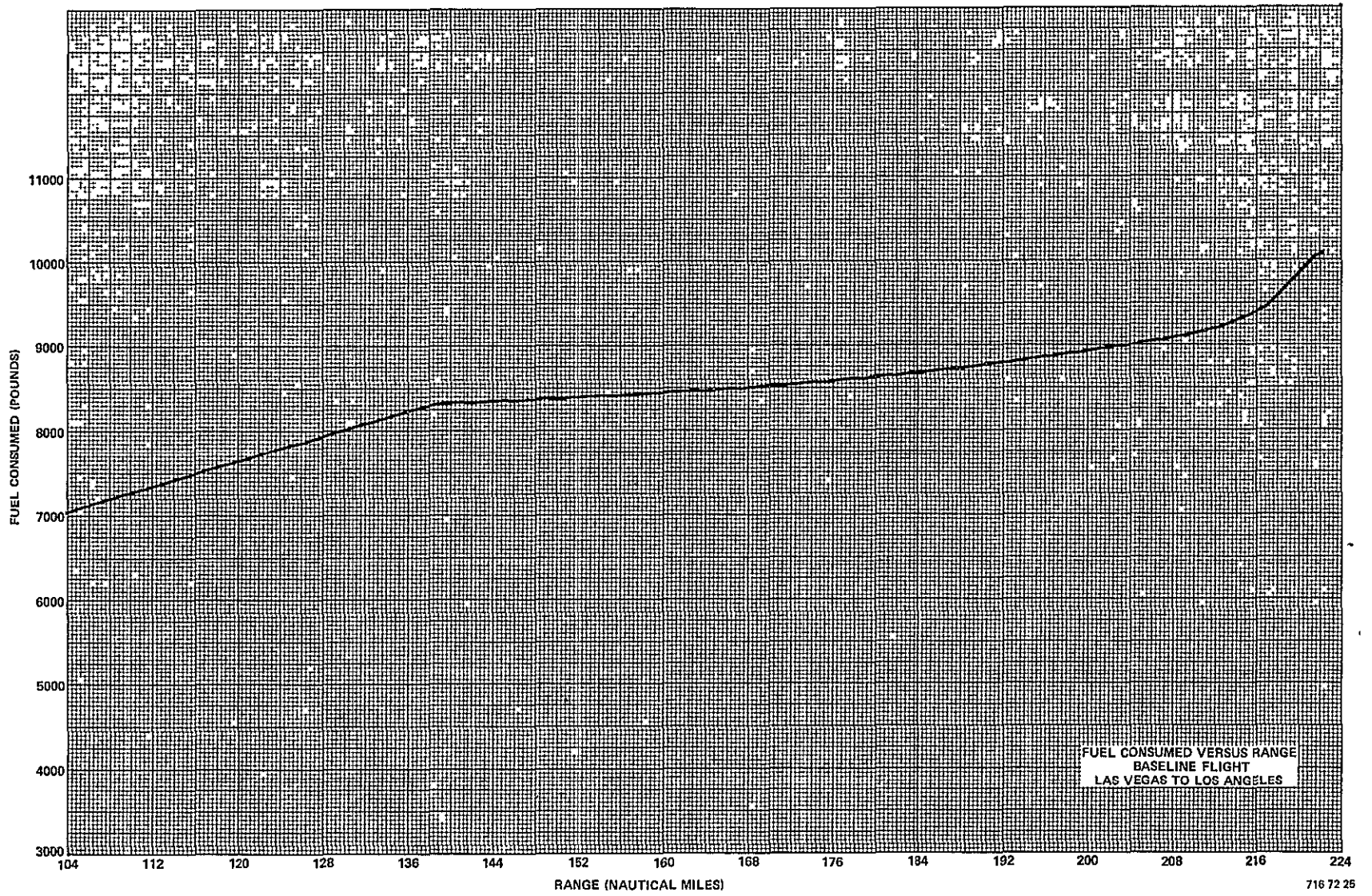


Figure 4-19

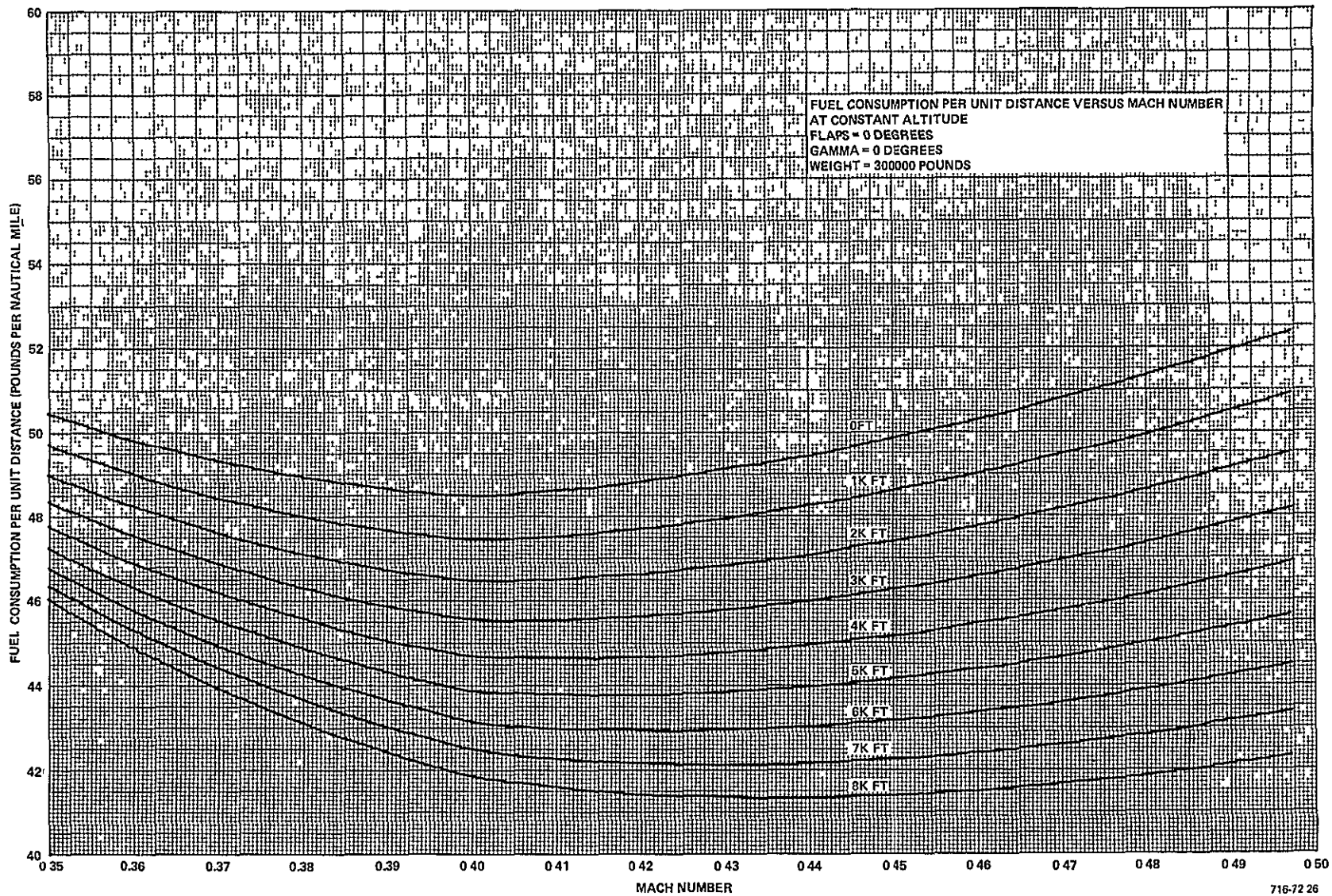


Figure 4-20

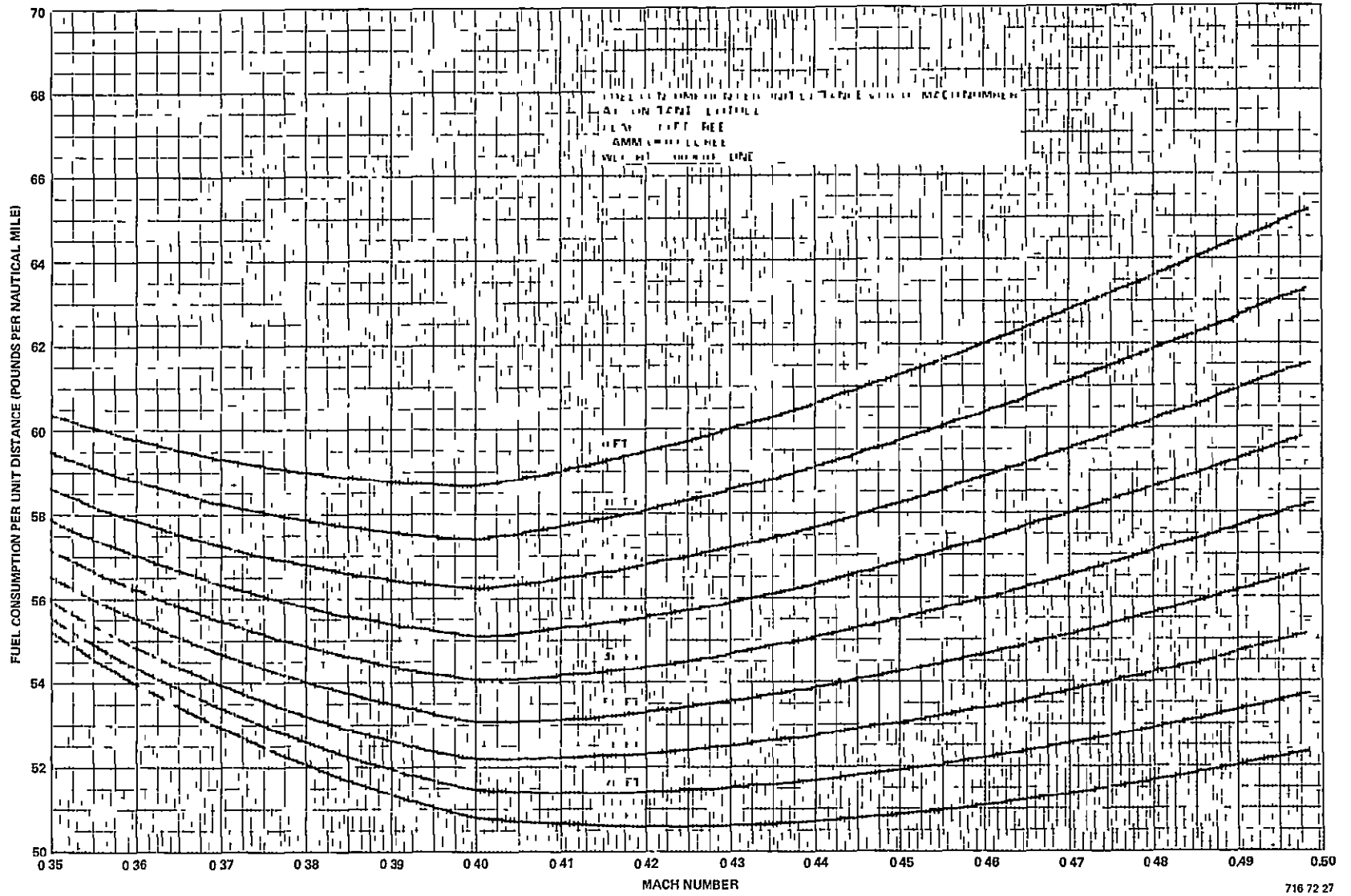


Figure 4-21



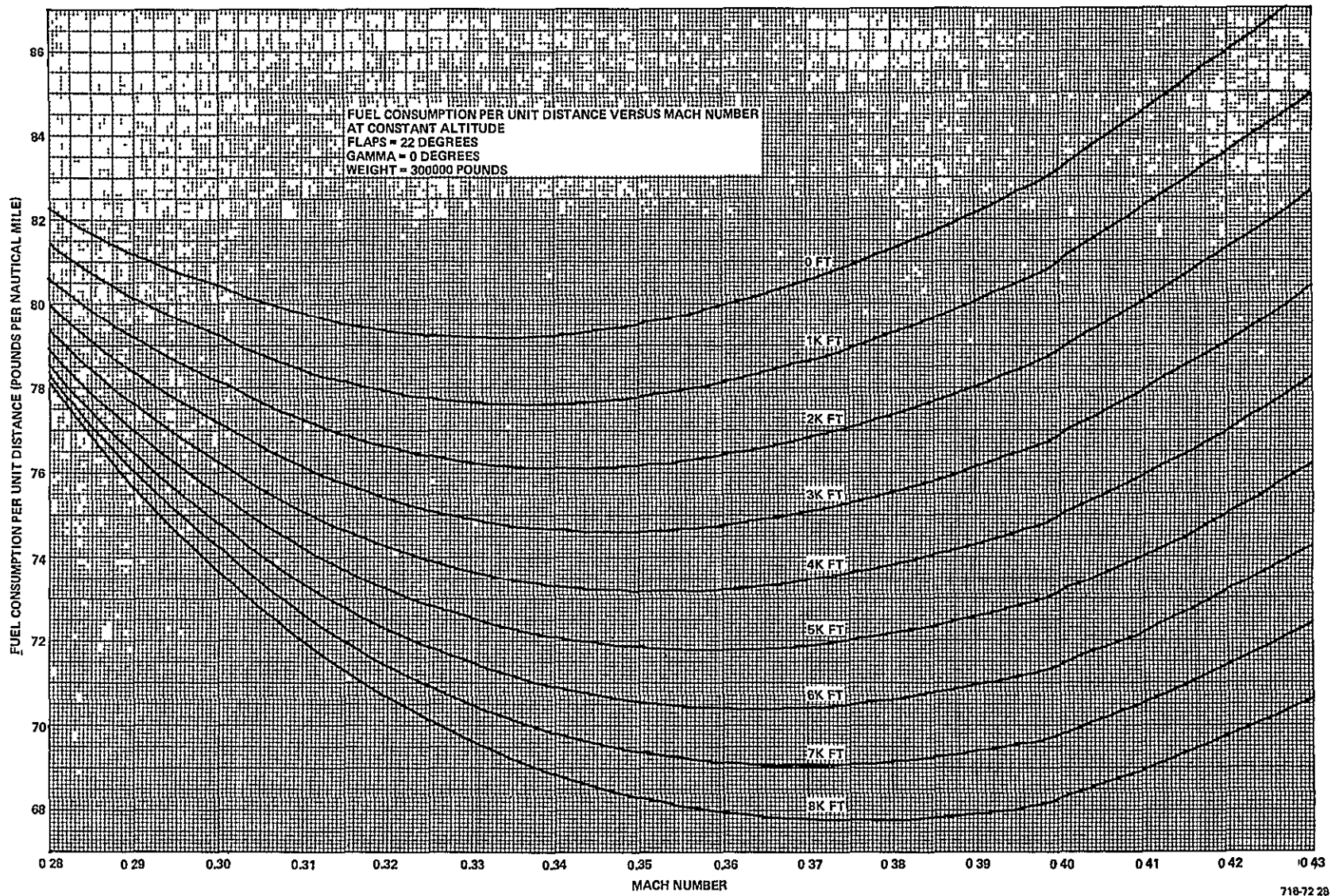
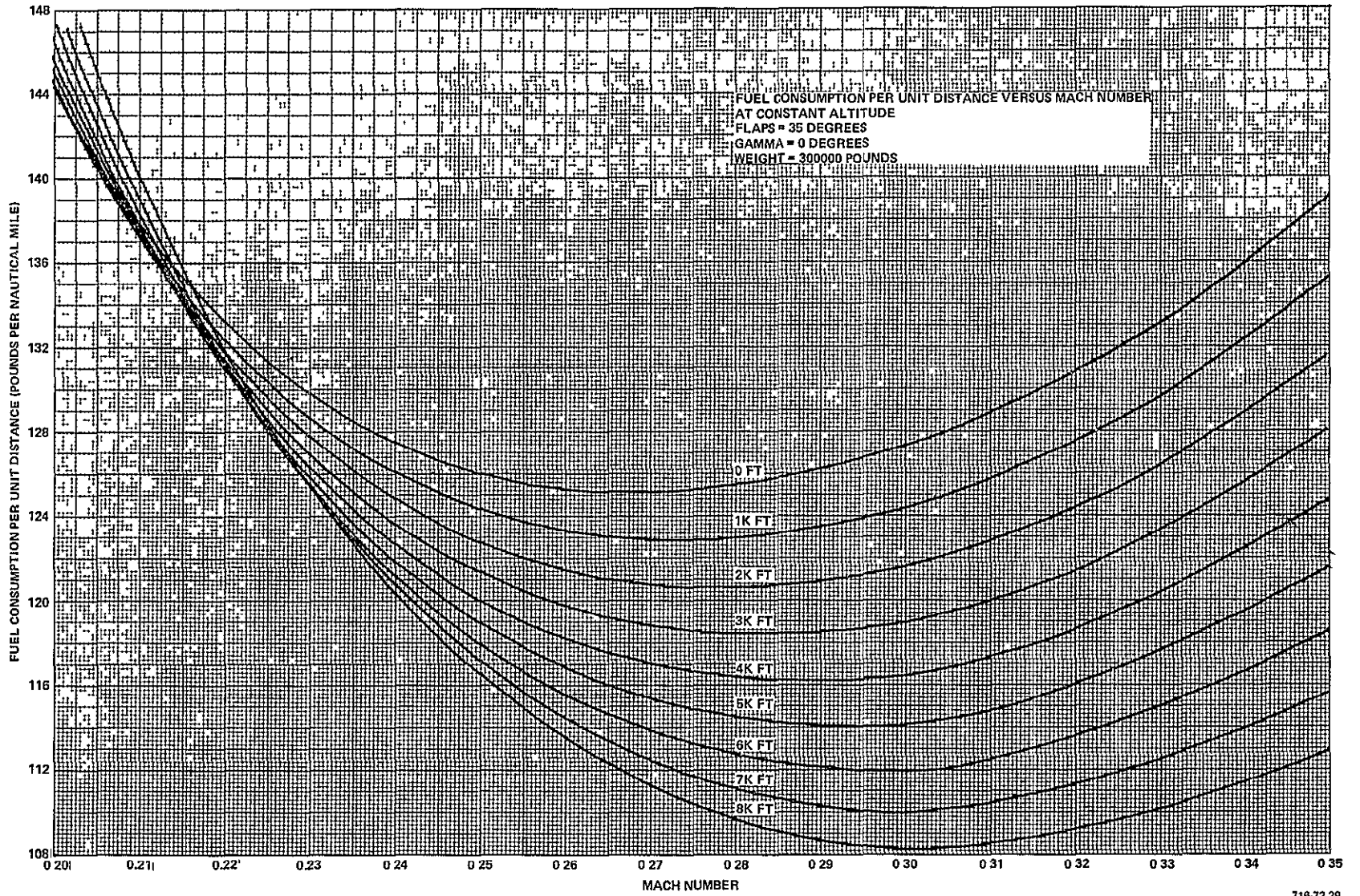


Figure 4-22

ORIGINAL PAGE IS  
OF POOR QUALITY

4-27



718-72 29

Figure 4-23



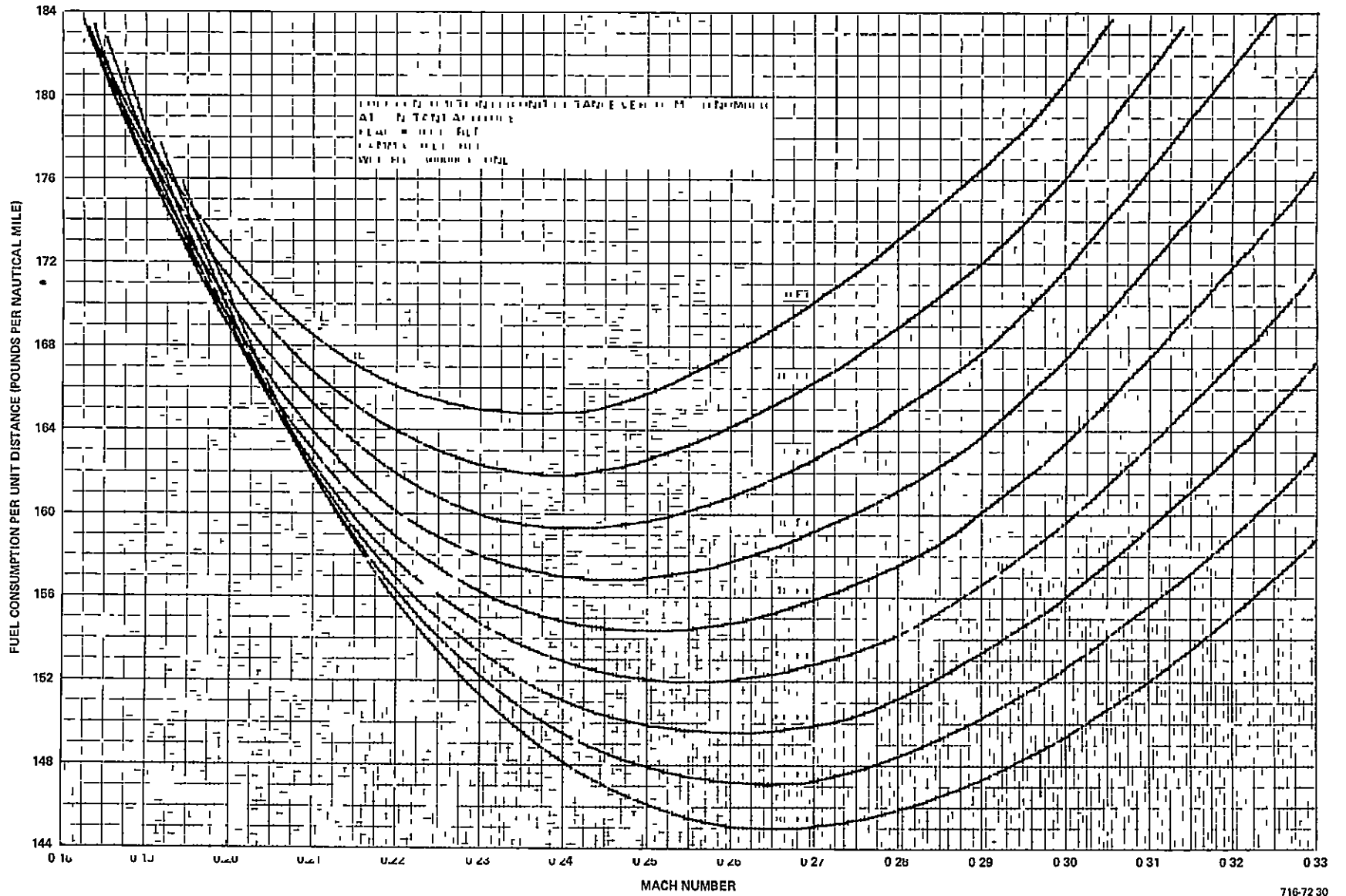


Figure 4-24

Obviously, increasing the amount of flaps increases the value of  $F_D$  as there is much more drag on the aircraft. The optimal Mach number, however, decreases with increased flaps. For instance, at 3,000 feet and zero flaps the optimal Mach number is about .405, while with 50 degrees of flaps the optimal Mach number is only .245.

It is interesting to note that as the amount of flaps increases, the  $F_D$  curves become steeper so that the minimums become more critically defined. This suggests that the approach speed becomes an important factor in the conservation of fuel when the flaps have been deployed. As an example, a .02 decrease in Mach number from the optimal at 3,000 feet causes  $F_D$  to increase by only .6 pound per nautical mile with zero flaps, while the same decrease in Mach number causes a 2 pound per nautical mile increase in  $F_D$  with 50 degrees of flaps.

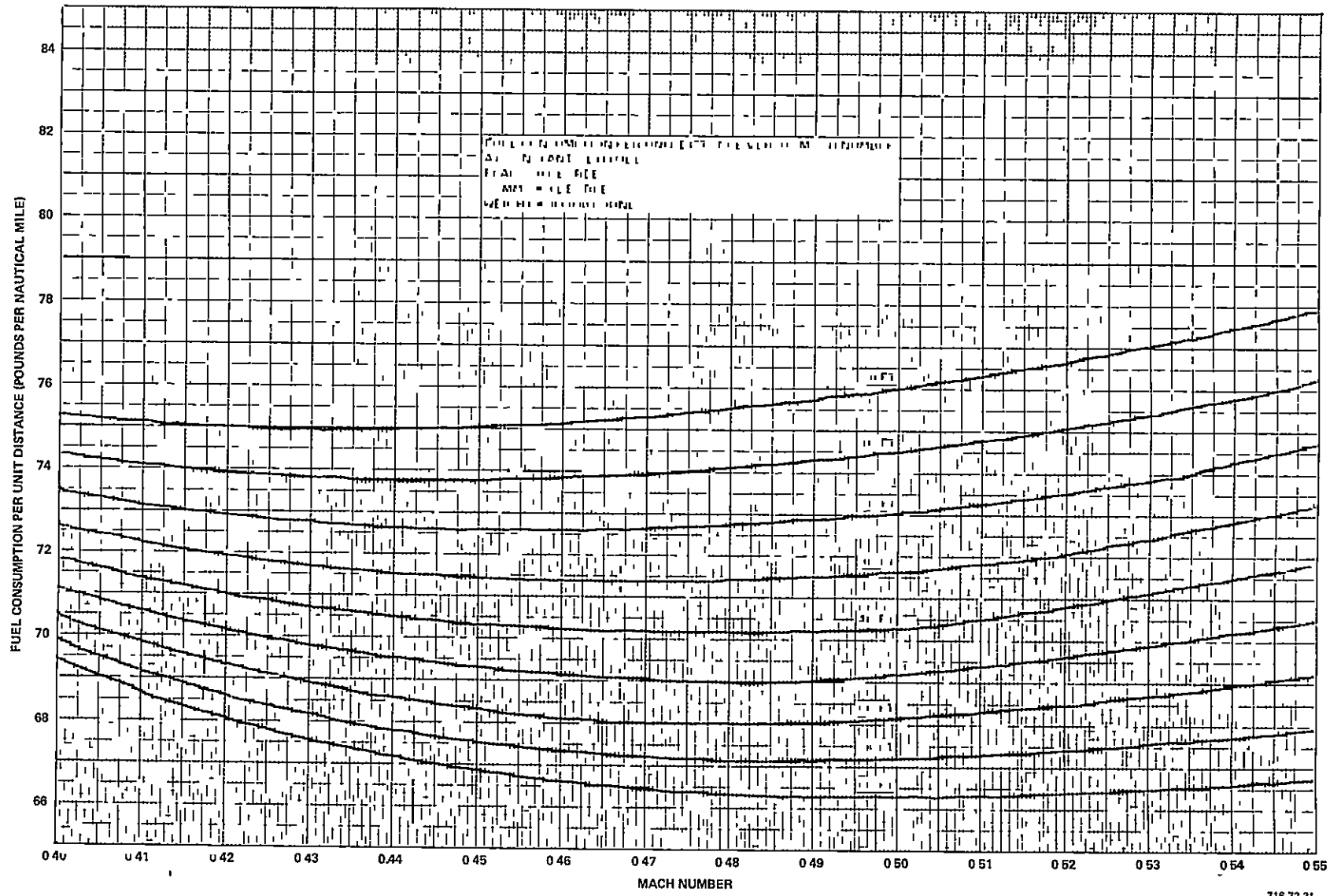
Figures 4-25 and 4-26 show  $F_D$  versus the Mach number for flap settings of 0 and 10 degrees, respectively, with a flight path angle of positive 3 degrees. As expected, the value of  $F_D$  increases with the higher gamma. Comparison of Figures 4-20 and 4-25 shows the optimal Mach number increases with increasing gamma. The increased gamma also tends to flatten the curves, suggesting that the higher the flight path angle, the less critical the Mach number for the conservation of fuel.

Figures 4-27 and 4-28 show  $F_D$  versus the Mach number for flap settings of 35 and 50 degrees, respectively, with a flight path angle of -2.75 degrees. The effects are just opposite those due to a positive gamma. Both the value of  $F_D$  and the optimal Mach number decrease with decreasing gamma. The relative steepness of the curves, however, does not appear to be greatly affected by a negative flight path angle, although the curves do exhibit some steepening.

Figure 4-29 shows the flight path angle versus the calibrated airspeed with retarded throttles at various flap settings. The altitude at which these curves were generated was 3,000 feet mean sea level while the aircraft weight was 300,000 pounds. Of the five different flap settings used, only zero degrees appears capable of equilibrium on a typical glide slope angle.

ORIGINAL PAGE IS  
OF POOR QUALITY

4-30

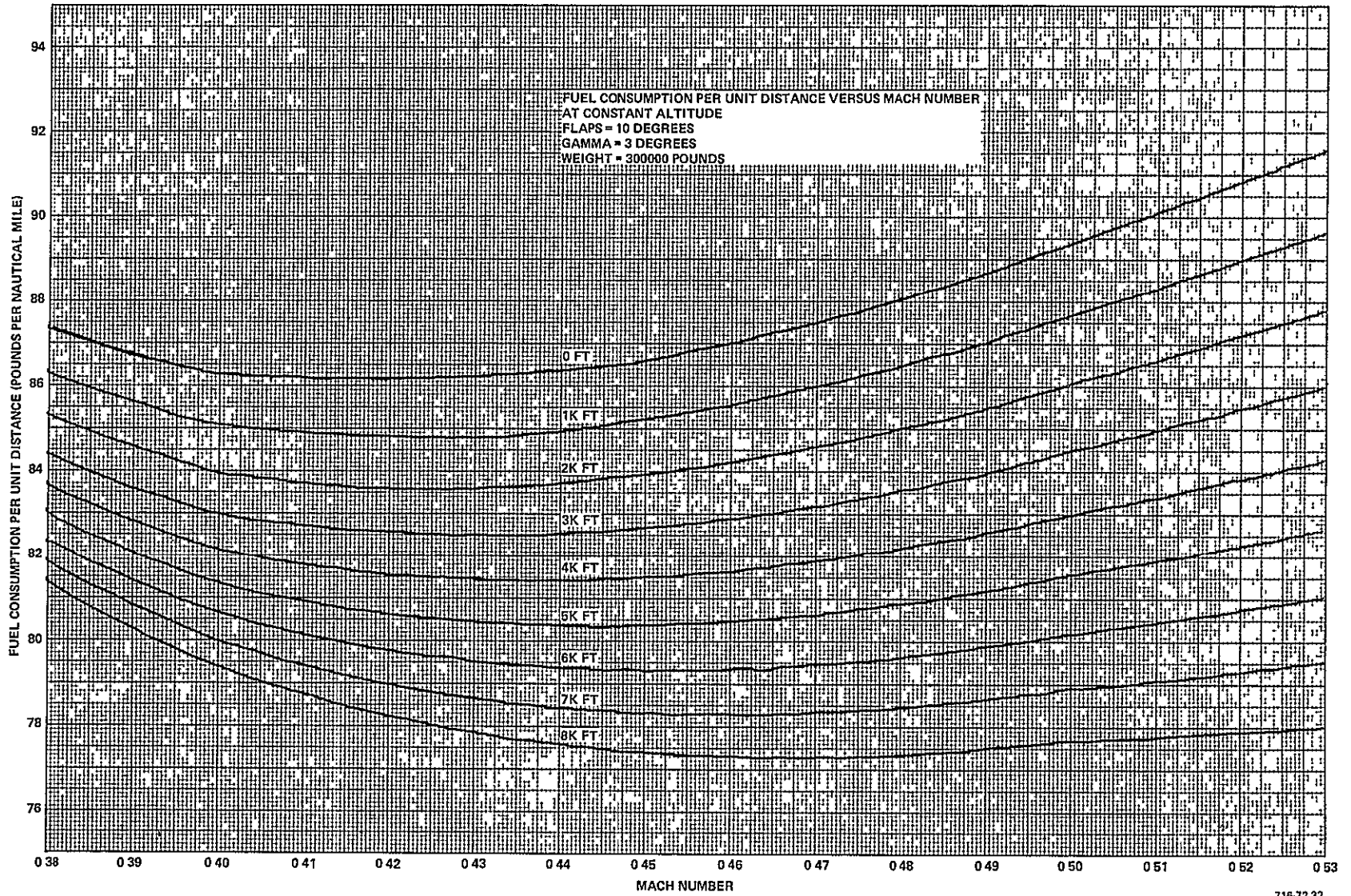


716 72 31

Figure 4-25

ORIGINAL PAGE IS  
OF POOR QUALITY

4-31



716-72 32

Figure 4-26

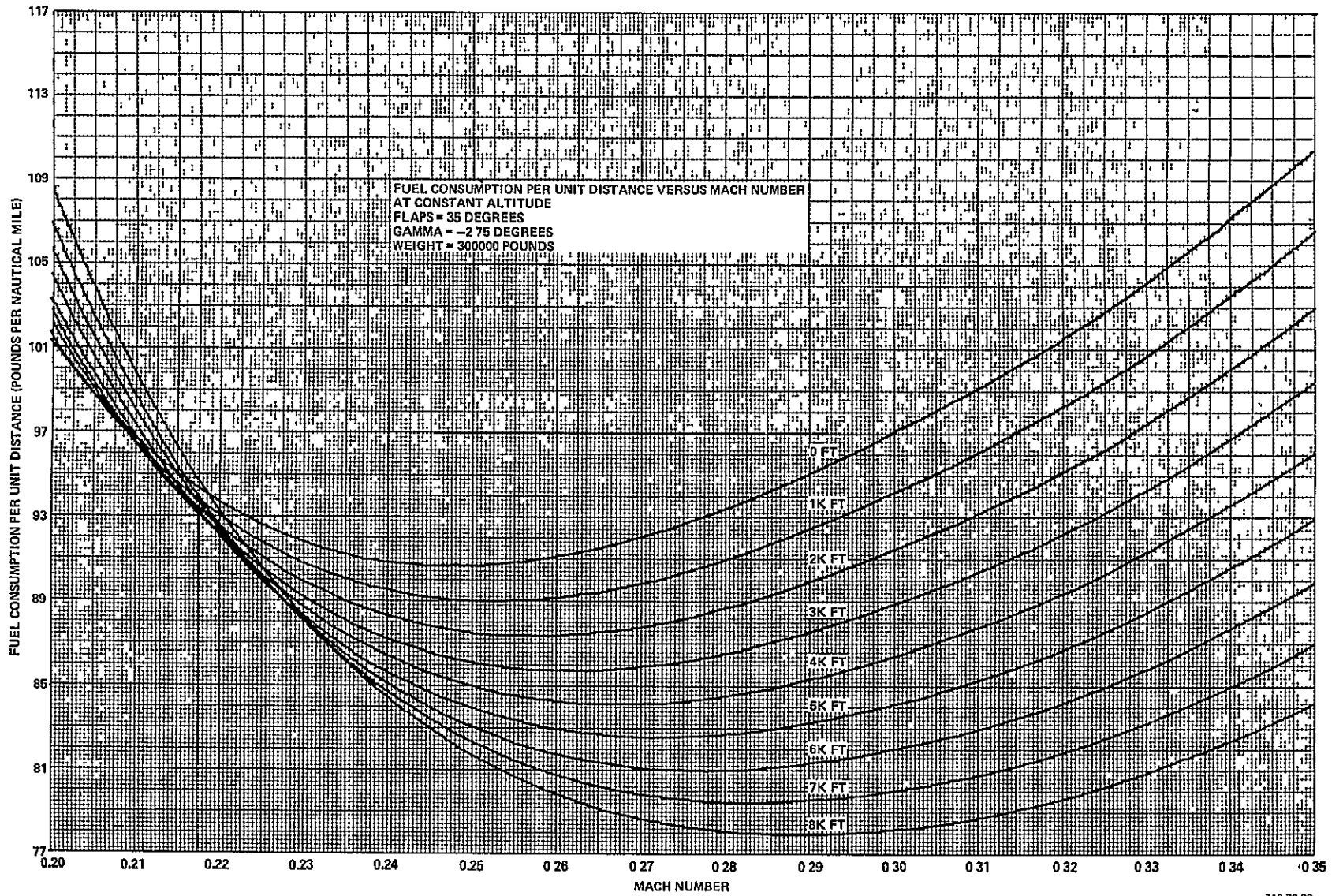


Figure 4-27

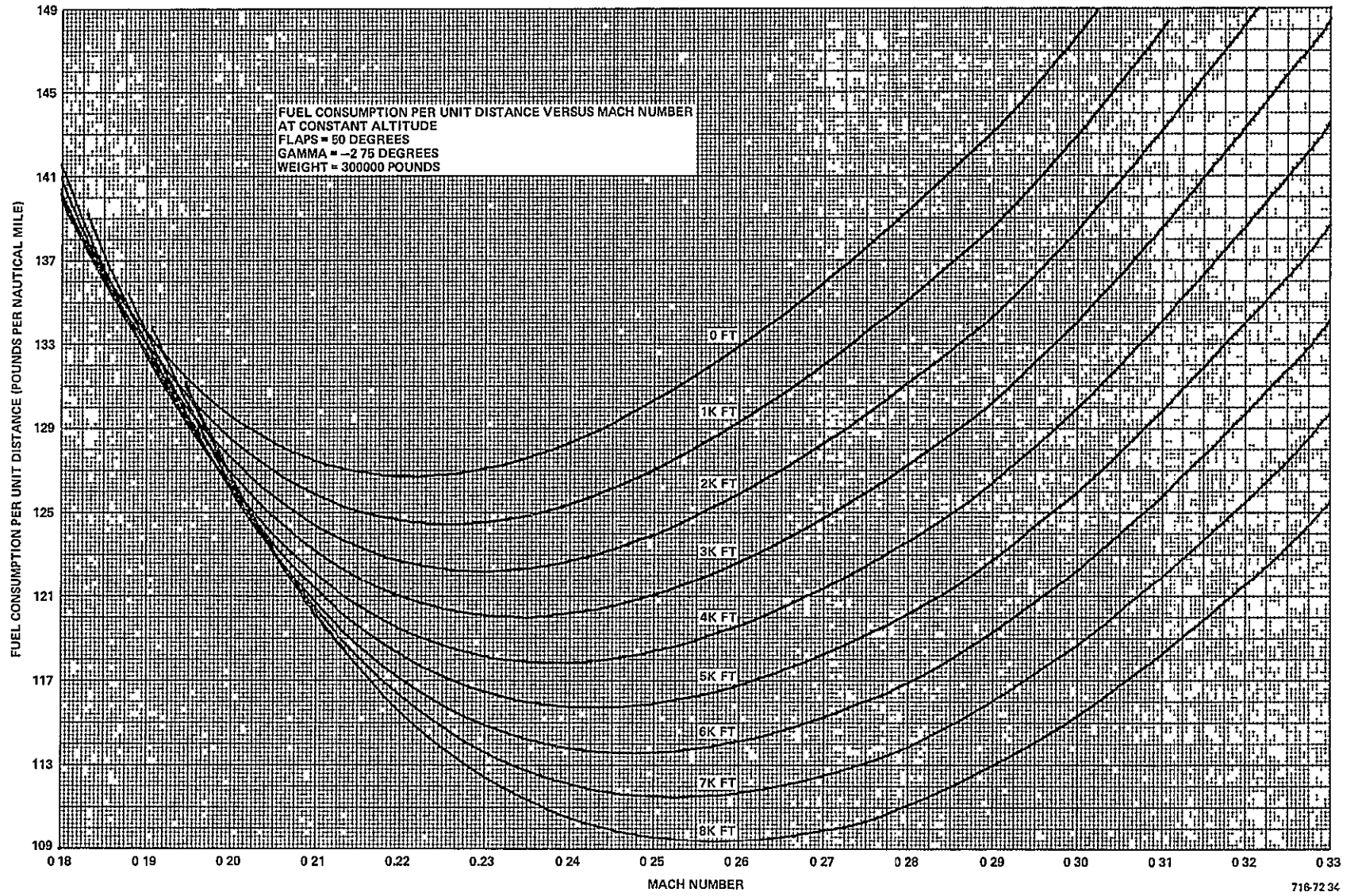


Figure 4-28



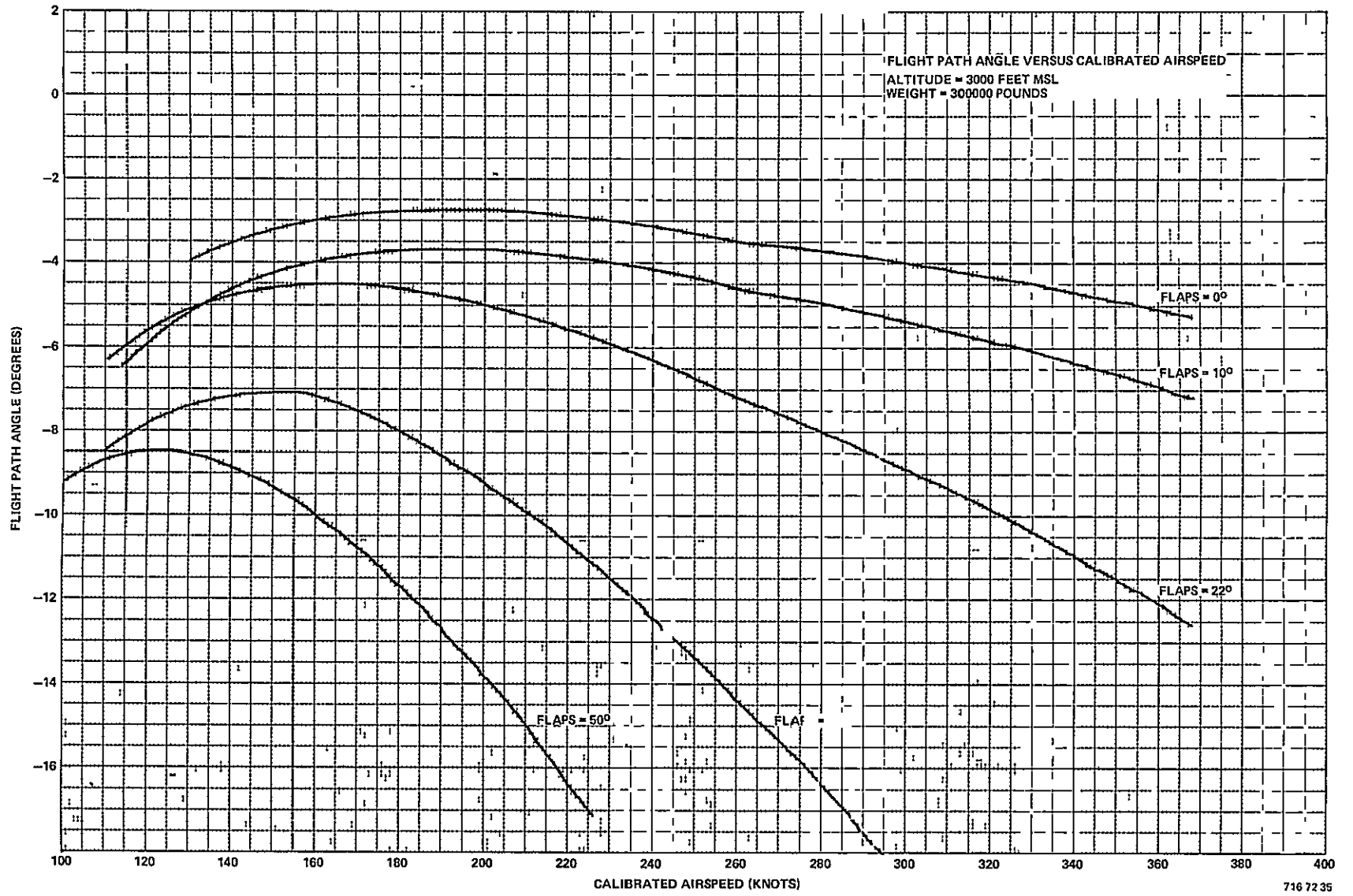


Figure 4-29

For example, with a 3 degree glide slope, the aircraft has equilibrium points at 230 and 160 knots. With 10 degrees of flaps, the glide slope would have to be 3.7 degrees to maintain an equilibrium speed of 195 knots. The required gammas for equilibrium and consequent speeds decrease with increasing flaps. Obviously, if the aircraft is on a typical glide slope, any amount of flaps will cause the aircraft to decelerate.

Figure 4-30 shows the calibrated airspeed versus distance for an aircraft on a 2.7 degree glide slope with retarded throttles at various flap settings. Obviously, the greater the flap setting, the greater the deceleration. Note that the curves are all relatively linear except when the airspeed approaches the stall speed of the aircraft (or less than 120 knots).

Table 4-2 shows the slope of each curve,  $\Delta V/\Delta X$  in units of knots per nautical mile and knots per foot. Note that the slopes represent decelerations. The slopes increase gradually until the flaps reach 20 degrees, at which time the slopes increase more rapidly. After the flaps reach 35 degrees, the increase in slope tails off again. The values in Table 4-2 define a function dependent on flaps that will hereafter be noted as  $K(\delta_f)$ .

TABLE 4-2  
 $\Delta V/\Delta X$  FOR VARIOUS FLAP SETTINGS  
 THROTTLES RETARDED,  $\gamma = -2.7$  DEGREES

Flaps (degrees)	$\frac{\Delta V}{\Delta X} \left( \frac{\text{knots}}{\text{nmi}} \right)$	$\frac{\Delta V}{\Delta X} \left( \frac{\text{knots}}{\text{ft}} \right)$
0	3.08	.000507
5	4.62	.00076
10	5.77	.00095
15	6.73	.001108
20	9.81	.001615
25	13.65	.002246
30	23.64	.003891
35	36.67	.006035
40	45.0	.007406



ORIGINAL PAGE IS  
OF POOR QUALITY

4-36

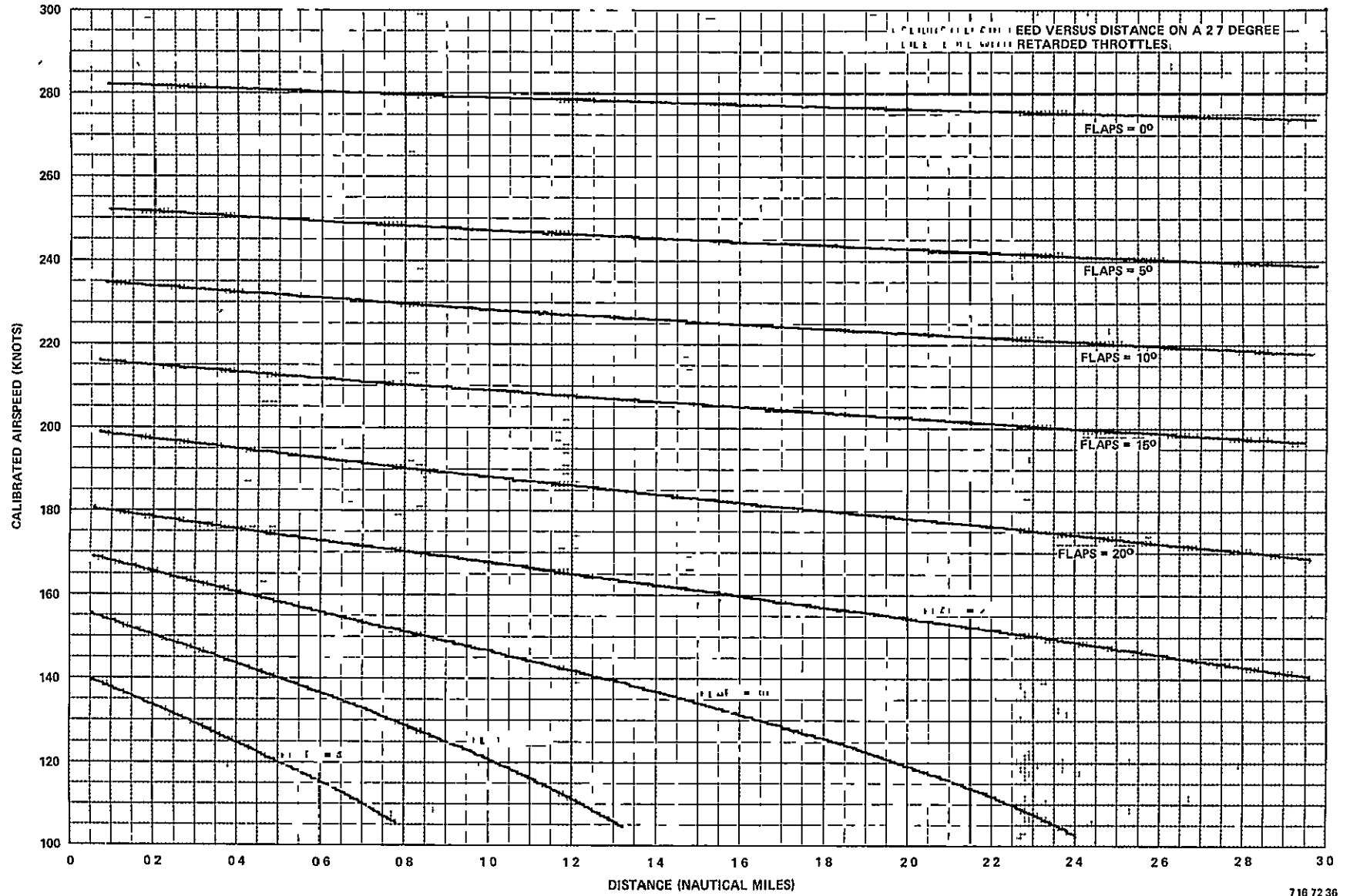


Figure 4-30

A second function that is basically a correction factor due to varying air referenced flight path angle and weight is defined as:

$$\hat{f}(\gamma_{air}, W) = \left( \frac{\dot{V}}{\dot{h}} \right) \frac{1}{K(\delta_f)} \quad (4-1)$$

where

$\dot{V}$  = Time rate of change in velocity

$\dot{h}$  = Time rate of change in altitude

$K(\delta_f)$  = Deceleration with actual flap setting as defined by Table 4-2

$W$  = Aircraft weight

This function is denoted as an estimate since it is obtained from measured data. By multiplying  $\hat{f}(\delta_{air}, W)$  by the deceleration expected from the aircraft at 300,000 pounds with 50 degrees of flaps on a 2.7 degree air referenced flight path angle,  $K(\delta_f = 50)$ , an estimate of the expected change in velocity for a change in altitude is obtained for the aircraft at its current weight and air referenced flight path angle.

$$\left( \frac{\hat{\Delta V}}{\Delta h} \right)_{\delta_f=50} = \hat{f}(\gamma_{air}, W) K(\delta_f = 50) \quad (4-2)$$

Similarly,  $\Delta V/\Delta h$  can be estimated for flap settings of 40, 30, 20, and 10 degrees.

For a given desired change in velocity for a particular flap setting, the corresponding change in altitude is given by:

$$\Delta h = \Delta V \left[ \frac{1}{\left( \frac{\hat{\Delta V}}{\Delta h} \right)_{\delta_f}} \right] \quad (4-3)$$

where

$\Delta V$  = Desired change in velocity

$\left( \frac{\hat{\Delta V}}{\Delta h} \right)_{\delta_f}$  = Estimate of deceleration with altitude for a particular  $\delta_f$

To ensure stabilization for a normal landing 500 feet above ground level, a base altitude of 700 feet AGL is used as the minimum altitude at which the flaps will be set to 50 degrees and the throttles will be increased to hold the approach airspeed. Table 4-3 gives the desired flap deployment schedule and the associated changes in velocity for the various flap settings. The altitude at which the flaps should be deployed to 50 degrees is given by:

$$h_{50} = 700 + 10 \left[ \frac{1}{\left( \frac{\Delta V}{\Delta h} \right)_{\delta_f=50}} \right] \quad (4-4)$$

The corresponding changes in altitude for the other flap settings simply add in succession yielding:

$$h_{40} = h_{50} + 10 \left[ \frac{1}{\left( \frac{\Delta V}{\Delta h} \right)_{\delta_f=40}} \right] \quad (4-5)$$

$$h_{30} = h_{40} + 20 \left[ \frac{1}{\left( \frac{\Delta V}{\Delta h} \right)_{\delta_f=30}} \right] \quad (4-6)$$

$$h_{20} = h_{30} + 30 \left[ \frac{1}{\left( \frac{\Delta V}{\Delta h} \right)_{\delta_f=20}} \right] \quad (4-7)$$

TABLE 4-3  
DESIRED FLAP DEPLOYMENT SCHEDULE

Flap Setting (deg)	Approximate V at Deployment (knots)	V (knots)
50	145	10
40	155	10
30	175	20
20	205	30
10	As needed	As needed

The  $\Delta V$  associated with the next flap deployment (10 degrees initially) is defined as the minimum between the actual airspeed or 5 knots less than the placard speed minus the airspeed for the next higher deployment - 20 degrees in this case. Thus:

$$h_{10} = h_{20} + \left[ \min (V, V_{\text{placard}} - 5) - 205 \right] \left[ \frac{1}{\left( \frac{\Delta V}{\Delta h} \right)_{\delta_f=10}} \right] \quad (4-8)$$

Equations (4-1) through (4-8) are computed continuously and the flaps are deployed whenever the computed altitude is reached. If the aircraft is going too fast for a particular flap deployment, the flap command will remain slightly below what the placard limit will allow. Once a particular flap deployment is made, the corresponding altitude is no longer computed and the next deployment altitude calculation takes the form of Equation (4-8) using the velocity given in Table 4-3 to calculate the new  $\Delta V$ . It should be noted that the glide slope is captured from above; therefore, there is no constant altitude approach segment. Also, power is not applied until there are 50 degrees of flaps.

#### D. BASELINE FLIGHT WITH DELAYED FLAP APPROACH: LAS VEGAS TO LOS ANGELES

The only difference between the baseline flight approach and the baseline flight with a delayed flap approach is during the descent, thus no new plots were taken for the climb-out segment. Figure 4-31 shows the barometric altitude versus the range for the baseline flight with the delayed flap approach. The point of descent is now 143 miles into the flight compared to 138 for the baseline. This results in glide slope capture at 207 miles without leveling off at an approach altitude.

The fuel flow per unit distance,  $F_D$ , versus the range for the descent is shown in Figure 4-32. The major difference between this curve and the corresponding curve for the baseline flight (Figure 4-17) is the lack of spikes due to flap deployment. The spikes are absent because no power is applied until there are 50 degrees of flaps.

ORIGINAL PAGE IS  
OF POOR QUALITY

4-40

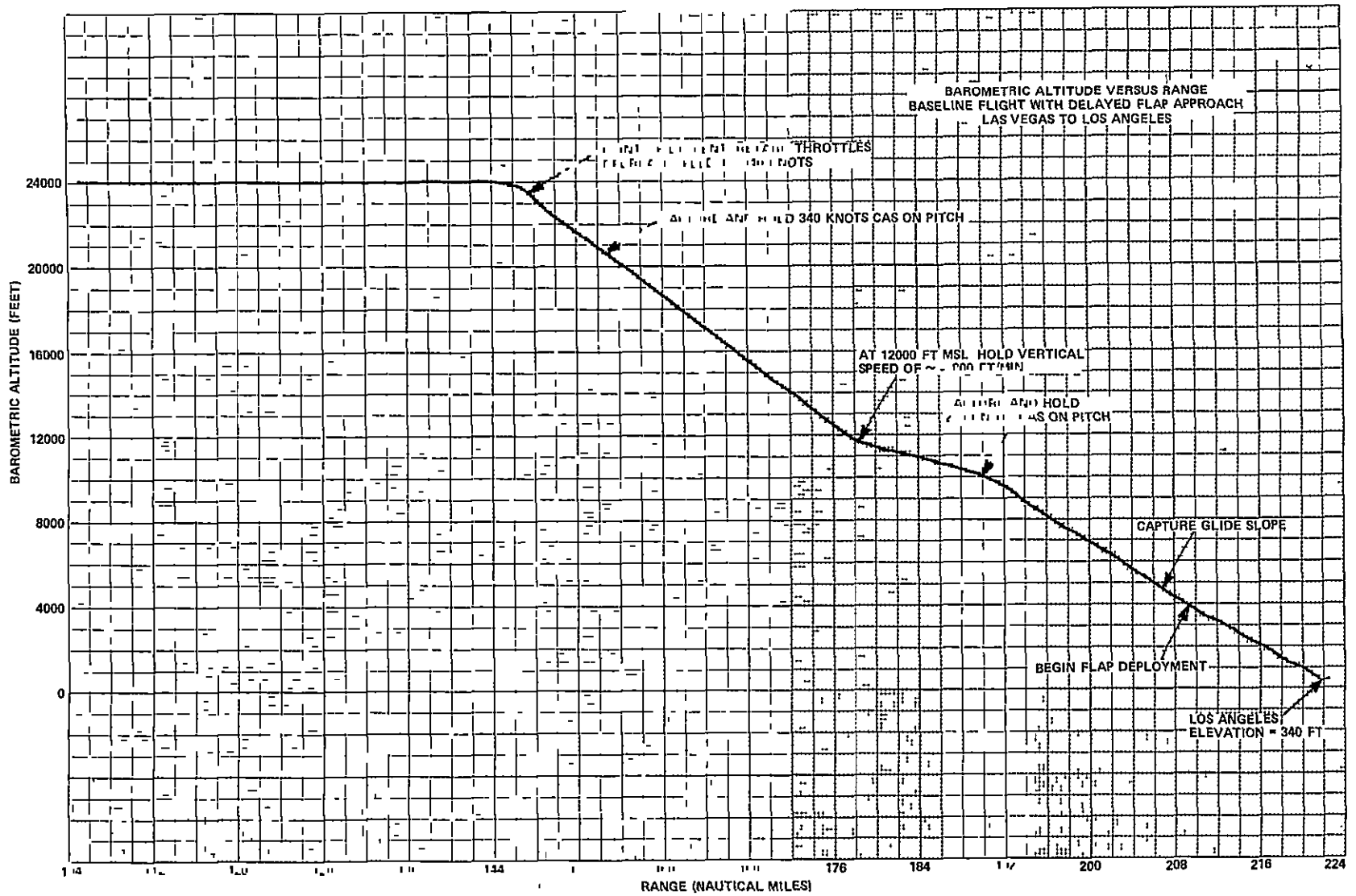


Figure 4-31

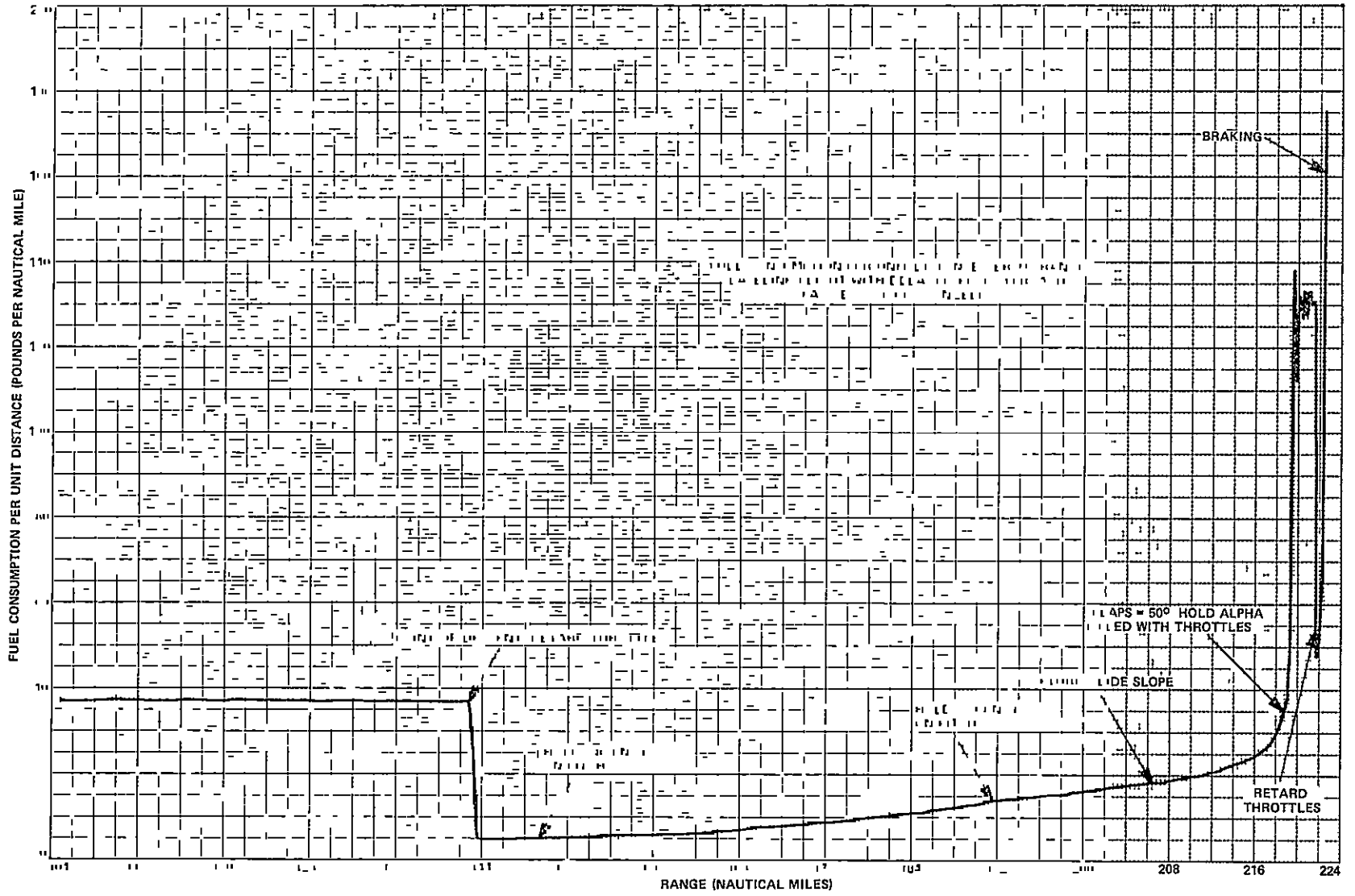


Figure 4-32

Flap deployment versus the range is shown in Figure 4-33. The initial flap deployment occurs at 211.2 miles and 3,100 feet AGL. It is only 8 degrees due to placard limitation. Final flaps are deployed at 219 miles and 860 feet AGL.

Figure 4-34 shows the calibrated airspeed versus the range for the baseline flight with a delayed flap approach. Note that the speed steadily decreases as the flaps are deployed and is held at about 135 knots only after full landing flaps (50 degrees) are achieved. Powered flight during approach and landing is at a minimum.

Results of several baseline flights with delayed flap approaches are given in Table 4-4. The average fuel consumption is 9,791 pounds, 281 pounds less than the baseline, or about a 2.79 percent fuel savings. Average flight time is 37 minutes and 8 seconds. This is 1 minute and 52 seconds less than the baseline, or 4.79 percent faster. The decrease in flight time and fuel consumption is obviously due to the delayed flap deployment.

TABLE 4-4  
FLIGHT DATA  
BASELINE FLIGHT WITH DELAYED FLAP APPROACH

Flight No.	Fuel Consumed (pounds)	$F_D$ (lb/nmi)	Time (min, sec)
1	9,790	44.02	37, 8
2	9,794	44.04	37, 9
3	9,788	44.01	37, 6
4	9,791	44.02	37, 8
Averages	9,791	44.02	37, 8

While making test runs for the delayed flap approach, it was discovered that the performance of the flap deployment algorithm was highly dependent on the flight condition. A slight variation in the altitude or speed at which the glide slope was captured caused a very noticeable difference in the flap deployment. This suggests that the linearized flap deployment algorithm inferred from the plots of CAS versus distance (Figure 4-30) is not adequately sophisticated to cope with a broad spectrum of flight conditions.

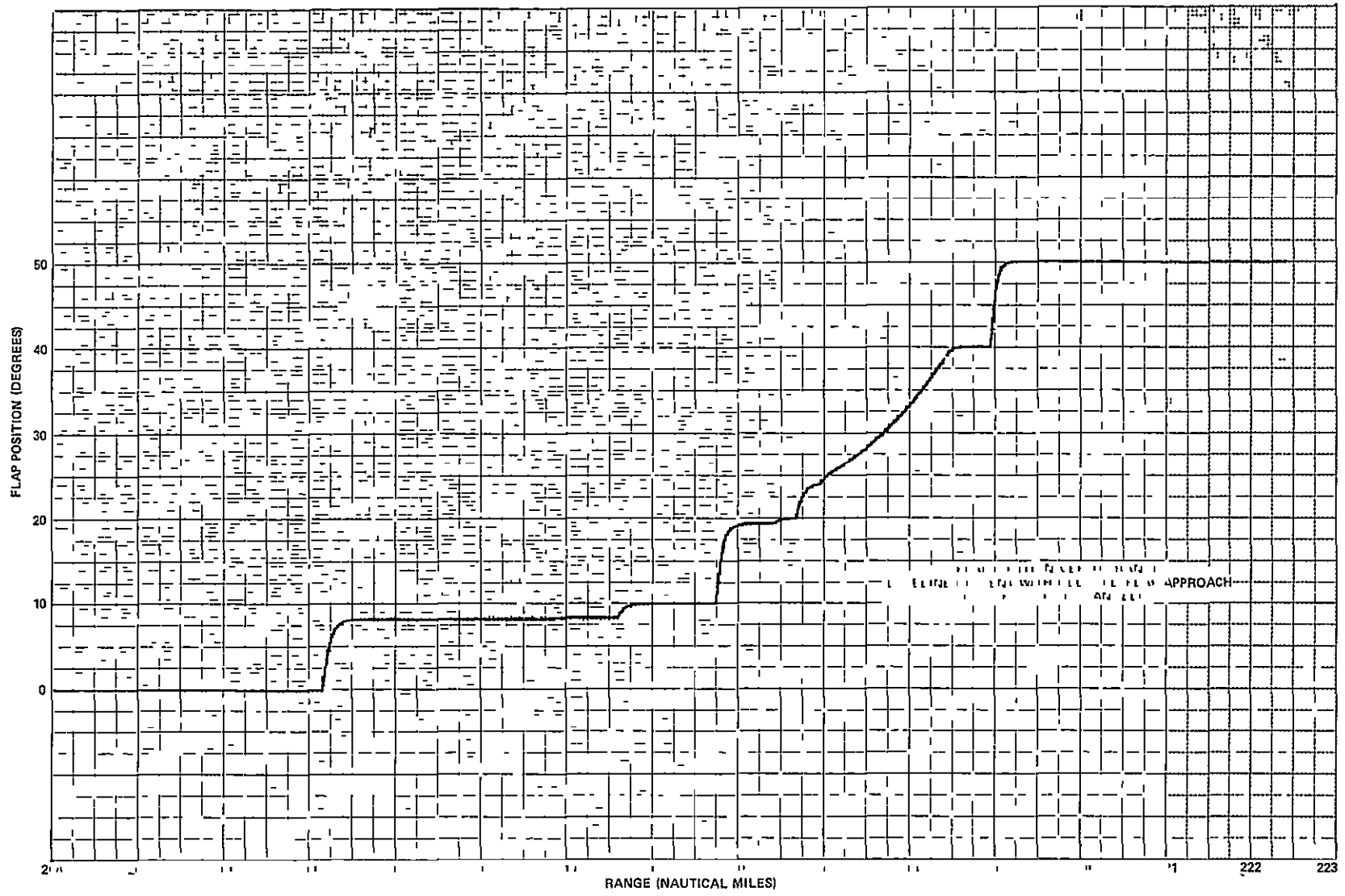


Figure 4-33



ORIGINAL PAGE IS  
OF POOR QUALITY

4-44

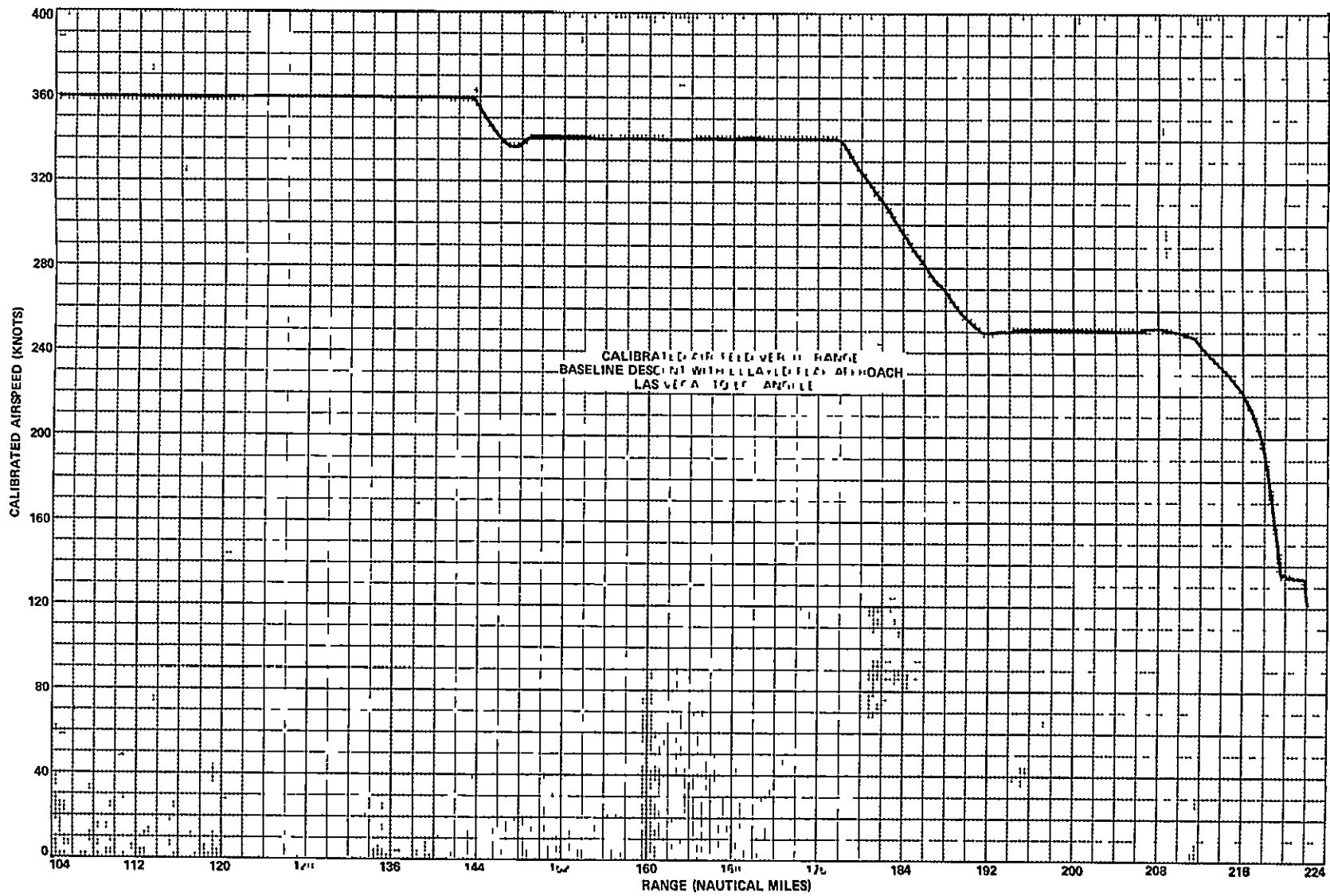


Figure 4-34

It further suggests that data of the type shown in Figure 4-30 should be taken over a more diverse speed (CAS) range and the flap deployment algorithm should be refined to fully account for the nonlinearities. This investigation is a prerequisite to obtaining a practical flap deployment scheme.

#### E. BASELINE FLIGHT AT OPTIMAL CRUISE MACH: LAS VEGAS TO LOS ANGELES

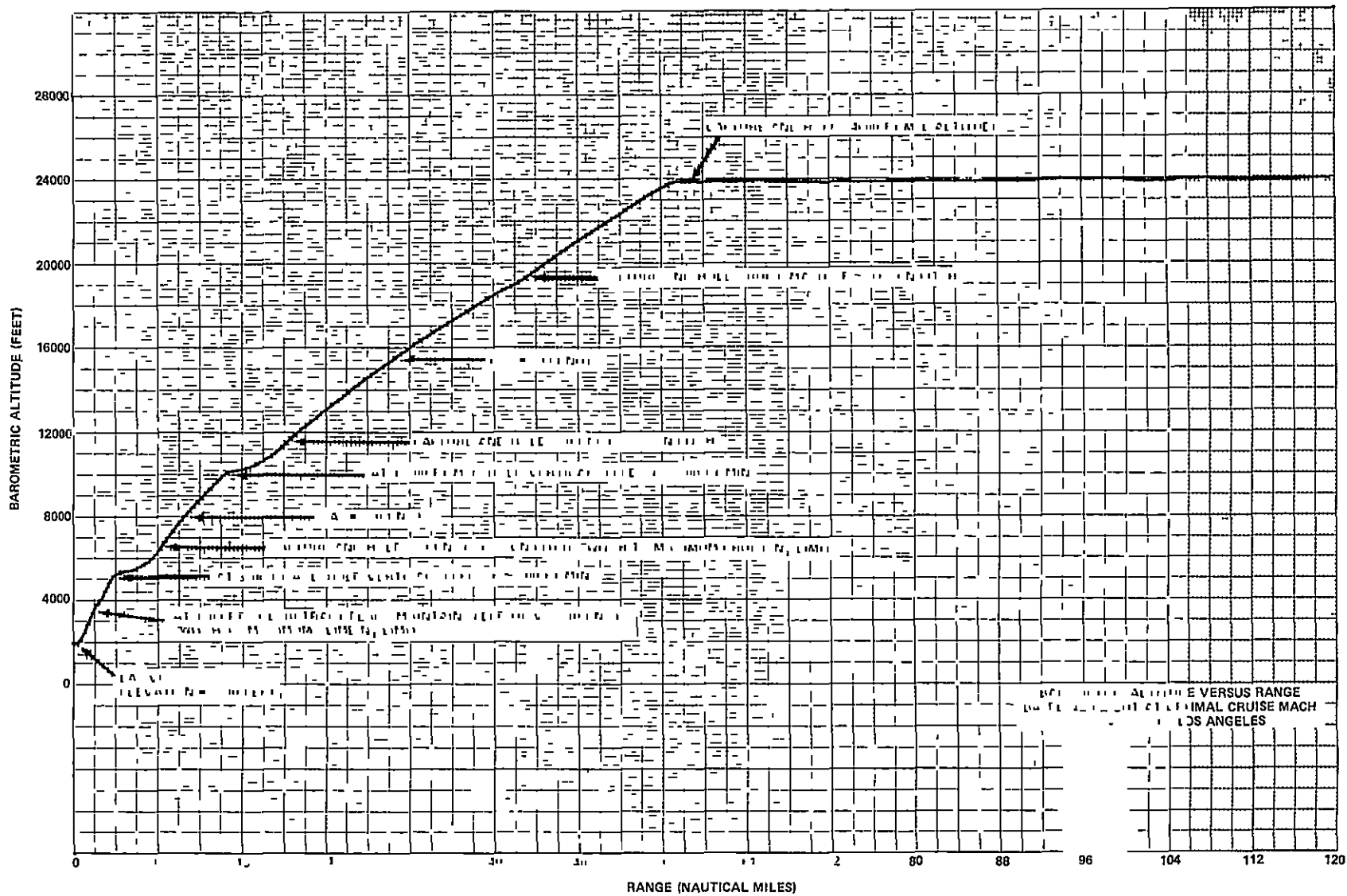
The optimal cruise Mach for an altitude of 24,000 feet MSL and a weight of about 320,000 pounds was estimated from interpolating on the  $F_D$  versus Mach curves presented in Part A of this section. A value of .62 was computed as the optimal cruise Mach number. The climb-out procedure only changes in that once .62 Mach is achieved, the Mach number, rather than calibrated airspeed, is held on pitch. The only change in descent procedure is that at the point of descent the aircraft must pitch down to increase the calibrated airspeed to 340 knots.

Figures 4-35 and 4-36 show the barometric altitude versus the range for the climb-out and descent of a baseline flight at the optimal cruise Mach. The optimal Mach of .62 is reached 46 miles into the climb-out and the cruise altitude is reached at 63 miles. This is only 1 mile further than that for the baseline flight. Descent is begun at 146.5 miles as a flight path angle of -5 degrees is commanded to increase the CAS to 340 knots. However, this value of CAS is not captured until 166 miles. The rest of the descent is then similar to the baseline flight.

The plots of fuel consumption per unit distance versus the range, Figures 4-37 and 4-38, are very similar to the baseline flight. When the cruise altitude is reached, however, the aircraft is already at the cruise Mach and the throttles can immediately pull back from the  $N_1$  limit to hold the Mach number. In the baseline flight the throttles must remain at the  $N_1$  limit once the cruise altitude is attained in order to increase the speed to the cruise Mach of .83. Flying at the optimal (slower) Mach number causes  $F_D$  to drop to the cruise value sooner in the flight, thus saving fuel. The value of  $F_D$  during cruise is 30.6 pounds per nautical mile for the optimal cruise Mach, while it is 37.5 pounds per nautical mile for the baseline cruise Mach.

ORIGINAL PAGE IS  
OF POOR QUALITY

4-46



716 72 41

Figure 4-35

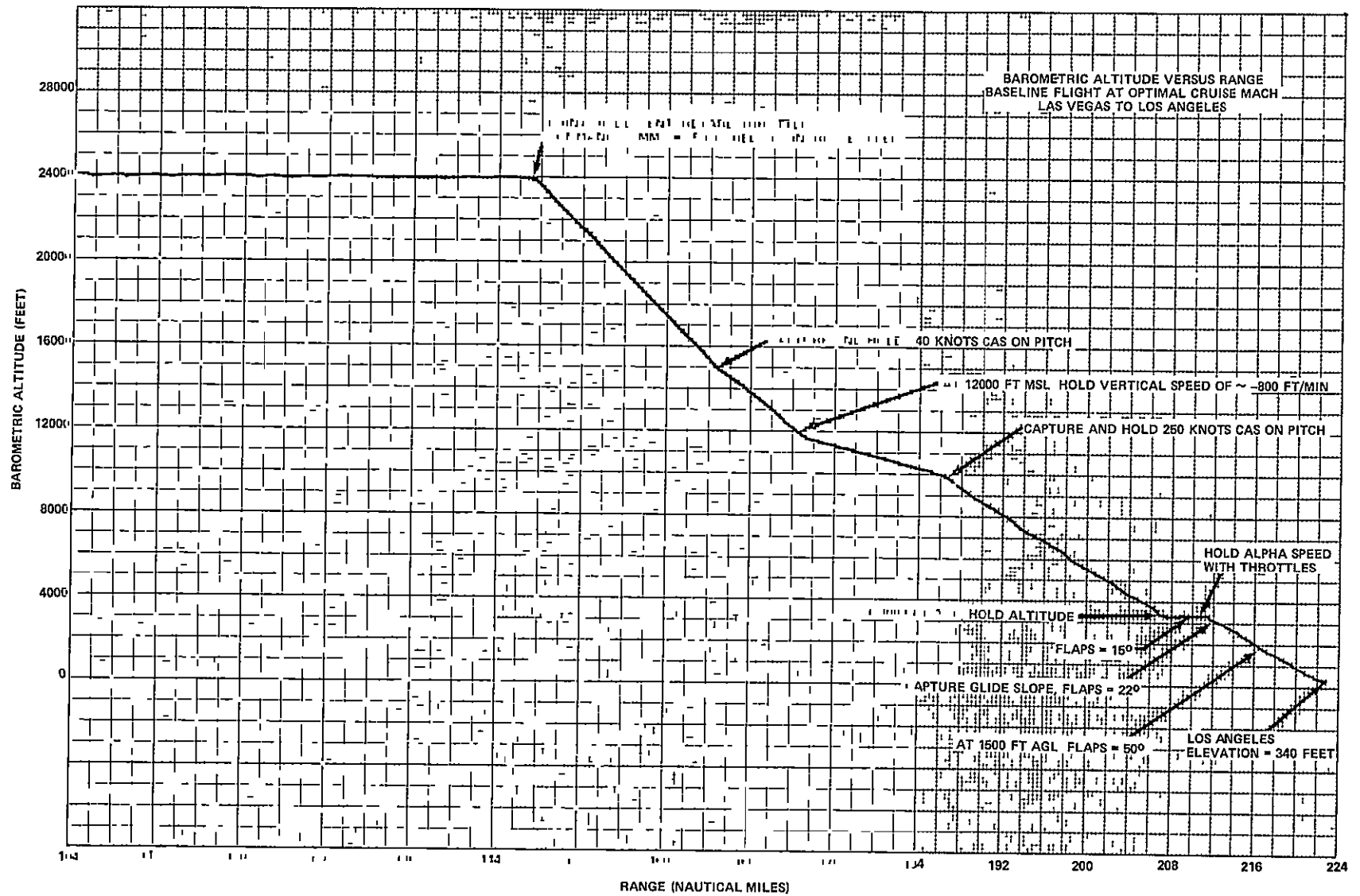


Figure 4-36

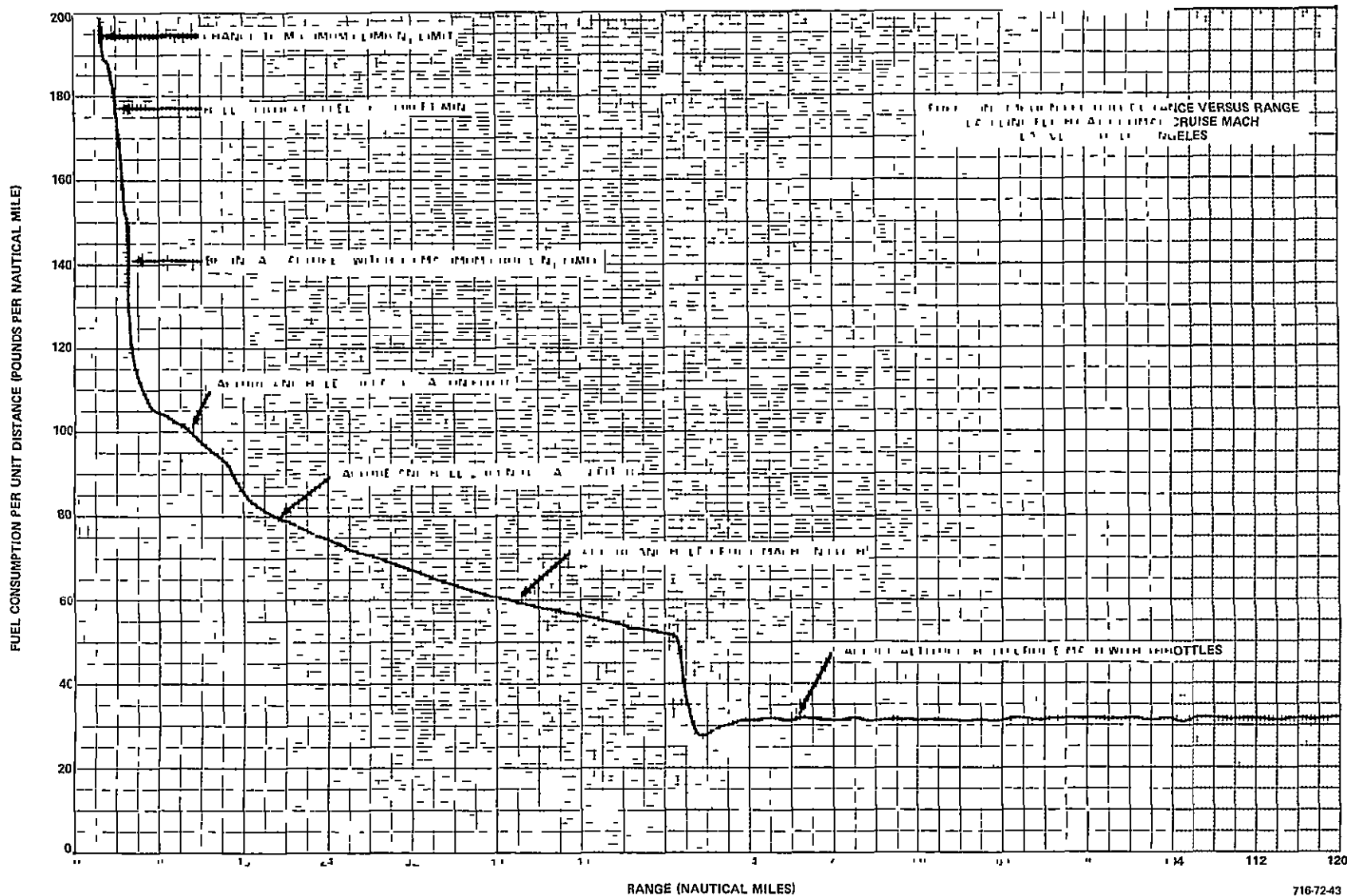


Figure 4-37

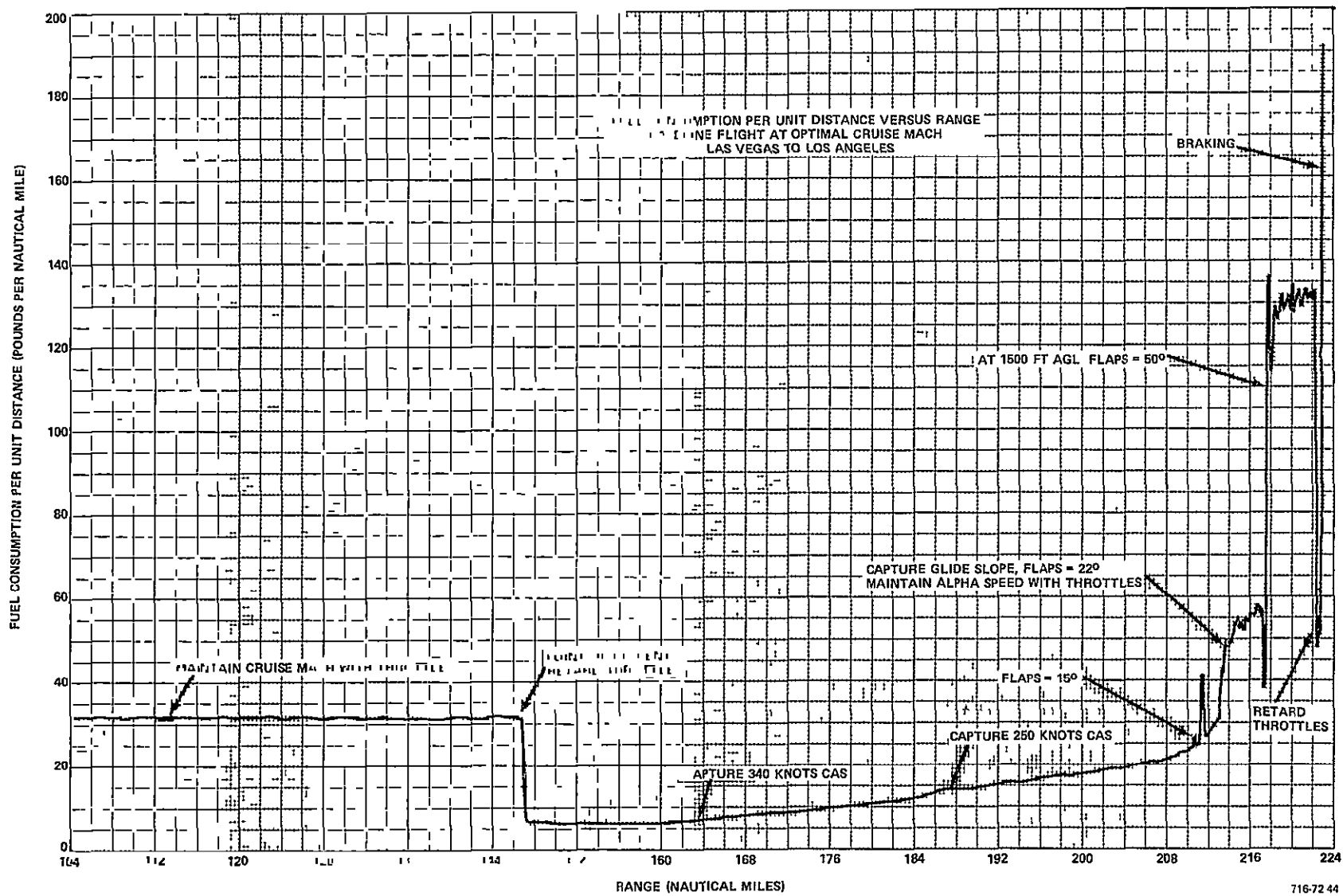


Figure 4-38

Table 4-5 gives the results of several flights using the baseline procedures, but cruising at the optimal Mach number. The average 9,638 pounds of fuel consumed is a 434 pound saving over the baseline flight or 4.31 percent. Average flight time is 42 minutes and 20 seconds, or 3 minutes and 20 seconds longer than the baseline. This represents an 8.55 percent increase due to cruising at a slower speed.

TABLE 4-5  
FLIGHT DATA  
BASELINE FLIGHT AT OPTIMAL CRUISE MACH

Flight No.	Fuel Consumed (pounds)	$F_D$ (lb/nmi)	Time (min, sec)
1	9,641	43.34	42, 20
2	9,644	43.34	42, 21
3	9,632	43.28	42, 19
4	9,634	43.29	42, 19
Averages	9,638	43.31	42, 20

#### F. FORTRAN FUEL OPTIMIZATION PROGRAM

A FORTRAN program for computing minimum fuel flight paths was developed at Stanford University and is documented in Reference 3.

The program was executed using the data provided by Stanford to verify the results obtained by Shoaee and Bryson. That successfully done, a number of changes were made so that the program would more accurately reflect the methods used in the simulation.

The first change was the replacement of table look-ups with equations for the air data (speed of sound and air density) and the coefficient of drag. This was done to increase their accuracy by eliminating linear interpolation of highly nonlinear functions. The subroutine SPLINE and function subroutine SP were eliminated and replaced with a new subroutine SONRO which calculates

the speed of sound and air density using the following equations based on the NASA Environment Data Model:

$$T_{AMB} = 288.16 - .0019812h + \Delta T \quad (4-9)$$

$$\theta_{AM} = T_{AMB}/288.16 \quad (4-10)$$

$$V_S = 1116.42 (\theta_{AM})^{\frac{1}{2}} \quad (4-11)$$

$$\delta_{AM} = \left[ \frac{T_{AMB} - \Delta T}{288.16} \right]^{5.255876} \quad (4-12)$$

$$\rho = .002378 \delta_{AM} / \theta_{AM} \quad (4-13)$$

where

$\Delta T$  = Temperature correction factor to allow for flights during hot or cold days

h = Altitude

$\rho$  = Air density

$V_S$  = Speed of sound

In addition, the function subroutine CD was changed to implement the equation for the coefficient of drag that is used in the simulation.

$$C_D = f_1 + K_{1flap} + \left\{ .0552778f_2 + K_{2flap} \right\} C_{L\alpha}^2 \quad (4-14a)$$

where

$$f_1 = \begin{cases} .0148 & M \leq .6 \end{cases} \quad (4-14b)$$

$$f_1 = \begin{cases} .014592 + \frac{6.47657 \times 10^{-5}}{(.91155-M)} & 6 \leq M \leq 9 \end{cases} \quad (4-14c)$$

$$f_2 = \left[ \frac{\min(f_1, .01822)}{.0148} \right]^4 \quad (4-14d)$$



The use of this equation also necessitated limiting the search for a minimum Hamiltonian to an upper value of .9 Mach. The functions  $K_{1flap}$  and  $K_{2flap}$  are correction factors due to flaps and are determined by linear interpolation and a table look-up. The tables used for  $K_{1flap}$  and  $K_{2flap}$  are given in Appendix H.

The updated program was executed in the cruise altitude mode to check the effects of these changes. The results, given in Appendix A-1, showed little difference from the Stanford results. In general, the new program yielded slightly lower Mach numbers and higher fuel consumption. Both gave an optimal cruise altitude of 33,000 feet for a weight of 400,000 pounds. The differences were greater with increasing altitude and Mach number since it is in these regions that the air data functions become more nonlinear.

The ascent and descent tables were then generated and are given in Appendices A-2 and A-3. The updated program resulted in higher ranges and fuel-used figures, and smaller Mach numbers and flight path angles ( $\gamma$ ). There were exceptions to these rules but the trends of a continually decreasing  $\gamma$  during the ascent and a decreasing, then increasing  $\gamma$  during the descent held throughout. It should be noted that exact comparison is difficult because the different flight path angles result in different altitude increments to be computed and printed.

The next change was to recompute the engine data (thrust, specific fuel consumption, maximum thrust, idle thrust, and idle fuel flow rate) using the simulation program with the  $N_1$  limit following the baseline procedure. This data proved to be significantly different from that furnished. The specific fuel consumption was higher while corresponding points in the other three categories were lower.

The new data generated the optimal cruise table shown in Appendix A-4. The results proved to be a continuation of the trends noted earlier in Appendix A-1, although the differences were much greater. Once again, an optimal cruise altitude of 33,000 feet occurred. The new data resulted in a 4 percent increase in minimum fuel consumption over the Stanford data.

The ascent and descent tables provided by this case (Appendices A-5 and A-6) continue to exhibit the general trends noted earlier in connection with Appendices A-2 and A-3. Once again, a large difference in flight path angle causes the altitude increments to vary. Nonetheless, a sufficient number of similar points exist to allow comparison.

A plot of the optimal ascent flight paths using different engine data, that provided by Stanford and that computed by the CF6-6 engine simulation (see Section II, Part B), is given in Figure 4-39. The great difference in engine data is illustrated in this figure.

A number of changes were made in the computer program to better reflect the actual aircraft performance. The most significant change was a rederivation of the necessary equations to include the effects of changes in the aircraft's kinetic energy. The program was originally derived based on the assumption that the energy provided by the engines was used only to acquire potential energy. While it is true that the majority is of this type, an appreciable amount of kinetic energy is also present. A few rough calculations demonstrate this point. At an altitude of 14,000 feet the program gives an optimal velocity of 558 feet per second. Thus, kinetic energy makes up 25.7 percent of the total energy present. The percentage changes throughout the flight; however, by including the kinetic energy effects a more accurate model is obtained.

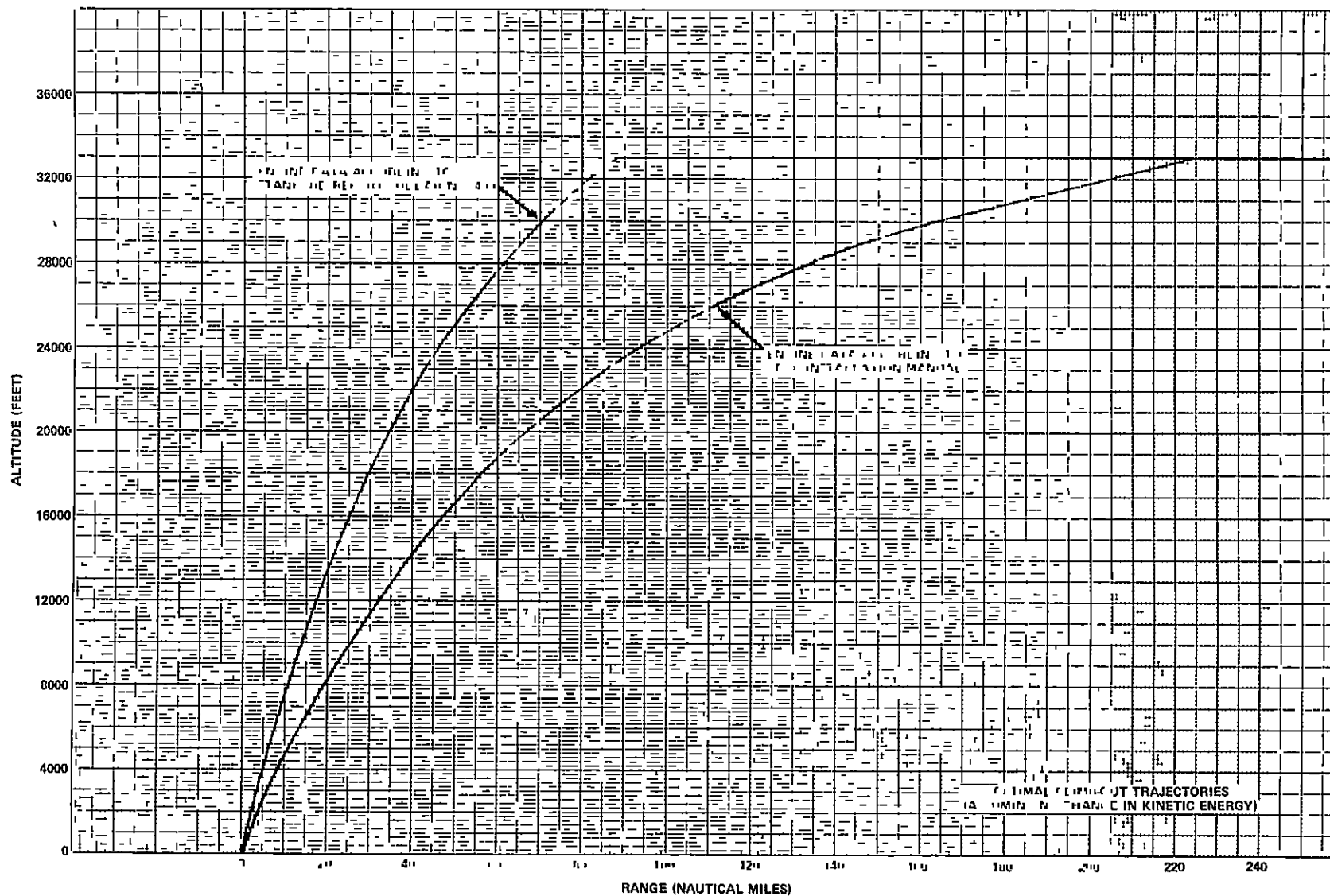
The new derivation follows closely that of the old one. The major difference is the use of the rate of change of energy instead of the rate of change of altitude as a state equation.

Let  $E$  be the energy divided by the mass

$$E = V^2/2 + g h \quad (4-15)$$

ORIGINAL PAGE IS  
OF POOR QUALITY

4-54



716-72-45

Figure 4-39

The differential equations are

$$m\dot{V} = T - D - m g \sin \gamma \quad (4-16)$$

$$\dot{x} = V \cos \gamma + Vw \quad (4-17)$$

$$\dot{h} = V \sin \gamma \quad (4-18)$$

Differentiating the energy with respect to time gives

$$\begin{aligned} \dot{E} &= V\dot{V} + g\dot{h} \\ &= V \left( \frac{T - D - m g \sin \gamma}{m} \right) + g V \sin \gamma \\ &= V \frac{(T - D)}{m} \end{aligned} \quad (4-19)$$

Using the range,  $x$ , as the independent variable, the problem of minimizing fuel use for a given range,  $R$ , may be stated as follows:

Find  $V$  and  $T$  to minimize

$$J = \int \dot{f} dt = \int_0^R \frac{df}{dx} dx = \int_0^R \frac{CT}{V \cos \gamma + Vw} dx \quad (4-20)$$

subject to

$$\frac{dE}{dx} = \frac{\dot{E}}{\dot{x}} = \frac{V (T - D)}{m (V \cos \gamma + Vw)} \quad (4-21)$$

The Hamiltonian for this problem is

$$H = \frac{CT}{V \cos \gamma + Vw} + \frac{\lambda V (T - D)}{m (V \cos \gamma + Vw)} \quad (4-22)$$

Since  $H$  is not an explicit function of  $x$ ,  $H$  is a constant.

The Hamiltonian must be minimized with respect to the control variables  $T$  and  $V$ . Minimizing with respect to  $T$  yields

$$T = \begin{cases} T_m & \text{for } \left(C + \frac{\lambda V}{m}\right) < 0 \\ T_i & \text{for } \left(C + \frac{\lambda V}{m}\right) > 0 \end{cases} \quad (4-23)$$

$T$  is not determined by minimizing  $H$  if  $C + \frac{\lambda V}{m} = 0$ . For this singular arc condition, the Lagrange multiplier,  $\lambda$ , is

$$\lambda = \frac{-Cm}{V} \quad (4-24)$$

so that  $H$  in this case is

$$H = \frac{-\lambda VD/m}{V \cos \gamma + Vw} = \frac{CD}{V \cos \gamma + Vw} \quad (4-25)$$

In order to minimize  $H$  with respect to  $V$ , the necessary condition is

$$\frac{\partial H}{\partial V} = 0$$

However, this condition is not used directly except on the singular arc. Since

$$H = \frac{df}{dx} + \lambda \frac{dE}{dx} \quad (4-26)$$

and

$$\lambda = \frac{H - \frac{df}{dx}}{dE/dx} \quad (4-27)$$

Then

$$\frac{\partial H}{\partial V} = \frac{\partial}{\partial V} \frac{df}{dx} + \lambda \frac{\partial}{\partial V} \frac{dE}{dx} = 0 \quad (4-28)$$

C.2

Substituting Equation (4-27) in Equation (4-28) yields

$$\frac{\partial H}{\partial V} = \frac{\partial}{\partial V} \frac{df}{dx} + \frac{\left[ H' - \frac{df}{dx} \right] \frac{\partial}{\partial V} \frac{dE}{dx}}{\frac{dE}{dx}} \quad (4-29)$$

Dividing by  $\frac{dE}{dx}$  and manipulating gives

$$\frac{\frac{dE}{dx} \frac{\partial}{\partial V} \frac{df}{dx} - \left[ \frac{df}{dx} - H \right] \frac{\partial}{\partial V} \frac{dE}{dx}}{\left( \frac{dE}{dx} \right)^2} = 0 \quad (4-30)$$

This can be rewritten as

$$\frac{\partial}{\partial V} \left[ \frac{df/dx - H}{dE/dx} \right] = 0 \quad (4-31)$$

Therefore, the value of V that minimizes H can be obtained by finding the value of V that minimizes

$$\begin{aligned} HAM &= \frac{\frac{df}{dx} - H}{dE/dx} \quad (4-32) \\ &= \frac{CT - H (V \cos \gamma + Vw)}{V \frac{(T - D)}{m}} \\ &= \frac{CT - H (V \cos \gamma + Vw)}{V (\dot{V} + g \sin \gamma)} \end{aligned}$$

The program uses the singular arc cruise Equation (4-25) to define H. Then Equation (4-32) is used for ascent and descent.

After incorporating the equations into the program, other changes became necessary. When the time increment (DELTA) was reduced from 30 to 5 seconds, the optimal ascent and descent Mach numbers tended to move in large jumps every few iterations while remaining constant between them. It was decided that this was caused by the shallowness of the optimal curve near the true

minimum. This, combined with the tolerance of the minimization routine, prevented it from finding the true optimal point until conditions had changed sufficiently to cause a large jump. Decreasing the tolerance of the minimization routine alleviated the problem.

The end conditions for the ascent and descent should be such that a relatively smooth transition from ascent to cruise and from descent to approach altitude is obtained. The program as constructed, however, provided a profile that resulted in an excess of kinetic energy for the aircraft at the transition points. For example, at 24,000 feet the optimal ascent Mach given by the program is .6822 while the optimal cruise Mach is .623. Therefore, the craft has overaccelerated and will have to slow down to obtain an optimal cruise. To achieve the proper end conditions, the program was changed to compute in reverse time. The optimal cruise end point then became the initial condition.

In the baseline procedure both the engine data for the maximum climb and maximum cruise  $N_1$  limits are used during the ascent. Appropriate logic was added to the program to accomplish the switch whenever the previously described conditions are met. Also, the aircraft weight is continually recomputed to account for the amount of fuel consumed.

The ascent exhibited a tendency to pitch down to attain sufficient speed to capture the ascent profile. The opposite was true of the descent. The problem was overcome by constraining the program to only select points for the optimal ascent and descent so that gamma does not change sign.

The original FORTRAN programs utilized a constant altitude minimization search (constant energy if one neglects kinetic energy). This search was initially used after the rederivation to include kinetic energy effects. At the suggestion of Arthur E. Bryson, Jr., the search was modified to include the kinetic energy effect on the minimization boundary (i.e., the search should be done on a constant energy boundary). This change gave a theoretically correct minimization under the assumptions, and did in fact slightly improve the results.

A new ascent table was produced by the program and is given in Appendix A-7. Figure 4-40 compares the results due to assuming no change in kinetic energy to those obtained from the final version of the program in which all of the above modifications had been incorporated. The significant difference in profiles is a good indication of the importance of including changes in the kinetic energy.

A complete listing of the current program is given in Appendix B. It is constructed to allow either derivation to be run by changing one variable (TCNST). A second variable (TCNST2) allows control over the use of the constant energy boundary search.

The FORTRAN program was then run for the Las Vegas to Los Angeles climb-out to a cruise altitude of 24,000 feet using both derivations. Mach-altitude profiles were generated from the computer printouts and test flights were run on the simulator. The test flight results were compared to the predicted (FORTRAN) results by examining a portion of the climb-out where the Mach-altitude profile was being tracked. For the case where the kinetic energy was neglected, this region was from 8,250 feet at .53 Mach to 23,625 feet at .665 Mach. In the flight where the kinetic energy was included, the region ran from 8,625 feet at .514 Mach to 23,063 feet at .637 Mach.

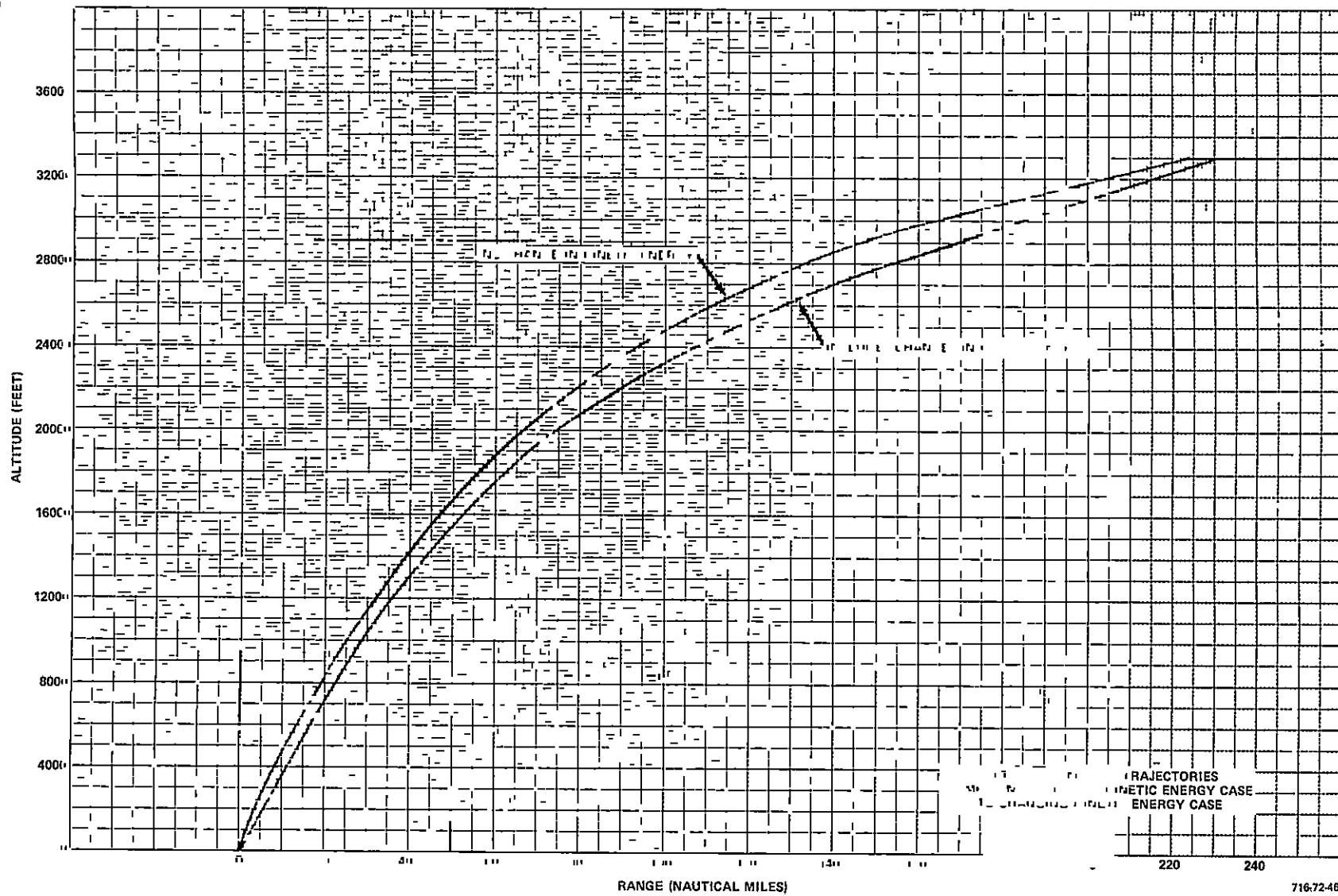
For the case neglecting kinetic energy, the FORTRAN program predicted the range during the climb-out region to be 45.21 nautical miles, while the predicted fuel consumption was about 2,852 pounds. The range covered in the test flight during the particular region was 50 nautical miles or 10.6 percent further than predicted. The test flight used 3,150 pounds of fuel or 9.47 percent more than that predicted by the FORTRAN program.

For the case that included the kinetic energy, the FORTRAN program predicted a range of 45.83 nautical miles and a fuel consumption of 2,956 pounds. The test flight range was only 45 miles or 1.81 percent less than predicted. Fuel consumption from the test flight was 2,900 pounds or 1.88 percent less than the predicted amount.



ORIGINAL PAGE IS  
OF POOR QUALITY

4-60



716-72-46

Figure 4-40

In comparing the two derivations, it is easy to see that the addition of the kinetic energy more closely predicts the actual performance of the flight simulator. A 10.6 percent error in range resulted by neglecting the kinetic energy, while including it resulted in only a 1.81 percent difference, which is on the order of acceptable measurement error.

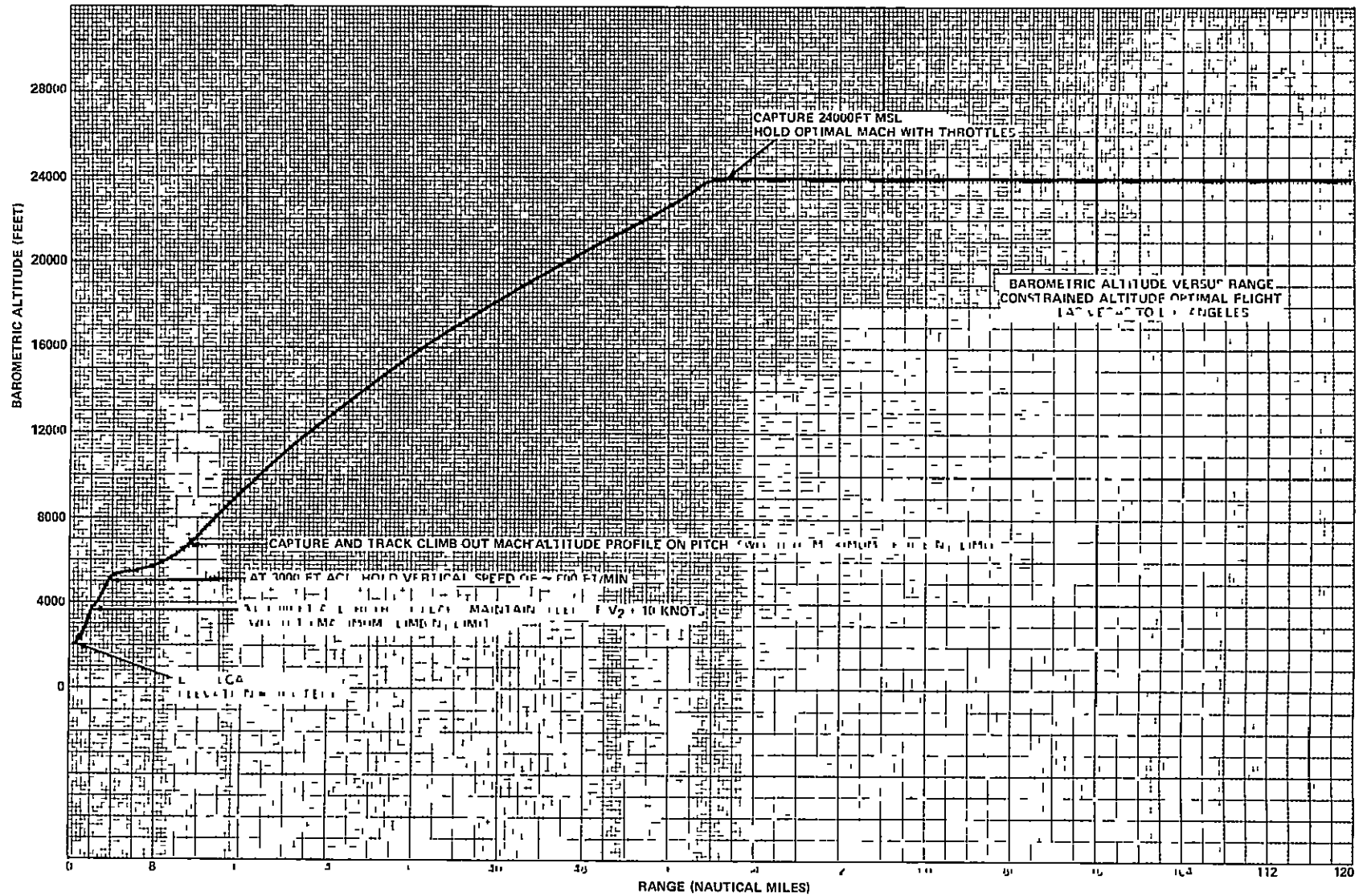
#### G. CONSTRAINED ALTITUDE OPTIMAL FLIGHT: LAS VEGAS TO LOS ANGELES

The FORTRAN fuel optimization program was used to generate the ascent and descent tables for a flight from Las Vegas to Los Angeles that was constrained to a cruise altitude of 24,000 feet MSL. Baseline climb-out procedure is used to 3,000 feet AGL at which point the autopilot begins to capture a Mach-altitude profile on pitch derived from the optimal ascent table. While at 24,000 feet, the aircraft cruises at the optimal Mach number for that altitude and weight. At the descent point, the aircraft captures the descent Mach-altitude profile and tracks it until 3,000 feet AGL. The aircraft then captures this approach altitude and baseline procedure is followed from there to touchdown. Actual ascent and descent tables as output by the FORTRAN program are given in Appendices C-1 and C-2. Table 4-6 shows the climb-out and descent Mach-altitude profiles derived from the computer output.

Figures 4-41 and 4-42 show the barometric altitude versus the range for the constrained altitude optimal flight from Las Vegas to Los Angeles. The climb-out is identical to the baseline to 3,000 feet AGL. After the climb-out profile is captured, a smooth ascent is made to the cruise altitude 61 miles into the flight. The throttles retard at the point of descent (139 miles), but the aircraft must maintain altitude to slow down to the descent profile before it can begin a capture. A smooth descent is then made to the approach altitude and the remainder of the flight is identical to the baseline.

ORIGINAL PAGE IS  
OF POOR QUALITY

4-62

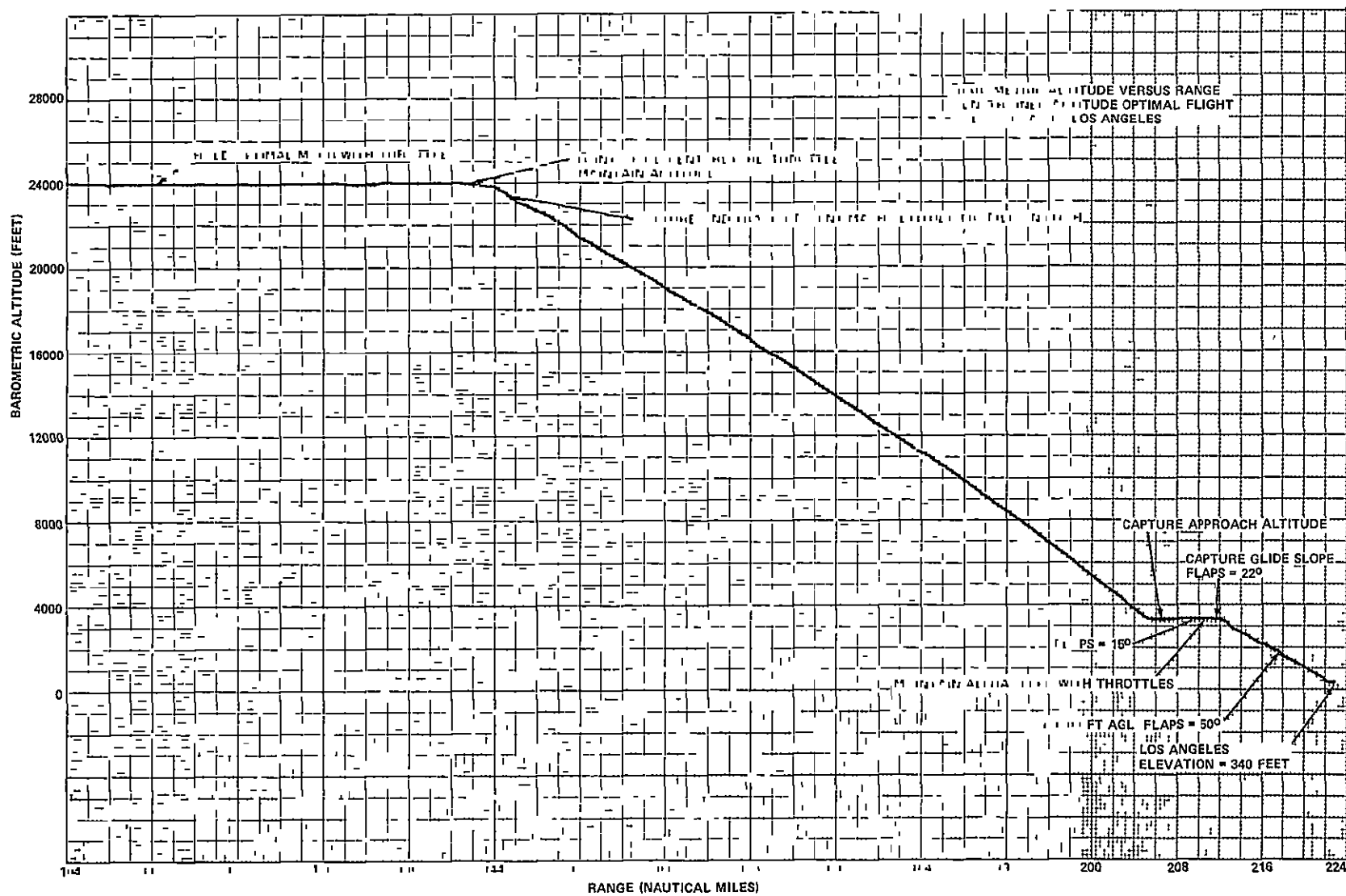


7167247

Figure 4-41

ORIGINAL PAGE IS  
OF POOR QUALITY

4-63



716-72 48

Figure 4-42

TABLE 4-6  
MACH-ALTITUDE PROFILE  
CONSTRAINED ALTITUDE OPTIMAL FLIGHT  
LAS VEGAS TO LOS ANGELES

Altitude (feet)	Climb-Out Mach	Descent Mach
3,000	--	.4552
4,000	--	.4544
5,000	.5193	.4527
6,000	.5252	.4531
7,000	.5316	.4538
8,000	.538	.4543
9,000	.5439	.4549
10,000	.5479	.4565
11,000	.5553	.4594
12,000	.5629	.4628
13,000	.5709	.4665
14,000	.5789	.4704
15,000	.5863	.4744
16,000	.5961	.4789
17,000	.6058	.4837
18,000	.6154	.489
19,000	.6251	.4981
20,000	.6356	.5075
21,000	.6455	.5155
22,000	.6528	.5243
23,000	.6516	.5346
24,000	.623	.552

Actual Mach-altitude profile for the climb-out is shown in Figure 4-43. The autopilot begins tracking the predetermined climb-out Mach-altitude profile of Table 4-6 to about 8,000 feet. Note that the profile peaks out at a little over .65 Mach and that the aircraft must then slow down to the cruise speed of .623 Mach.

Figure 4-44 shows Mach number versus barometric altitude for the descent. The aircraft has to slow down prior to beginning the Mach capture and does so

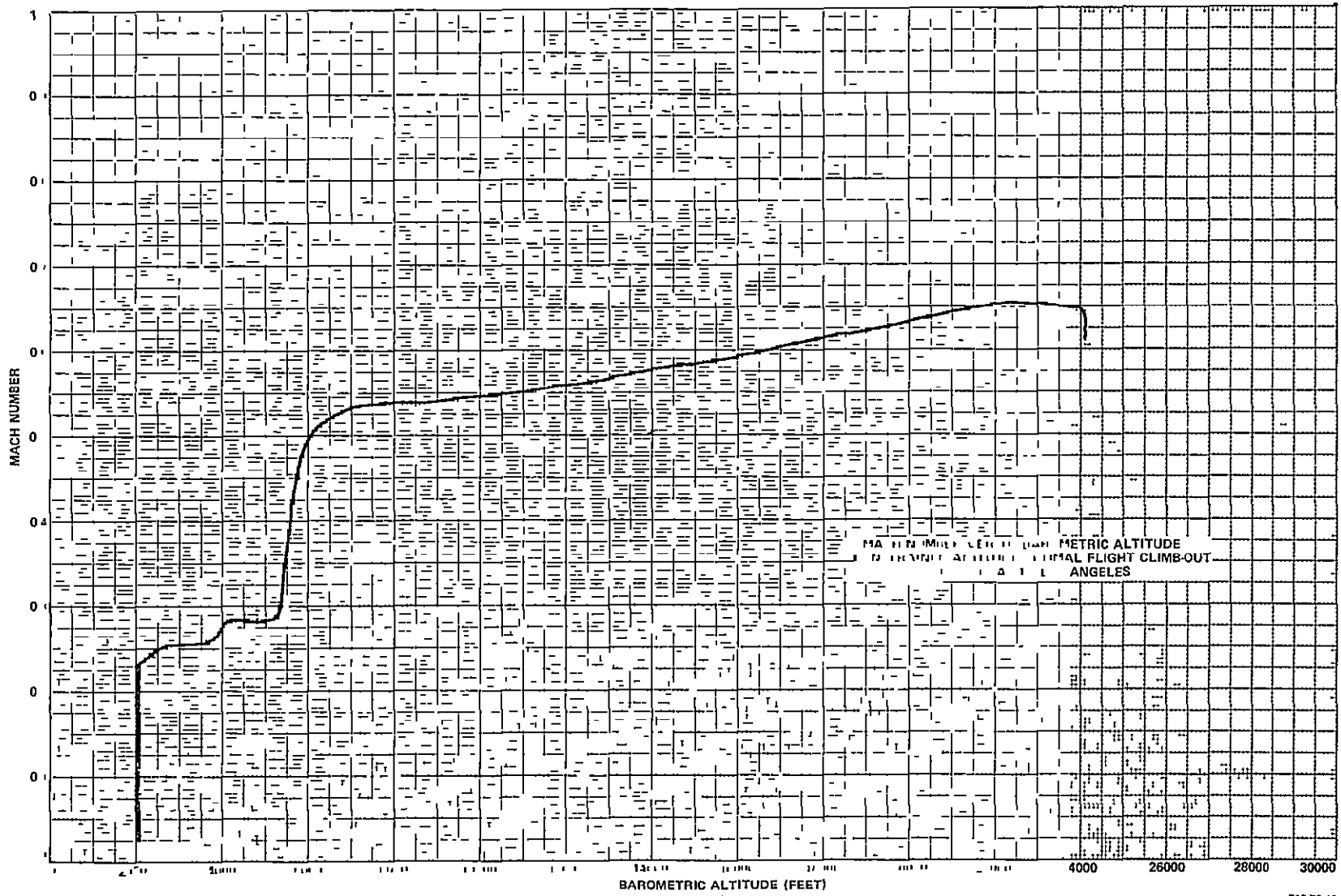


Figure 4-43

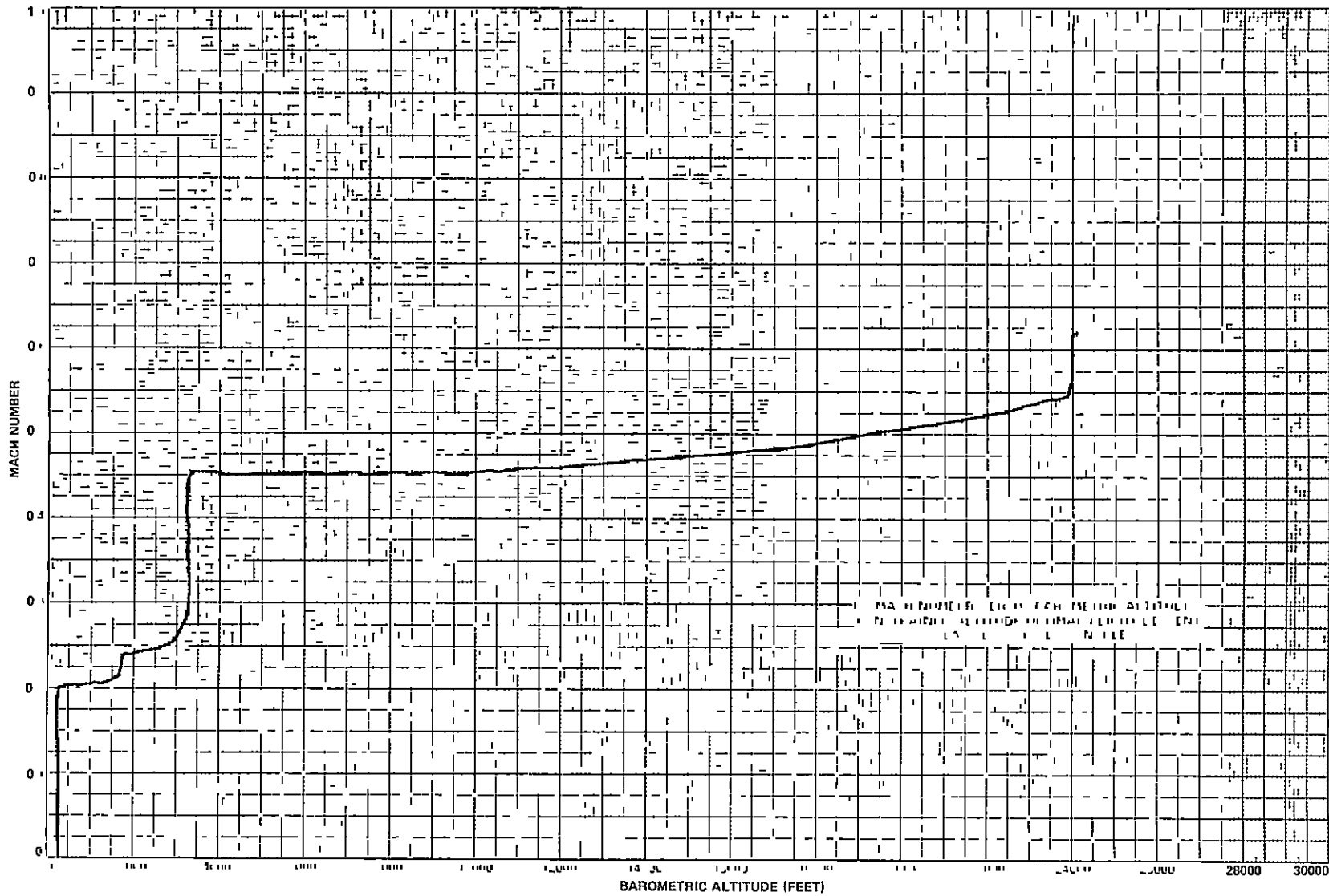


Figure 4-44

by maintaining altitude while the throttles are retarded. The descent Mach profile is then captured and tracked from about 23,000 feet down to the approach altitude of 3,000 feet AGL.

Calibrated airspeed versus the range is shown in Figures 4-45 and 4-46 for the climb-out and descent, respectively. While the climb-out Mach-altitude profile is being tracked, the calibrated airspeed is relatively constant, varying only from 300 to 290 knots. During the descent, however, the calibrated airspeed increases steadily from 230 knots up to 280 knots.

Figures 4-47 and 4-48 show flight path angle versus range for climb-out and descent. Again, it should be noted that the scale is somewhat exaggerated. The depression beginning at 4 miles in Figure 4-47 is due to the autopilot holding a vertical speed of about 600 feet per minute before the Mach capture begins. The large peak at 59 miles is due to the autopilot pitching the aircraft up slightly in order to slow down to the cruise Mach number. Once the cruise altitude is reached, the flight path angle goes to zero. When the descent Mach-altitude profile capture begins, the flight path angle drops sharply. It then slowly decreases as the profile is tracked until the approach altitude is reached. Behavior after this is the same as in the baseline flight.

Fuel consumption per unit distance,  $F_D$ , versus the range for the climb-out is shown in Figure 4-49. The large depression beginning at 60 miles is due to the transition to the cruise mode. The altitude capture begins and the autothrottle changes from holding the  $N_1$  limit to holding the cruise Mach. Since the cruise Mach is slower than the aircraft Mach number at the time of the transition, the throttles pull back to allow the aircraft to slow down. As the Mach approaches the cruise value, the throttles increase to hold this value.

Figure 4-50 shows the fuel consumption per unit distance versus the range for the descent. The general appearance of the curve is nearly identical to that for the baseline flight (Figure 4-17). There are only very slight differences in the value of  $F_D$  and the points at which events occur.



ORIGINAL PAGE IS  
OF POOR QUALITY

89-4

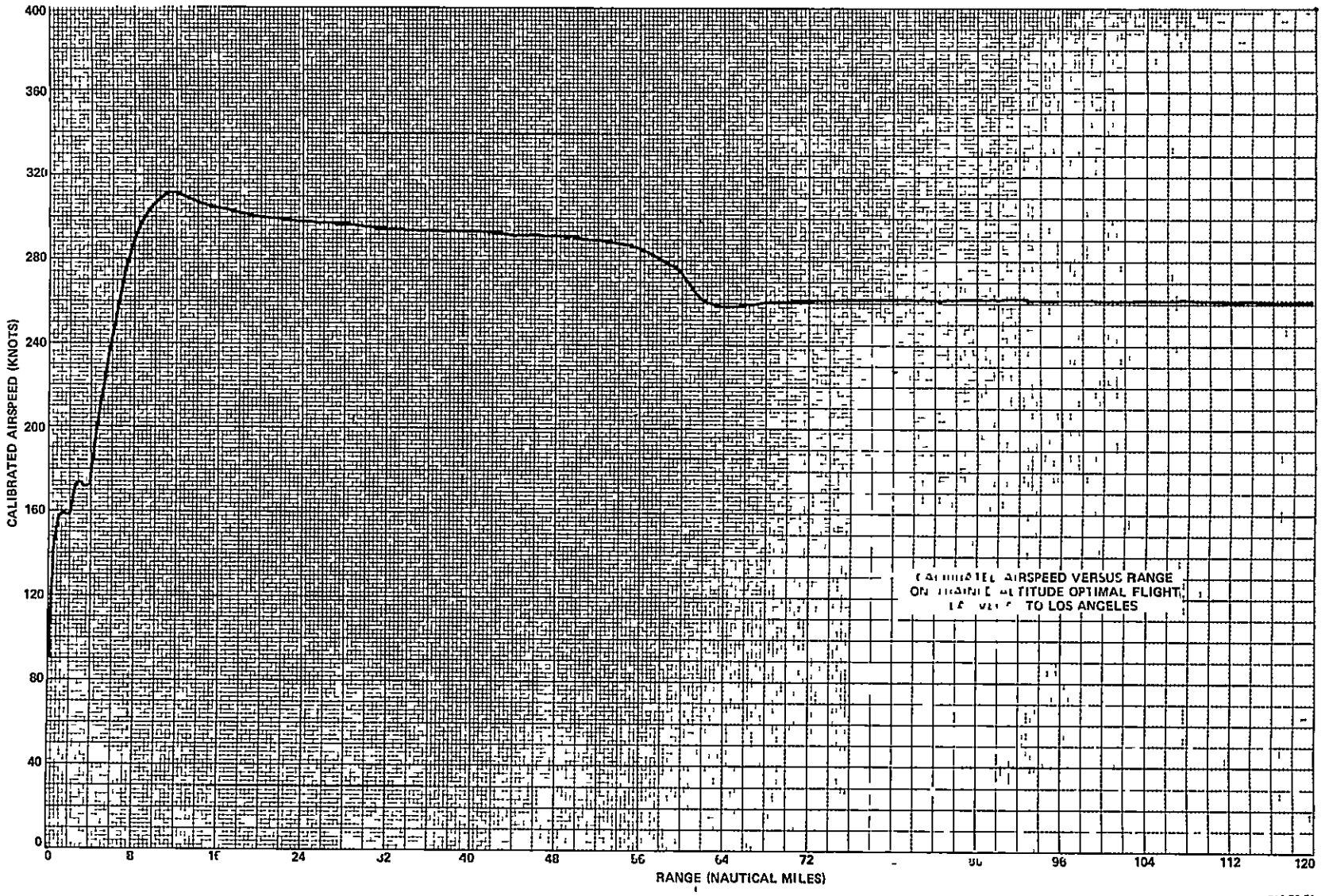


Figure 4-45

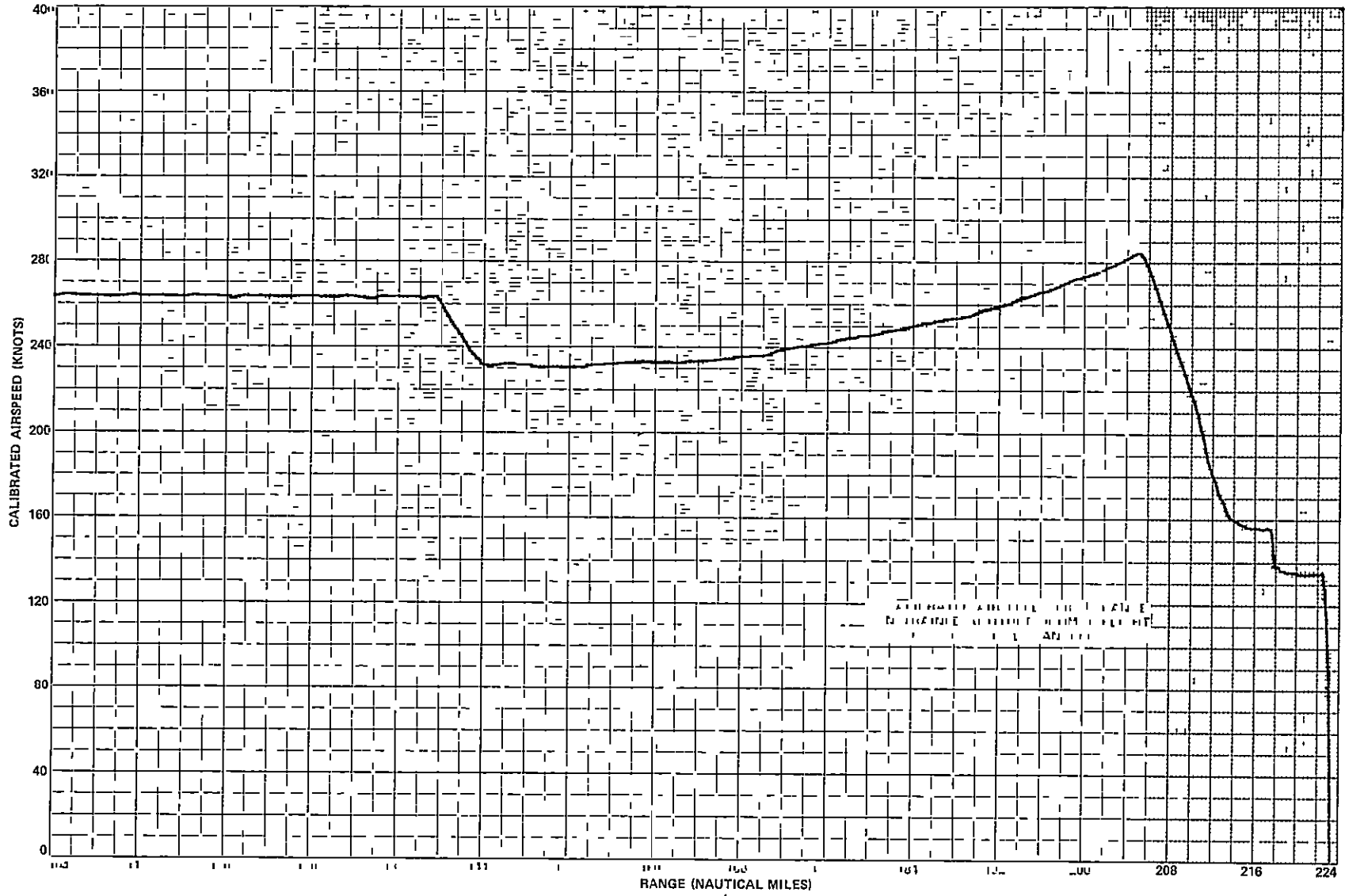


Figure 4-46

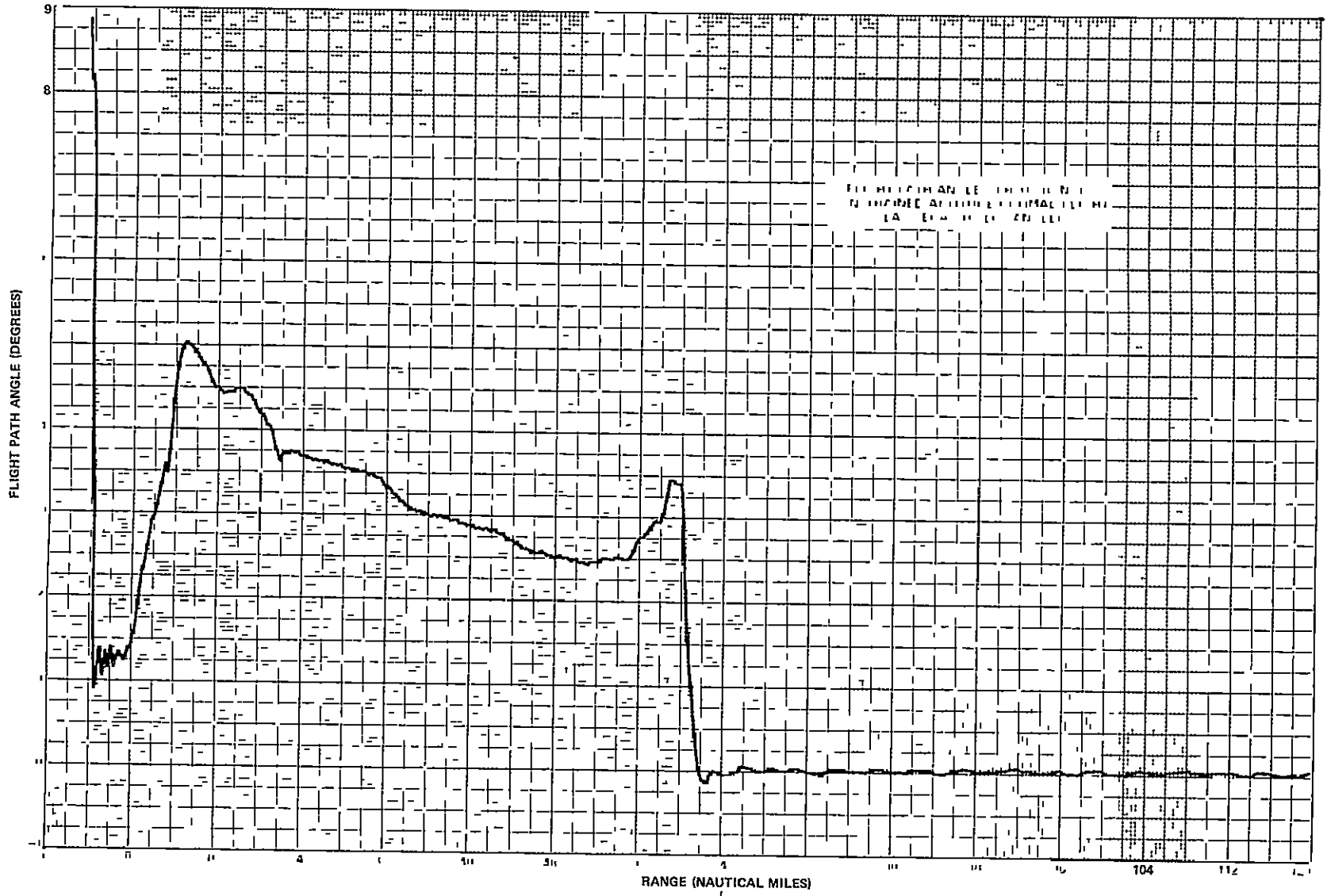


Figure 4-47

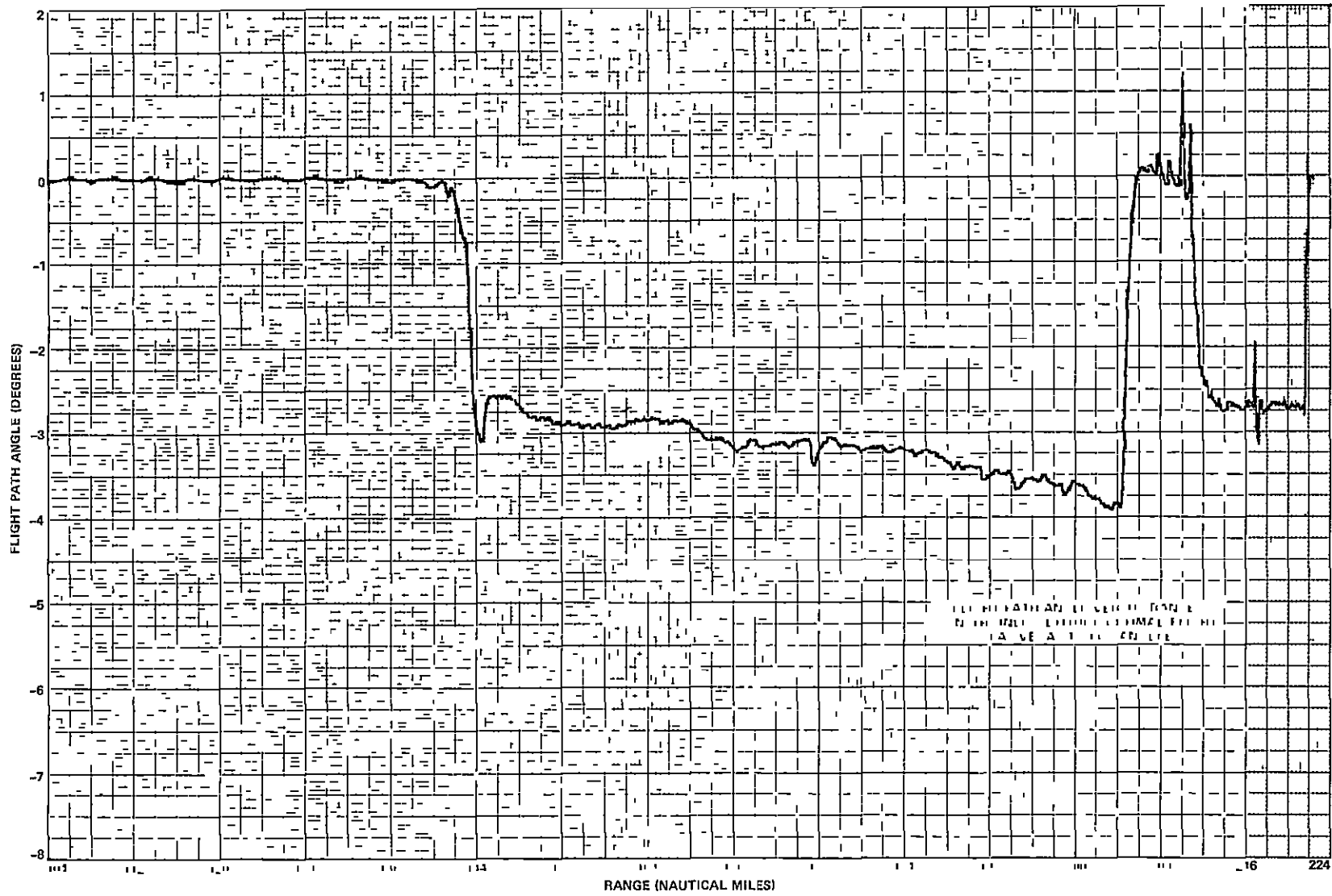


Figure 4-48

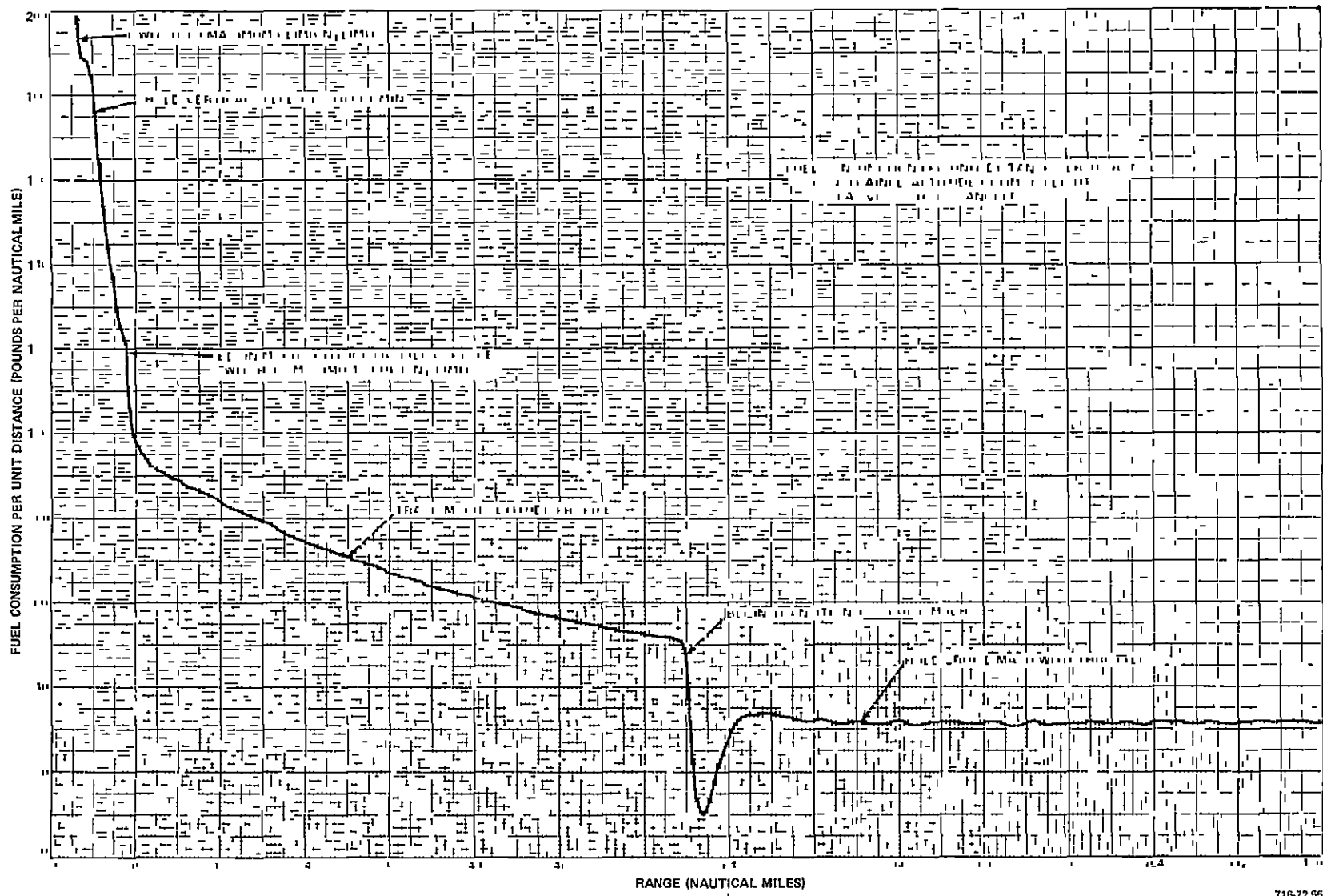


Figure 4-49

ORIGINAL PAGE IS  
OF POOR QUALITY

4-73

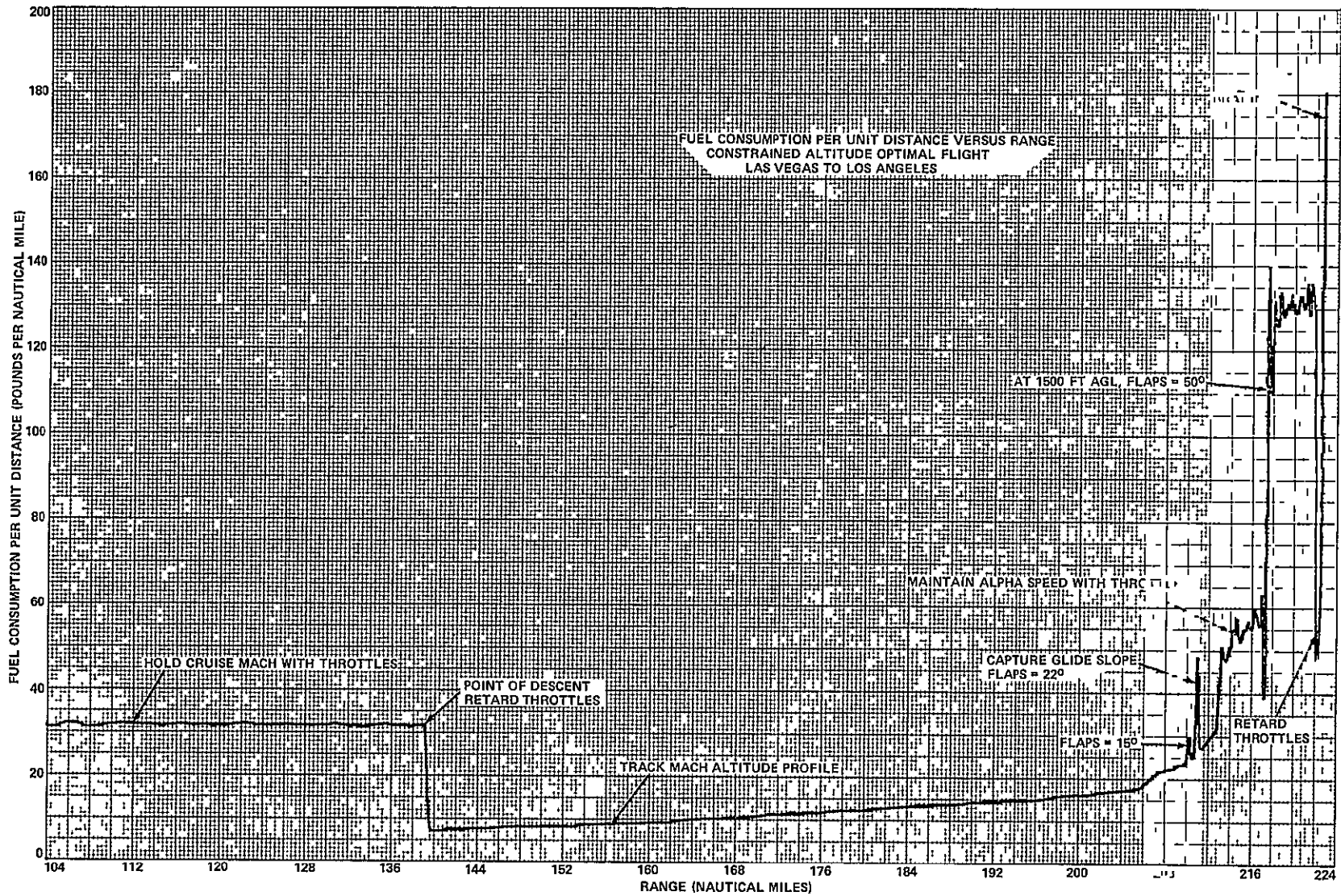


Figure 4-50

The total fuel consumed versus the range is shown in Figures 4-51 and 4-52. The slope change at 60 miles is due to the lower  $F_D$  value when the cruise begins. A second slope change at 140 miles is due to the throttles being retarded at the point of descent. The slope increases again near the end of the flight because of the increase in drag caused by the flap deployment and the necessary increase in fuel flow to maintain the approach speed.

Table 4-7 shows the results of several constrained altitude optimal flights from Las Vegas to Los Angeles. Average fuel consumption of 9,480 pounds is 592 pounds (5.9 percent) less than the baseline value. Average fuel consumption per unit distance is 42.58 pounds per nautical mile for a 2.67 pound per nautical mile saving over the baseline. Flight time increased 9.4 percent to 43 minutes and 6 seconds.

TABLE 4-7  
CONSTRAINED ALTITUDE OPTIMAL FLIGHT  
LAS VEGAS TO LOS ANGELES

Flight No.	Fuel Consumed (pounds)	$F_D$ (pounds/nmi)	Time (min, sec)
1	9,483	42.59	43, 8
2	9,478	42.58	43, 7
3	9,480	42.58	43, 8
4	9,480	42.58	43, 3
Averages	9,480	42.58	43, 6

#### H. UNCONSTRAINED ALTITUDE OPTIMAL FLIGHT: LAS VEGAS TO LOS ANGELES

The FORTRAN program was used to determine the optimal climb-out and descent profiles for the unconstrained altitude case from Las Vegas to Los Angeles. Table 4-8 shows the implemented profiles that were derived from the computer printout, which is given in Appendix D. The aircraft climbs out on the ascent profile to an altitude of 31,450 feet. At this point, the throttles are retarded and the autopilot begins to capture the descent profile. This requires the aircraft to maintain altitude for about 6 nautical miles in order to slow down to the descent profile.

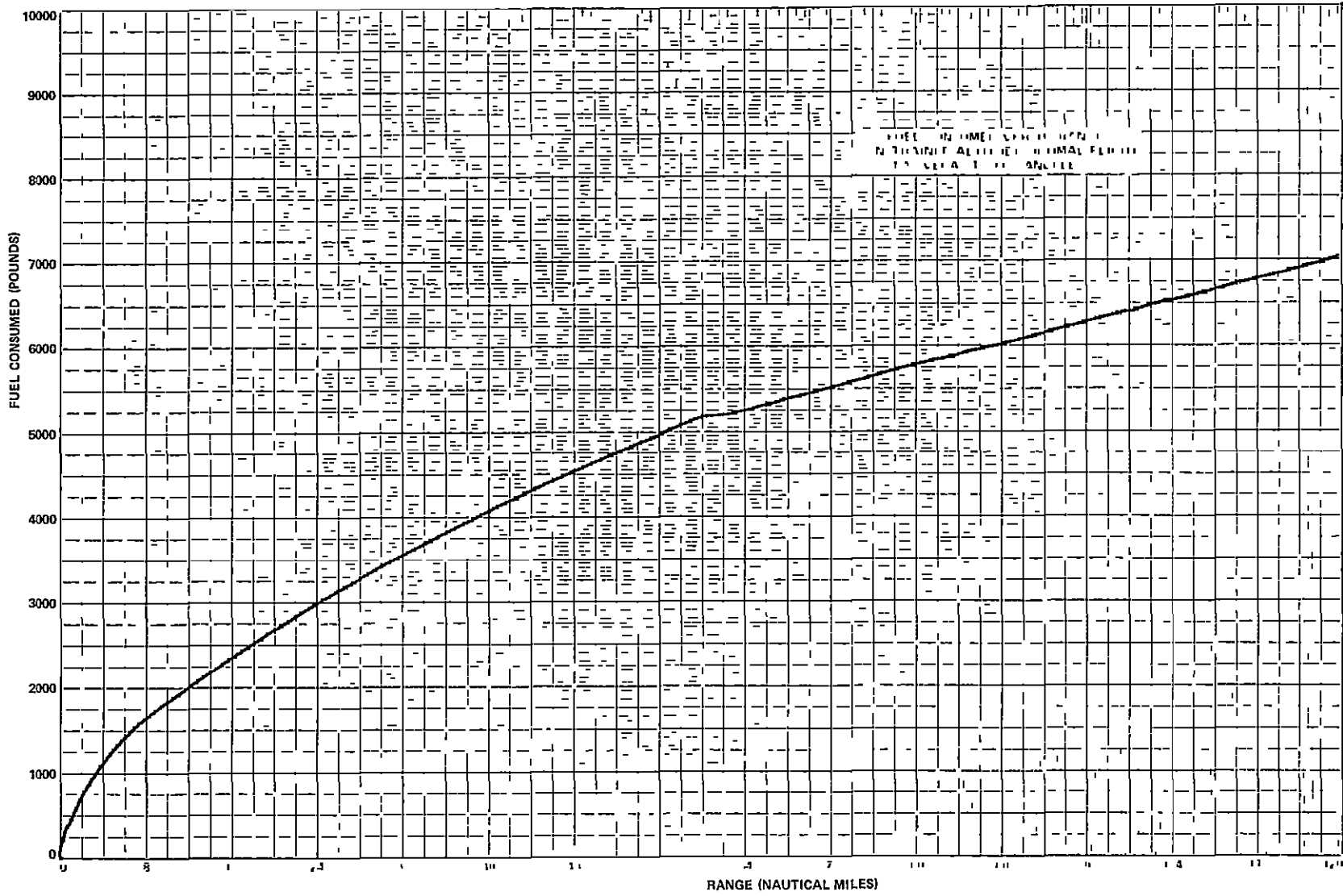


Figure 4-51



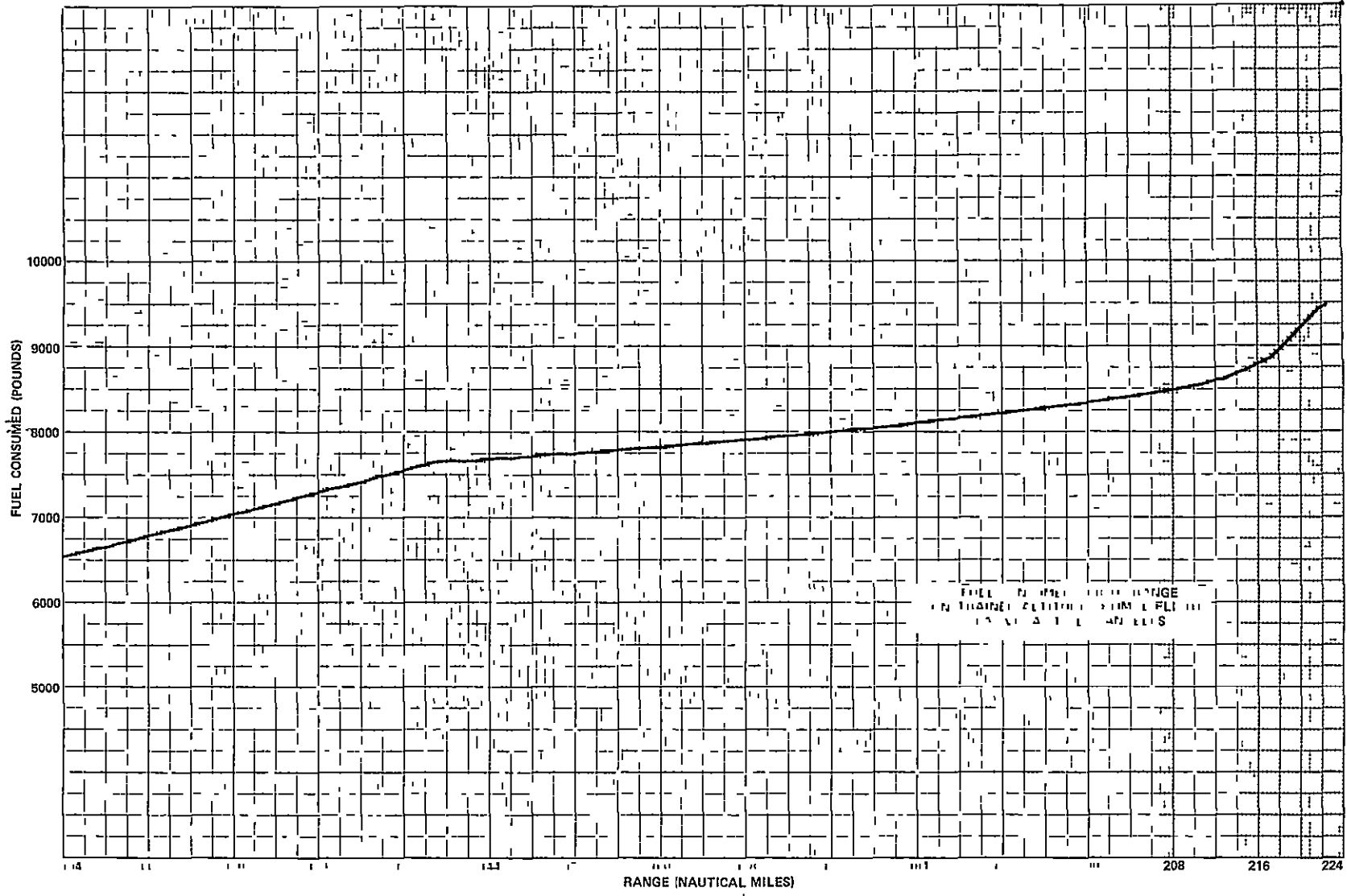


Figure 4-52

TABLE 4-8  
MACH-ALTITUDE PROFILE  
UNCONSTRAINED ALTITUDE OPTIMAL FLIGHT  
LAS VEGAS TO LOS ANGELES

Altitude (feet)	Climb-Out Mach	Descent Mach
3,000	--	.4717
4,000	--	.4600
5,000	.5152	.4653
6,000	.5206	.4646
7,000	.5266	.4653
8,000	.5329	.4654
9,000	.5386	.4655
10,000	.5417	.4626
11,000	.5486	.4691
12,000	.5556	.4707
13,000	.5628	.4742
14,000	.5701	.4779
15,000	.5768	.4831
16,000	.5859	.4859
17,000	.5951	.4894
18,000	.6040	.4941
19,000	.6133	.5025
20,000	.6238	.5109
21,000	.6335	.5189
22,000	.6432	.5273
23,000	.6543	.5358
24,000	.6651	.5454
25,000	.6758	.5541
26,000	.6910	.5649
27,000	.7013	.5759
28,000	.7126	.5922
29,000	.7248	.6084
30,000	.7309	.6193
31,000	.7286	.6357
32,000	.7034	.6521

Table 4-9 summarizes the data for the optimal flight path with unconstrained altitude. The average fuel consumption of 9,316 pounds is a 756 pound saving over the baseline flight, or 7.51 percent. The average  $F_D$  is 41.85 pounds per nautical mile which is 3.4 pounds per nautical mile (7.51 percent) less than the baseline flight. The flight time increased 3 minutes and 28 seconds (8.89 percent) over the baseline for a total of 42 minutes and 28 seconds.

TABLE 4-9  
FLIGHT DATA  
UNCONSTRAINED ALTITUDE OPTIMAL FLIGHT  
LAS VEGAS TO LOS ANGELES

Flight No.	Fuel Consumed (pounds)	$F_D$ (lb/nmi)	Time (min, sec)
1	9,320	41.86	42, 30
2	9,321	41.87	42, 30
3	9,311	41.82	42, 25
4	9,311	41.83	42, 28
Averages	9,316	41.85	42, 28

Figures 4-53 and 4-54 show the altitude versus the range for the optimal flight path with unconstrained altitude. Various flight events are indicated on each curve. As mentioned earlier, the short cruise segment is due to the slow-down period required to capture the descent profile.

Figures 4-55 and 4-56 show the fuel consumption per unit distance versus the range for the unconstrained optimal flight path. At peak altitude, the throttles are immediately retarded and the fuel flow drops from 38 pounds per nautical mile to 5 pounds per nautical mile with no cruise segment.

I. UNCONSTRAINED ALTITUDE OPTIMAL FLIGHT WITH DELAYED FLAP APPROACH:  
LAS VEGAS TO LOS ANGELES

Since the delayed flap approach does not require holding an approach altitude, the cruise segment can be longer. In the case of an unconstrained altitude flight from Las Vegas to Los Angeles, this means the aircraft can climb to a higher altitude before beginning the descent. Thus, the FORTRAN

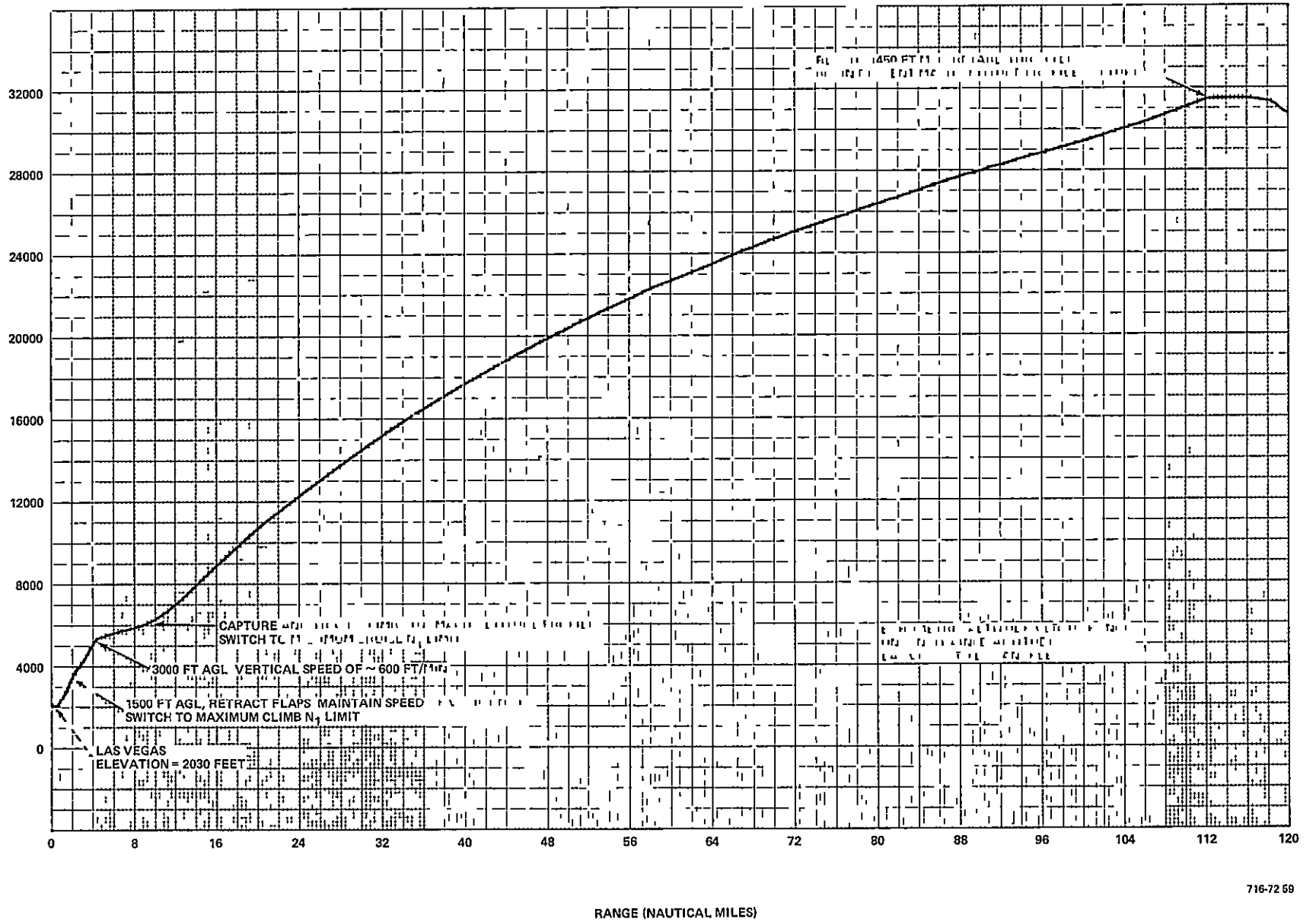


Figure 4-53

BAROMETRIC ALTITUDE (FEET)

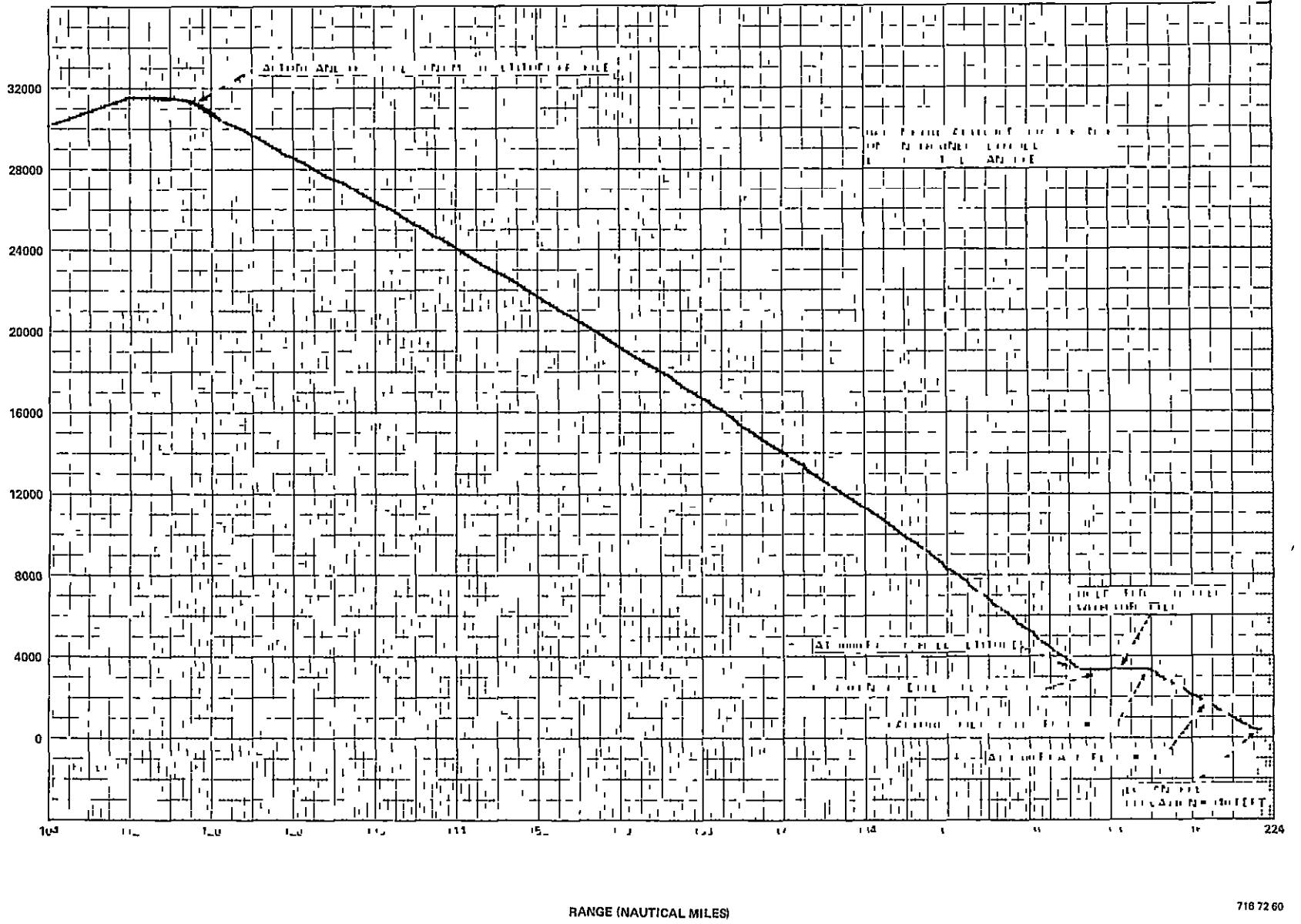


Figure 4-54

FUEL CONSUMPTION PER UNIT DISTANCE (POUNDS PER NAUTICAL MILE)

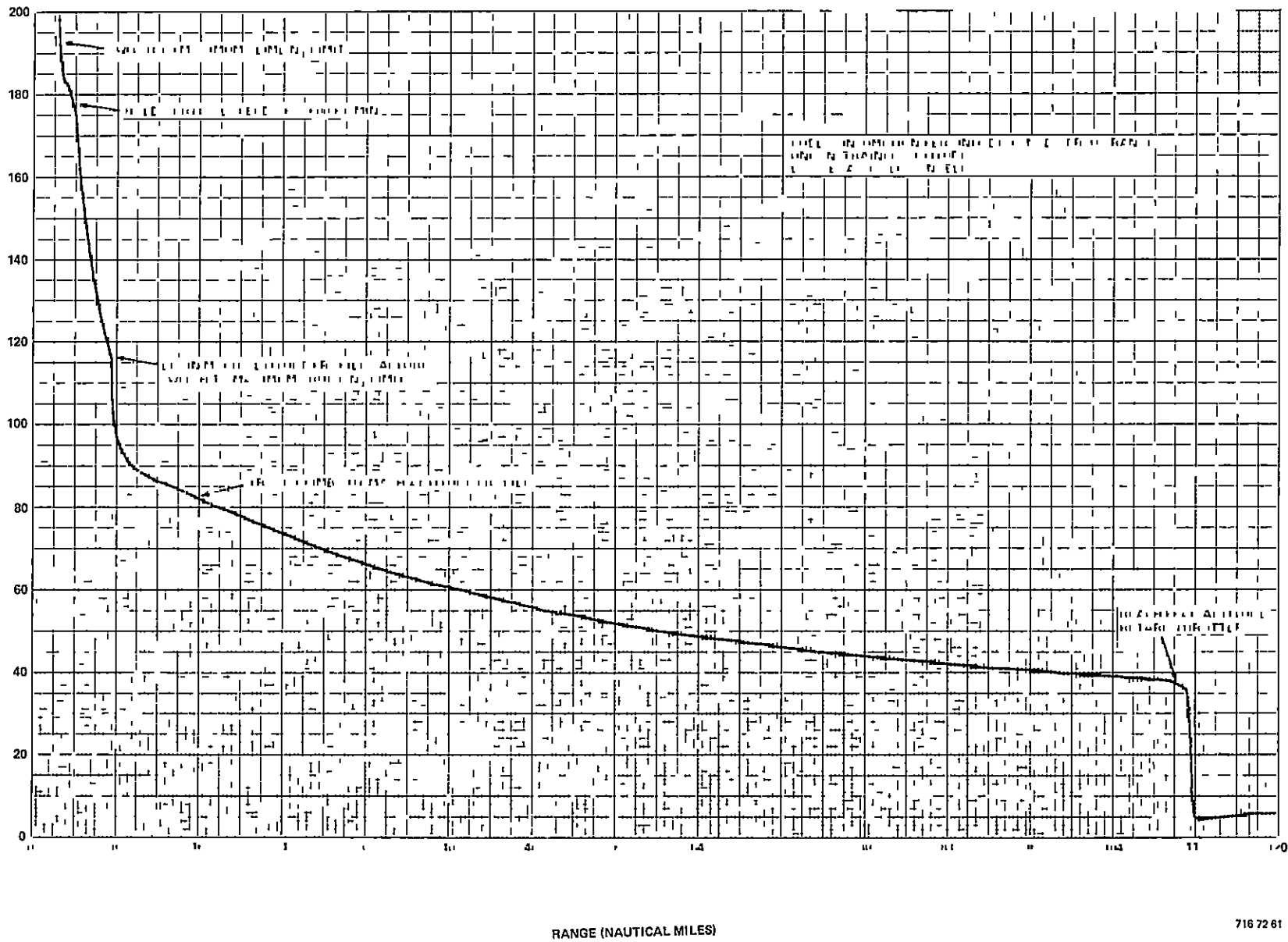


Figure 4-55

FUEL CONSUMPTION PER UNIT DISTANCE (POUNDS PER NAUTICAL MILE)

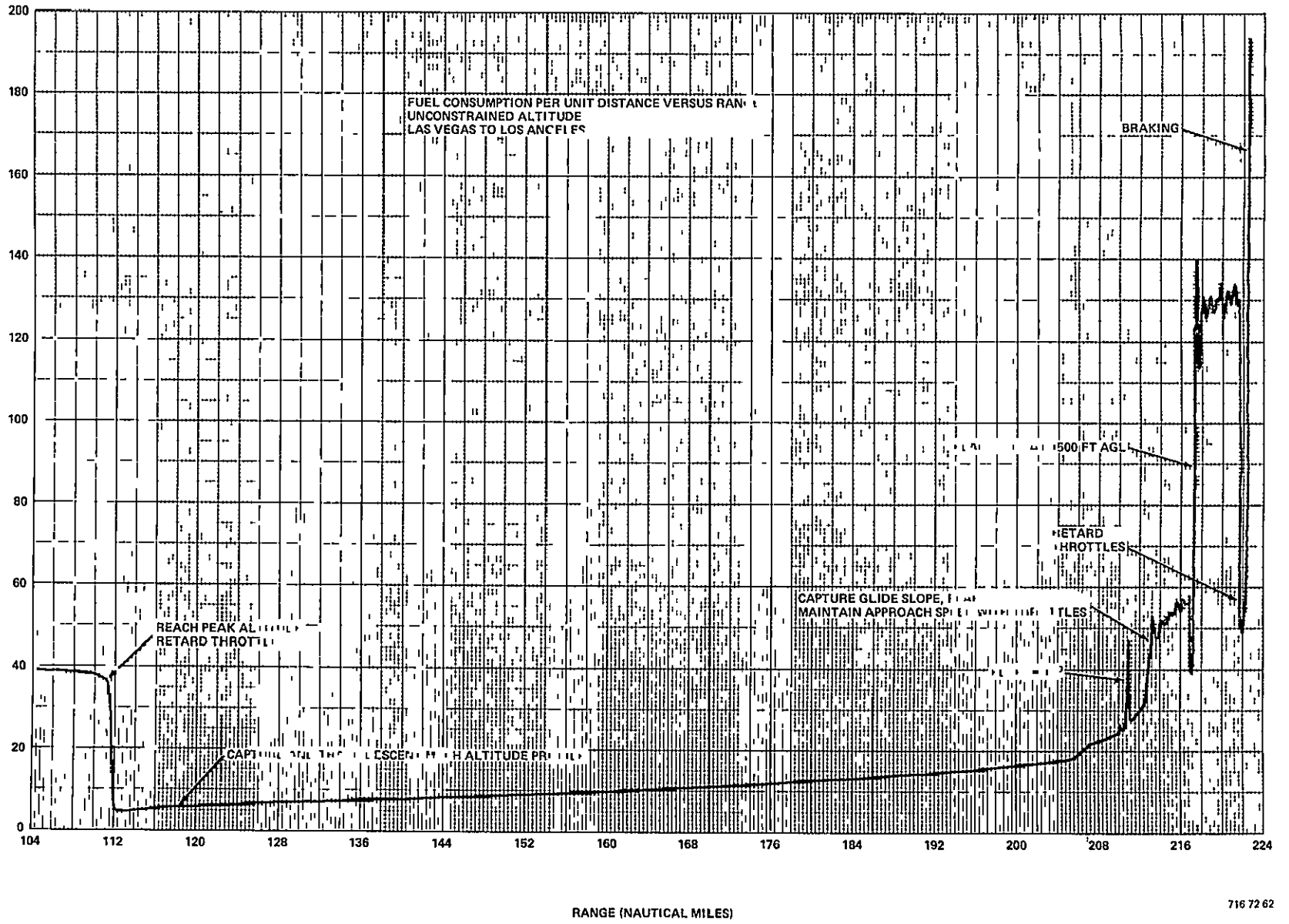


Figure 4-56

optimization program was used to generate new Mach-altitude profiles. Appendix E contains the actual computer printout while Table 4-10 shows the Mach-altitude profiles derived from that printout.

TABLE 4-10  
MACH-ALTITUDE PROFILE  
UNCONSTRAINED ALTITUDE OPTIMAL FLIGHT WITH DELAYED FLAP APPROACH  
LAS VEGAS TO LOS ANGELES

Altitude (feet)	Climb-Out Mach	Descent Mach
5,000	.5145	.4706
6,000	.5201	.4706
7,000	.5260	.4705
8,000	.5321	.4704
9,000	.5372	.4711
10,000	.5409	.4713
11,000	.5477	.4710
12,000	.5546	.4735
13,000	.5617	.4753
14,000	.5689	.4785
15,000	.5756	.4813
16,000	.5845	.4854
17,000	.5936	.4895
18,000	.6025	.4956
19,000	.6117	.5029
20,000	.6222	.5108
21,000	.6318	.5190
22,000	.6415	.5272
23,000	.6507	.5362
24,000	.6626	.5450
25,000	.6727	.5549
26,000	.6856	.5647
27,000	.6991	.5763
28,000	.7123	.5920
29,000	.7216	.6083
30,000	.7287	.6159
31,000	.7401	.6291
32,000	.7492	.6417
33,000	.733	.6573



Barometric altitude versus the range is shown in Figures 4-57 and 4-58. Note that the peak altitude is reached at the same distance (112 miles) into the flight as the unconstrained altitude flight with a normal approach (Figure 4-53). The altitude, however, is 32,600 feet MSL instead of 31,450 feet MSL. Seven miles are now required for slow-down before the descent profile can be captured. Glide slope is captured at 200 miles.

Figures 4-59 and 4-60 show the fuel consumption per unit distance versus the range. The throttles begin to pull back as the altitude capture begins in order to hold the cruise Mach and then quickly retard when the capture is completed. As in the baseline case with delayed flaps, there are no spikes in  $F_D$  during the approach until full landing flaps are deployed and power is applied to maintain airspeed.

The flap position during the approach is shown versus the range in Figure 4-61. Initial flap deployment begins at 202.6 miles while full landing flaps (50 degrees) are deployed at 219.5 miles.

Figures 4-62 and 4-63 show the calibrated airspeed versus the range. Again, the calibrated airspeed changes little during climb-out, varying only from 300 to 270 knots. The same is true for the descent, except at the lower altitudes where the calibrated airspeed increases more rapidly.

Table 4-11 shows the results for several unconstrained altitude flights with the delayed flap approach. Average fuel consumption of 8,993 pounds is 1,079 pounds (or 10.7 percent) less than that for the baseline flight. Fuel consumption per unit distance thus decreased 10.7 percent to 40.42 pounds per nautical mile. Flight time, however, only increased 5.8 percent to 41 minutes and 16 seconds.

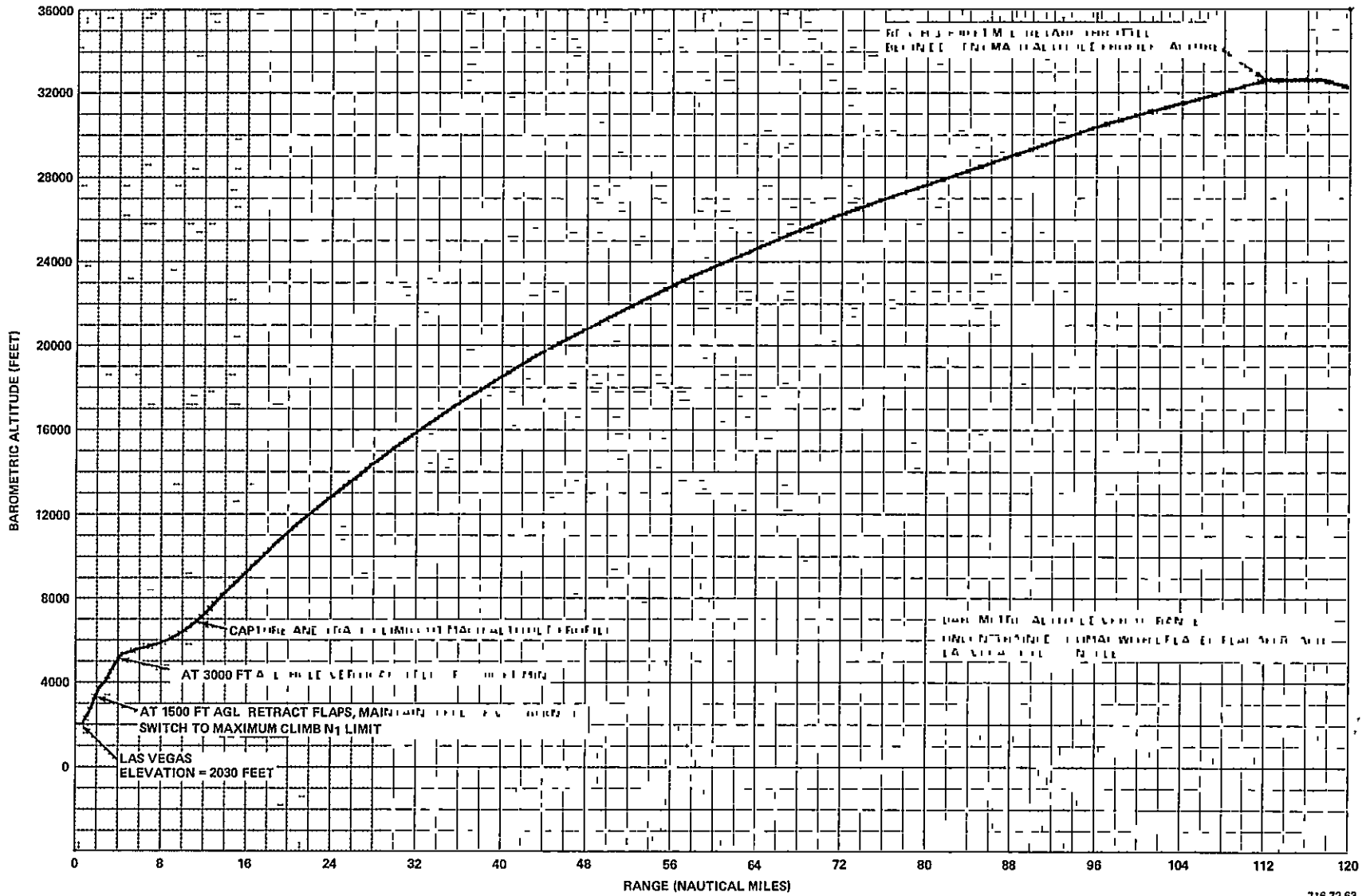


Figure 4-57

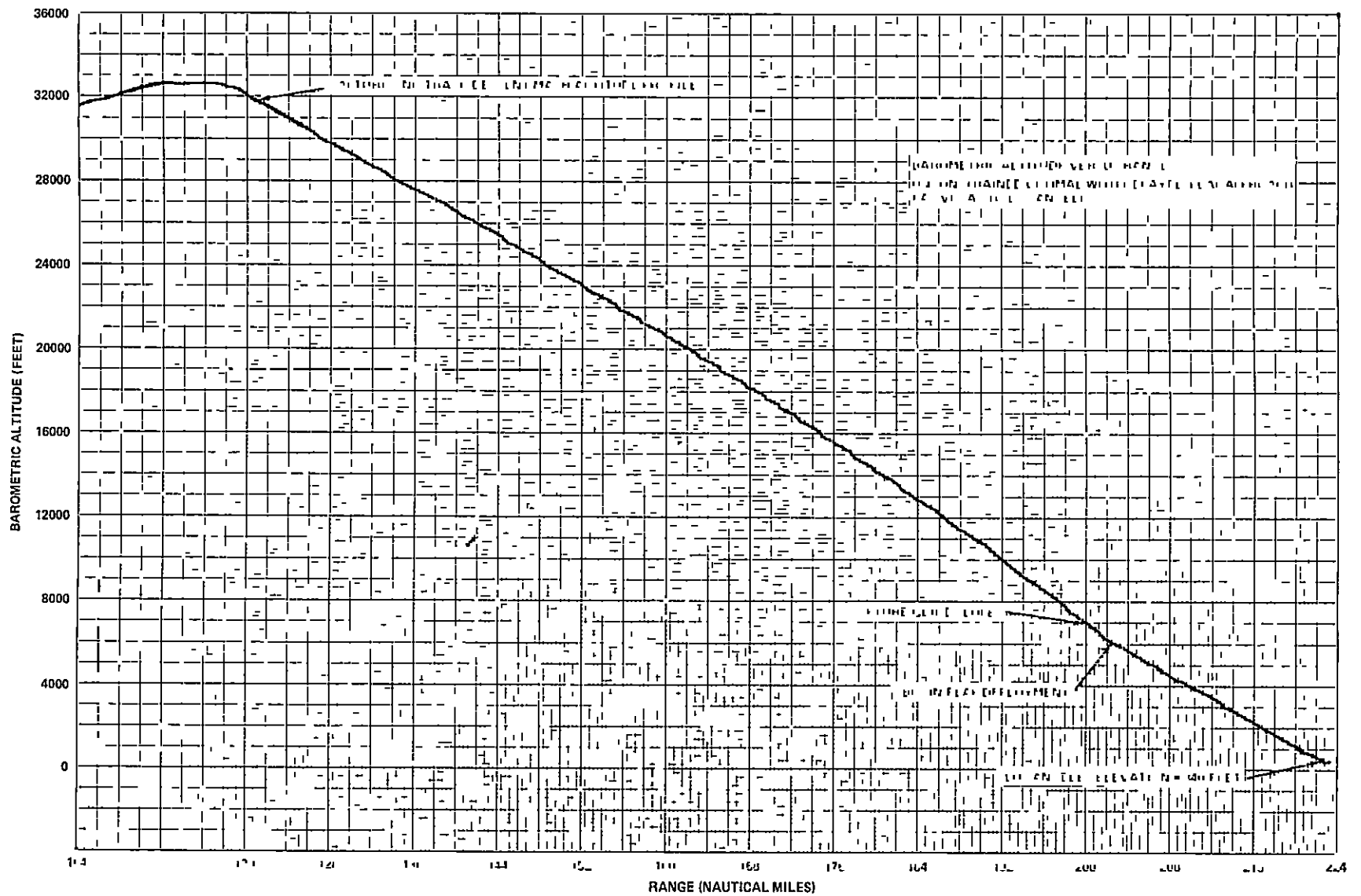


Figure 4-58

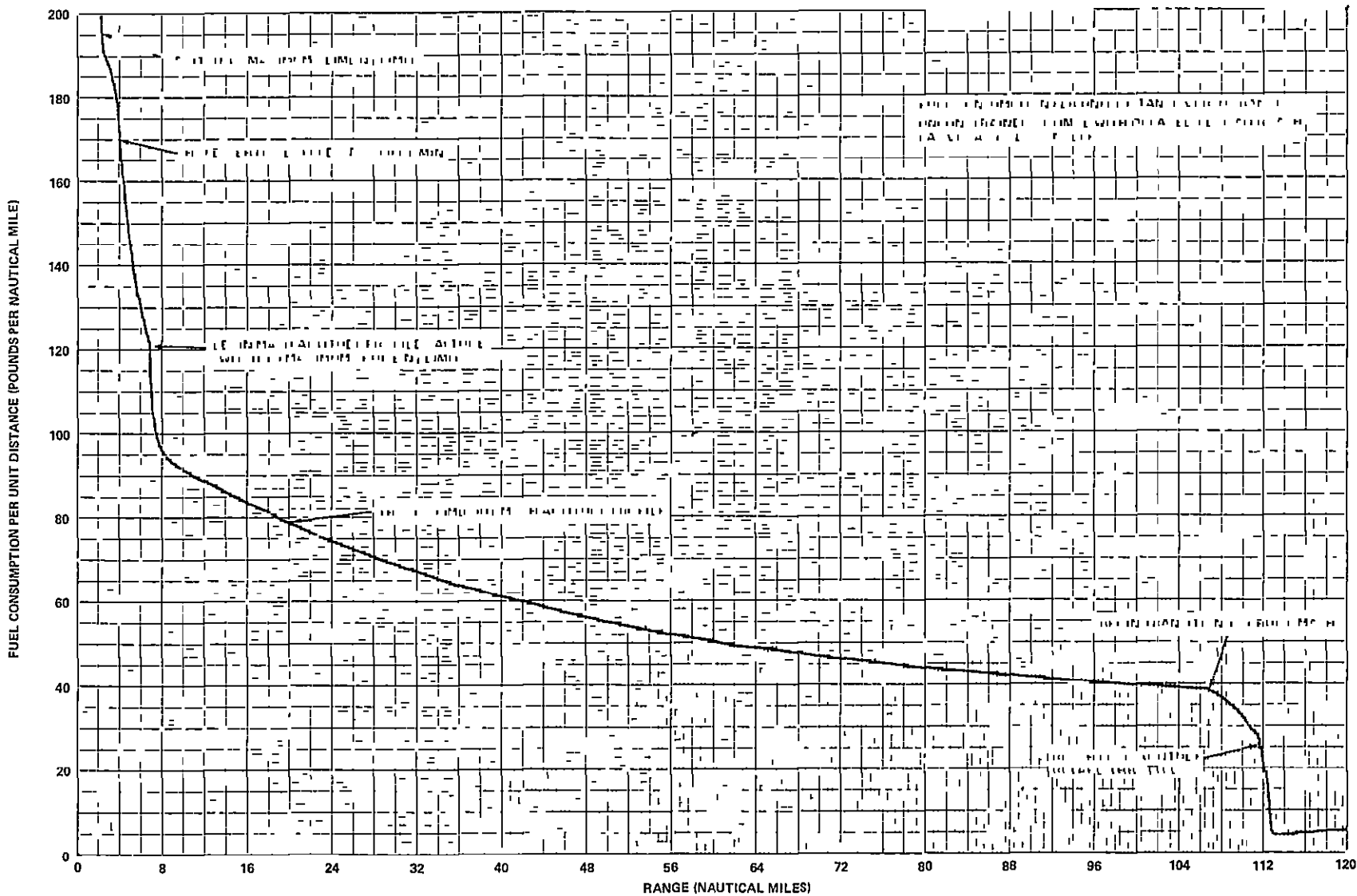


Figure 4-59

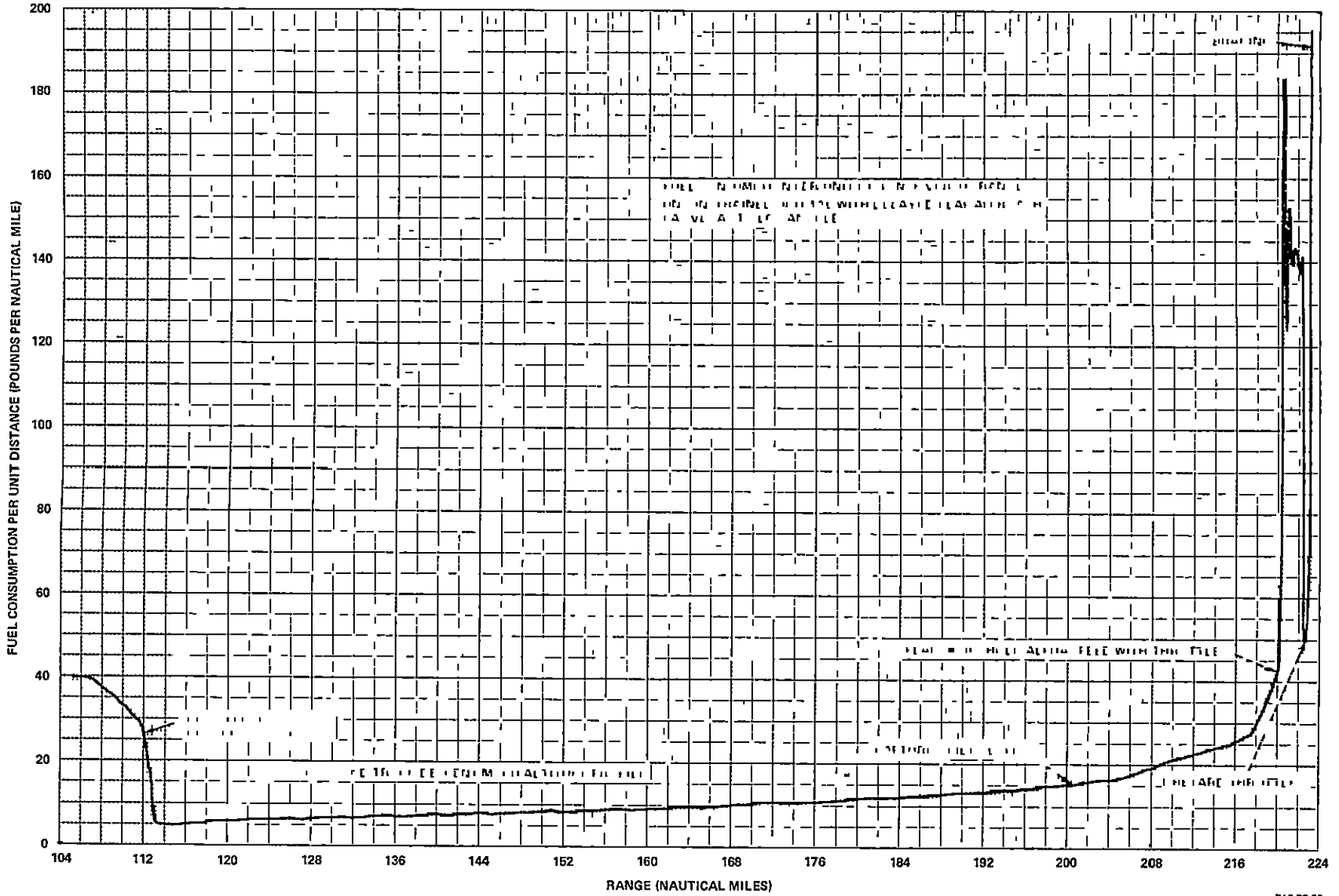


Figure 4-60

ORIGINAL PAGE IS  
OF POOR QUALITY

68-7

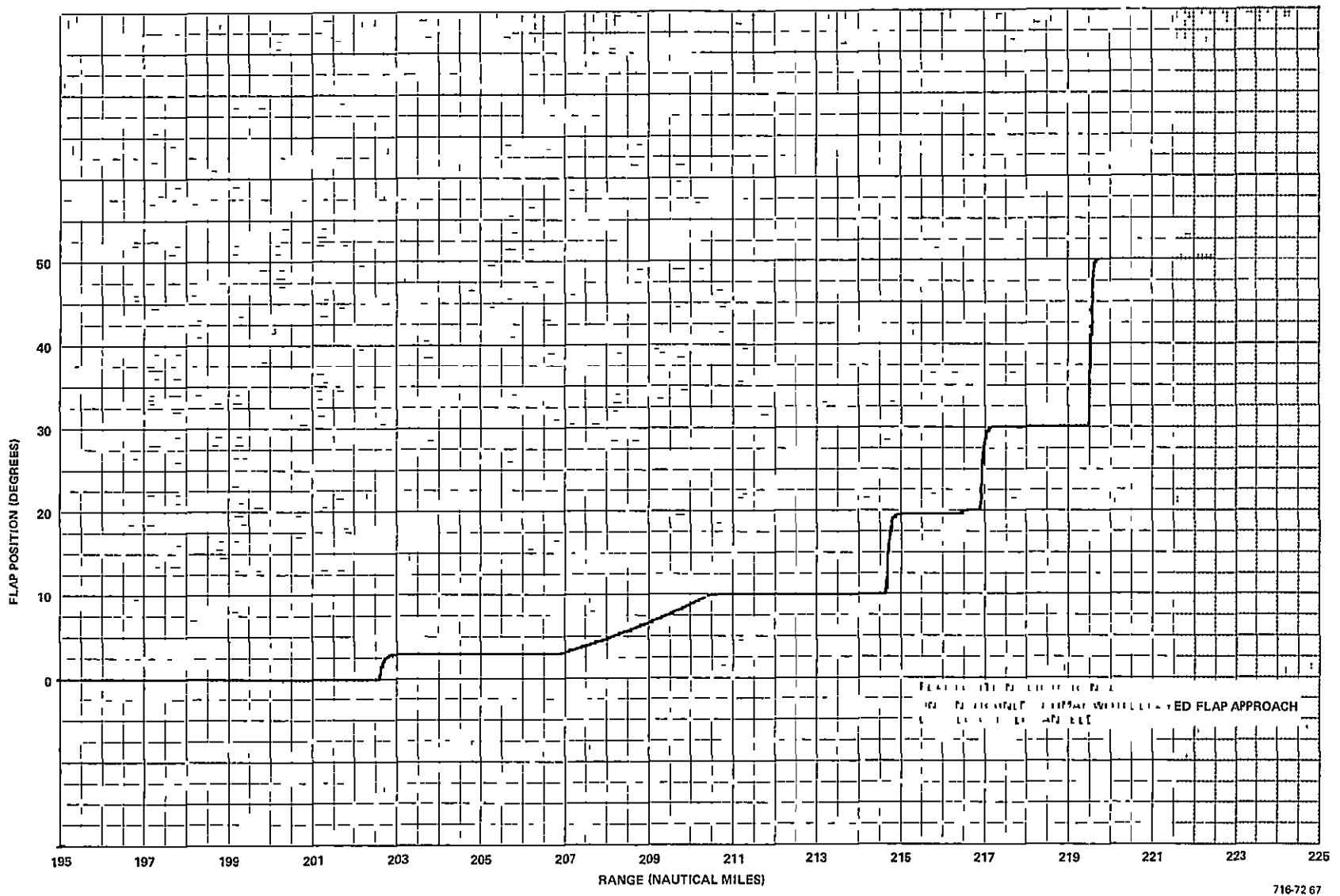


Figure 4-61

06-7

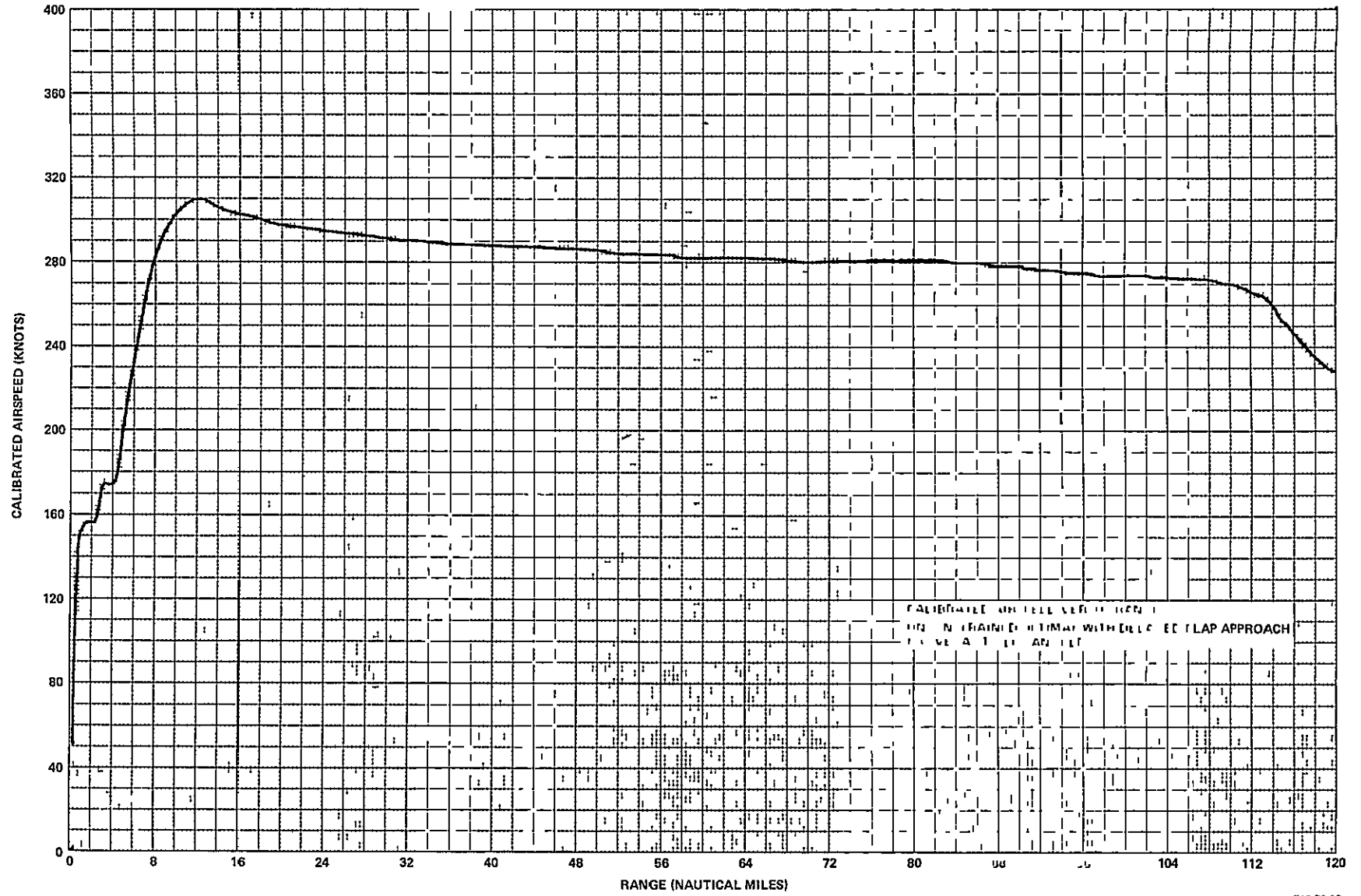


Figure 4-62

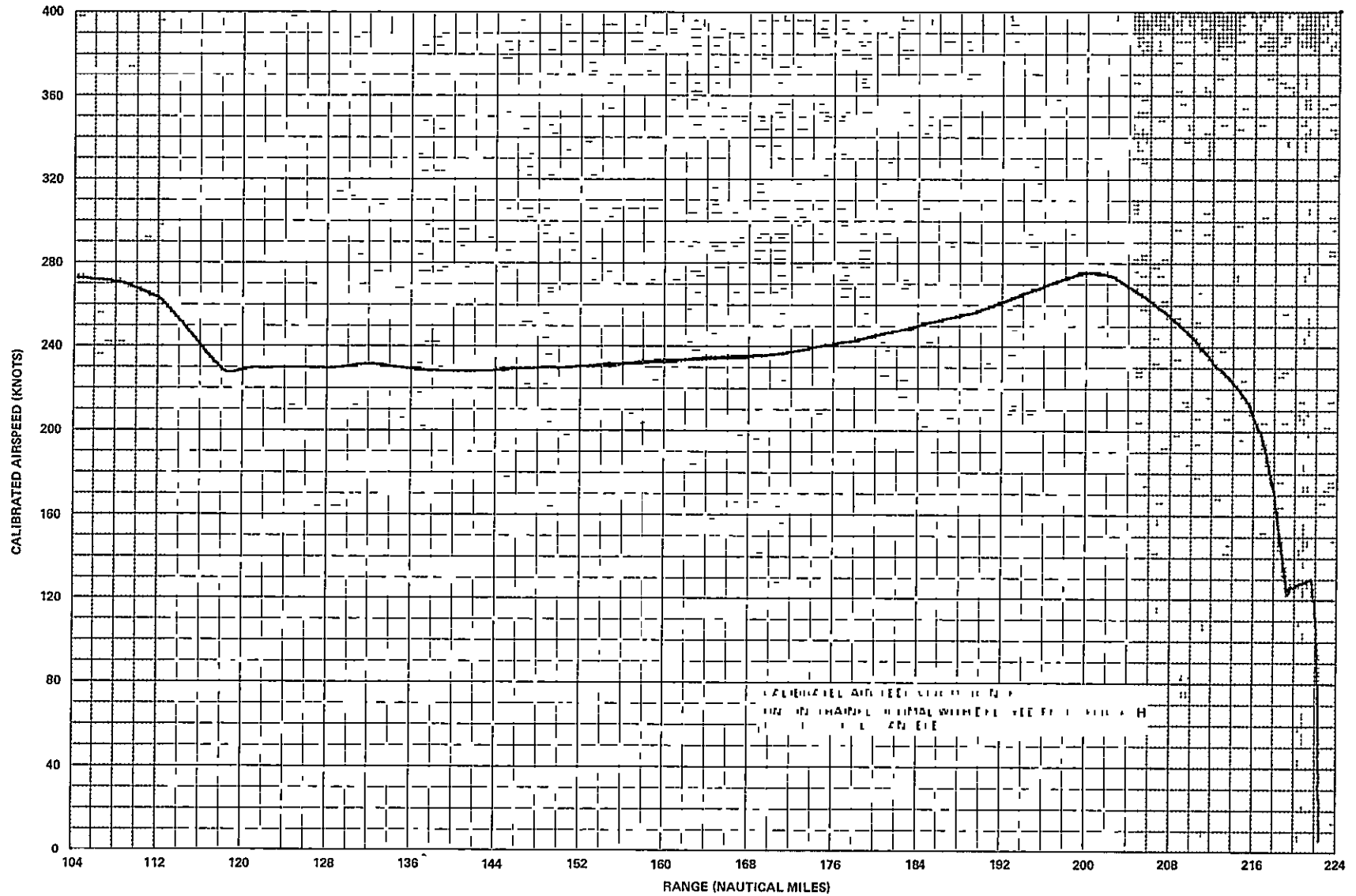


Figure 4-63



TABLE 4-11  
 FLIGHT DATA  
 UNCONSTRAINED ALTITUDE OPTIMAL FLIGHT WITH DELAYED FLAP APPROACH  
 LAS VEGAS TO LOS ANGELES

Flight No.	Fuel Consumed (pounds)	$F_D$ (lb/nmi)	Time (min, sec)
1	9,005	40.44	41, 17
2	8,983	40.37	41, 18
3	9,001	40.47	41, 14
4	8,972	40.32	41, 15
5	9,006	40.48	41, 14
Averages	8,993	40.42	41, 16

J. BASELINE FLIGHT: CHICAGO TO LAS VEGAS

To provide some insight into the effects of fuel optimization strategies on intermediate range flights, the leg from Chicago to Las Vegas was studied. The baseline profile for this leg was included in Section III. Figure 4-64 shows the lateral flight path in terms of the latitude and longitude for the flight from Chicago to Las Vegas.

Figure 4-65 shows barometric altitude versus range for the initial climb-out and cruise segment of the baseline flight. At about 30,000 feet MSL, the  $N_1$  limit is changed back to the maximum climb mode because the rate of climb drops below 1,000 feet per minute. The cruise Mach of about .83 is attained, then held on pitch from 33,500 feet to the initial cruise altitude of 35,000 feet MSL. Cruise altitude is reached 156 miles into the flight.

The enroute climb in altitude is shown in Figure 4-66. At 652 miles, the throttles are increased to the maximum climb  $N_1$  limit and the Mach is held on pitch. The new cruise altitude of 39,000 feet MSL is achieved 43 miles later, and the aircraft returns to the cruise mode.

Figure 4-67 shows the barometric altitude versus the range for the descent segment of the baseline flight. Descent begins at 1,242 miles as the throttles are retarded and the aircraft pitches down to increase the calibrated airspeed. The rest of the descent is then the same as for the

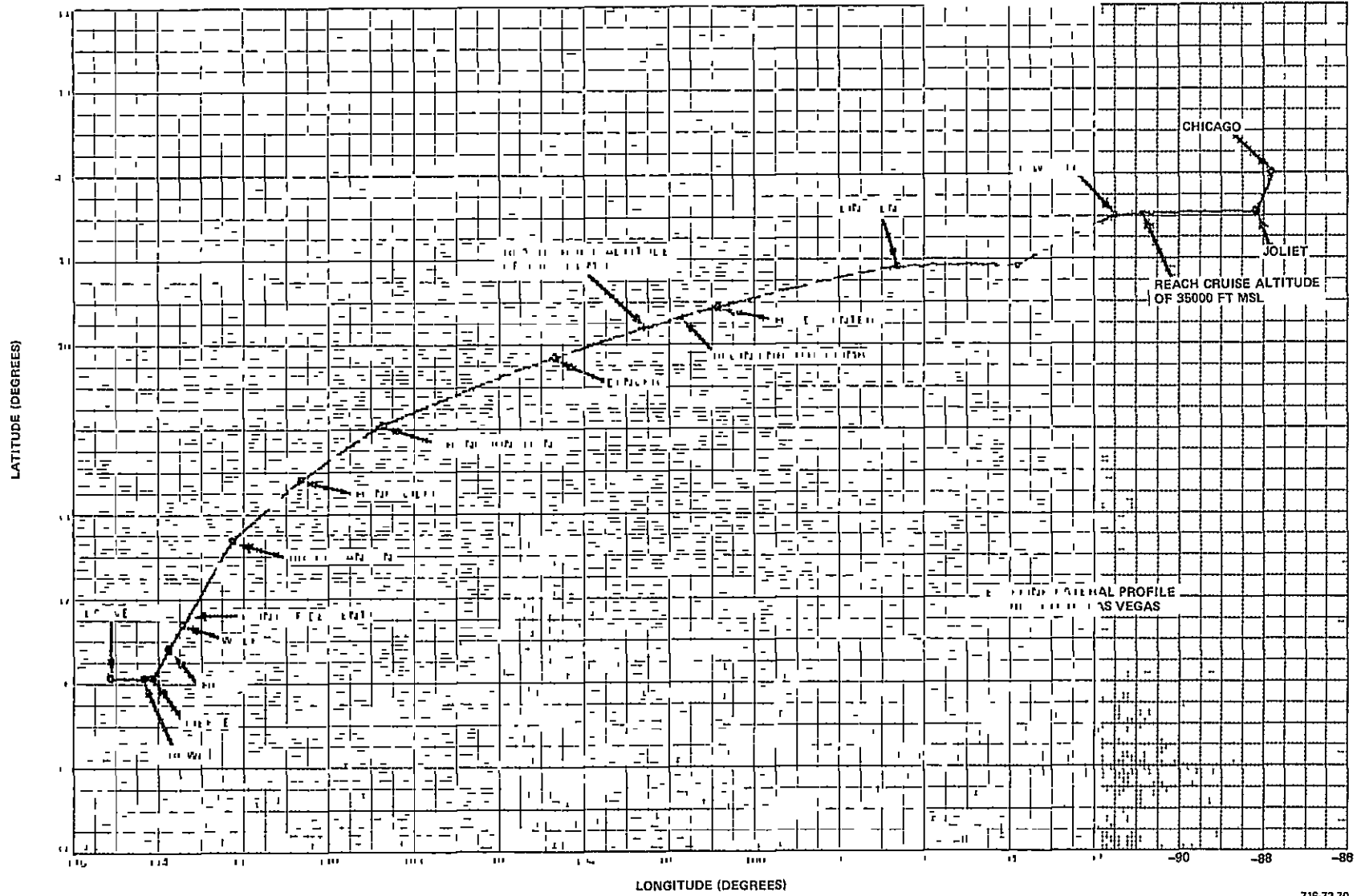


Figure 4-64

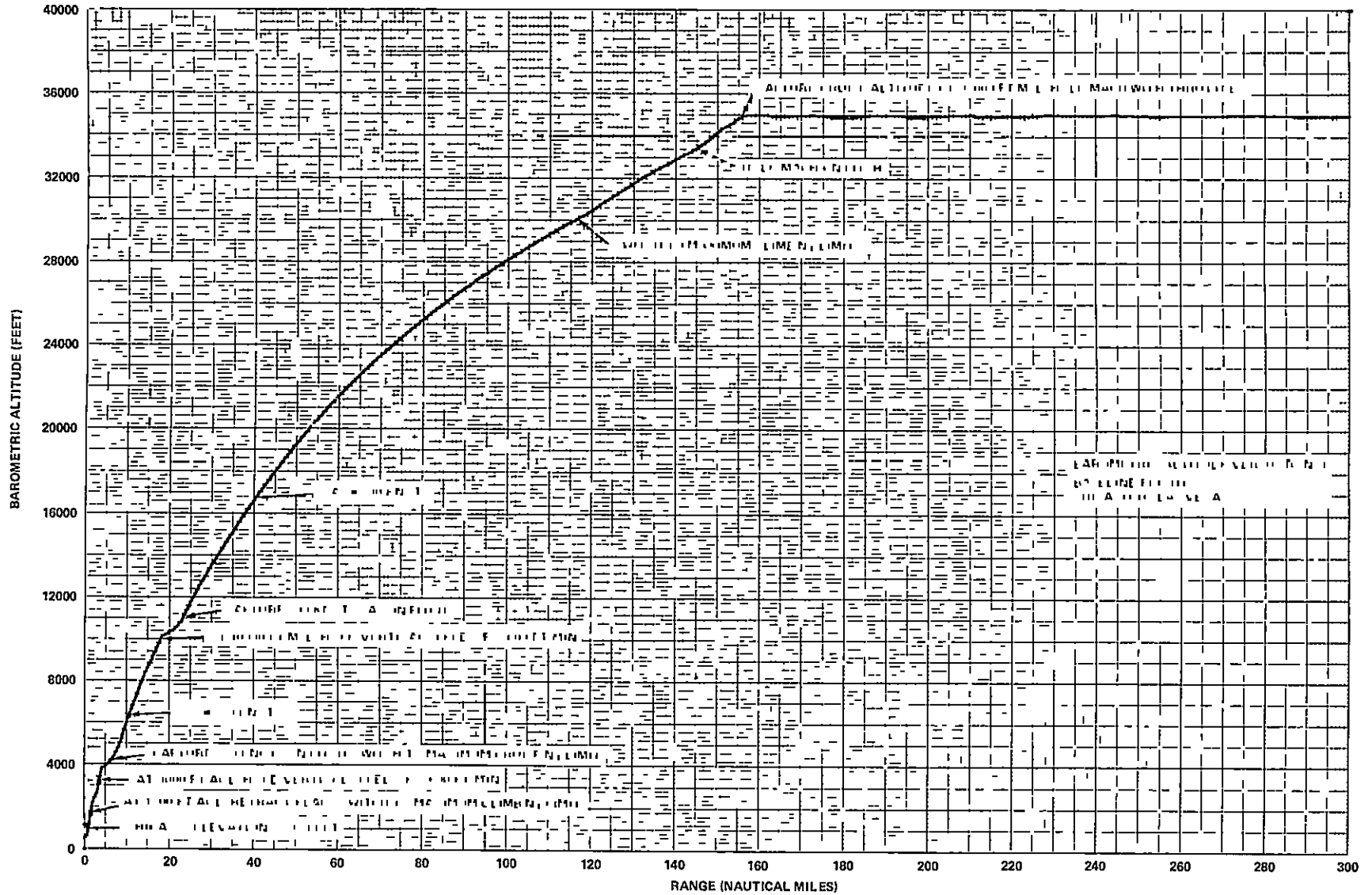


Figure 4-65

ORIGINAL PAGE IS  
OF POOR QUALITY

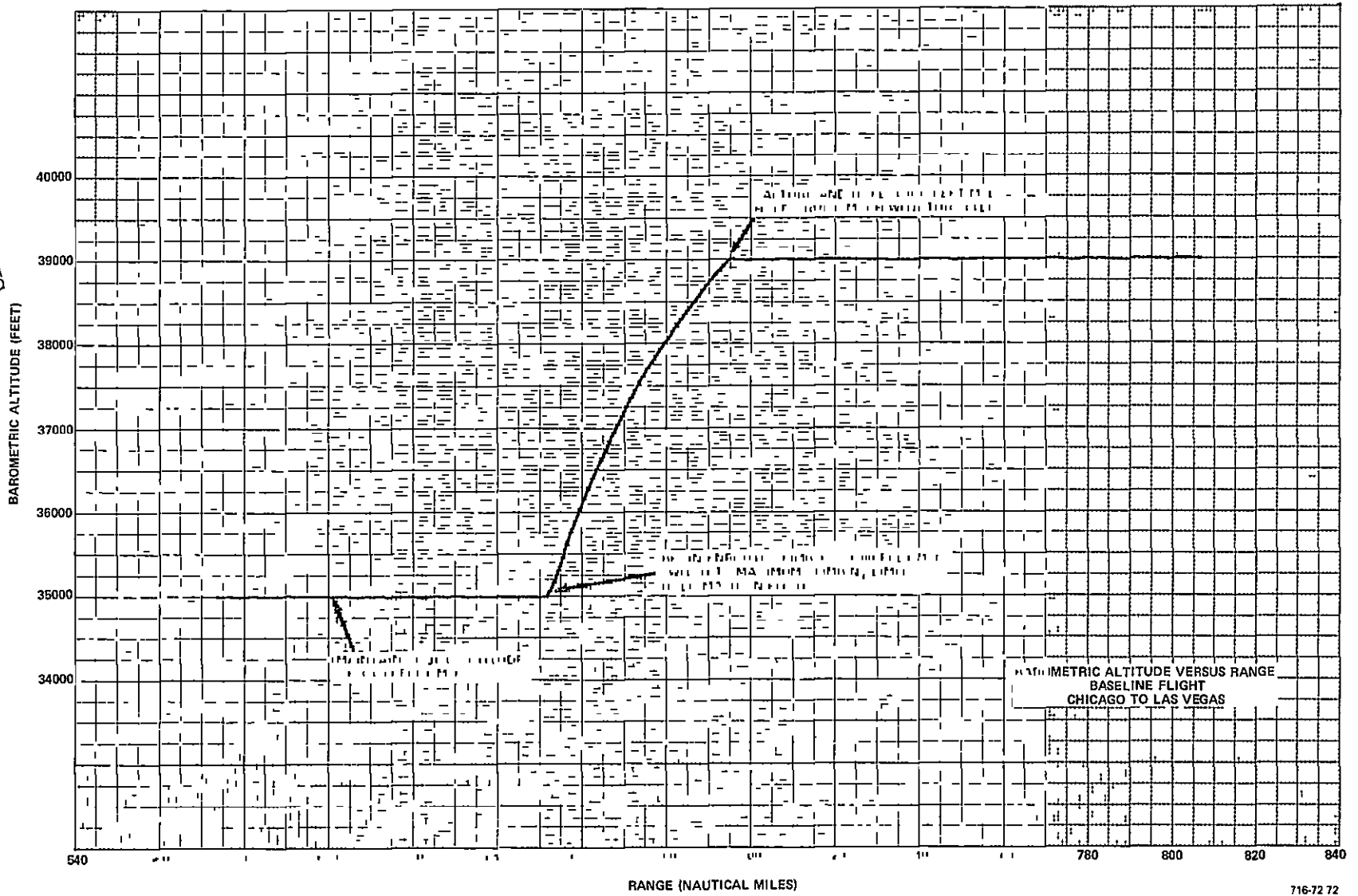


Figure 4-66

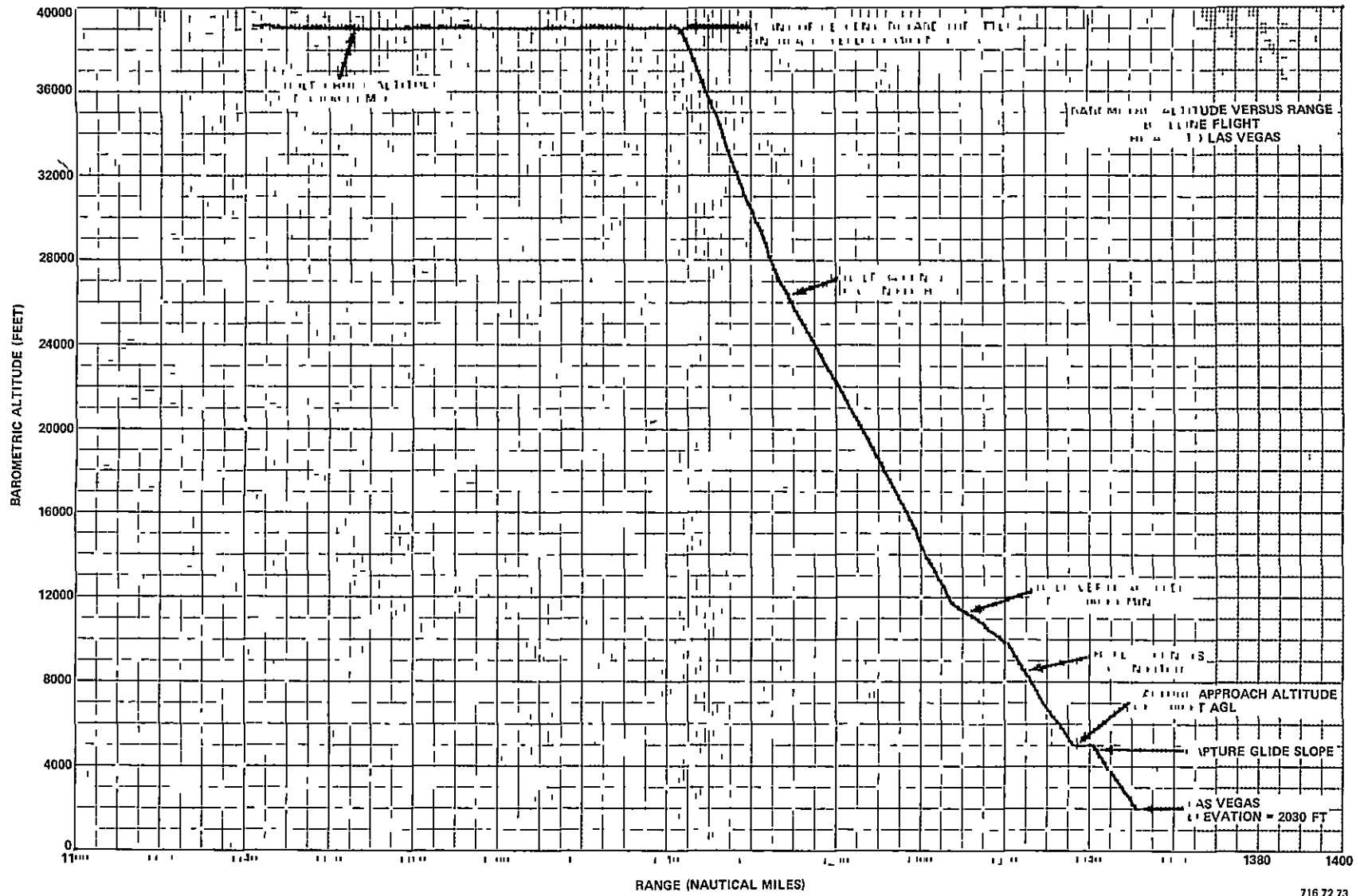


Figure 4-67

short range flight. Approach altitude is captured at 1,336 miles and the glide slope is captured at 1,340.5 miles. Total range for the flight is 1,350 nautical miles.

Fuel consumption per unit distance versus the range is shown in Figure 4-68 for the climb-out segment of the baseline flight. The increase in  $F_D$  at 117.5 miles is due to changing to the maximum climb  $N_1$  limit. Cruise altitude capture begins at 155 miles and the throttles begin to pull back to hold the cruise Mach, causing  $F_D$  to decrease.

Figure 4-69 shows  $F_D$  during the enroute climb. While cruising at 35,000 feet, the average value of  $F_D$  is 28 pounds per nautical mile. When the throttles are increased to the  $N_1$  limit,  $F_D$  increases to a peak of 37 pounds per nautical mile. After the new cruise altitude of 39,000 feet is captured, the average value of  $F_D$  is only 27 pounds per nautical mile.

Fuel consumption per unit distance during the descent and approach versus range is shown in Figure 4-70. Again, the appearance of the plot is the same as for the short haul flight (Figure 4-17) although it is compressed somewhat due to the larger range scale.

Average fuel consumption for the baseline flight from Chicago to Las Vegas is 41,566 pounds. The range of 1,350 miles gives an average  $F_D$  of 30.79 pounds per nautical mile. Average flight time is 3 hours, 3 minutes, and 15 seconds.

#### K. CONSTANT ALTITUDE CRUISE OPTIMAL FLIGHT WITH DELAYED FLAP APPROACH: CHICAGO TO LAS VEGAS

A total ascent fuel burnout of 10,400 pounds was assumed for the flight from Chicago to Las Vegas. A cruise table was generated by the FORTRAN program using the new weight and an optimal cruise altitude of 37,520 feet. The cruise table is given in Appendix F. The FORTRAN program was then used to generate the ascent and descent tables for the Chicago to Las Vegas flight; these are also included in Appendix F. Table 4-12 shows the Mach-altitude profiles derived from these tables.

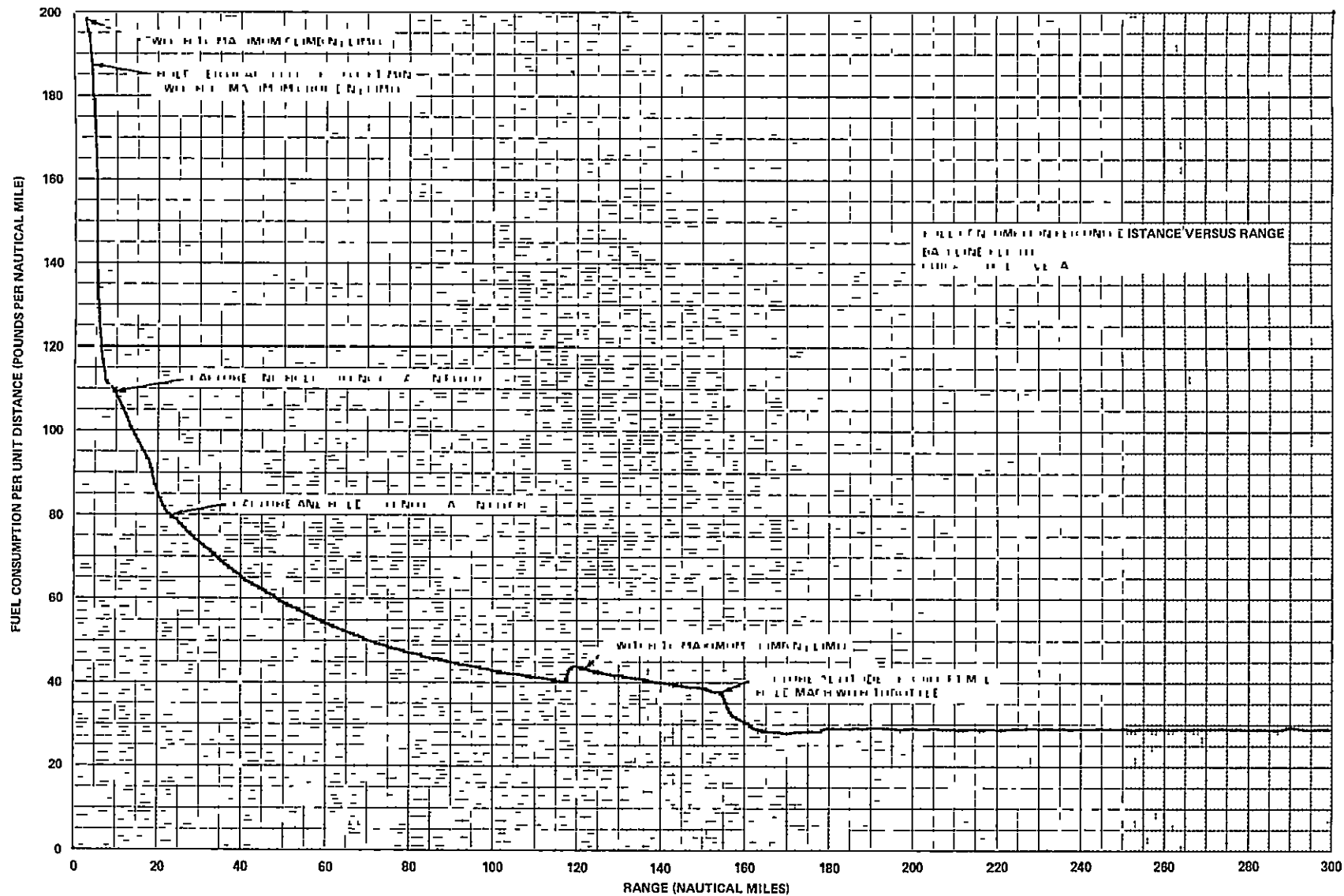


Figure 4-68

ORIGINAL PAGE IS  
OF POOR QUALITY

66-7

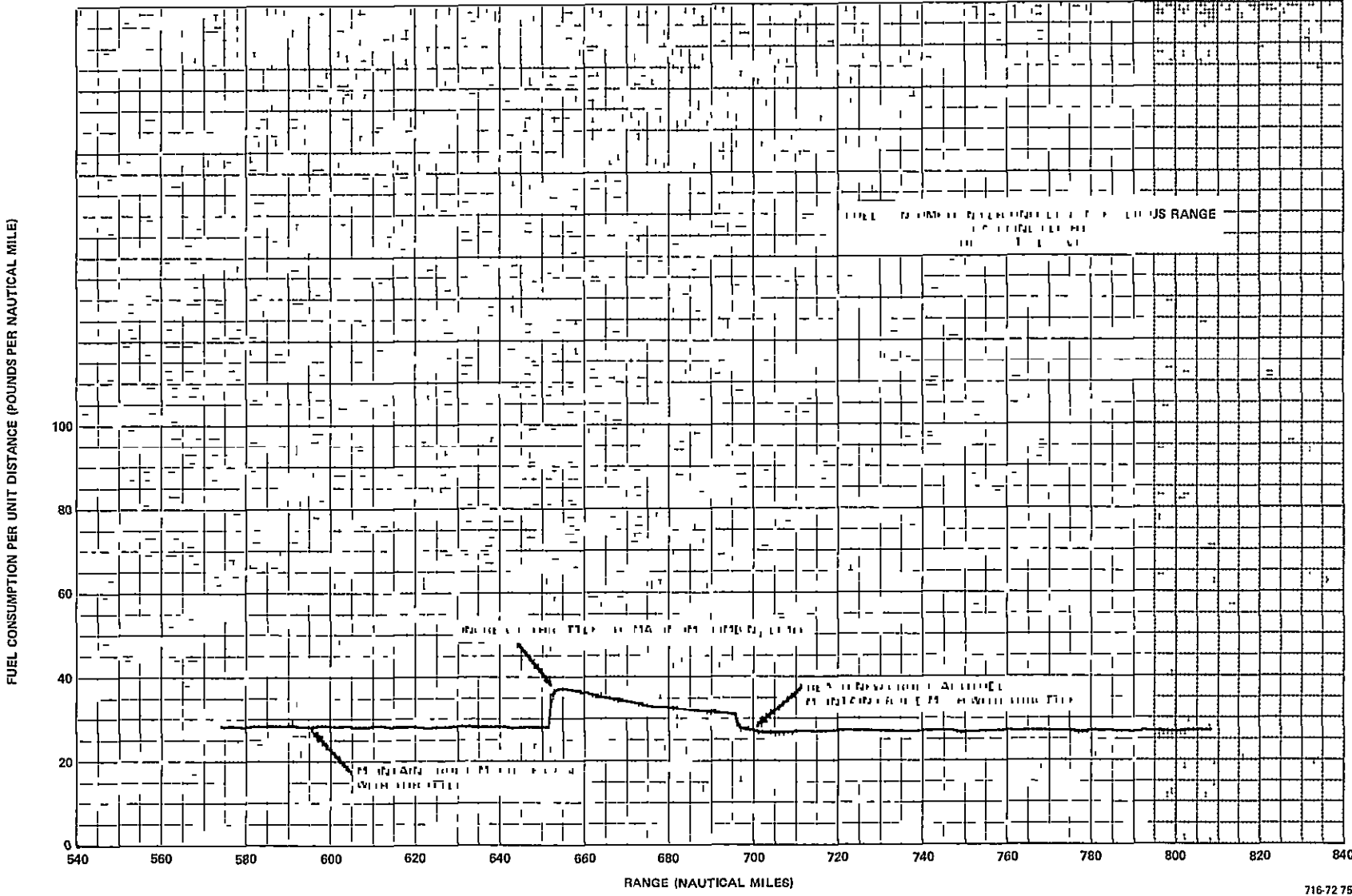


Figure 4-69



ORIGINAL PAGE IS  
OF POOR QUALITY

4-100

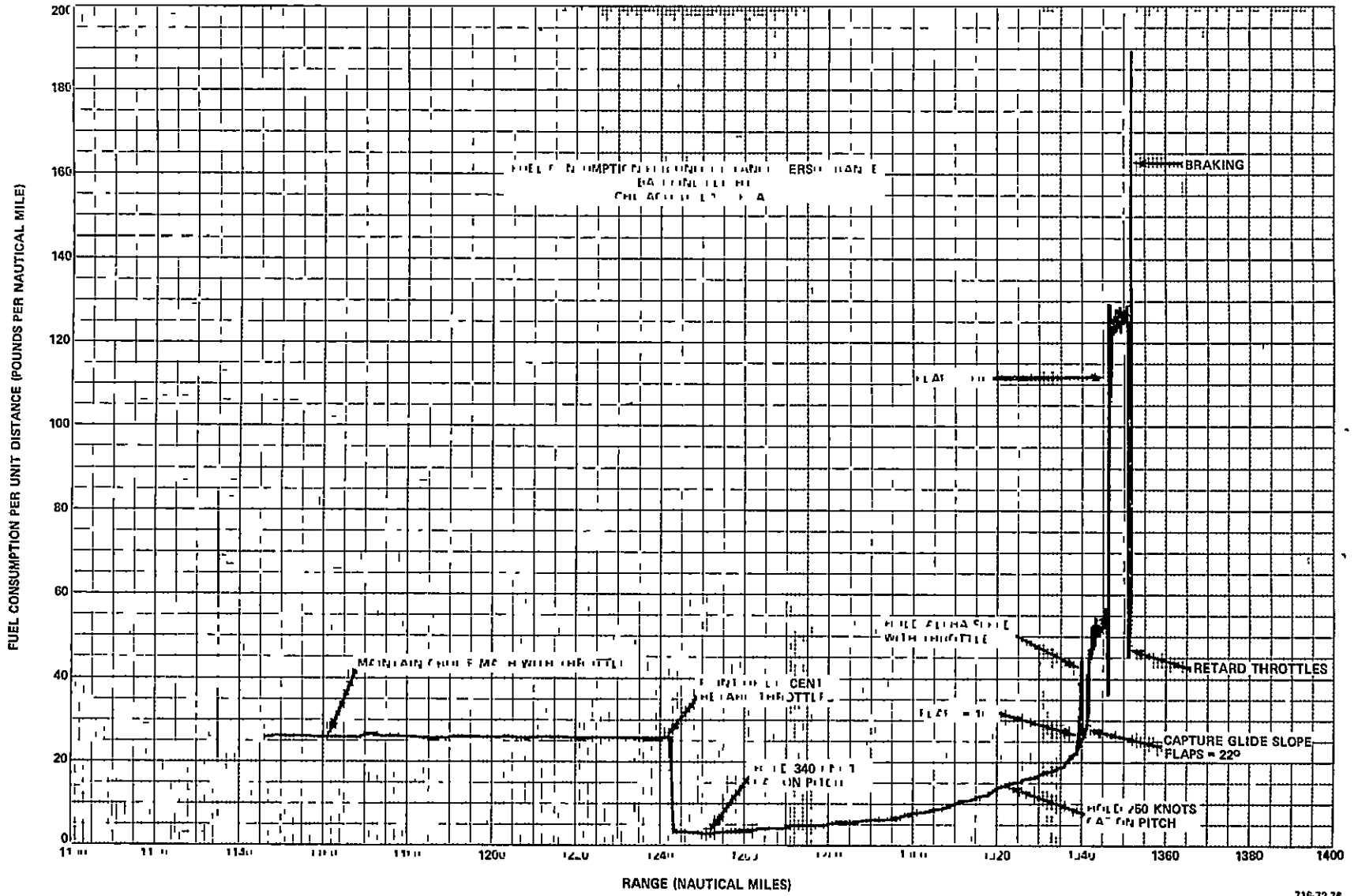


Figure 4-70

TABLE 4-12

MACH-ALTITUDE PROFILE  
OPTIMAL FLIGHT WITH DELAYED FLAP APPROACH  
CHICAGO TO LAS VEGAS

Altitude (feet)	Ascent	Descent
3,000	.5097	--
4,000	.5128	.4554
5,000	.519	.4520
6,000	.5249	.4516
7,000	.5312	.4516
8,000	.5377	.453
9,000	.5428	.4552
10,000	.5471	.4577
11,000	.5541	.4598
12,000	.5614	.463
13,000	.5689	.4638
14,000	.5765	.4677
15,000	.5835	.4704
16,000	.5928	.4746
17,000	.6016	.4792
18,000	.6106	.4842
19,000	.62	.4904
20,000	.6307	.5011
21,000	.6406	.5089
22,000	.6505	.5169
23,000	.6601	.526
24,000	.673	.5349
25,000	.6836	.5447
26,000	.6968	.5548
27,000	.7087	.5652
28,000	.7196	.5767
29,000	.7313	.5903
30,000	.7382	.6054
31,000	.7494	.6161
32,000	.7582	.6266
33,000	.7655	.6368

TABLE 4-12 (cont)  
MACH-ALTITUDE PROFILE  
OPTIMAL FLIGHT WITH DELAYED FLAP APPROACH  
CHICAGO TO LAS VEGAS

Altitude (feet)	Ascent	Descent
34,000	.7719	.6478
35,000	.7783	.6607
36,000	.7815	.6775
37,000	.7829	.6891
38,000	.7829	.6945

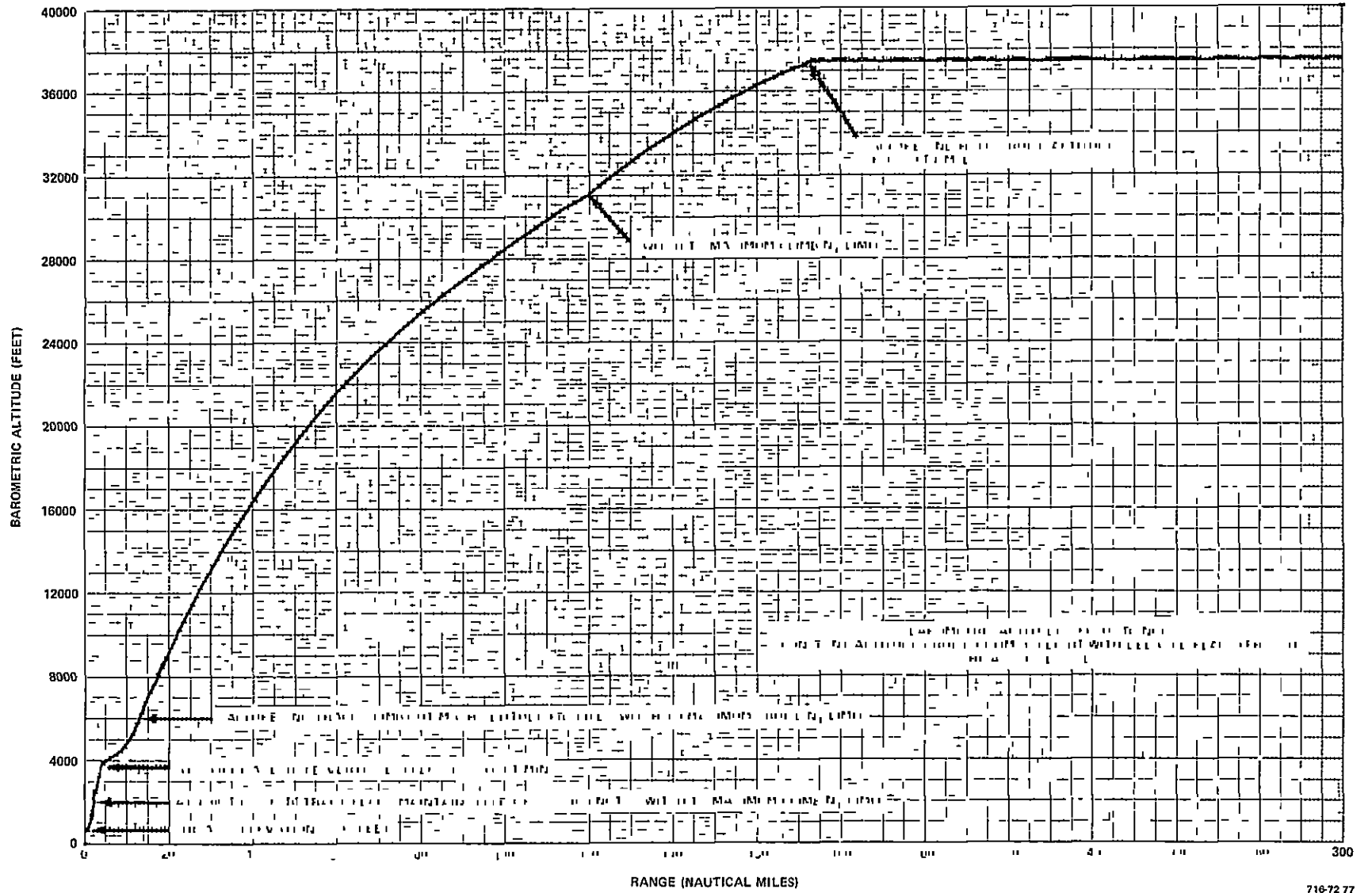
Figure 4-71 shows the barometric altitude versus the range for the climb-out from Chicago. In this case, the throttles change back to the maximum climb  $N_1$  limit at 31,000 feet compared to 30,000 feet for the baseline flight. The cruise altitude of 37,520 feet is achieved 173 miles into the flight, or 17 miles further than the baseline. Once the cruise altitude is captured, it is held on pitch until the descent point.

A plot of altitude versus range for the descent is shown in Figure 4-72. At the descent point (1,229 miles), the aircraft must maintain altitude for 4 miles to slow down to the descent Mach-altitude profile. Glide slope is captured at 1,333 miles (the total range being 1,350 miles).

Figures 4-73 and 4-74 show the fuel consumption per unit distance versus the range for the climb-out and descent, respectively. Average  $F_D$  at the beginning of the cruise segment is 27 pounds per nautical mile while at the descent point it is only 25.5 pounds per nautical mile. The difference is due to the optimal Mach number and consequently,  $F_D$ , being dependent on the weight of the aircraft.

The flap position versus the range is shown in Figure 4-75. Initial flap deployment begins at 1,335 miles (2 miles after glide slope capture) and full landing flaps are deployed at 1,347 miles.

Figures 4-76 and 4-77 show the calibrated airspeed (CAS) versus the range for the climb-out and descent, respectively. Note that there is a somewhat



RANGE (NAUTICAL MILES)

Figure 4-71

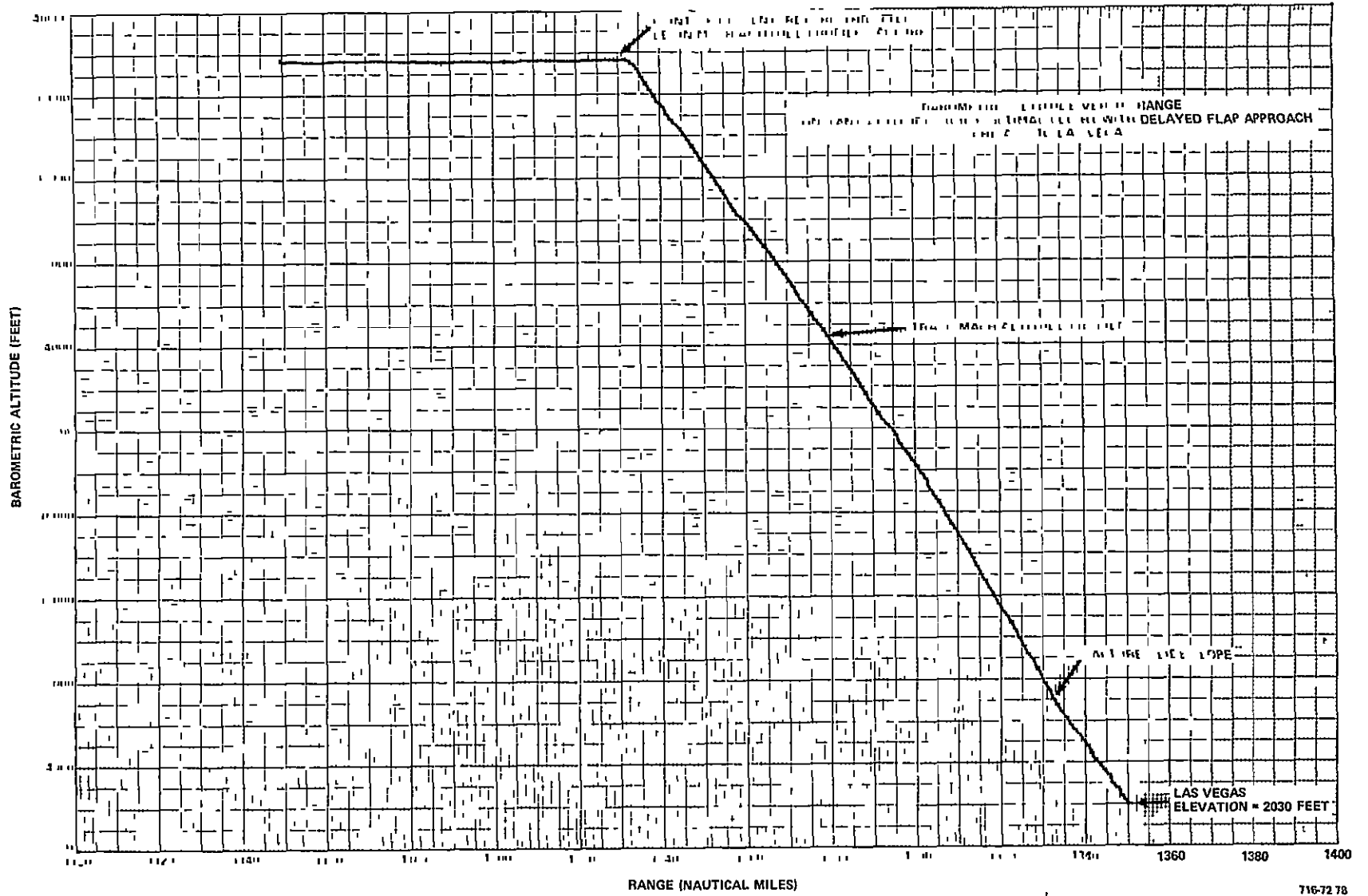


Figure 4-72

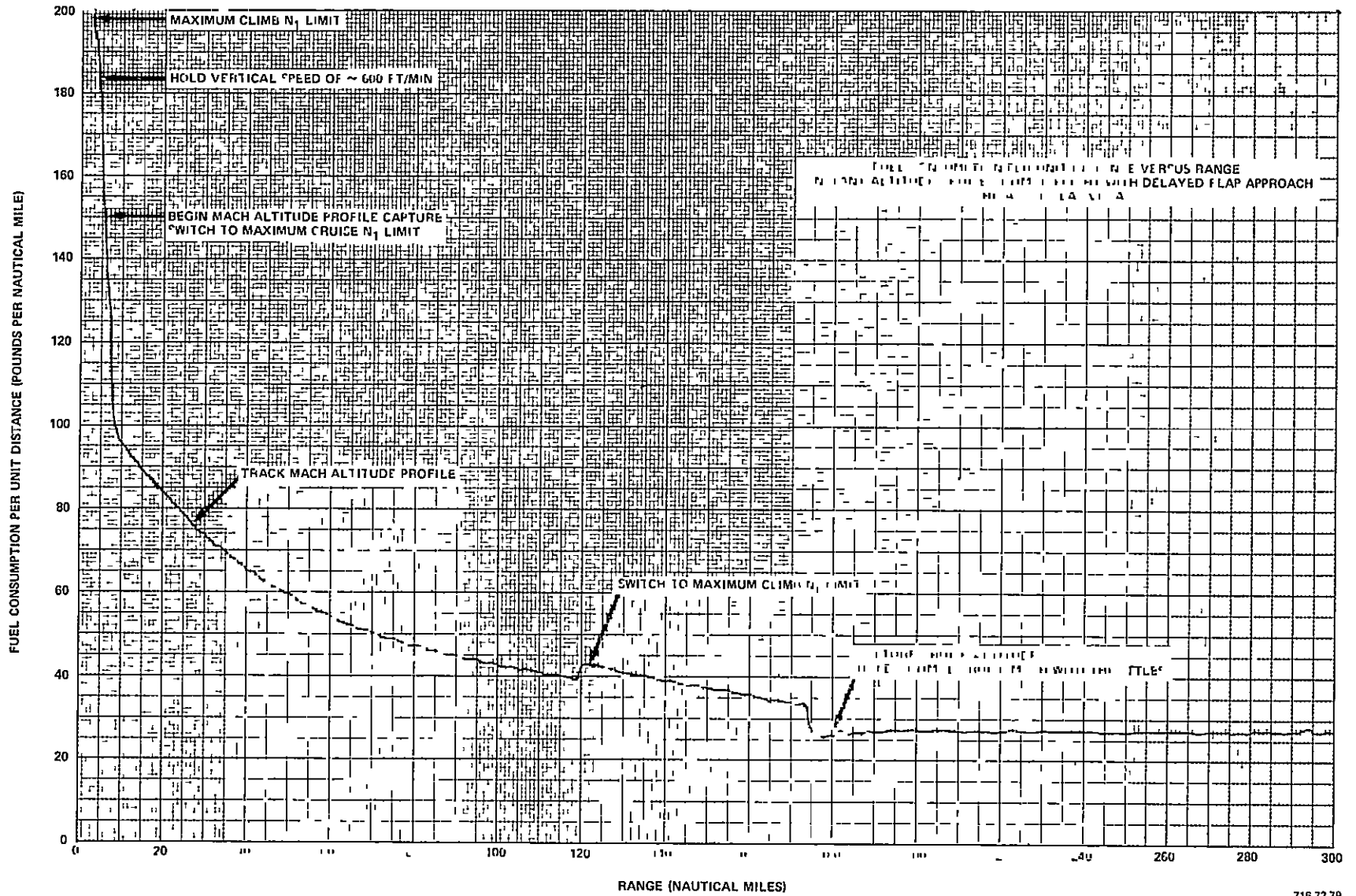


Figure 4-73

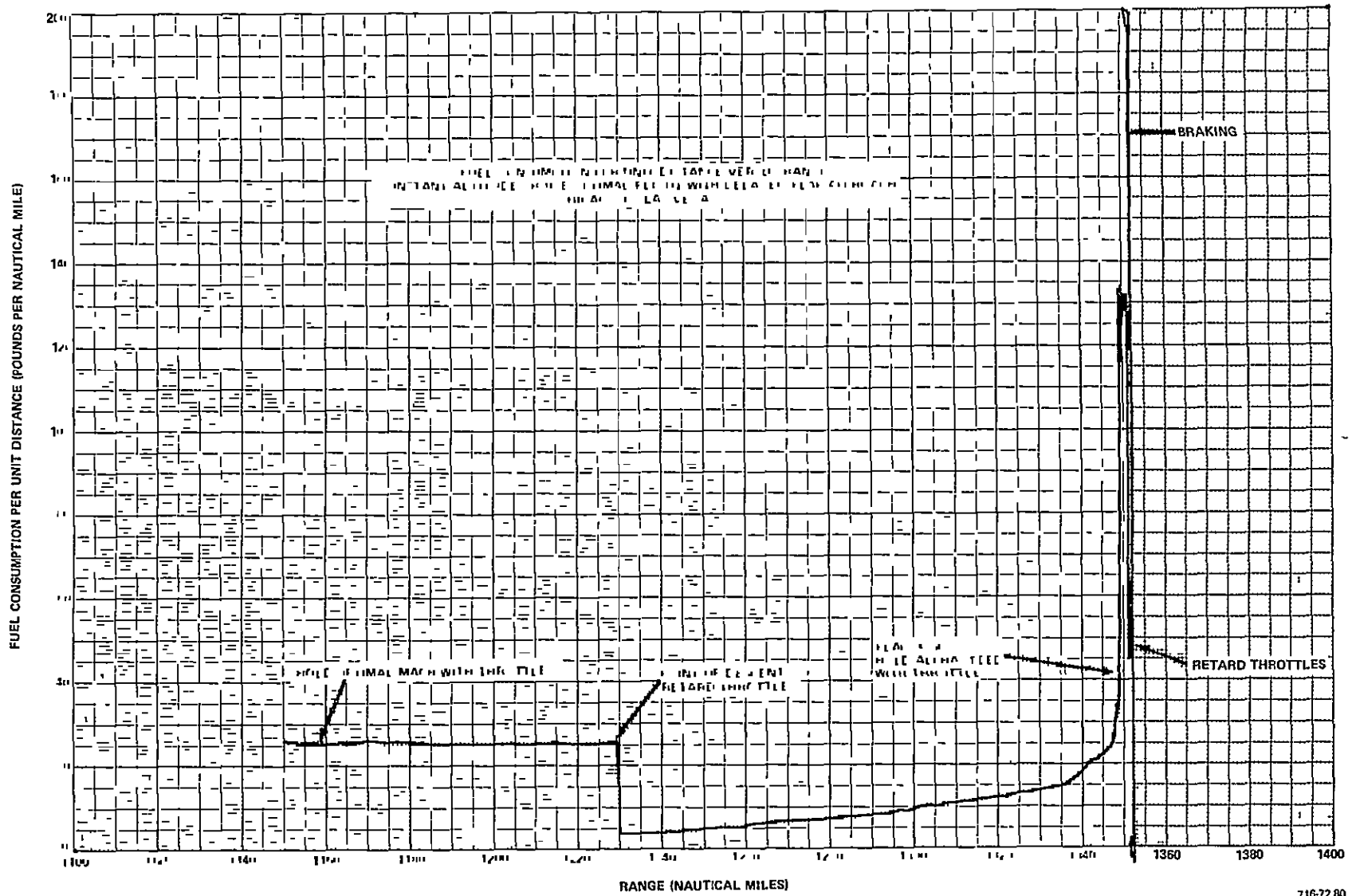
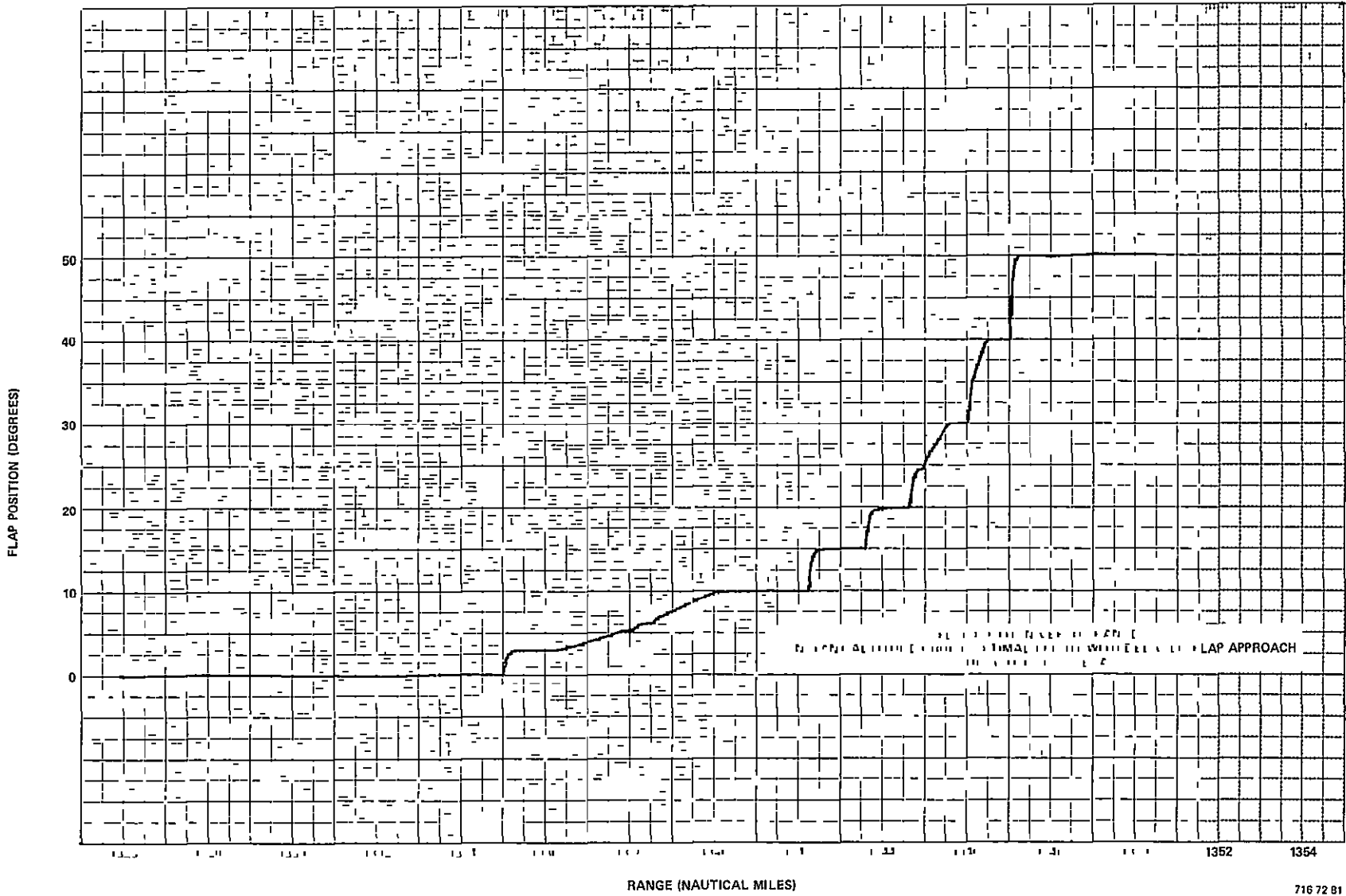


Figure 4-74

ORIGINAL PAGE IS  
OF POOR QUALITY

4-107

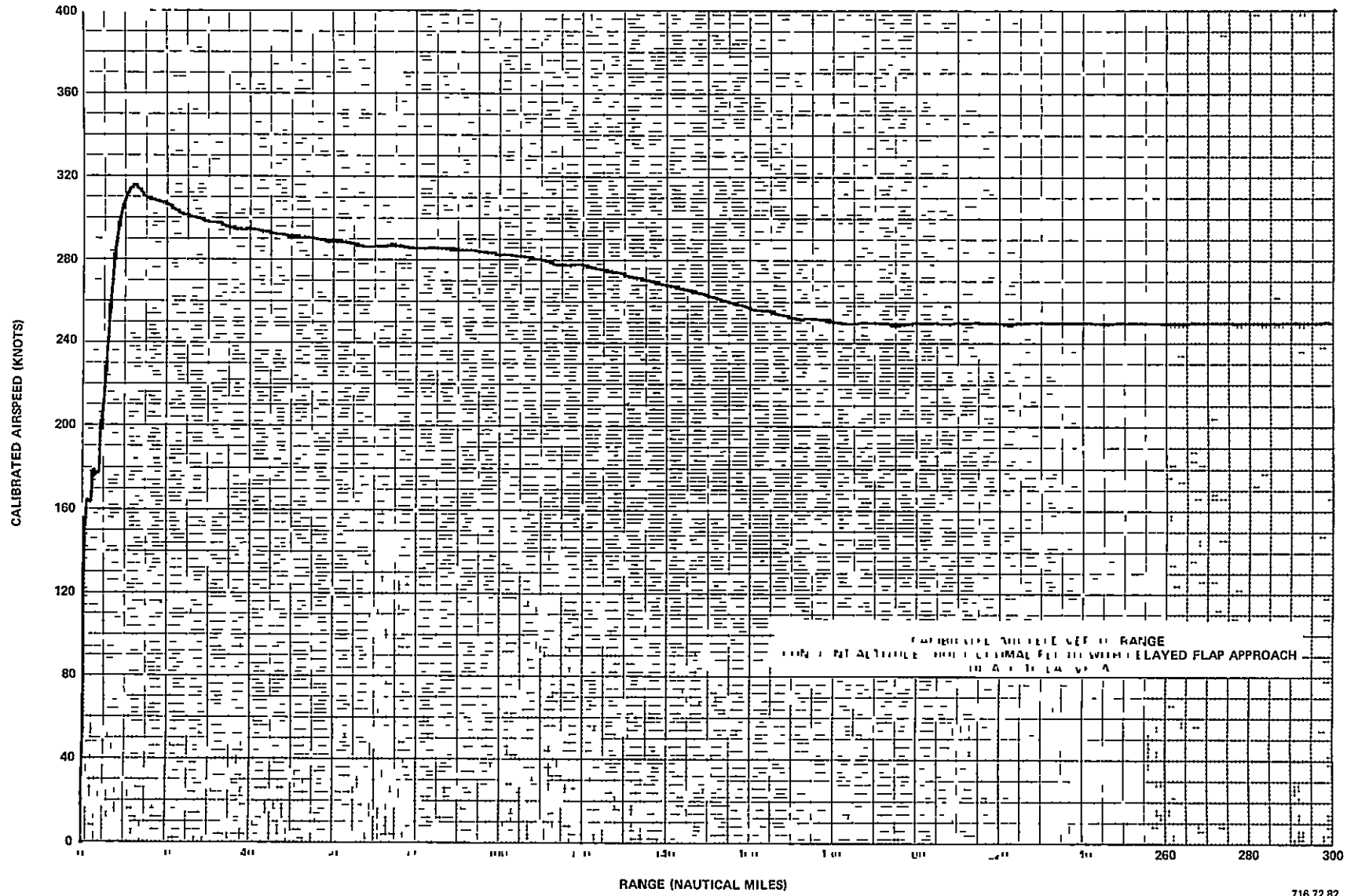


RANGE (NAUTICAL MILES)

716 72 81

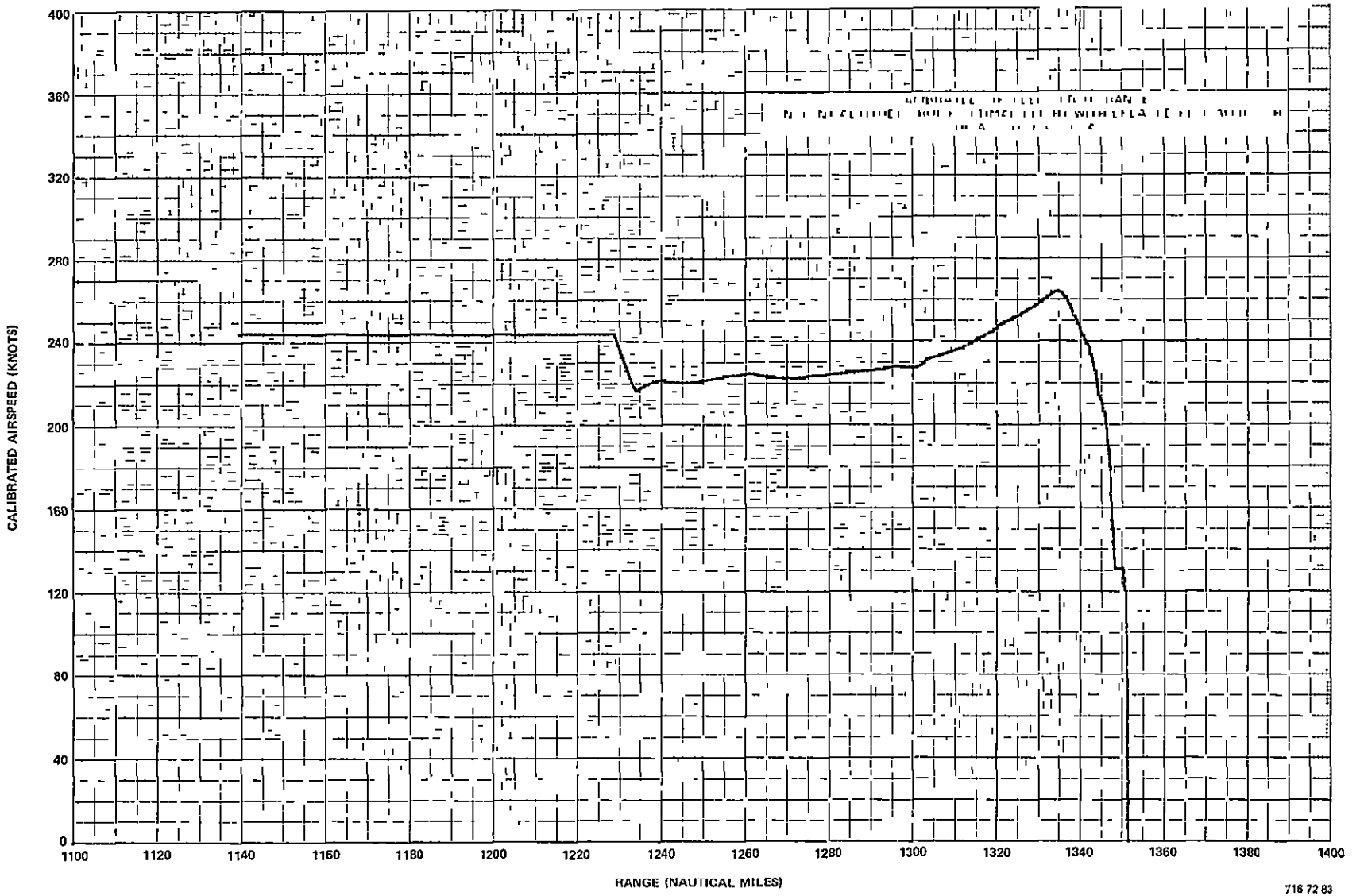
Figure 4-75





RANGE (NAUTICAL MILES)

Figure 4-76



RANGE (NAUTICAL MILES)

Figure 4-77

larger variation in CAS while the climb-out profile is being tracked than in the other optimal flights. This is a result of flying to a higher altitude.

The average fuel consumption for the constant altitude cruise optimal flight with a delayed flap approach is 39,914 pounds. The difference of 1,652 pounds from the baseline represents a 4 percent savings in fuel. Average  $F_D$  dropped the same percentage to 29.56 pounds per nautical mile. The flight time increased 11 minutes and 54 seconds (6.5 percent) to 3 hours, 15 minutes, and 9 seconds.

#### L. CLIMBING CRUISE OPTIMAL FLIGHT WITH DELAYED FLAP APPROACH: CHICAGO TO LAS VEGAS

Cruise tables for several different weights were generated by the FORTRAN program and are included in Appendix G. The results were incorporated into the airborne program to vary the optimal cruise altitude reference as the aircraft weight changed during the flight. In this manner the aircraft will always fly at the optimal altitude even with large changes in weight.

The same profiles as for the constant cruise altitude flight were used for the climbing cruise. Initial cruise altitude is 37,400 feet. The weight change of 27,500 pounds during cruise causes the altitude to be 39,200 feet at the descent point. Figures 4-78 and 4-79 show barometric altitude versus range for the climb-out and descent, respectively.

Fuel consumption per unit distance versus the range is shown in Figures 4-80 and 4-81. The average  $F_D$  at the beginning of the cruise segment is 27.5 pounds per nautical mile. At the descent point, the aircraft is 1,800 feet higher and the  $F_D$  is down to about 26 pounds per nautical mile.

Figure 4-82 shows flap position during the approach while Figures 4-83 and 4-84 show the calibrated airspeed for the climb-out and descent, respectively. All three curves are very similar to those for the constant cruise altitude flight.

Average fuel consumption for the climbing cruise optimal flight with a delayed flap approach is 39,860 pounds. This is 1,706 pounds (4.1 percent)

ORIGINAL PAGE IS  
OF POOR QUALITY

4-111

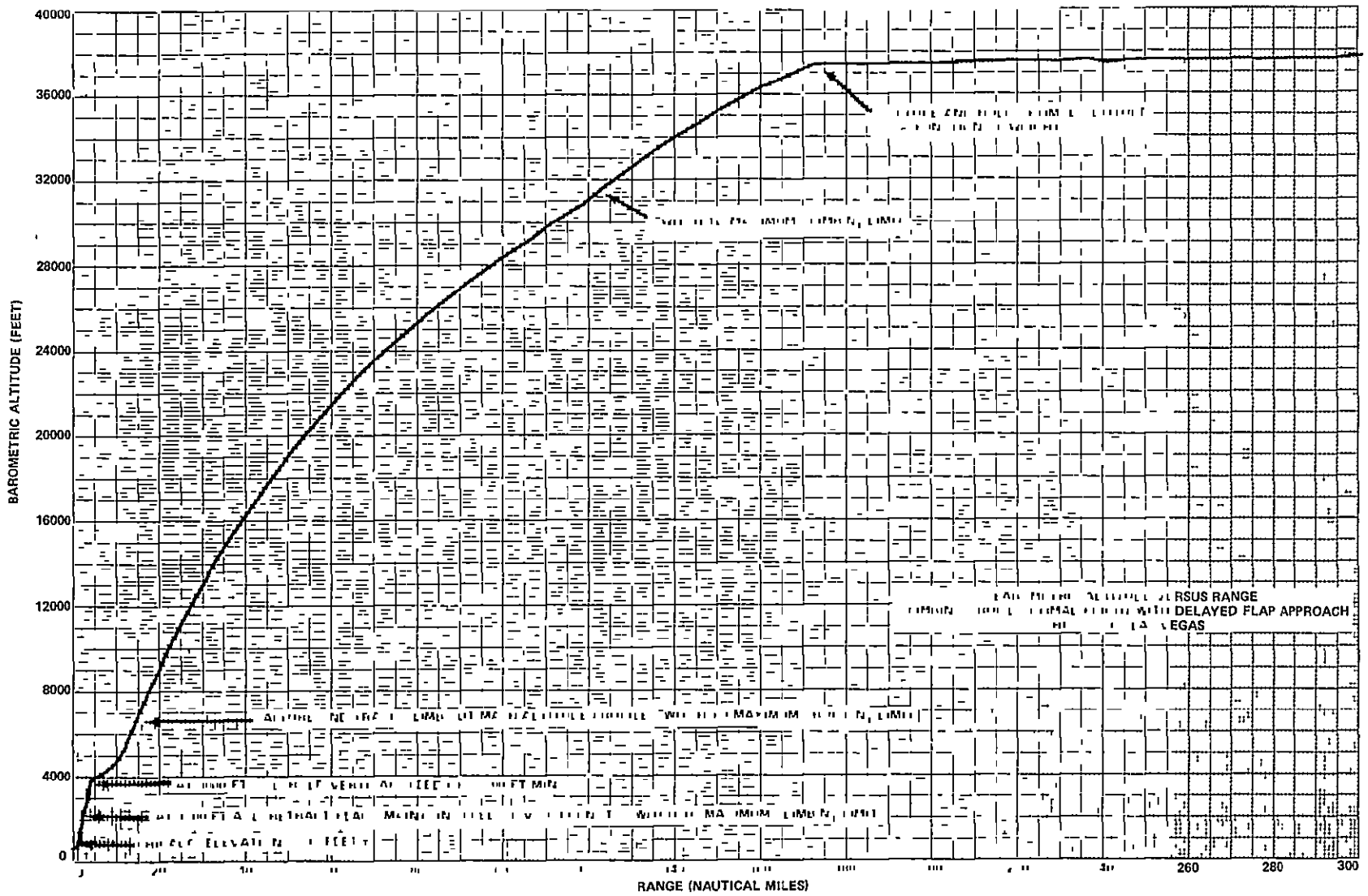


Figure 4-78

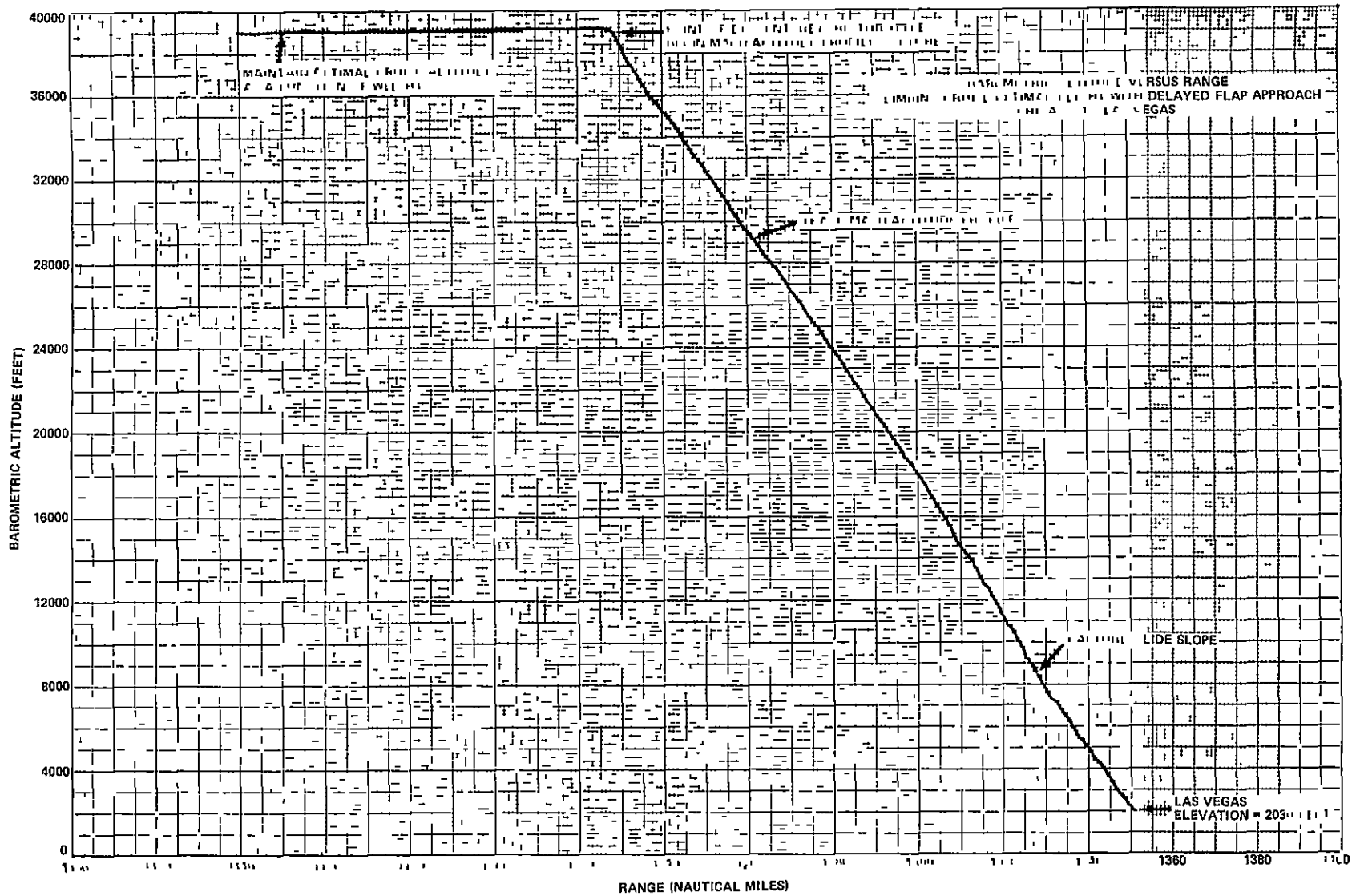
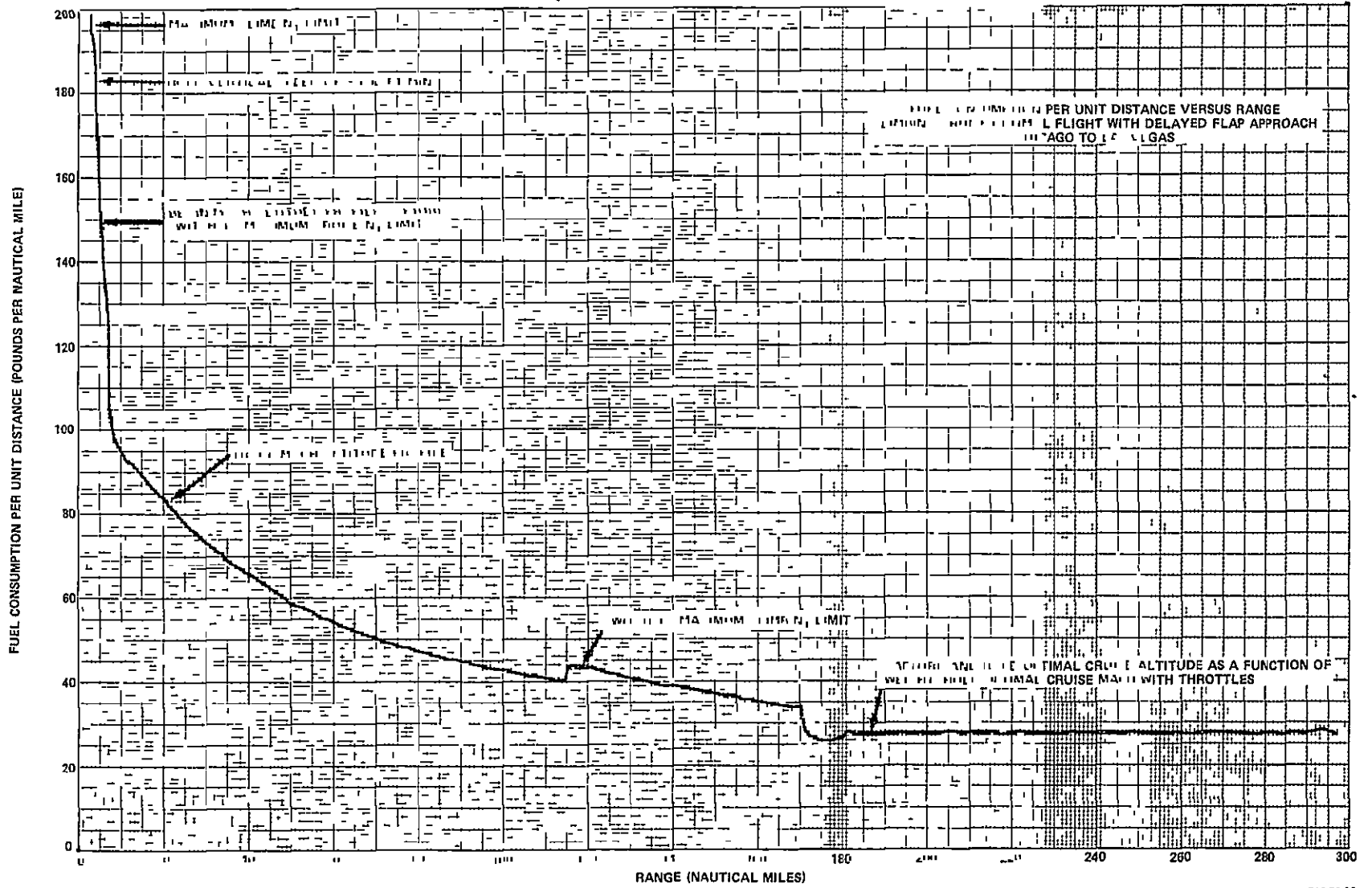


Figure 4-79

ORIGINAL PAGE IS  
OF POOR QUALITY

4-113



716 72 86

Figure 4-80

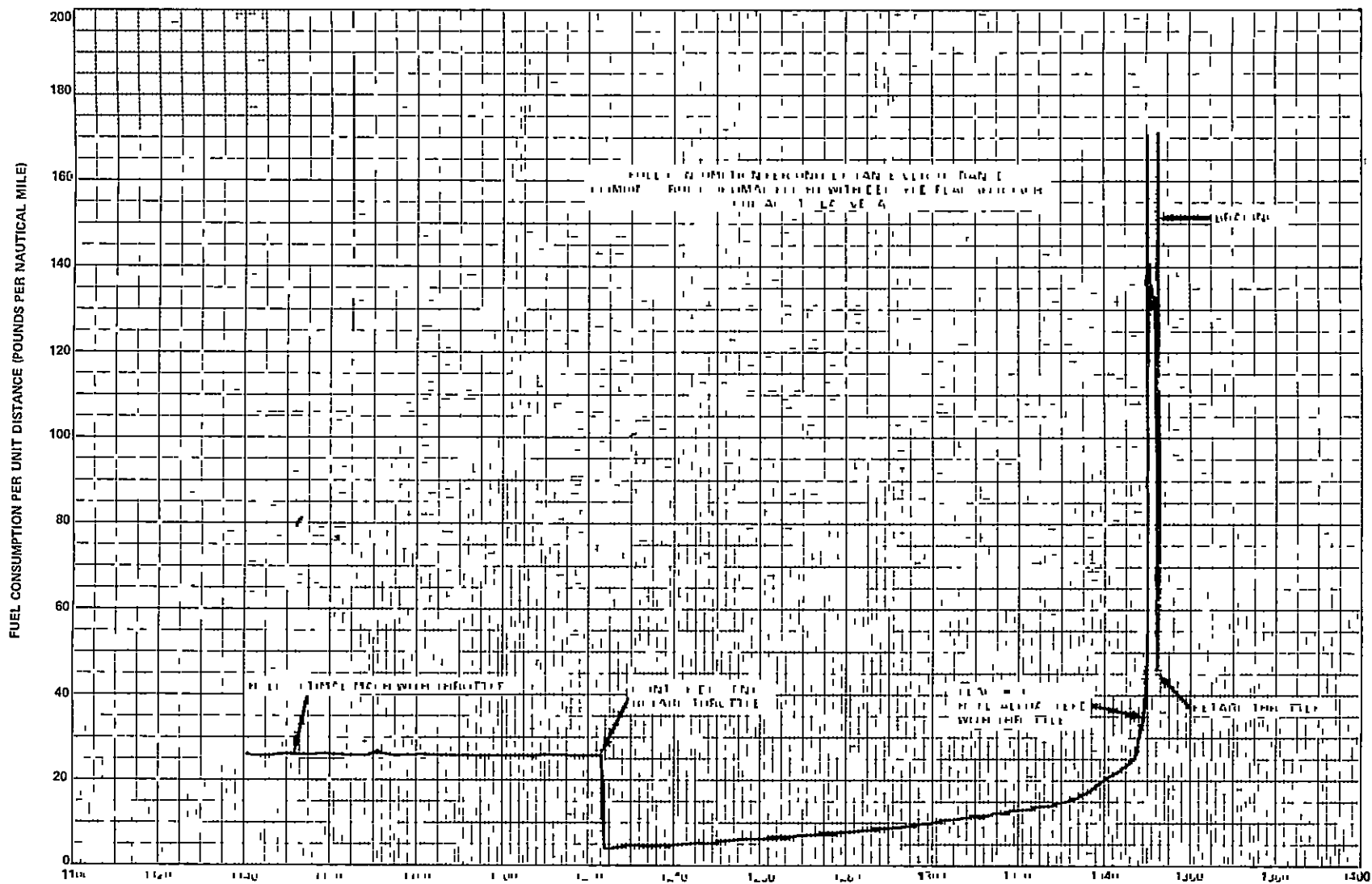


Figure 4-81

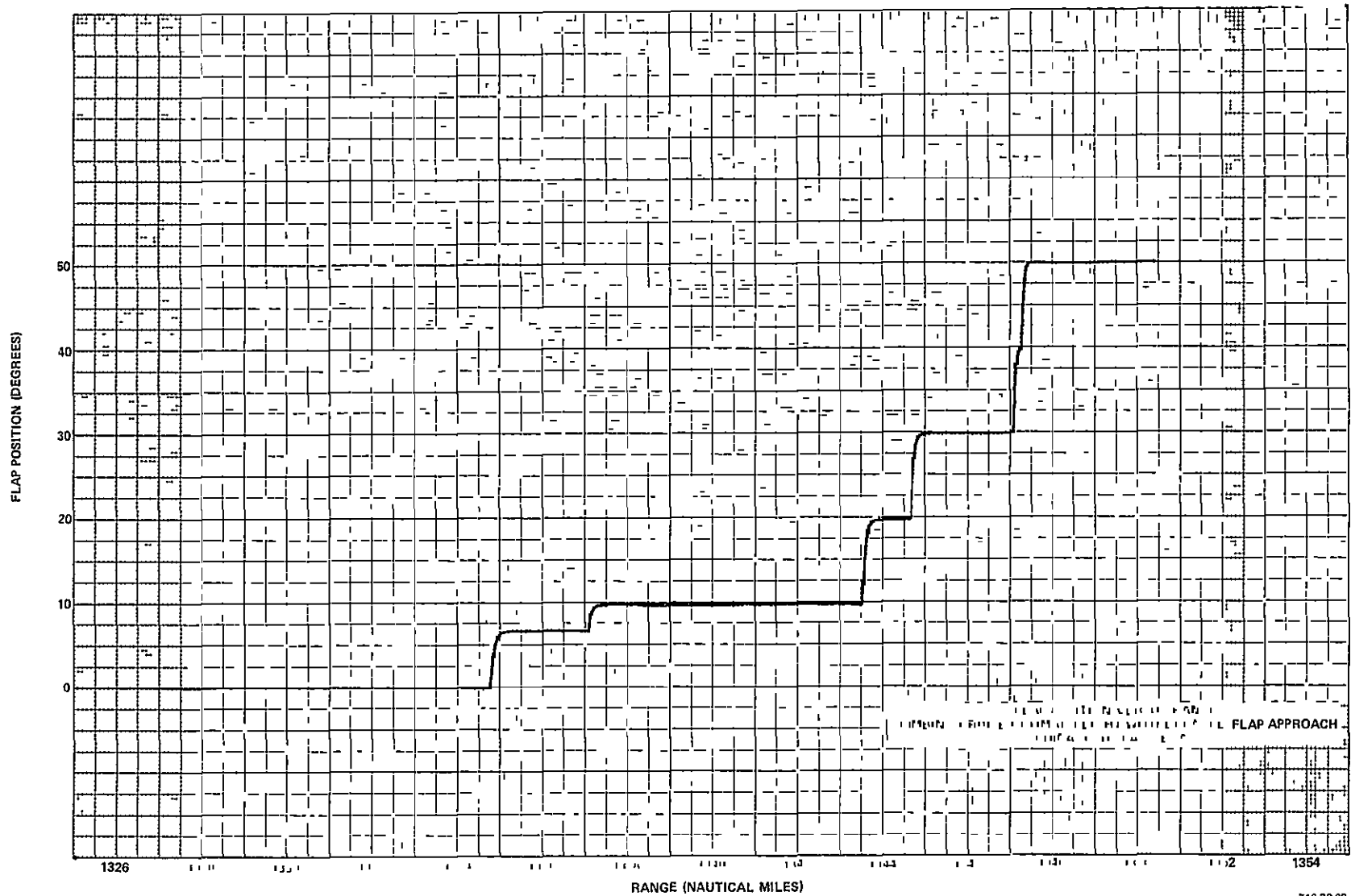


Figure 4-82



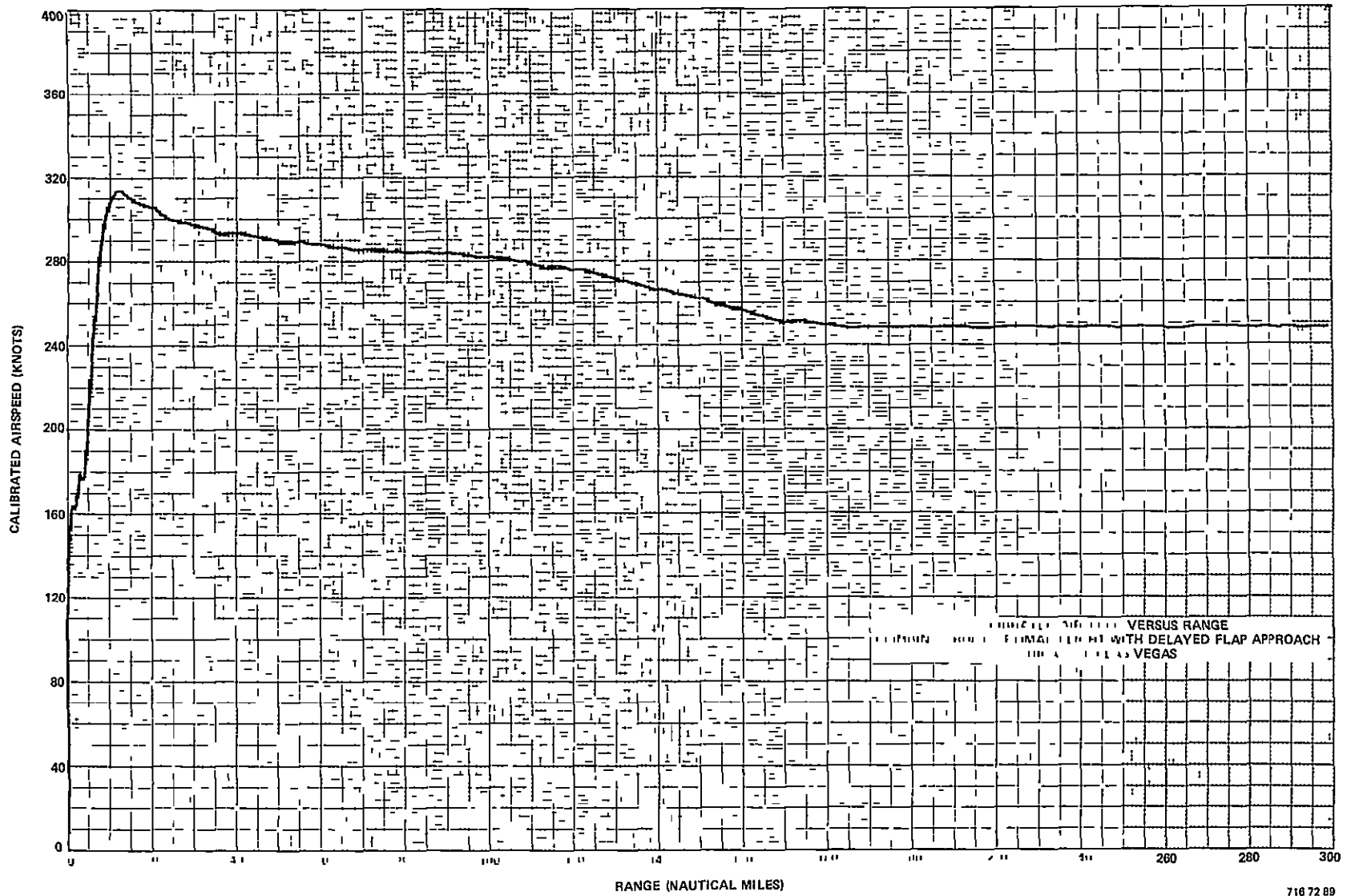
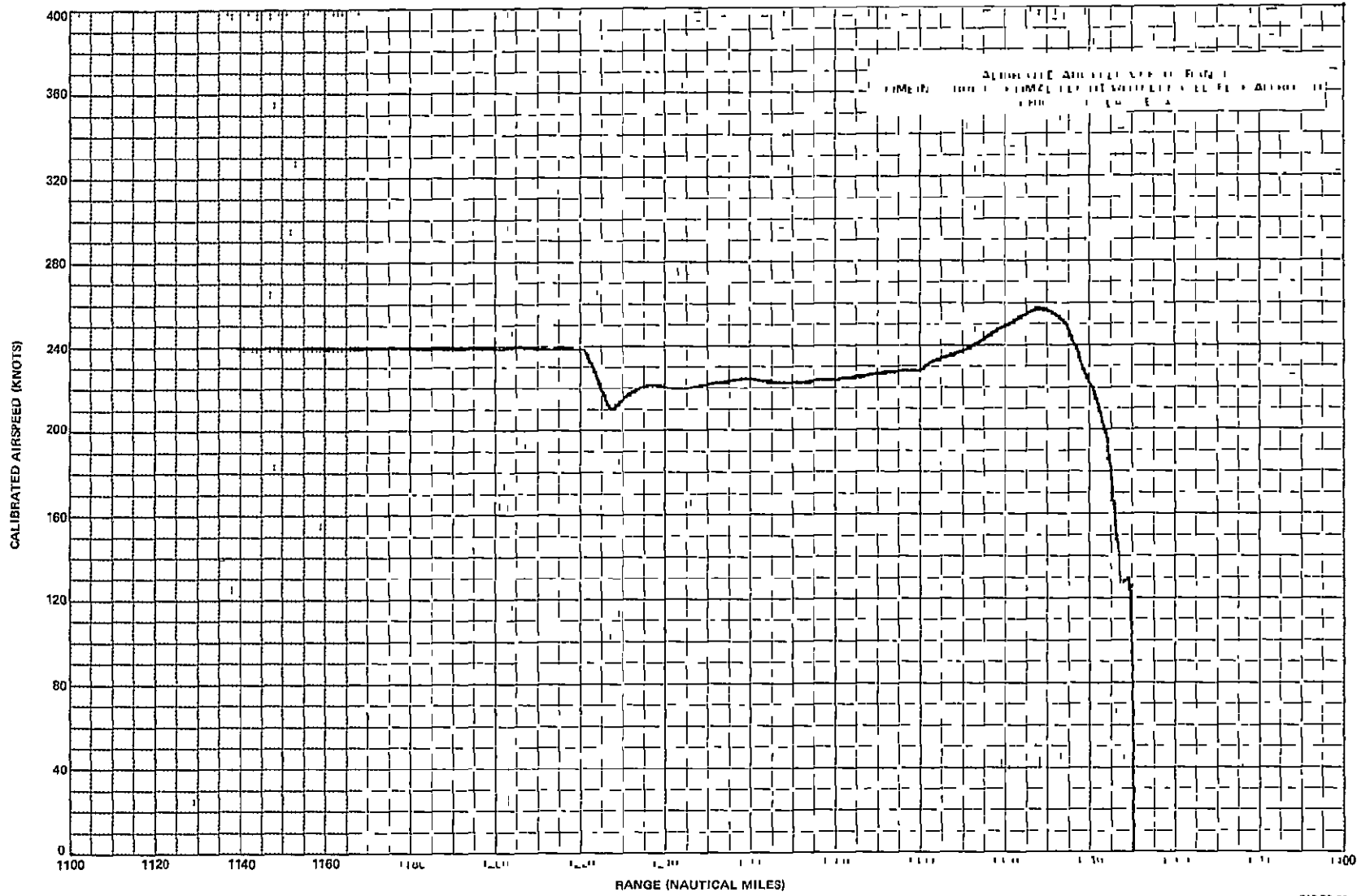


Figure 4-83

4-117



716-72 80

Figure 4-84

less than the baseline and 54 pounds (.14 percent) less than the constant cruise altitude flight. Average  $F_D$  is 29.52 pounds per nautical mile. Flight time decreased 14 seconds from the constant cruise altitude flight to 3 hours, 14 minutes, and 55 seconds. This is 6.37 percent longer than the baseline flight.

#### M. GREAT CIRCLE ROUTE ANALYSIS

From spherical geometry, the great circle distance between point A and point B is

$$\text{Distance} = 3456.484 \cos^{-1} \left[ \sin \text{Lat}_A \sin \text{Lat}_B + \cos \text{Lat}_A \cos \text{Lat}_B \cos \Delta\lambda \right] \quad (4-33)$$

where

$\text{Lat}_A$  = Latitude of point A

$\text{Lat}_B$  = Latitude of point B

$\Delta\lambda$  = Longitude of point A minus longitude of point B

Using this equation for the distance between Las Vegas and Los Angeles results in a great circle route of 207 nautical miles. This is 15 miles less than the baseline flight. Since this distance would come out of the cruise segment, the average  $F_D$  during cruise can be used to compute the potential fuel savings from flying a great circle route. For the baseline cruise Mach of .83, average  $F_D$  is 37.5 pounds per nautical mile during cruise, which results in a 562.5 pound (5.58 percent) savings in fuel. For the baseline flight at the optimal cruise Mach of .62,  $F_D$  is 31.25 pounds per nautical mile which yields a 468.75 pound (4.65 percent) savings. At the faster speed, the flight time would be 1 minute and 48 seconds (4.62 percent) less, while the slower speed would result in a 2 minute and 24 second decrease (5.67 percent) in flight time.

The baseline distance from Chicago to Las Vegas is 1,350 nautical miles. Equation (4-33) yields a great circle distance of 1,320 nautical miles, or 30 miles less than the baseline. At an average cruise  $F_D$  of 27 pounds per nautical mile, the fuel savings would be 810 pounds, or 1.95 percent. A

flight at the optimal cruise Mach of .778 would be 4 minutes and 5 seconds faster for a 2.1 percent decrease in flight time.

It should be noted that the possible savings due to flying a great circle route are dependent on the current FAA flight route from city to city. The results discussed above are thus valid only for the two routes studied and generalizations for other routes cannot be made.

SECTION V

CONCLUSIONS AND RECOMMENDATIONS

## SECTION V

## CONCLUSIONS AND RECOMMENDATIONS

In general, it was found that the shorter the route length the greater the potential improvement in fuel efficiency. The results shown in Table 5-1 for the Las Vegas to Los Angeles flight (low altitude) versus the results in Table 5-2 for the Chicago to Las Vegas flight (high altitude) illustrate this point. The former achieved a 1,079 pound fuel savings over a distance of 222 miles, while the latter realized a 1,706 pound savings in 1,350 miles.

TABLE 5-1  
SUMMARY OF SIMULATOR FLIGHT RESULTS  
LAS VEGAS TO LOS ANGELES

Flight	Average Fuel Consumed (lb)	Average $F_D$ (lb/nmi)	Average Flight Time (min,sec)	Fuel Saved		Time Change	
				(lb)	%	(min,sec)	%
Baseline	10,072	45.25	39,0	-	-	-	-
Baseline with Delayed Flap Approach	9,791	44.02	37,8	281	2.79	-(1,52)	-4.79
Baseline at Optimal Cruise Mach	9,638	43.31	42,20	434	4.31	3,20	8.55
Optimal with Constrained Altitude	9,480	42.58	43,6	592	5.9	4,6	9.4
Optimal with Unconstrained Altitude	9,316	41.85	42,28	756	7.51	3,28	8.89
Optimal with Unconstrained Altitude and Delayed Flap Approach	8,993	40.42	41,16	1079	10.7	2,16	5.8
Optimal with Unconstrained Altitude and Delayed Flap Approach on Great Circle Route	8,524	41.18	38,52	1548	15.4	-(0,8)	-.34

TABLE 5-2  
SUMMARY OF SIMULATOR FLIGHT RESULTS  
CHICAGO TO LAS VEGAS

Flight	Average Fuel Consumed (lb)	Average $F_D$ (lb/nmi)	Average Flight Time (hr,min,sec)	Fuel Saved		Time Change	
				(lb)	%	(hr,min,sec)	%
Baseline	41,566	30.79	3,3,15	-	-	-	-
Constant Altitude Cruise Optimal with Delayed Flap Approach	39,914	29.56	3,15,9	1652	3.97	0,11,54	6.5
Climbing Cruise Optimal with Delayed Flap Approach	39,860	29.52	3,14,55	1706	4.1	0,11,40	6.37
Climbing Cruise Optimal with Delayed Flap Approach on Great Circle Route	39,050	29.58	3,10,50	2516	6.05	-(0,4,5)	-2.1

On short haul flights, the current practice of flying a relatively low altitude cruise segment at a high calibrated airspeed results in an inefficient (high drag) condition, far removed from the optimal fuel condition.

In order to achieve full potential fuel savings, these departures from current FAA regulations or procedures were made:

- The restriction of calibrated airspeed to 250 knots maximum below 10,000 feet was ignored.
- The normally assigned altitudes were ignored.

The first point bears further study to fully assess the penalty paid in adhering to this restriction. From the results of the baseline flight at the optimal cruise Mach and the constrained altitude optimal flight (see Table 5-1), the total penalty for a baseline climb-out and descent is less than 150 pounds of fuel.

The second point bears discussion as to what procedures might be acceptable on a short route such as Las Vegas to Los Angeles. The best fuel savings on a short route were obtained by climbing until it was necessary to begin the descent. The optimal cruise altitude is generally not achieved on a short flight and a required cruise segment at a lower flight level obviously decreases the potential fuel savings.

Periodic altitude reassignments on longer routes could give results quite close to optimum. The climbing cruise flight from Chicago to Las Vegas saved 54 pounds of fuel over the constant altitude cruise flight (see Table 5-2). This difference would probably have been somewhat less had the constant cruise altitude been chosen as a compromise between the optimal altitudes for the weights at the beginning and the end of the cruise segment.

It can be inferred from the data that the fuel consumption sensitivity to suboptimal airspeeds is least during climb-out (see Figures 4-25 and 4-26). It can also be said that the fuel consumption sensitivity to changes in airspeed near the optimal value is quite small for all conditions (see Figures 4-1 through 4-6). This implies that time can be introduced into the cost function without drastically affecting fuel consumption.

The optimal cruise condition is observed to be a function of weight. The optimal altitude increases with decreasing weight while the optimal Mach



number remains approximately constant. At a fixed altitude the optimal Mach number decreases with decreasing weight. If these results were used in combination by flying at the optimal Mach between periodic enroute climbs (to an altitude close to optimum), the results would be quite close to optimal.

As mentioned previously, the fuel optimal cruise basically requires a slower airspeed than current airline procedure dictates. The resultant time penalty raises the valid question of the total operating cost difference between current procedures and fuel optimal procedures. This question must be addressed as well as the question of what savings in operating costs are available. As was mentioned, it would appear from the low sensitivity of fuel consumption to a change in airspeed near the optimal value that the time penalty could be significantly reduced without a drastic increase in the fuel consumption. However, this strategy warrants quantitative investigation before any further conclusions are made as to its effectiveness.

Further work which we recommend is:

- Include time in the cost function in order to obtain an operating cost optimal formulation.
- Refine the delayed flap/decelerating approach to include nonlinear effects and better glide slope acquisition.
- Investigate feasibility and effectiveness of establishing a lower flight idle throttle setting.
- Investigate the effectiveness of an adaptive-optimal system.
- Investigate performance degradation due to throttle hysteresis.
- Investigation of various procedure-oriented drag reductions through improved stabilizer trim (Differential Engine Thrust).
- Evaluation of the various concepts in a manual environment (including pilot workload).
- Determination of a practical system incorporating all procedures judged to be worthwhile.
- Flight test the system in manual, automatic, and semi-automatic configurations.

## REFERENCES

## REFERENCES

1. Osder, S. S., Mossman, D. C., and Devlin, B. T., "Flight Test of a Digital Guidance and Control System in a DC-10 Aircraft," Journal of Aircraft, Volume 13, No. 9, September 1976, pp. 676-686.
2. Bryson, A. E., Jr., Desai, M. N., and Hoffman, W. C.: "Energy State Approximation in Performance Optimization of Supersonic Aircraft," Journal of Aircraft, Vol. 6, No. 6, Nov-Dec 1969, pp. 481-488.
3. Shoaee, Hamid, and Bryson, Arthur E., Jr., Airplane Minimum Fuel Flight Paths for Fixed Range, Department of Aeronautical Engineering, Stanford University, SUDDAR No. 499, NASA Grant NGL 05-020-007, March 1976.
4. Erzberger, H., McLean, John D., Barman, John F.: "Fixed Range Optimum Trajectories for Short-Haul Aircraft," NASA TN D-8115, December 1975.
5. Blaschke, A. C., et al., Aerodynamic Data for Stability and Control Calculations Model DC-10 Series 10 Jet Transport, Report No. DAC-67489, Revised November 30, 1971, Douglas Aircraft Division, McDonnell Douglas Corporation, Long Beach, California.
6. The CF6-6 Engine Installation Manual, GEK 9286, Revision July 1, 1975, Aircraft Engine Group, General Electric Company, Cincinnati, Ohio.